BINDING SERVICES
Tel +44 (0)29 2087 4949
Fax.+44 (0)29 2037 1921
E-Mail Bindery@Cardiff.ac.uk

Investigating the role of NFκB in the pathology of osteoarthritis

Sarah Nicol Lauder

A thesis submitted to Cardiff University for the Degree of Doctor of Philosophy

Department of Rheumatology
School of Medicine
Cardiff University
Cardiff
UK

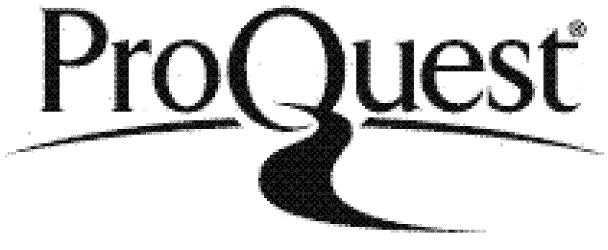

ProQuest LLC
789 East Eisenhower Parkway
P.O. Box 1346
Ann Arbor, MI 48106-1346

DECLARATION

This work has not previously been accepted in substance for any degree and is not concurrently submitted in candidature for any degree.

Signed ..... (candidate) Date 1/JUN/07

STATEMENT 1

This thesis is being submitted in partial fulfillment of the requirements for the degree of PhD (insert MCh, MD, MPhil, PhD etc, as appropriate)

Signed ..... (candidate) Date 1/JUN/07

STATEMENT 2

This thesis is the result of my own independent work/investigation, except where otherwise stated.
Other sources are acknowledged by explicit references.

Signed ..... (candidate) Date 1/JUN/07

STATEMENT 3

I hereby give consent for my thesis, if accepted, to be available for photocopying and for inter-library loan, and for the title and summary to be made available to outside organisations.

Signed ..... (candidate) Date 1/JUN/07

STATEMENT 4 - BAR ON ACCESS APPROVED

I hereby give consent for my thesis, if accepted, to be available for photocopying and for inter-library loans **after expiry of a bar on access** approved by the Graduate Development Committee.

Signed ..... (candidate) Date .....

Acknowledgements

During the past three years numerous people have helped and supported my work, I would like to extend my gratitude to all of them.

First, and foremost, I would like to thank my supervisors Dr Anwen Williams and Dr Paul Brennan, for their guidance and direction during my studies and for teaching me the way research should be conducted. I am grateful to you both for giving me the opportunity to continue my PhD studies within the School of Medicine.

To the members of the Rheumatology Department, I would like to thank Mr Nick Amos for all his technical advice and assistance over the past three years, for teaching me numerous skills and for his patience during the early days. Thanks to Sara and Clare for their help and cooperation throughout my studies and to Kate for her assistance during the latter stages. I would also like to thank Prof. Bryan Williams for his support.

I would like to acknowledge Dr Rhian Goodfellow, and all the theatre staff at the Royal Glamorgan Hospital, for providing the regular supply of synovial tissue that have made this project possible, and both Dr Ron Hill and Dr Francisco Talamas at Roche who provided the IKK inhibitors used throughout these studies.

Thanks to the Arthritis Research Campaign for financial support during the first 18 months of my project and to the School of Medicine for providing financial assistance during the latter half of my studies.

On a more personal note I'd like to thank my 'chinas' for always being at the end of a phonecall or an email, in particular, Bex, Angie, Lindsay, Wilko, Parselle and Sarah, and to Gilly for his patience and support.

Finally, I would like to thank my Mom and Dad, for their continued, unconditional love and support, both emotionally and financially.

Abstract

Globally the most prevalent muscoskeletal condition affecting humans, osteoarthritis is a complex, multifactorial disease characterised by deterioration of articular cartilage and varying degrees of synovial inflammation. The catabolic cytokine interleukin-1beta (IL-1β), a potent inducer of the transcription factor NFκB, induces the production of cartilage destructive aggrecanases and matrix metalloproteinases (MMPs) and the inflammatory cytokine, interleukin-6 (IL-6), within the joint.

The aim of the work described in this thesis was to investigate the role of NFκB within the osteoarthritic joint and its potential as a therapeutic target for disease intervention. NFκB activation was inhibited using adenoviral gene transfer or by two novel pharmacological inhibitors of IKK, RO100 and RO919.

Inhibition of the NFκB signalling cascade in human synovial fibroblasts from osteoarthritic patients suppressed the IL-1β induction of IL-6, MMP-1 and MMP-3 but did not affect the levels of tissue inhibitor of metalloproteinases-1 (TIMP-1). To further investigate the effects of these IKK inhibitors, cartilage degradation was investigated by culturing murine patellas with human synovial fibroblasts. Early stage cartilage deterioration, induced by IL-1β, was prevented by NFκB inhibition.

An animal model of OA, that reflected the early stage pathological changes, was set up as part of this study. The therapeutic efficacy of RO100 and RO919 was tested *in vivo*. It was observed that neither inhibitor prevented pathological changes associated with OA, for example cartilage degradation. The basis of the lack of efficacy demonstrated by RO100 and RO919 is unknown but may be due to poor bioavailability of the agents within the joint.

In conclusion, the studies conducted during this thesis have shown, in various systems, that inhibiting NFκB can prevent changes such as cartilage degradation that occur in OA. Increasing the bioavailability of these or other inhibitors of NFκB may be key in the development of successful novel therapeutic modalities in the future.

Publications

Lauder SN, Carty SM, Carpenter CE, Hill RJ, Talamas F, Bondeson J, Brennan P, Williams AS. Interleukin-1β induced activation of nuclear factor-κB can be inhibited by novel pharmacological agents in osteoarthritis. Rheumatology (Oxford). 2007;**46(5)**:752 - 8.

Bondeson J, Lauder S, Wainwright S, Amos N, Evans A, Hughes C, Feldmann M, Caterson B. Adenoviral gene transfer of the endogenous inhibitor IκBα into human osteoarthritis synovial fibroblasts demonstrates that several matrix metalloproteinase and aggrecanases are nuclear factor-κB-dependent. J Rheumatol. 2007; **34(3)**:523 – 33.

Amos N, Lauder S, Evans A, Feldmann M, Bondeson J. Adenoviral gene transfer into osteoarthritis synovial cells using the endogenous inhibitor IκBα reveals that most but not all inflammatory cells and destructive mediators are NFκB dependent. Rheumatology (Oxford). 2006; **45(10)**:1201 – 9.

Bondeson J, Wainwright SD, Lauder S, Amos N, Hughes CE. The role of synovial macrophages and macrophage produced cytokines in driving aggrecanases, matrix metalloproteinases and other destructive and inflammatory responses in osteoarthritis. Arthritis Res Ther. 2006; **8(6)**:R187.

Published Abstracts

Lauder SN, Carty SM, Carpenter CE, Hill R, Talamas F, Brennan P, Williams AS. Targeting NFκB modifies pathogenic processes in Osteoarthritis. Arthritis & Rheumatism 2006; **54(9)**:S78

Amos N, Lauder S, Evans A, Bondeson J. Adenoviral gene transfer into cells from diseased tissue as a tool to investigate the regulation of inflammatory and destructive mediators in the osteoarthritic synovium. Scandinavian Journal of Rheumatology 2005; **34(Suppl 120)**:S26

Table of Contents

Table of Figures

List of Tables

Abbreviations

Ab	Antibody
ACLT	Anterior Cruciate Ligament Transection
ADAM	a disintegrin and metalloprotease
ADAMTS	a disintegrin and metalloprotease with thrombospondin type I motif
AdV	Adenovirus
AIA	Antigen Induced Arthritis
BSA	Bovine Serum Albumin
CIA	Collagen Induced Arthritis
COMP	Cartilage Oligomeric Protein
D-MEM/F12	Dulbecco's Modified Eagle's Media
ELISA	Enzyme Linked Immunoabsorbent Assay
EMSAs	Electrophoretic Mobility Shift Assays
FCS	Fetal Calf Serum
GAG	Glycosaminoglycans
ICE	IL-1β converting enzyme
IGF-1	Insulin-Like Growth Factor-1
IKK	IkappaB Kinase
IL-	Interleukin-
IL-1RA	IL-1 specific Receptor Antagonist
LIF	Leukaemia Inhibitory Factor
MIA	Monosodium Iodoacetate
MMP	Matrix Metalloproteinase
MOI	Multiplicity of Infection
NBFS	Neutral Buffered Formalin Saline
NEMO	NFκB Essential Modifier
NFκB	Nuclear Factor-kappaB
NO	Nitric Oxide
OA	Osteoarthritis
OA-COCUL	OA CoCultures
OA-EXP	OA Explants
OA-SF	OA Synovial Fibroblasts
OSM	Oncostatin-M
PBS	Phosphate Buffered Saline
RA	Rheumatoid Arthritis
TACE	TNFα Cleavage Enzyme
TBS	Tris Buffered Saline
TGFβ	Transforming Growth Factor-beta
TIMP	Tissue Inhibitor of Metalloproteinase
TMB	Tetramethylbenzidine
TNFα	Tumour Necrosis Factor-alpha

CHAPTER ONE

General Introduction

1.1 The Joint.

With a critical role in skeletal function, the synovial joints of the body dissipate the mechanical stresses imposed upon them, allowing the joint to function correctly in a pain free manner. Synovial joints are comprised of 4 constituent connective tissues; articular cartilage, bone, synovium and the joint capsule, the importance of each will be discussed in detail (Figure 1.1).

Figure 1.1 The synovial joint.

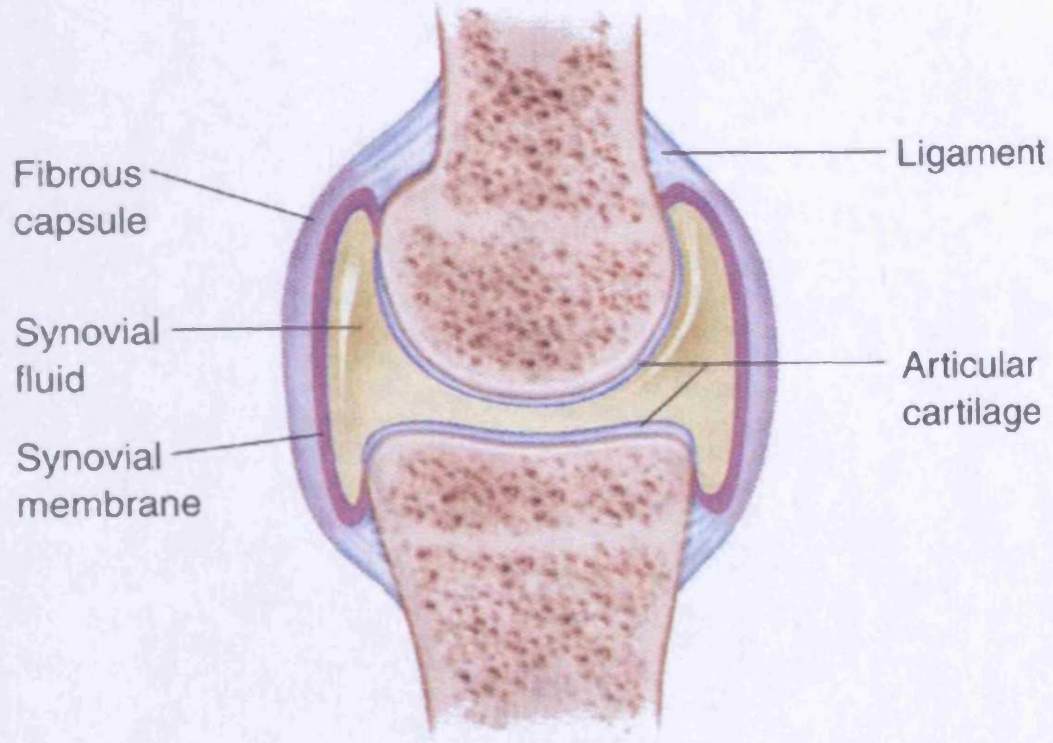

(Raven & Johnson., 1999)

1.1.1 Articular Cartilage.

William Hunter performed the first study into cartilage structure in 1743, today articular cartilage is still the most well studied of all the connective tissues within the joint (Benedek, 2006). An aneural, avascular tissue, the primary function of articular cartilage is to maintain skeletal shape and distribute loads effectively across the joint (Bora *et al.*, 1987). Due to its remarkable strength, cartilage provides an effective load bearing surface for decades, unless the composition of the tissue or the mechanics of the joint become damaged or altered.

Chondrocytes are the resident cell type present within articular cartilage. With a sparse distribution within the tissue they comprise around 2% of the total cartilage volume (Poole *et al.*, 2001). Chondrocytes have two distinct morphological forms; those at the joint surface have a flattened ellipsoidal appearance, whilst chondrocytes residing deeper within the tissue have a more rounded morphology (Archer *et al.*, 2003). Chondrocytes have a distinctive cellular structure, with each chondrocyte encased by a cavity known as the lacunae, which cytoplasmically isolates each cell. The pericellular rim surrounds the lacunae, the matrix of which is particularly rich in non-collagenous proteins and proteoglycans, but is notably lacking in collagen (Youn *et al.*, 2006) (Figure 1.2).

Articular cartilage is a highly organised tissue, displaying a zonal structural arrangement. The composition of the matrix of articular cartilage varies enormously between the different zones and in proximity to the chondrocytes. The territorial matrix, which immediately surrounds the lacunae of the chondrocyte, is comprised of collagen fibres that extend around the

chondrocytes, whilst the interterritorial matrix between chondrocytes consists of crosslinked collagen fibrils with large proteoglycan complexes interspersed in the interfibrillar spaces (Poole *et al.*, 1982) (Figure 1.3). The constituent matrix proteins of both regions are produced by the chondrocytes during neo-natal development and post-natal growth; in the adult the matrix proteins are actively maintained by the chondrocytes (Martin *et al.*, 2000).

The different zones of articular cartilage extend from the joint surface to the underlying subchondral bone (Figure 1.4). The uppermost layer, the superficial zone, faces the joint cavity, with discoidal chondrocytes orientating themselves parallel to the cartilage surface (Lorenz *et al.*, 2006). The interterritorial matrix in this zone comprises a fine mesh of collagen fibrils orientated parallel to the surface (Clark, 1990). The percentage of proteoglycan is much lower in the superficial zone than in any other zone. The intermediate and radial zones together comprise approximately 60% of the total thickness of cartilage and are situated directly beneath the superficial zone (Poole *et al.*, 2001). Chondrocytes often aggregate forming vertical clusters, referred to as chondrones, in the lower regions of the cartilage. A haphazard arrangement of large collagen fibrils with high proteoglycan content is typical of the interterritorial matrix of the intermediate and radial strata (Poole *et al.*, 2001). A thin layer of calcified cartilage connects the articular cartilage to the subchondral bone below. Due to their appearance chondrocytes located in this deep zone were initially believed to be necrotic, subsequent studies have demonstrated that the chondrocytes present are fully functional and metabolising (Aigner *et al.*, 2001; Marles *et al.*, 1991). Calcified cartilage was originally articular cartilage but as a result of juvenile growth the matrix in this zone was mineralised due to

the growth plate of the subchondral bone advancing. Further mineralisation of the articular cartilage is prevented once an individual reaches adulthood by the chondrocytes of the lower radial zone adjacent to the tidemark.

Cartilage proteins fall into two major classes; collagens and proteoglycans. A number of other matrix proteins are present in articular cartilage at much lower levels, although it is believed their role in cartilage destruction and OA pathology is not as great as that of collagens and proteoglycans.

Figure 1.2 The Chondrocyte.

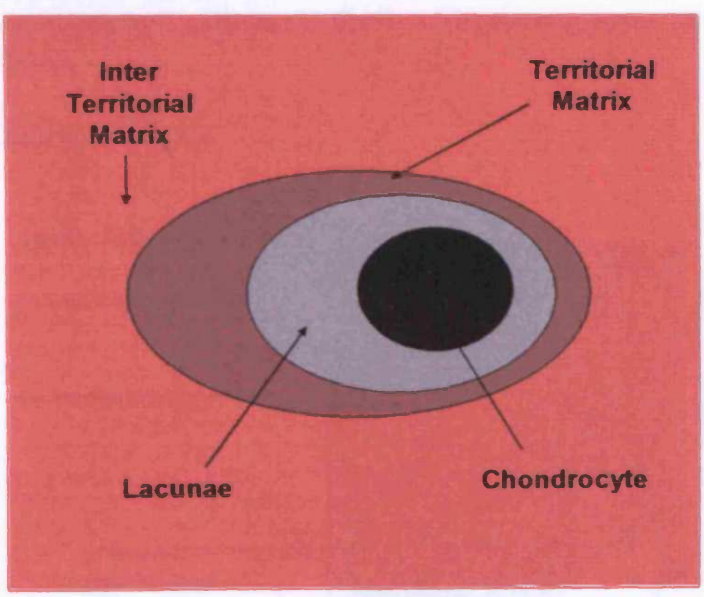

Schematic representation of an articular chondrocyte surrounded by interterritorial matrix.

Figure 1.3 Composition of the interterritorial matrix of articular cartilage.

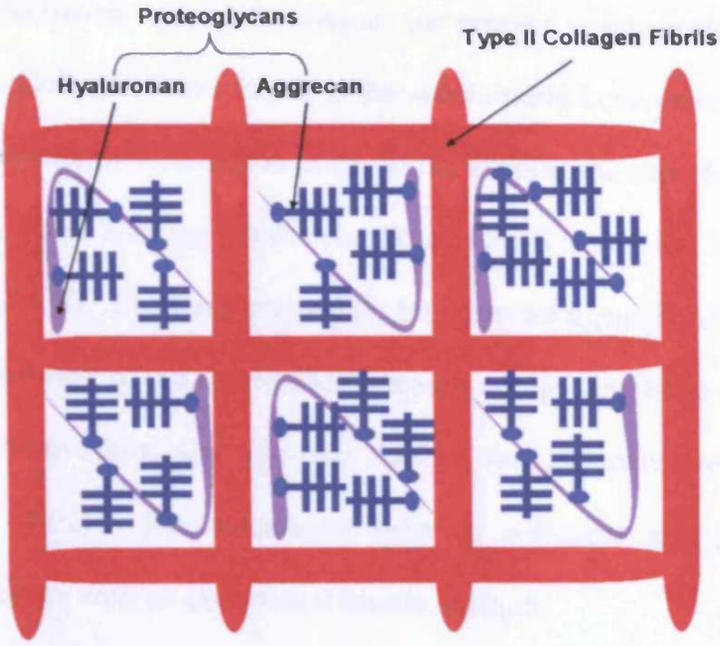

Simplified schematic of the interterritorial matrix of articular cartilage illustrating the crosslinked collagen II fibrils with proteoglycans interspersed between the fibres.

Figure 1.4 Cartilage Strata.

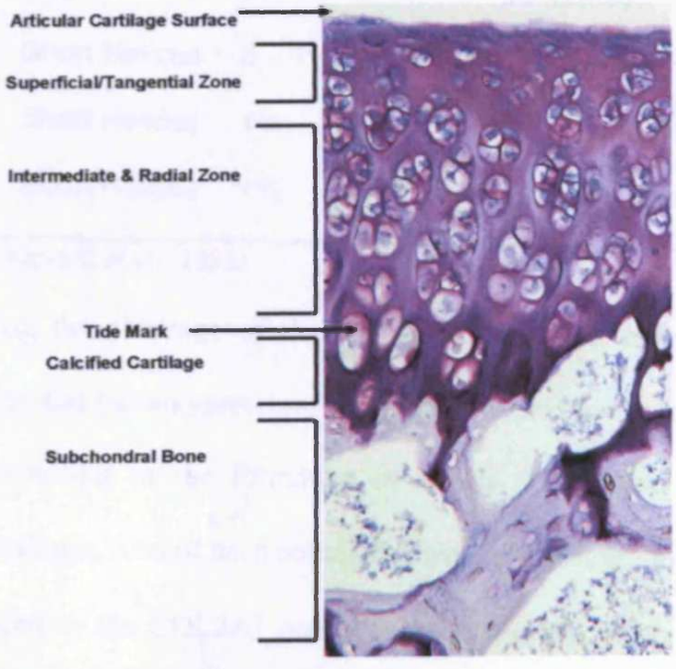

Histological section of articular cartilage, stained with Toluidine Blue. The different zones present are identified on the left hand side of the image.

1.1.1.1 Collagens.

Five different types of collagen are present within articular cartilage (Table 1.1). Collagen fibres attach to the subchondral bone extending upwards in a radial fashion, the orientation of the fibrils alters at the superficial zone with the collagen fibres running parallel to the surface forming the laminia propia (Eyre *et al.*, 2006). Covalent interactions between collagens II, IX and XI form the fibrillar network of the interterritorial matrix encapturing large proteoglycans such as aggrecan whilst also allowing smaller, less abundant proteoglycans to bind (Eyre, 2002). The association between collagens and proteoglycans provides cartilage with its exceptional tensile strength.

Table 1.1 Collagens of Articular Cartilage.

Collagen	Formation	Total Collagen (%)	Articular Cartilage Location
Type II	Fibril	95%	All Zones
Type XI	Fibril	3%	All Zones
Type VI	Short Helices	0 – 1%	Pericellular Zone
Type IX	Short Helices	1%	All Zones
Type X	Short Helices	1%	Calcified Zone

(*Adapted from Sandell *et al.*, 1992)

Following the cleavage of their N and C terminal extensions by the aminoproteinases and carboxyproteinases secreted by the chondrocytes, collagen II aggregates resulting in the formation of fibrils (Hollander *et al.*, 1994). Collagen II constitutes 90% of each collagen fibril, comprising three identical α_1 II chains produced by the COL2A1 gene. Together the chains combine to form the triple helix (Poole *et al.*, 2001). Collagen II fibrils vary enormously in

diameter dependent upon their location ranging from 20nm at the articular surface to >100nm in the deeper zones (Clarke, 1971).

Comprising 1% of the overall collagen content of adult cartilage, type IX collagen is a heterotrimer consisting of 3 triple helical domains; COL1, COL2 and COL3. Collagen type IX binds periodically in an antiparallel fashion to the surface of crosslinked collagen type II fibrils, where it is believed to play a role in fibril initiation (Aigner *et al.*, 2006; Buckwalter *et al.*, 1997; Mendler *et al.*, 1989; Wu *et al.*, 1995).

The normal turnover of collagens within healthy articular cartilage is regulated by the matrix metalloproteinase (MMP) family of enzymes, which are discussed in detail in section 1.3.10

1.1.1.2 Proteoglycans.

Located in the interfibrillar spaces proteoglycans have a hydrophilic role attracting water into the interterritorial matrix of articular cartilage (Pasternack *et al.*, 1974). Structurally, proteoglycans consist of a core protein backbone with branching glycosaminoglycans (GAG) chains (Roughley *et al.*, 1994). The constituent proteoglycan of articular cartilage is usually aggrecan, or the smaller proteins decorin and biglycan, whilst the GAG side chains are typically comprised of chondroitin sulfate, keratan sulfate and dermatan sulfate (Buckwalter *et al.*, 1997).

Aggrecan is the most abundant proteoglycan within articular cartilage, a large aggregating monomer, structurally composed of a 2000 amino acid core protein filament, with three globular domains G1, G2 and G3 (Dudhia, 2005). The 3 interglobular domains provide the attachment sites for keratan sulfate and chondroitin sulfate to bind to the protein backbone of aggrecan and form the

GAG side chains (Knudson *et al.*, 2001). The association of aggrecan with hyaluronic acid forms large proteoglycan aggregates, which stabilise the interterritorial matrix arrangement and enhance the tensile strength of collagen (see Figure 1.3) (Buckwalter *et al.*, 1994).

Like collagen, the turnover of proteoglycans in healthy cartilage is tightly regulated. Two members of the a disintegrin and metalloproteinases with thrombospondin type I motifs (ADAMTS) family, the aggrecanases, in combination with MMPs, are responsible for the regulation of proteoglycans in articular cartilage (Nagase *et al.*, 2003). The aggrecanase members of the ADAMTS family are discussed in detail in section 1.3.11

1.1.2 Subchondral bone.

In a healthy joint the subchondral bone, in association with the articular cartilage, transmits mechanical loading forces through the joint (Eckstein *et al.*, 1998; Eckstein *et al.*, 1992). The subchondral bone lies directly beneath the calcified zone of articular cartilage, with the subchondral growth plate extending from the tidemark of articular cartilage to the bone marrow below. A highly vascular tissue, subchondral bone has the ability to remodel and repair in the event of damage occurring (Clark, 1990). As a viscoelastic tissue, subchondral bone acts as a shock absorber for the overlying articular cartilage and protects the cartilage from damage that could be induced by excessive loads (Radin *et al.*, 1970).

1.1.3 Synovium.

The synovial membrane of the joint is composed of three constituent tissue types; adipose, fibrous and areolar tissue. The aggregation of adipocytes (fat cells) results in the formation of adipose tissue whilst fibrous tissue, as the

name suggests, is composed of a collection of protein fibrils of fibrin, collagen, elastin and keratin (Wysocki *et al.*, 1972). Areolar tissue contains fibroblasts and macrophages encased in a matrix of collagen and elastin fibrils with glycoproteins and proteoglycans densely embedded in the spaces between fibrils (Slack, 1959).

The synovial membrane has three definable layers; the intimal layer, vascular net and subintimal layer (Figure 1.5). The intimal layer of the synovial membrane faces the joint space cavity and is very thin, typically only 2 or 3 cells deep (Roy, 1967). The major cell types present within the intimal layer are the synoviocytes, type A macrophages and type B fibroblasts (Iwanaga *et al.*, 2000). Initimal layer synoviocytes are highly metabolically active secreting hyaluronic acid and other synovial fluid proteins, which lubricates the cartilage allowing correct joint functioning (Iwanaga *et al.*, 2000; Revell *et al.*, 1995). The presence of adipocytes in the intimal layer varies between individuals, with mast cells, leukocytes, and T & B lymphocytes present in very small numbers, typically during inflammatory periods (Smith *et al.*, 2003).

Directly beneath the intimal layer the vascular net is situated. It is responsible for supplying the synovium with blood and has a significant role in promoting synovial inflammation through the circulatory recruitment of leukocytes to the intimal layer (Revell *et al.*,1988).

The subintimal layer is composed of a relatively unspecialized tissue type that provides structural support to the intimal layer and vascular net above (Edwards, 2000). It provides a reservoir of fibroblasts to replace those present within the intimal layer. During inflammation leukocytes are also recruited to

the subinitimal layer via the circulation, forming a local source of macrophages that can migrate to the initimal layer when required.

Figure 1.5 Synovial Membrane Structure.

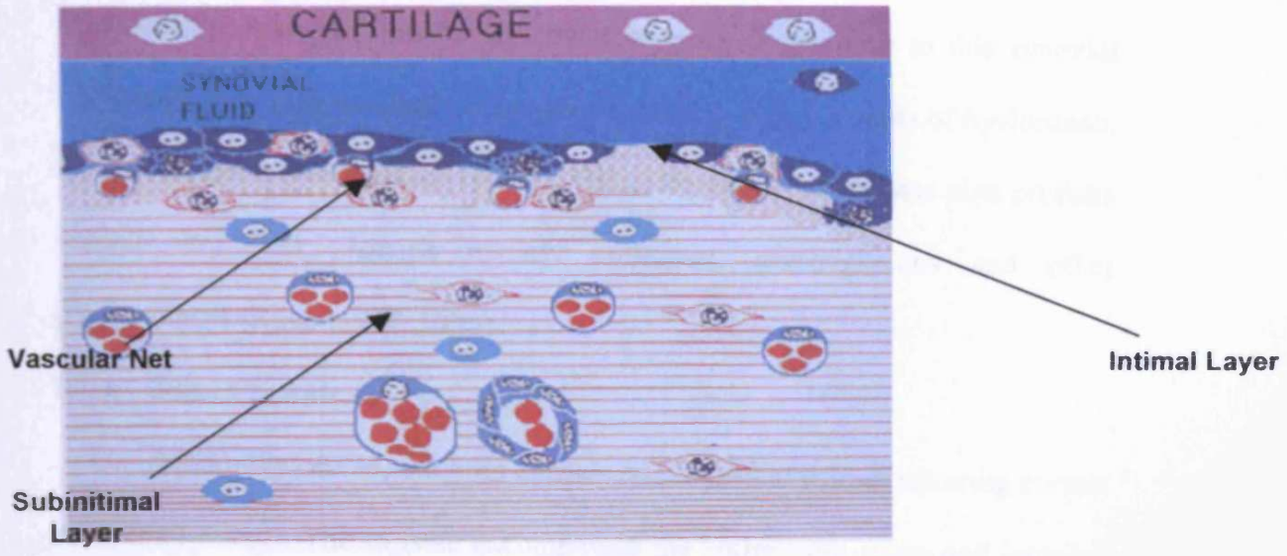

Schematic representation of the synovial membrane, illustrating the different zones present within the membrane. (Edwards, 2000).

1.1.3.1 Macrophages.

Historically referred to as type A cells, synovial macrophages are derived from a population of bone marrow derived monocytes recruited to the synovium via the circulation. As antigen presenting immune cells, macrophages are a member of the leukocyte family, involved in both adaptive and innate immune response (Adrem *et al.*, 1999; Sasmono *et al.*, 2004). A critical function of macrophage immune response is the phagocytosis of foreign bodies, synovial macrophages in the intimal layer are responsible for clearing any foreign 'debris' from the synovial fluid.

1.1.3.2 Fibroblasts.

Type B synoviocytes or synovial fibroblasts as they are typically known, constitute approximately 90% of all the cells present within the synovial membrane. With a unique morphology fibroblasts are easily recognisable by their distinctive branched cytoplasm and single nucleus. The role of fibroblasts in connective tissues is one of structural support, in addition to this synovial fibroblasts have a specialised phenotype producing large amounts of hyaluronan, a vital component of healthy synovial fluid. Synovial fibroblasts also produce several structural proteins namely collagens, proteoglycans and other glycoproteins (Revell *et al.*,1995).

1.1.4 Joint Capsule.

Often overlooked, the joint capsule has a critical role in ensuring correct joint functioning. The capsule encompasses the entire joint space and includes the tendons and ligaments of the joint. Surrounding the synovial membrane, the capsule is comprised of a dense fibrous connective tissue composed of collagen fibres that attach to the adjacent bone (Ralphs *et al.*, 1994). The tendons and ligaments of the capsule are especially important providing the joint with mechanical stability.

1.2 Osteoarthritis (OA).

Globally the most prevalent musculoskeletal condition, OA is a disorder of the synovial joints that is characterised by the loss of articular cartilage, combined with a degree of synovial inflammation and subchondral bone remodelling. The etiology, pathology, mechanical, biochemical and clinical presentation of OA will be discussed in detail.

1.2.1 Historical Perspective.

The term OA was first employed during the 19th century, to describe arthritic joint changes. In 1890 Garrod listed OA as an interchangeable term for rheumatoid arthritis (RA) leading to confusion as to whether the two diseases were one and the same at this time (Benedek, 1999). By the early 20th century it was evident that 'arthritis' was not a single disease and in reality encompassed a number of conditions, each unique in terms of pathology and disease outcome. A number of individuals, including Merrins (1903), Goldthwait (1904), and Nichols & Richardson (1909) employed the term 'osteoarthritis' to accurately describe degenerative joint changes. At this time OA was considered to be a consequence of ageing, with simple wear and tear processes driving the characteristic joint destruction. This perspective of OA continued for several decades, until Ehrlichs' pioneering study in the 1970's led to a shift in perception.

In 1975 Ehrlich provided evidence that cohorts of OA patients experienced an acute inflammatory episode at disease onset (Ehrlich, 1975). Consequently it is now postulated that OA as a disease lies somewhere between the degenerative joint changes, classically observed with old age, and the highly inflammatory, autoimmune disease RA. OA is currently defined by the American College of Rheumatology as a *"heterogeneous group of conditions that leads to joint symptoms and signs which are associated with defective integrity of articular cartilage, in addition to related changes in the underlying bone at joint margins"* (Altman *et al.*, 1986).

Historically much of the research conducted in OA has focused on understanding the destructive processes that occur in the articular cartilage, it is now speculated that to fully elucidate the pathogenic mechanisms that drive OA,

all aspects of the joint need to be studied in unison, with particular focus upon the cartilage, bone and synovium.

1.2.2 The Osteoarthritic Joint.

OA is initiated primarily by damage or alterations to the articular cartilage integrity, with disease progression each of the constitutive joint tissues becomes involved and plays an intrinsic role in OA pathology. Figure 1.6 depicts the key changes observed in an osteoarthritic joint. The changes that occur to each tissue during OA pathology will be discussed in detail.

Figure 1.6 Schematic of pathological changes in the osteoarthritic joint.

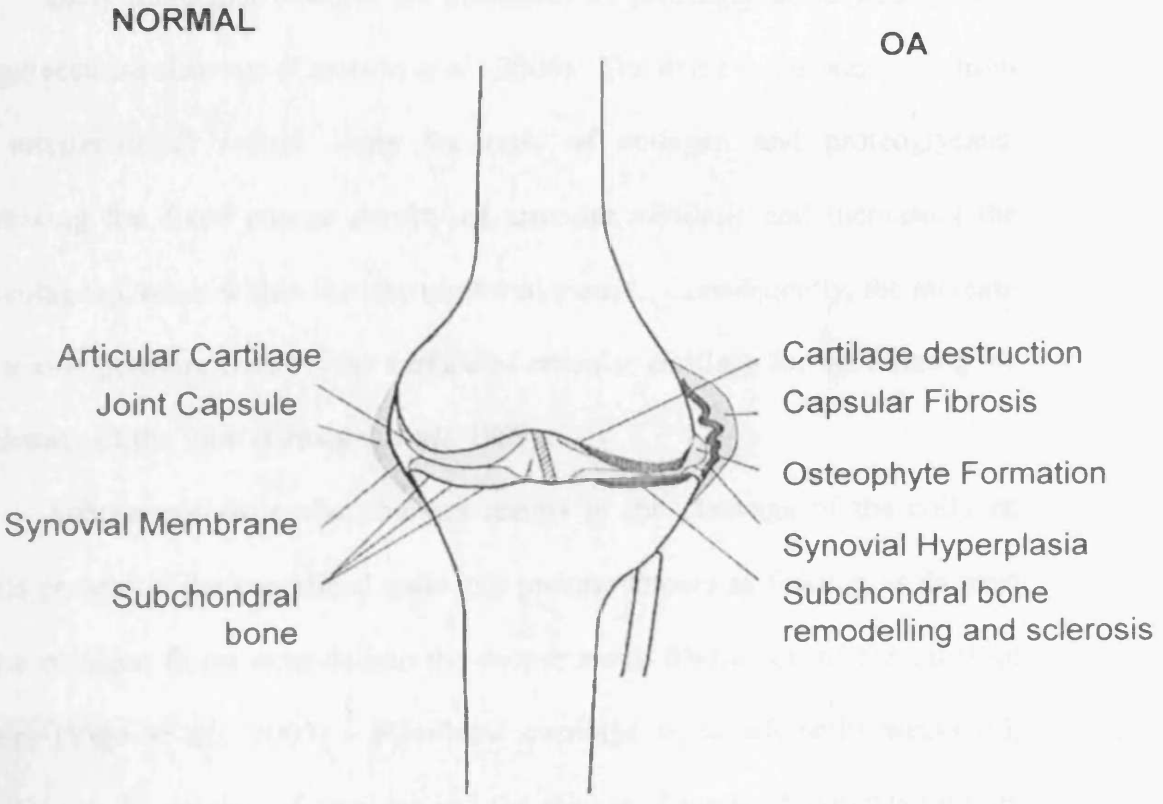

The four main connective tissues of a healthy articular joint are compared on the left hand side, with the major pathological changes that occur in an osteoarthritic joint on the right hand side. Each pathological change in the constituent tissues will be discussed. (Adapted from Aigner *et al.*, 2006).

1.2.2.1 Osteoarthritic Articular Cartilage.

Initial osteoarthritic changes typically represent some degree of roughening of the cartilage, followed by fibrillation of the surface zone and the formation of lesions (Bullough, 2004). Chondrocytes attempt to repair the damage by increasing their anabolic activity resulting in the formation of 'repair fibrous cartilaginous' tissue (fibrocartilage) which is produced as a result of the chondrocytes ability to upregulate collagen II production but not aggrecan (Eyre, 1980; Mankin, 1981). Unfortunately fibrocartilage does not possess the tensile strength of natural articular cartilage and consequently is unable to withstand the same degree of mechanical loading, thus degradation continues.

Early molecular changes are illustrated by proteoglycan loss as a result of aggrecanase cleavage (Caterson *et al.*, 2000). The depletion of aggrecan from the interterritorial matrix alters the ratio of collagen and proteoglycans, decreasing the fixed charge density of articular cartilage and increasing the percentage of water within the interterritorial matrix. Consequently, the increase in osmotic pressure contorts the surface of articular cartilage further altering the mechanics of the joint (Grushko *et al.*, 1989).

Subsequent molecular changes results in the cleavage of the collagen fibrils present in the superficial zone in a process known as flaking; as damage to the collagen fibres extends into the deeper zones fibrillation of the cartilage occurs (Veje *et al.*, 2003). Fibrillated cartilage is significantly weakened, resulting in the erosion of cartilage and the release of matrix fragments into the joint space. The erosion can be so severe that during the latter stages of OA the underlying subchondral bone is often exposed (Pfander *et al.*, 1999). The molecular changes in proteoglycan and collagen content that result in cartilage

degeneration are attributable to the action of a range of specific proteolytic enzymes, the mode of action and effect of these mediators will be discussed in detail in 1.3.10 & 1.3.11

1.2.2.2 Osteoarthritic Suchondral Bone Changes.

It has been demonstrated that alterations in the density and structure of the subchondral bone has a profound effect in both the initiation of cartilage destruction and subsequent cartilage loss (Bobinac *et al.*, 2003). Currently it remains unclear whether damage occurring to the articular cartilage or subchondral bone is initially responsible for osteoarthritic changes. At present two schools of thought exist, either;

1) As a result of cartilage erosion, the subchondral bone stiffens due to sclerosis which further enhances the rate of articular cartilage destruction (Vellet *et al.*, 1991),

OR

2) Microfractures in the trabecular bone that heal become stiffer and consequently the bone no longer has the same shock absorbing capacity. As a result, altered stresses and mechanical forces exist within the joint, leading to cartilage erosion (Lajeunesse, 2004; Lindau *et al.*, 2003).

Two separate studies conducted in a spontaneous guinea pig model of OA have demonstrated that subchondral bone remodelling occurs prior to any gross histopathological change within the articular cartilage (Anderson-McKenzie *et al.*, 2005 ; Quashnickia *et al.*,). It remains to be seen if this effect occurs in OA patients. Extensive bone remodelling occurs during the latter stages of the disease, with the areas where bone changes are greatest correlating with the areas where the greatest cartilage destruction is evident. Eburnated

bone is often apparent in patients with severe OA at end stage (Wieland *et al.*, 2005). The formation of osteophytes, bony outgrowths produced by the remodelling subchondral bone, are typically associated with OA progression and are an attempt to restabilise the joint. It is suggested that the presence of osteophytes correlates with the rate of cartilage destruction (van Osch *et al.*, 1996). Consequently subchondral bone remodelling is a useful prediction of the severity of OA pathology, although the processes occurring within the subchondral bone during OA still remain to be fully elucidated.

1.2.2.3 Osteoarthritic Synovial Membrane Changes.

In contrast to the historical perception of OA, synovial inflammation has been demonstrated in both early and late stages of the disease (Benito, 2005; Lindblad *et al.*, 1987). Cartilage destruction and the subsequent release of matrix fragments into the joint space, is speculated to result in synovial hypertrophy and hyperplasia (Athanasou, 1991; Edwards, 1982). In some patients the release of fragments from the cartilage surface can result in shards of cartilage becoming embedded within the synovial membrane and eliciting a highly inflammatory response locally (Revell, 1988). During inflammatory periods it has been demonstrated that the intimal layer increases in thickness to a depth of 5 - 6 cells (Smith, 1992). Several studies have demonstrated that inflammation within the joint is not uniform and is typically localised in the synovial membrane adjacent to cartilage lesions and areas of erosion (Lindblad, 1987).

Synovial macrophages are believed to play a critical role in inducing and maintaining synovial inflammation due to their ability to secrete IL-1β and TNFα. The release of such highly inflammatory cytokines within the synovial

membrane results in the upregulation of an array of cytokines, chemokines, MMPs and other inflammatory mediators that perpetuate the inflammatory response within the synovium.

1.2.2.4 Osteoarthritic Joint Capsule Changes.

Damage to the tendons and ligaments of the joint capsule can result in an alteration of the mechanics of the joint, which can severely impair joint functioning and enhance the pathogenic processes associated with OA (Sharma *et al.*, 1999; von Porat *et al* 2004). In the larger weight bearing joints of the body, ligament laxity can be a significant contributing factor in accelerating disease progression (Roos *et al.*, 1995). In the latter stages of OA, capsular fibrosis typically occurs as a consequence of thickening of the collagen fibres, resulting in increased stiffness of the affected joint and reduced motion (Ralphs *et al.*, 1994).

1.2.3 Clinical Presentation.

As the 8th most frequent cause of disability globally, OA is the most prevalent rheumatic condition seen clinically (Birchfield, 2001). Patients with OA initially seek clinical advice due to the increasing pain associated with the osteoarthritic joint. Typically a diagnosis of OA is made based upon the patient's history, the symptoms described and a physical examination of the joint, in combination with radiographic evidence, such as joint space narrowing or bone remodelling. Patients with OA routinely present with a number of common symptoms and signs of the disease, these are outlined in Table 1.2.

OA can affect any joint within the body, but is particularly prevalent in the peripheral joints, namely the interphalangeal joints of the hands particularly the distal and proximal joints, and the large weight bearing joints such as the

knees and hips. OA can take a monoarticular form, whereby a single joint is affected or a polyarticular form involving several joints (Arden *et al.*, 2006). Typically OA primarily affects a single joint with subsequent involvement of secondary joints, this is particularly prevalent in the larger weight bearing joints such as the knees and hips, as a consequence of the contralateral joint compensating for the osteoarthritic joint. This typically results in altered mechanical loading which can, over a period of time, initiate the disease within the healthy joint.

During the course of this study, synovial samples taken from end stage patients undergoing either hip or knee replacement surgery have been utilised, consequently only OA affecting the hip and knee joints are discussed in detail in this thesis.

Table 1.2 Signs & Symptoms of OA.

Symptoms	Signs
Pain	Altered Gait
Stiffness	Tenderness
Swelling	Enlargement
Altered function	Crepitus
Weakness	Limitation of Motion
Grinding or Clicking	Deformity
Instability	

* Adapted from Altman *et al.*, 2003

1.2.3.1 Hip OA.

Marginally more prevalent in males than females, OA of the hip typically arises during the 5th and 6th decade of a patient's life (Kellgren *et al.*,

1958). Hip OA demonstrates the best correlation between the symptoms described by the patient and radiographic changes. Often the disease affects both joints and a primary diagnosis of OA in one hip increases the probability of secondary OA developing in the other hip (Cooper *et al.*, 1996). Cartilage destruction of the femoral head of an osteoarthritic hip is more common in the superior plane than the medial or axial plane, although superomedial and medial-axial patterns are more common in women than men, which maybe a consequence of altered joint loading in the female form (See Figure 1.7).

The pain associated with hip OA is not solely confined to the hip socket, it is typical for an individual to experience pain throughout the tibia and femur of the affected leg (Moskowitz *et al.*, 2001). In such cases the hip is not initially suspected as the cause of the pain, it is often believed to originate from the knee joint. During early OA pain usually results from the patient using the hip joint for a length of time, for example after a period of walking. As the disease progresses pain can occur at any time and is particularly problematic during periods of rest and during sleep when the joint is immobilised. Stiffness is a common symptom of an osteoarthritic hip and can make it difficult for an individual to complete even simple tasks as movement within the joint is often severely restricted (Moskowitz *et al.*, 2001).

Figure 1.7 Structure of the hip joint.

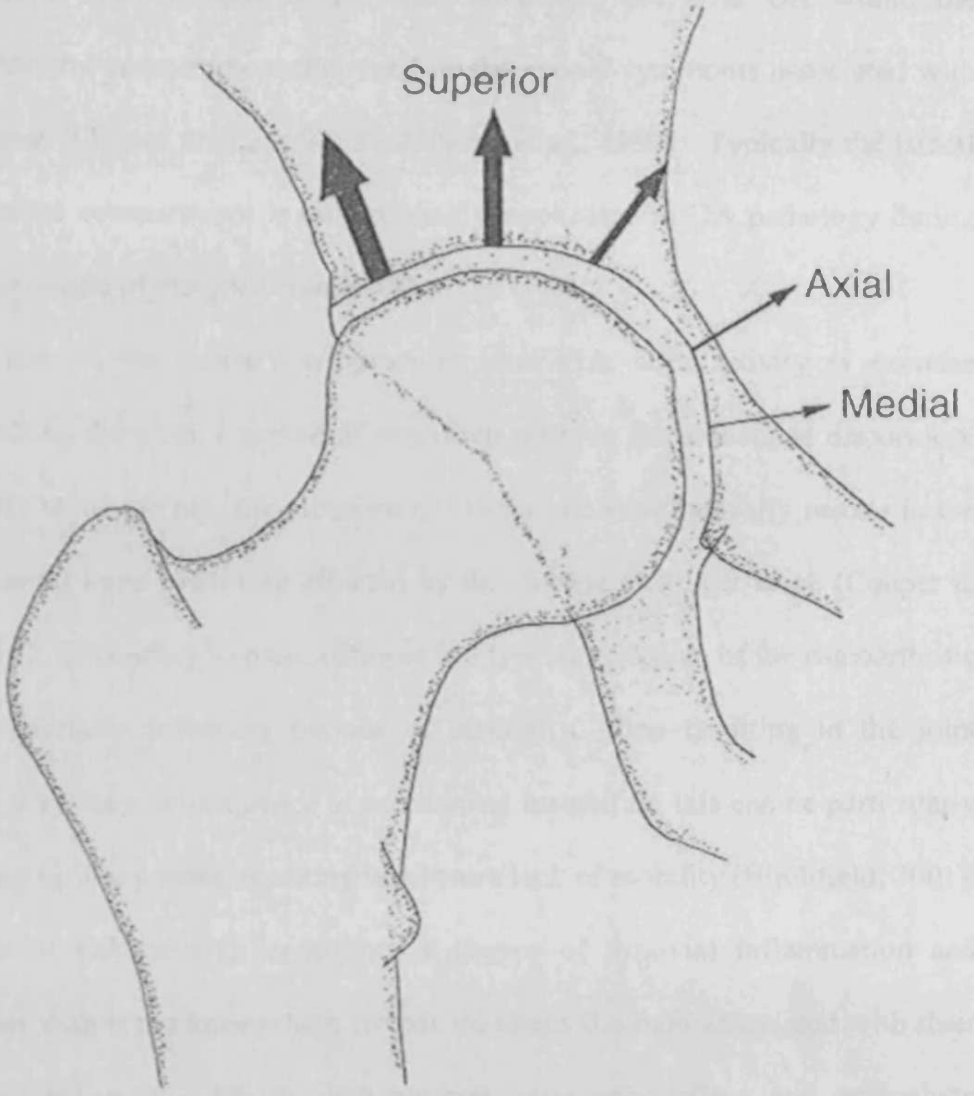

Schematic of the femoral head of the hip joint, demonstrating the planes of cartilage destruction (O'Reilly *et al.*, 2000).

1.2.3.2 Knee OA.

As the largest weight bearing joint of the body, OA of the knee is highly common, and is particularly prevalent both in women and obese patients (Petersson *et al.*, 2002). The knee is a complex structure comprised of 3 major compartments; the medial tibiofemoral, lateral tibiofemoral and the patellofemoral as illustrated in Figure 1.8 (Last, 1948). OA can affect any of

these compartments either individually or in combination. OA of the medial tibiofemoral compartment is the most prevalent, but it is OA within the patellofemoral compartment that exhibits the classic symptoms associated with the disease (Cooper *et al.*, 1992; McAlindon *et al.*, 1992). Typically the lateral tibiofemoral compartment is only routinely implicated in OA pathology during the latter stages of disease (Figure 1.8).

Pain is the primary symptom of knee OA, with activity or exercise exacerbating the pain, a period of rest often relieves the associated discomfort. As with OA of the hip, the presence of OA in one knee typically results in the contralateral knee becoming affected by the disease at a later stage (Cooper *et al.*, 1996). Secondary to pain, stiffness is a typical symptom of the osteoarthritic knee, especially following periods of inactivity, often resulting in the joint 'giving way' as a consequence of mechanical instability, this can be particularly disabling for the patient, resulting in a severe lack of mobility (Birchfield, 2001). Cohorts of OA patients experience a degree of synovial inflammation and effusions within the knee which further increases the pain associated with their disease (Hill *et al.*, 2001). Subchondral bone remodelling and osteophyte formation are common in knee OA and such joint modifications are believed to be a source of pain during the latter stages.

Figure 1.8 Compartmentalisation of the knee joint.

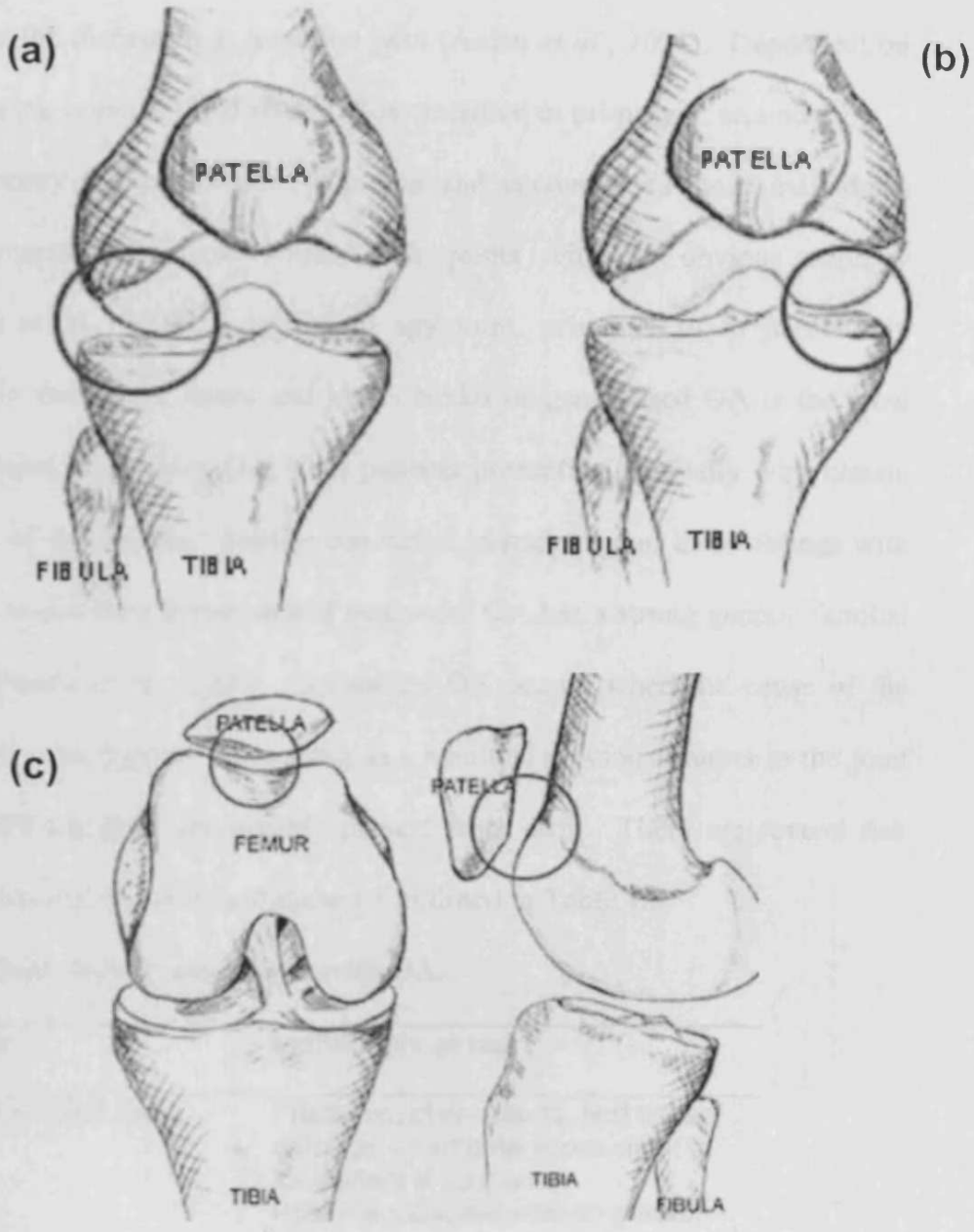

Schematic representation of the three compartments, lateral (a), medial (b) and patello-femoral (c) compartments affected by OA in the human knee joint (www.kneeguru.co.uk)

1.2.4 OA classification.

OA is a disease associated with increasing age, the disease is rare in individuals under 30, whilst in the 80+ population 80% of individuals are affected by the disease in at least one joint (Arden *et al.*, 2006). Dependent on the underlying cause of the disease OA is classified as primary or secondary.

Primary OA is the more common and encompasses those individuals with degenerative changes within their joints with no obvious etiology (Hochberg *et al.*, 2003). Arising in any joint, primary OA is particularly prevalent in the hands, knees and hips. Nodal or generalised OA is the most common form of primary OA, with patients presenting clinically with classic symptoms of the disease. Studies conducted in patients and their siblings with heberdens nodes have demonstrated that nodal OA has a strong genetic familial link (Irlenbusch *et al.*, 2006). Secondary OA occurs when the cause of the disease is known, typically occurring as a result of previous trauma to the joint or an underlying joint abnormality present from birth. There are several risk factors associated with OA and these are outlined in Table 1.3

Table 1.3 Risk factors associated with OA.

Risk factor	Individuals at risk
Previous Joint Trauma	Fractures, dislocations, soft tissue damage – particularly prevalent in footballers & runners
Sex	Post-menopausal women greater risk than men – joint specific
Body Mass Index (BMI)	Obesity increases risk of OA by 4 x for women & 4.8 x for men
Genetic Factors	Genetic link of Heberden Nodes, a number of candidate genes implicated in OA pathology
Bone Density	Link between high bone density and OA
Occupational factors	Typically farmers, carpenters & floor layers, footballers etc

1.3 Cytokines, Chemokines & Matrix Metalloproteinases.

Cytokines and chemokines are intercellular messengers released by cells as a result of specific signals, exerting a specific response on either an adjacent paracrine target or an autocrine target. A single cytokine can elicit both a positive and negative effect dependent upon its cellular target. Typically cytokine signalling mediates a relatively local effect but they can in some circumstances elicit a distant endocrine effect. The matrix metalloproteinases (MMPs) are a family of enzymes responsible for tissue remodelling within the body.

Within the healthy joint a balance of cytokines, chemokines and MMPs are known to be responsible for maintaining normal physiology and joint function. However, an imbalance of anabolic cytokines (those mediators responsible for the synthesis of articular cartilage matrix) and catabolic mediators (those mediators responsible for the destruction of the interterritorial matrix of articular cartilage) results in the classic osteoarthritic changes within the joint (Pelletier *et al.*, 1993).

Cytokines and other mediators present within the joint are derived from either the chondrocytes of the articular cartilage, or the macrophages and fibroblasts of the synovium. Both chondrocytes and macrophages express a very similar cytokine profile. In the healthy joint cartilage homeostasis is achieved by the chondrocytes maintaining a balance between catabolic IL-1β and TNFα and the anabolic mediators present (Goldring *et al.*, 2004). Only once cartilage destruction has been initiated do activated macrophages become a significant source of catabolic cytokines.

At disease onset the homeostatic balance between anabolism and catabolism shifts in favour of the latter and cartilage destruction proceeds. The disease initiating event or factor that results in a shift to catabolism is largely unknown. Following the initiation of cartilage destruction the chondrocytes will initially make an attempt to repair the damaged cartilage as described in 1.2.2.1. During the latter stages of OA cytokines derived from the synovial membrane are believed to be instrumental in promoting cartilage destruction within the joint (See Figure 1.9).

Two critical cytokines have been implicated in the pathology of an array of arthritic conditions; IL-1β and TNFα. In RA it is thought that TNFα drives the IL-1β induced cartilage destruction and consequently is the predominant cytokine in RA pathology (van den Berg, 1999). In OA it is speculated that the process is different, with both IL-1β and TNFα acting independently of each other. IL-1β is speculated to initiate and promote cartilage destruction within the joint whilst also playing a significant role in inflammation, whilst TNFα is postulated to play the major role in the inflammatory processes of the synovium (Caron *et al.*, 1996; van de Loo *et al.*, 1995; van den Berg *et al* 2001).

Fig 1.9 Phases of joint destruction.

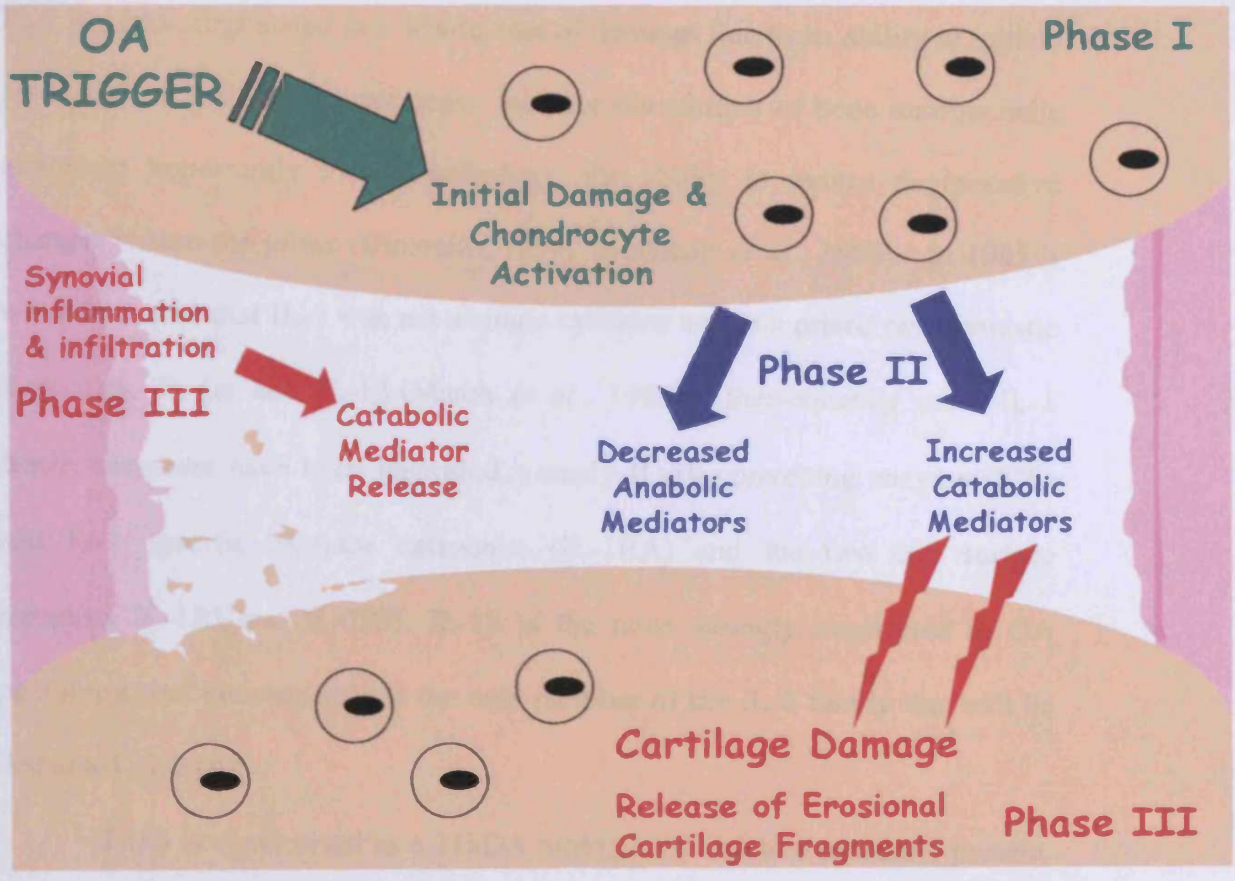

Schematic representation of the three pathological phases of OA (Adapted from van den Berg *et al.*, 2000)

1.3.1 The Interleukin(IL)-1 family.

First identified as a pro-inflammatory cytokine during the late 1970's, IL-1 has been implicated in a whole host of diseases due to its ability to initiate fever, induce lymphocyte responses, increase the number of bone marrow cells and most importantly to OA pathology, the ability to induce degenerative changes within the joints (Dinarello, 1994; Westacott *et al.*, 1996). In 1985 it was discovered that IL-1 was not a single cytokine and comprised two agonistic molecules, IL-1α and IL-1β (March *et al.*, 1985). Subsequently other IL-1 family members have been identified, namely IL-1β converting enzyme (ICE) and IL-1 specific receptor antagonist (IL-1RA) and the two cell surface receptors IL-1RI and IL-1RII. IL-1β is the most strongly implicated in OA pathology, and consequently is the only member of the IL-1 family that will be discussed in detail.

IL-1β is synthesised as a 31kDA biologically inactive precursor protein, pro-IL-1β, which is cytosolically located (Dinarello, 1994). Activation of biologically active IL-1β requires peptide cleavage by ICE (Black *et al.*, 1988). ICE itself is initially produced as an inactive molecule requiring cleavage to become enzymatically active. The active ICE heterodimer forms a tetramer with 2 molecules of pro-IL-1β and cleaves pro-IL-1β at the aspartic acid residue at position 116 yielding a 17kDA biologically active peptide; IL-1β. Active IL-1β is comprised of 14 β strands (Preistle *et al.*, 1989) that combine forming β sheets. Trypsin, elastase, granzyme A and chymotrypsin can also enzymatically cleave pro-IL-1β to release active IL-1β.

IL-1β signalling is a highly amplified and efficient process, with only 5% of receptors requiring occupation for IL-1β to elicit a biological response

(Dinarello, 1994). Signalling is initiated by IL-1β forming a heterodimer complex between itself, the IL-1 receptor, and the IL-1β receptor accessory protein (Dinarello, 1996). IL-1RA acts as the natural inhibitor of this process, mimicking the action of IL-1β by binding to the IL-1 receptor, upon binding no biological response is elicited and IL-1β itself is prevented from binding (Arend *et al.*, 1998). IL-1β gene expression is a transient effect, upon stimulation IL-1β is typically present within 15 – 30 minutes and after 4 hours the levels begin to subside (Fenton *et al.*, 1988). Although IL-1β gene expression induced by IL-1 itself, can last for 24 hours or more. Typical IL-1β inducers include stress factors such as UV, inflammatory substances such as C reactive protein (CRP) and urate crystals, phorbol esters, and other cytokines such as TNFα. Of the most importance to OA pathology, is the induction of IL-1β by cell matrix factors such as fibronectin and collagen (Dinarello, 1996).

Whilst IL-1β plays a critical role in maintaining cellular response and function, the margin between normal physiology and damaging destructive responses is very narrow (Dinarello, 1996). In the osteoarthritic joint IL-1β is postulated to have a dual role inducing both matrix protein synthesis and the enzymes associated with cartilage destruction. It has been demonstrated that both IL-1α and IL-1β are produced by the chondrocytes with those cells in the superficial zone predominating in IL-1β production (Ollieverre *et al.*, 1986; Pelletier *et al.*, 1989). IL-1β induces collagen type I and III, but represses collagen type II and IX production (Goldring *et al.*, 1988). In the context of OA the elevated levels of IL-1β result in the collagen type I and III produced aggregating to form fibrous cartilage as an attempted repair mechanism.

Elevation of IL-1β in the joint results in upregulation of MMPs within the joint, enhancing the destructive environment.

Increased numbers of IL-1 receptors are found on the surface of OA chondrocytes and synovial cells when compared with the same cell types in a normal joint. Hence, IL-1β elicits a greater effect in OA than healthy joints as demonstrated by the upregulation of MMPs and other cytokines (Martel-Pelletier *et al.*, 1992; Sadouk *et al.*, 1995). It has been postulated that IL-1RA could be clinically beneficial in OA patients in preventing the destructive effects that IL-1β induces. Locally the levels of IL-1RA are not great enough to inhibit the action of IL-1β, however it is speculated that a 100 fold excess of IL-1RA within the joint would eliminate the effect of IL-1β altogether (Pelletier *et al.*, 2001).

1.3.2 Tumour Necrosis Factor-alpha (TNFα).

In 1975 TNFα was first discovered as a protein capable of causing the necrotic repression of tumours (Carswell *et al.*, 1975). Subsequently it was demonstrated that this effect was tumour specific and that TNFα had a broader role and was implicated in a number of disease processes as well as apoptosis. TNFα has an intrinsic role in both acute inflammation such as the response seen in septic shock, and in chronic inflammation typical of RA and psoriatic arthritis (Warren, 1990).

First isolated in 1984 from activated macrophages, TNFα is typically produced by macrophages and monocytes, although T and B lymphocytes and neutrophils are amongst the other cell types known to secrete the cytokine (Fiers, 1991). Structurally TNFα is a trimeric cone shaped peptide that can be either membrane bound or soluble (Jones, 1989). Each monomer of the TNFα

trimer is comprised of β-pleated sheets orientated into a 'jelly-roll' like formation (Porter, 1990). Initially TNFα is produced as a membrane bound 157 amino acid precursor molecule with a molecular weight of 26kDa (Idriss, 2000). TNFα cleavage enzyme (TACE) (also known as ADAM-17) is responsible for the proteolytic cleavage of membrane inactive TNFα releasing the 17kDa active form (Black, 2002). TNF receptor 1 (TNFRI, p55) a 55kDA receptor and TNF receptor 2 (TNFRII, p75) a 75 kDa receptor, are the two cell membrane receptors through which TNFα elicits its biological effects.

In OA, the exact role of TNFα within the joint remains to be fully elucidated. Elevated levels of TNFRI upon the surface of chondrocytes within the osteoarthritic joint indicated a role for TNFα in cartilage destruction (Westacott *et al.*, 1994). Increased numbers of TNFRI have also been demonstrated on synovial fibroblasts (Alaaeddine *et al.*, 1997). Consequently in OA, TNFα has been speculated to drive synovial inflammation within the joint, with a secondary role demonstrated in cartilage destruction.

Of the two inflammatory cytokines; IL-1β and TNFα, it would appear that IL-1β is the driving force behind OA pathology, with TNFα involved to a lesser extent.

1.3.3 IL-6.

The exact physiological role of IL-6 in OA is unclear. Associated with immune response and a whole host of disease processes, IL-6 is believed to play an inflammatory role as demonstrated in murine models of RA (de Hooge *et al.*, 2000; Takagi *et al.*, 1998). In contradiction to this study, IL-6 exhibited an anti-inflammatory role in studies involving TNFα induced leukaemic cells (Aderka *et al.*, 1993). Produced by a vast array of cell types, including macrophages and

fibroblasts, it would appear that IL-6 can play either an inflammatory or anti-inflammatory role (Wong *et al.*, 2003).

First cloned in 1986, the glycoprotein IL-6 is known to be a 184 amino acid peptide with a molecular weight range of 23kDA to 32kDA (Santham *et al.*, 1989). The IL-6 signalling cascade is a complicated pathway, with IL-6 signalling via a cell surface receptor or through the association of IL-6 and soluble IL-6 receptor complex in a process known as trans signalling (Kallen, 2002). The IL-6 receptor is typically expressed by macrophages, neutrophils and certain cohorts of lymphocytes, whilst the signal-transducing membrane protein, gp130, which allows transsignalling, is expressed by almost all cells (Desgeorges *et al.*, 1997).

The aforementioned inflammatory cytokines, IL-1β and TNFα, are known to induce the production of IL-6, and elevated levels of the cytokine have been demonstrated in OA joints (Venn *et al.*, 1993). The inflammatory and anti-inflammatory properties exhibited by IL-6, appears to provide it with a dual role in OA pathology. IL-6 elicits an anabolic role within the joint through its induction of the tissue inhibitor of metalloproteases-1 (TIMP-1), a mediator responsible for naturally inhibiting the action of the destructive enzymes the MMPs. The association of IL-6 with IL-1β, thus preventing the synthesis of proteoglycans within the cartilage matrix, demonstrates a catabolic role for the cytokine (Neitfeld *et al.*, 1990). It remains to be seen if IL-6 is a true driving force in OA pathology or if it simply plays a minor role in response to the biological effects that other cytokines and mediators evoke within the joint.

1.3.4 Leukaemia Inhibitory Factor (LIF).

A member of the IL-6 family, LIF is a cytokine speculated to play a dual role in both normal physiology and pathology. Associated with normal physiological processes such as promoting growth and differentiation, LIF also plays an intrinsic role in inflammation (Alexander *et al.*, 1994). Structurally LIF consists of a single chain glycoprotein, eliciting its effects by binding to a receptor constituting the gp130 common IL-6 receptor and a second gp receptor, gp190 (Kishimoto *et al.*, 1994).

With the ability to upregulate both MMP production and nitric oxide production, LIF appears to play a catabolic role within the joint (Lotz *et al.*, 1992). This is further substantiated by the involvement of LIF in the breakdown of proteoglycans (Bell *et al.*, 1995; Carroll *et al.*, 1993).

1.3.5 IL-17.

Secreted solely by T cells, IL-17, is a cytokine only involved in the pathology of OA patients who exhibit a significant T cell infiltrate, typically those with Erosive OA (EOA) (Moseley *et al.*, 2003). IL-17 has been shown to upregulate the production of IL-6 and nitric oxide whilst synergistically enhancing the effect of IL-1β and TNFα upon cartilage destruction (Chaubad *et al.*, 2000; Shalom-Barak *et al.*, 1998).

1.3.6 CXCL8.

Intrinsically implicated in the pathology of RA, CXCL8 a potent inflammatory chemokine, has been associated with OA pathology as a consequence of the upregulation of CXCL8 via IL-1β and TNFα (Yoshida *et al.*, 1999). The chondrocytes, fibroblasts and macrophages of the joint are known to secrete CXCL8 (Hirota *et al.*, 1992; van Damme *et al.*,1990). It is speculated that secreted CXCL8 is involved in the synovial inflammatory response.

1.3.7 CCL2

A member of the C-C family of chemokines, CCL2 is a monocyte chemoattractant protein, with an intrinsic role as the name suggests in the recruitment of monocytes from the circulation into tissues during periods of inflammation (Vergunst *et al.*, 2005). Osteoarthritic chondrocytes have been shown to release significantly reduced levels of CCL2 in comparison to normal chondrocytes in reponse to both IL-1β and TNFα stimulation (Yuan *et al.*, 2001). However synovial fibroblasts isolated from osteoarthritic patients demonstrated increased production of CCL2 following stimulation with TNFα (Fiorito *et al.*, 2005).

1.3.8 CCL5

A second member of the C-C family of chemokines, CCL5, historically referred to as RANTES (regulated upon activation, normal T cell expressed and secreted), has been associated with the pathology of RA where it has a role in the recruitment of T cells into the synovial membrane (Yuan *et al.*, 2001, Vergunst *et al.*, 2005). CCL5 expression by osteoarthritic chondrocytes has been demonstrated to be enhanced in comparison to normal chondrocytes, whilst synovial fibroblasts derived from OA patients also produce CCL5 (Alaaeddine *et al.*, 2001, Seitz *et al.*, 1994).

1.3.9 Nitric Oxide (NO).

An inorganic free radical, NO is proposed to have a highly significant role in OA pathology (Martel Pelletier, 1999). Elevated levels of NO are produced by the chondrocytes resident in the osteoarthritic joint (Grabowski *et al.*, 1997). NO has a dual role within the joint, upregulated by IL-1β it induces

the production of catabolic MMPs (Murrel *et al.*, 1995), whilst also preventing the synthesis of matrix proteins (Taskiran *et al.*, 1994).

1.3.10 Transforming Growth Factor-beta (TGFβ).

Associated with the synthesis of matrix, TGFβ induces production of collagen and proteoglycan (Qi *et al.*, 2000; van Osch *et al.*, 1998). Elevated levels of TGFβ are found in the cartilage, synovium and subchondral bone of an osteoarthritic joint, this is speculated to be a consequence of the attempted repair response initiated during the early stages of OA. Like a number of other cytokines, TGFβ elicits a dual role within the joint. In one respect TGFβ evokes an anabolic response, inhibiting the IL-1β induced cartilage destruction (Malemud *et al.*, 2004) and under certain conditions upregulating the induction of TIMP-1 and TIMP-3 by chondrocytes (Hui *et al.*, 2003). In contrast TGFβ is implicated in the induction of MMP-13 and aggrecanases which induce a catabolic effect (Moldovan *et al.*, 2000; Yamanishi *et al.*, 2002). An *in vivo* lapine study demonstrated administration of TGFβ via adenoviral gene transfer, did not elicit a repair response and under certain conditions it may induce degradation of the cartilage matrix (Mi *et al.*, 2003).

1.3.11 Insulin-Like Growth Factor-1 (IGF-1).

Whilst IGF-1 levels are relatively low in the serum of OA patients, chondrocyte associated levels of IGF-1 are elevated (Middleton *et al.*, 1992). The synthesis of proteoglycans within the cartilage is modulated by IGF-1 (van Osch *et al.*, 1998). A second anabolic effect IGF-1 elicits is its ability to inhibit the destruction of cartilage (Hui *et al.*, 2001; Hui *et al.*, 2003). In contrast IGF-1 mediates catabolic effects, promoting subchondral bone remodelling, osteophyte formation and sclerosis of the underlying bone (Schouten *et al.*, 1993).

1.3.12 Matrix Metalloproteases (MMPs).

MMPs or matrixins as they are collectively referred to, are zinc dependent, calcium containing endopeptidases responsible for the degradation of all constituent proteins of the extracellular matrix (Kontogiorgis *et al.*, 2005). 23 different MMPs are known to exist in humans, eliciting a proteolytic effect at neutral pH. Each MMP belongs to one of 5 subgroups, as a result of their substrate specificity and structure, specifically the collagenases, gelatinases, stromeolysins, matrilysins, and the membrane bound MMPs (see Table 1.4) (Murphy *et al.*, 2002).

Structurally MMPs are comprised of five main domains; a signal peptide domain, a propeptide domain, a catalytic domain, a hinge region also known as the linker domain, and a hemopexin domain (illustrated in Figure 1.10), (Lemaître *et al.*, 2006). In addition to these domains the membrane bound MMPs (MT-MMPs) also possess a transmembrane domain including a cytoplasmic tail, which ensures they remain bound to the cell membrane. The signal peptide, a 20 amino acid protein, is proteolytically cleaved from the proteinase during extracellular secretion of MMPs (Bode *et al.*, 2003 ; Murphy *et al.*, 2002). Adjacent to the signal peptide is the 80 amino acid propeptide domain, containing the cysteine switch, responsible for holding the MMP in its latent form prior to activation (Lemaître *et al.*, 2006; Nagase *et al.*, 2006). The catalytic domain is approximately 170 amino acids in size and globular in formation, comprised of 5-stranded β-pleated sheets, with 3 α-helices and bridging loops that form a 'Met turn' structure (Mengshol *et al.*, 2002). Within the catalytic domain a catalytic zinc resides supported by the Met turn, its association with three histidines in the catalytic domain and the cysteine switch

motif in the propeptide domain, prevents peptide hydrolysis of the catalytic zinc by a water molecule and consequently activation (Visse *et al.*, 2003). The 10 - 70 amino acid hinge region is responsible for separating the catalytic domain from the hemopexin domain and is notably absent along with the hemopexin domain in the matrilysin subgroup of proteinases. The C-terminal hemopexin domain is the final domain of secreted MMPs, approximately 200 amino acids in size it has a four bladed β-propeller like structure and is responsible for the interactions between MMPs and their substrates or inhibitors (Lemaître *et al.*, 2006; Pardo *et al.*, 2005). The hemopexin domain appears to be critical in the proteolytic cleavage of collagens, as a result of its ability to bind to fibrillar collagens (Murphy *et al.*, 2002).

The proteinases, highlighted in bold in Table 1.4 (the collagenases; MMP-1 and MMP-13, the stromelysin; MMP-3, and the gelatinase; MMP-9), are intrinsically involved in the pathological degradation of the articular cartilage extracellular matrix during OA. The aforementioned enzymes and their role in disease will be discussed in further detail.

Figure 1.10 The MMP domains.

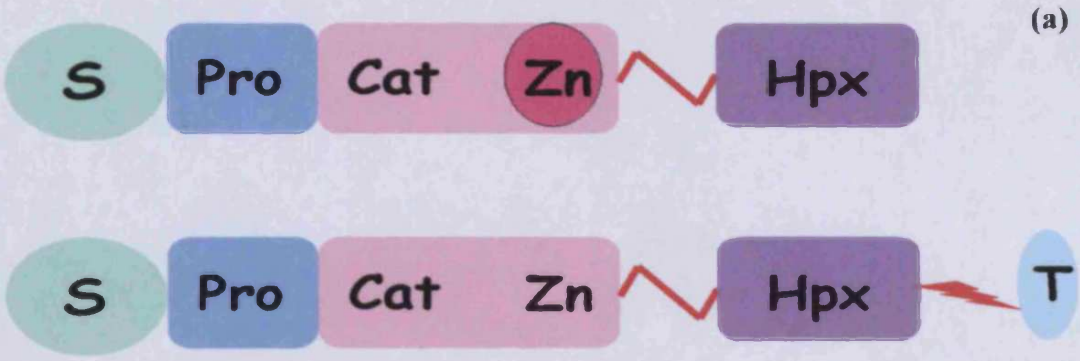

S: Signal Peptide
Pro: Propeptide domain
Cat: Catalytic domain
Zn: Catalytic Zinc
Hpx: Hemopexin domain
T: Transmembrane domain & cytoplasmic tail

Schematic overview of the MMP domains present in (a) secreted MMPs and (b) membrane bound MMPs (adapted from Das *et al.*, 2003).

Table 1.4 The MMP family.

MMP	ENZYME	ECM SUBSTRATE	ACTIVATED BY	ACTIVATOR OF
MMP-1	**Collagenase(-1) (Interstitial Collagenase)**	**Collagens (I, II, III, VII, VIII & X), aggrecan, link protein, versican, gelatin**	**MMP-3 & MMP-10**	**MMP-2**
MMP-2	Gelatinase (-A)	Collagens (I, IV, V, VII, X, XI & XIV), gelatin, elastin, fibronectin, aggrecan, decorin, link protein	MMP-1, -7, -13, -14, -15, -16, -17, -24, -25	MMP-9 & MMP-13
MMP-3	**Stromelysin (-1)**	**Collagens (III, IV, V & IX), gelatin, aggrecan, versican, perlecan, decorin, link protein, fibronectin**	**N/A**	**MMP-1, -7, -8, -9, -13**
MMP-7	Matrilysin-1 (PUMP-1)	Collagens (IV & X), gelatin, aggrecan, decorin, link protein, fibronectin, elastin, laminin	MMP-3 & MMP-10	MMP-2
MMP-8	Collagenase(2) Neutrophil Collagenase	Collagens (I, II, III, V, VII, VIII, & X), gelatin, aggrecan	MMP-3 & MMP-10	Not Defined
MMP-9	**Gelatinase (-B)**	**Collagens (IV, V, VII, X & XIV), gelatin, aggrecan, fibronectin, link protein**	**MMP-2, MMP-3 & MMP-13**	**Not Defined**
MMP-10	Stromeolysin (-2)	Collagens (III, IV, V & IX), gelatin, aggrecan, elastin, link protein	N/A	MMP-1, -7, -8, -9, -13
MMP-11	Stromeolysin (-3)	Collagen IV, fibronectin, gelatin, laminin, casein	N/A	Not Defined
MMP-12	Metalloelastase	Collagen IV, gelatin, elastin, fibronectin, laminin, casein	Not Defined	Not Defined
MMP-13	**Collagenase (-3)**	**Collagens (I, II, III, IV, IX, X, XIV), gelatin, aggrecan, perlecan, fibronectin**	**MMP-2, -3, -10, -14, -15**	**MMP-2 & MMP-9**
MMP-14	MT1-MMP (Membrane Bound)	Collagens (I, II & III), elastin, fibronectin, gelatin, laminin, vitronectin, casein	N/A	MMP-2 & MMP-13
MMP-15	MT2-MMP (Membrane Bound)	Fibronectin, laminin, aggrecan, perlecan	Not Defined	MMP-2 & MMP-13
MMP-16	MT3-MMP (Membrane Bound)	Collagen III, gelatin, fibronectin, casein	Not Defined	MMP-2
MMP-17	MT4-MMP (Membrane Bound)	Not Defined	Not Defined	MMP-2
MMP-26	Matrilysin-2	Collagen IV, gelatin, fibronectin	Not Defined	Not Defined

(Adapted from Chakraborti *et al.*, 2003)

Upon activation the collagenases degrade native collagen present within the articular cartilage, by unwinding the triple helical domain of the fibrils of collagen. The resulting relaxation of collagen results in the formation of gelatin,

which can be further degraded by additional members of the matrixin family (Pardo *et al.*, 2005). Cleavage of collagen I, II and III, induced by the collagenases, occurs as a result of the hemopexin domain targeting the triple helix ¾ from the N terminus of the molecule (Murphy *et al.*, 2002). Collagen II is the most abundant collagen present in articular cartilage, the degradation of this molecule by the collagenases results in the irreversible fibrillation of cartilage that is an intrinsic feature of OA. MMP-1 and MMP-13 of the four known collagenases are strongly implicated in OA pathology, the importance of each in disease pathogenesis is examined.

1.3.12.1 MMP-1.

Interstitial collagenase or MMP-1 was the first MMP isolated from synovial fibroblasts (Bramano *et al.*, 2004), it is secreted at high levels from the synovial membrane of the osteoarthritic joint. Although less specific in its cleavage of collagen II than MMP-13, MMP-1 expression within the joint is 200 fold greater than that of MMP-13 (Martel-Pelletier *et al.*, 1999). Within the cartilage itself MMP-1 levels are elevated by the chondrocytes present in the superficial zone. A study in a canine model of OA demonstrated that MMP-1 levels increased with cartilage destruction, suggesting that MMP-1 was critically involved during the latter stages of disease (Fernades *et al.*, 1998). MMP-1 is a multifunctional molecule, effectively degrading collagen, it also has the ability to degrade the most abundant proteoglycan of articular cartilage, aggrecan, thus demonstrating its critical role in the turnover of the matrix of articular cartilage (McCawley *et al.*, 2001).

1.3.12.2 MMP-13.

Often considered the dominant collagenase within the joint, MMP13 is 5 – 10 times more specific in its cleavage of collagen II than MMP-1 (Martel-Pelletier *et al.*, 2001). MMP-13 is predominantly secreted by chondrocytes (Forysth *et al.*, 2005), and is preferentially secreted by those cells located in the deep zone of cartilage (Fernades *et al.*, 1998; Moldovan *et al.*, 1997). MMP-13 expression is consequently elevated during the earlier bone remodelling stages of the disease (Leeman *et al.*, 2002). Aside from its critical role in the degradation of collagen II, it also degrades type I and II collagen and of all the collagenases elicits the greatest effect on gelatin, consequently it not only degrades collagen fibrils but also degrades the gelatin produced from their cleavage (Leeman *et al.*, 2002). The proteolytic activation of proMMP-9 occurs as a result of cleavage by MMP-13, which further enhances cartilage destruction, as a result of the gelatinase degradation of MMP-9 (Mengshol *et al.*, 2002).

1.3.12.3 MMP-3 (Stromelysin).

Initially identified in stromal cells hence the origin of the name, MMP-3 is produced in the joint by the fibroblasts, chondrocytes and osteoblasts (a resident cell type within the growth plate of the subchondral bone) (Bramano *et al.*, 2004). Structurally MMP-3 shares a homology with the collagenases, but is unable to degrade the fibrillar collagens present in articular cartilage. MMP-3 levels have been demonstrated to be elevated in cohorts of OA patients (Masuhara *et al.*, 2002), with broad specificity against a number of matrix proteins, it has been intrinsically linked to catabolism within the joint. Proteoglycans, and in particular aggrecan, are a major substrate of MMP-3 with studies demonstrating that elevated levels of MMP-3 result in severe

proteoglycan depletion from the articular cartilage (Gunja-Smith *et al.*, 1989; Nguyen *et al.*, 1989). Aggrecan cleavage within the joint is known to occur during the early stages of disease, hence MMP-3 levels are increased during early disease. Collagen type IX, responsible for maintaining the integrity of the extracellular matrix of articular cartilage through its linkage of collagen II fibrils with the proteoglycans, is also degraded by MMP-3 resulting in structural weakening of the cartilage (Okada *et al.*, 1989). A secondary, but equally important role of MMP-3, is its ability to proteolytically cleave both proMMP-1 and proMMP-9. The release of the two active forms of these enzymes results in an enhanced rate of cartilage destruction within the joint due to their collagenolytic and gelatinlytic activity respectively (Dreier *et al.*, 2004; Unemori *et al.*, 1991; van Meurs *et al.*, 1999). The levels of proMMP-3 have been highlighted as a potential prognostic marker of an individual with joint trauma consequently developing OA (Tchetverikov *et al.*, 2005).

1.3.12.4 MMP-9.

Expressed by neutrophils, macrophages and synovial fibroblasts the levels of MMP-9, in comparison to RA, are lower in OA (Yoshihara *et al.*, 2000). MMP-9, like other MMPs, degrades a number of different substrates, of particular importance is its ability to further degrade the unwound collagen II fibrils that form gelatin as a result of MMP-1 and MMP-13 proteolysis. MMP-9 has an additional role within the joint, its ability to activate the pro-inflammatory cytokine IL-1β resulting in an enhanced inflammatory environment (Ito *et al.*, 1996).

1.3.13 Adamlysins (The ADAMs & ADAMTS family).

Aside from the MMPs, a second group of proteolytic enzymes exist namely the ADAMs (a disintegrin and metalloprotease) and ADAMTSs (a disintegrin and metalloprotease and thrombospondin motifs). The ADAMs are a family of 34 enzymes anchored to the cell surface via a transmembrane domain with a diverse role in cellular function (Duffy *et al.*, 2003), of importance to OA is ADAM-17 or TACE as its also known (Black, 2002). ADAM-17 is expressed as a latent zymogen that is activated by removal of its prodomain. Upon activation membrane bound ADAM-17 cleaves inactive pro-TNFα into its active form as previously discussed in 1.3.2.

Of greater importance to OA pathology is the ADAMTS family. First identified in 1997, 20 different ADAMTSs are currently known to exist in mammals (Jones *et al.*, 2005). Structurally similar to MMPs, they comprise a signal peptide domain, a pro-domain, and a metalloproteinase catalytic domain with an altered amino acid sequence from the sequence present in MMPs. Unlike MMPs a disintegrin-like domain is located adjacent to the catalytic domain, which is followed by a thrombospondin (TS) repeat, a cysteine rich domain, a spacer domain and finally a variable number of TS repeats (Porter *et al.*, 2005). ADAMTS-4 and ADAMTS-5, also known as aggrecanase-1 and aggrecanse-2, are the ADAMTSs responsible for aggrecan degradation in OA (Jones *et al.*, 2005). Both ADAMTS-4 and ADAMTS-5 cleave aggrecan within residues Glu^{373} and Ala^{374} at 4 sites located in the chondroitin-sulphate-rich region (Arner *et al.*, 2002).

1.3.14 Regulation of MMP & ADAMTS activity.

The activity of MMPs is tightly regulated at three different stages, transcriptional regulation, activation of the inactive proMMP (post-transcriptional regulation), and inhibition of activity via a family of endogenous regulators namely the 'tissue inhibitors of metalloproteinases' (TIMPs). Within the healthy joint these three regulatory mechanisms act in unison to ensure that a homeostatic balance exists between anabolism and catabolism.

1.3.14.1 Transcriptional Regulation.

MMP transcription is tightly regulated in normal tissues, with MMP expression relatively low unless extracellular remodelling is required then gene expression may be elevated. In OA the levels of MMP are greatly increased. A number of external stimuli induce MMP transcription these include stress factors, chemical agents and cytokines. IL-1β and TNFα in particular are known to stimulate the four key MMPs: MMP-1, MMP-3, MMP-9 and MMP-13 implicated in OA pathology (Pelletier *et al.*, 2001). MMP induction is reliant on the presence of an activator protein-1 (AP-1) site located at the proximal promoter region of MMP genes (Martel-Pelletier *et al.*, 2001). MMP expression in response to inflammatory cytokines such as IL-1β and TNFα is known to stimulate a number of signal transduction pathways, including the Nuclear Factor kappa B (NFκB) pathway. MMP-1, MMP-3 and MMP-9 all possess a canonical binding site for NFκB, stimulation with IL-1β and TNFα results in activation of this signalling cascade and expression of these MMPs (Smith, 2006). Whilst MMP-13 itself does not possess a binding site for NFκB, blockade of NFκB signalling resulting in the inhibition of IL-1β and TNFα results in MMP-13 inhibition by an unknown mechanism, demonstrating partial

dependency of MMP-13 induction upon NFκB signalling (Burrage *et al.*, 2006; Mengshol *et al.*, 2000). Other signalling pathways involved in MMP induction include the mitogen activated protein kinase pathways (MAPKs) including the JNK, ERK and p38 pathways which results in MMP gene expression (Liang *et al.*, 2007; Reuben *et al.*, 2006; Wu *et al.*, 2004).

1.3.14.2 Post Transcriptional Regulation.

All MMPs are initially secreted in an inactive, latent pro-enzyme form. Activation can be induced by other MMPs and proteases such as plasminogen activator, or thrombin (proteolytic cleavage), alternatively cleavage can be achieved by chemical activation (Smith, 2006). Proteolytic activation involves the cleavage of the bait region present within the catalytic domain resulting in destabilisation of the domain (Visse *et al.*, 2003). Intermolecular processing involving MMP intermediates or other active MMPs results in the release of the active MMP, in a process often referred to as 'stepwise activation' (Nagase *et al.*, 2006). Alternatively chemical activation targets the cysteine switch, with full activation achieved as a result of the intermolecular processing steps described above. Activation of numerous MMPs requires cleavage by a different active member of the MMP family, hence the matrixin family is able to self regulate, illustrating the fine balance that exists between anabolic and catabolic processes (Sternlicht *et al.*, 2001).

1.3.14.3 The TIMPs.

The final stage of regulation of MMP activity is achieved through the association of active MMPs and their endogenous regulator, the TIMPs. Structurally TIMPs are 184 – 194 amino acids in size and morphologically comprise an elongated wedge form, with an N-terminal and C-terminal

subdomain (Bode *et al.*, 1999). The C terminal region of the TIMP protein interacts with the C-terminal region of the hemopexin region of the MMP whilst also binding to the active site of the protease (Chakraborti *et al.*, 2003). All TIMPs inhibit all active MMPs and bind to the enzyme at a stoichometric ratio of 1:1, in the healthy joint this ratio ensures MMP activity is tightly regulated (Nagase *et al.*, 1999). TIMP-1, TIMP-3 and TIMP-4 are known to be produced by both chondrocytes and fibroblasts within the osteoarthritic joint (Huang *et al.*, 2002; Su *et al.*, 1999). In OA, TIMP-1 appears to be the most important in regulating the action of MMPs, with TIMP-3 inhibiting the action of ADAMTS-4 and ADAMTS-5 (Nagase *et al.*, 2006). TIMP-2 and TIMP-4 have been demonstrated to effectively inhibit membrane bound MT-MMPs.

It is postulated that elevated levels of TIMPs within the osteoarthritic joint would prove beneficial, as a balance between anabolism and catabolism could be re-established as a consequence of the TIMPS binding to, and therefore inactivating the catabolic processes of the MMPs. However, such a treatment strategy has yet to be fully realised for OA (Baker *et al.*, 2002).

1.4 Nuclear Factor kappa B (NFκB).

A ubiquitously expressed transcription factor, NFκB was first discovered in the mid 1980s by Sen & Baltimore. Initially isolated from B cells, NFκB has subsequently been isolated from a whole host of cell types (Sen *et al.*, 1986). The transcription factor has been significantly implicated in immune and inflammatory responses, in a whole host of disease processes including cancers, RA, asthma and muscular dystrophy (Yates *et al.*, 2006)

The transcription factor is comprised of 5 proteins sharing structural homology, namely: NFκB1 (p105/p50), NFκB2 (p100/p52), c-Rel, RelA (p65) and RelB (Figure 1.11). NFκB1 and NFκB2 are initially synthesised in an inactive form, as p105 and p100 respectively, the ankyrin repeats present ensure the latency of the two subunits (Bonizzi *et al.*, 2004). Post-translational processing of the p105 and p100 subunits results in the formation of the DNA-binding subunits p50 and p52 (Ghosh *et al.*, 1998). Both NFκB1 and NFκB2 possess a Rel-Homology-Domain (RHD), but lack a transcription activation domain. A transcription activation domain is present in the three Rel transcription factors, with the Rel family of NFκB subunits also lacking the inhibitory ankyrin repeats (Ryseck *et al.*, 1992). RelA and c-Rel have a transcriptional activation role within the cell, whilst RelB can act as either an activator or a repressor of transcription (Ruben *et al.*, 1992). In the majority of cell types NFκB is present as a heterodimer of the NFκB1 (p50) subunit and the RelA (p65) subunit, which is retained latently within the cytoplasm by the IκB proteins present (Reigner *et al.*, 1997).

Two NFκB activation pathways exist; the classical or canonical signalling pathway and the alternative signalling pathway. The two separate modes of signalling are speculated to arise from their different regulatory function, with the classical pathway involved in innate immunity and the alternative pathway involved in adaptive immunity (Bonizzi *et al.*, 2004).

Figure 1.11 The five NFκB subunits.

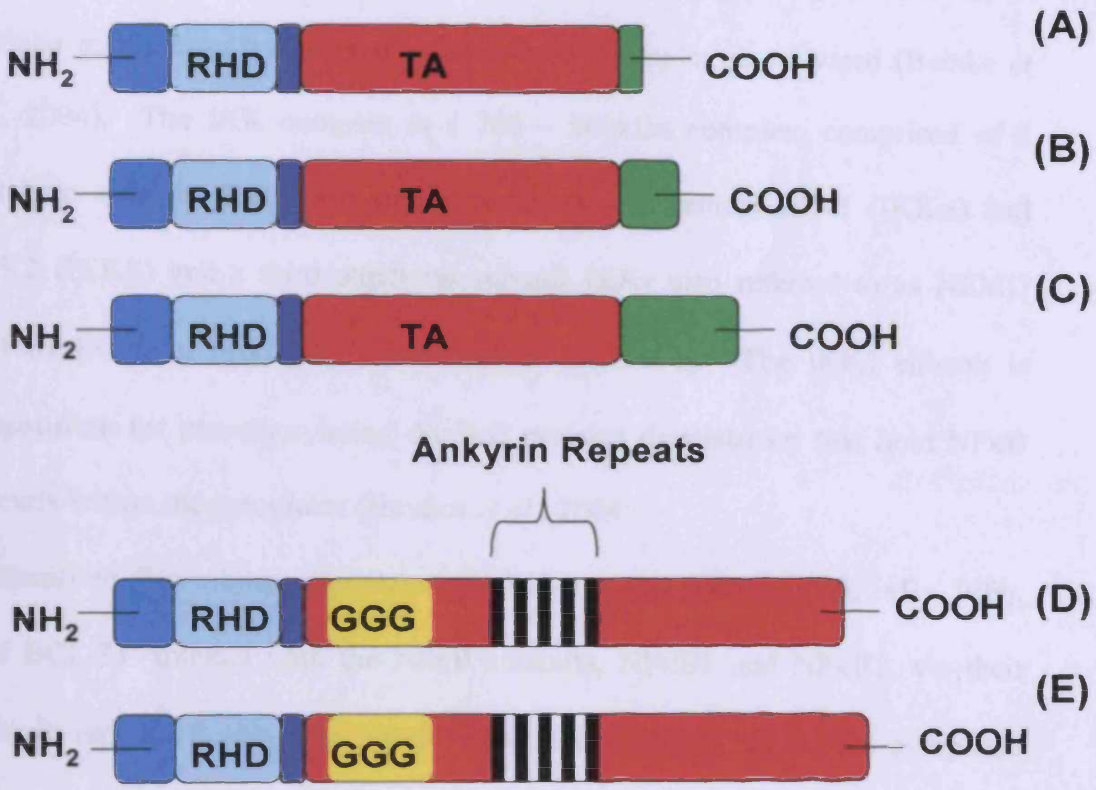

(A) p65 (RelA)
(B) RelB
(C) c-Rel
(D) NFκB1 (p105/p50)
(E) NFκB2 (p100/p52)

Simplified outline of the 5 NFκB subunits present with mammals. Depicted are the RHD domain, a 300 amino acid sequence which includes the nuclear localisation sequence. The GGG and region present in the NFκB1 and NFκB2 subunits are glycine hinge region, adjacent to this are the C terminal inhibitory ankyrin repeats (adapted from Yates *et al.*, 2006).

1.4.1 The classical pathway.

Classical signalling occurs as a result of inflammatory cytokine stimulation, typically IL-1 and TNFα, or in response to bacterial or viral products. Upon cellular stimulation the IkappaB kinase (IKK) complex is activated (Beinke *et al.*, 2004). The IKK complex is a 700 – 900kDa complex, comprised of 2 catalytic subunits that share structural homology, namely IKK1 (IKKα) and IKK2 (IKKβ) and a third structural subunit IKKγ also referred to as NEMO (NFκB Essential Modifier) (Stancovski *et al.*, 1997). The IKK2 subunit is responsible for phosphorylating the IκB proteins downstream that hold NFκB latently within the cytoplasm (Hayden *et al.*, 2004).

A family of five inhibitory proteins, the IκB proteins (IκBα, IκBβ, IκBε, IκBγ, and BCL-3) interact with the NFκB subunits, NFκB1 and NFκB2, via their ankyrin repeats, holding the NFκB homodimers latently within the cytoplasm (Roman-Blas *et al.*, 2006). Active IKK2 phosphorylates the N terminal serine residues 32 and 36 for IκBα and residues 19 and 23 for IκBβ (Hayden *et al.*,2004). The tertiary structure of the IκB proteins becomes modified in response to phosphorylation, exposing motifs that signal for the ubiquitin ligase to bind to the IκB proteins, resulting in rapid degradation by the 26S proteasome. Consequently the nuclear localisation sequence present in the RHD domain of the released NFκB subunits is exposed, allowing NFκB to shuttle to the nucleus where it induces the transcription of the gene of interest. A simplified overview of the classical pathway is depicted in Figure 1.12.

Figure 1.12 The classical NFκB activation pathway.

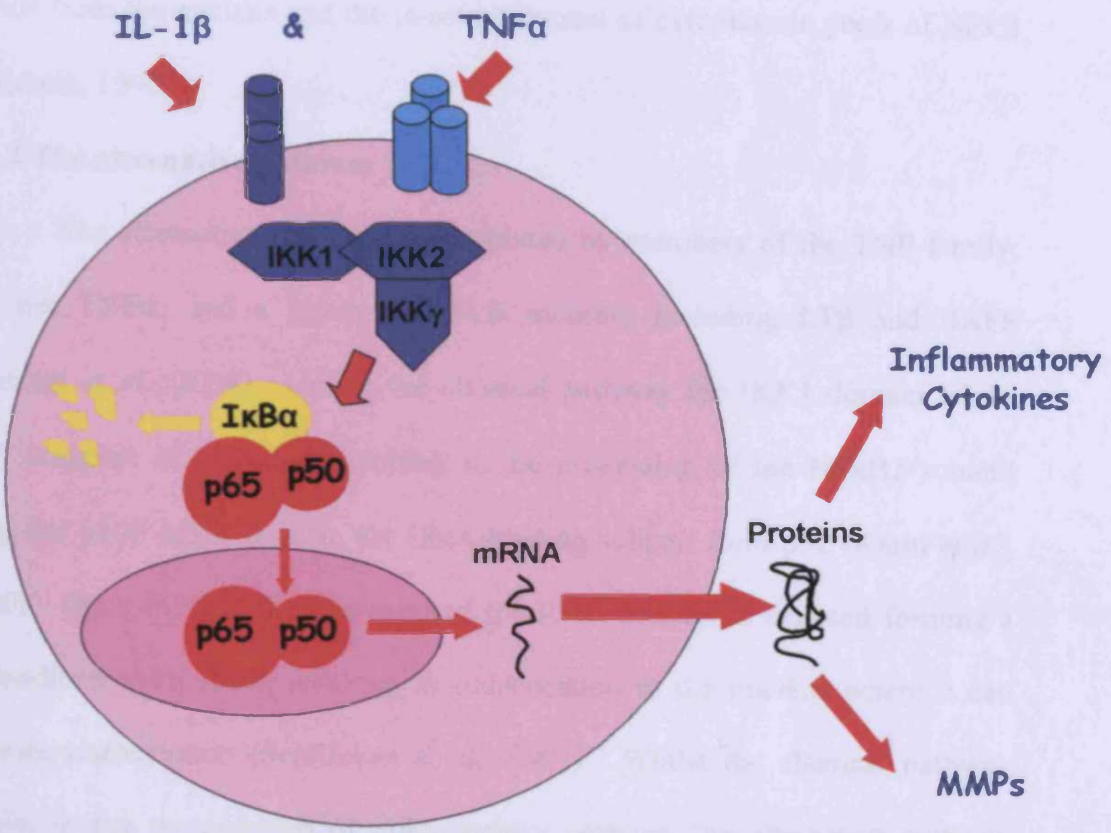

A simplified overview of the major steps of the classical NFκB activation pathway (adapted from Bonizzi *et al.*, 2004).

NFκB is a transient process that is tightly regulated. The IκBα gene contains multiple NFκB binding sites, hence the translocation of NFκB to the nucleus results not only in the upregulation of the gene of interest, but also the IκBα proteins. The newly synthesised IκBα is responsible for the removal of NFκB from the nucleus and the re-establishment of cytoplasmic pools of NFκB (Baldwin, 1996).

1.4.2 The alternative pathway

The alternative pathway is stimulated by members of the TNF family, but not TNFα, and a group of NFκB inducers including LTβ and BAFF (Bonizzi *et al.*, 2004). Unlike the classical pathway the IKK1 domain of the IKK complex is activated, resulting in the processing of the NFκB2 subunit from the p100 latent form to the DNA-binding subunit form p52 (Karin *et al.*, 2000). Once the p52 form is released the RHD domain is exposed forming a heterodimer with RelB, resulting in translocation to the nucleus where it can activate transcription (Senftleben *et al.*, 2001). Whilst the classical pathway results in the upregulation of inflammatory proteins, the alternative pathway results in the expression of genes involved in development and the maintenance of secondary lymphoid organs (Bonizzi *et al.*, 2004).

1.4.3 The role of NFκB in OA.

The NFκB signalling cascade has been demonstrated to induce the transcription of approximately 150 genes (Roman-Blas *et al.*, 2006). Its association with OA results from the ability of the transcription factor to upregulate a number of mediators associated with disease pathology, namely IL-6, and the MMPs; MMP-1, MMP-3, MMP-9 and MMP-13. Elevated levels of the inflammatory cytokines IL-1β and TNFα have been demonstrated within the

OA joint, as previously described IL-1β and TNFα are potent inducers of the classical pathway, and are themselves further upregulated by NFκB activation.

1.5 Animal models of OA.

The advent of animal models for the study of OA has enhanced our understanding of the mechanisms of pathology and the clinical progression of the disease. A range of animal models of OA exist, in a variety of species, each with their own unique advantages and disadvantages. Such models typically fall into one of four broad categories; spontaneous models, genetically modified models, enzymatically or chemically induced models and mechanically induced models. Each *in vivo* OA model mimics certain aspects of the disease precisely whilst other clinical aspects of the disease are not as accurately represented, consequently depending upon the study or the treatment strategy under investigation, certain models maybe more advantageous than others.

1.5.1 Spontaneous OA Models.

A number of aging species develop spontaneous OA, mimicking the slow, progressive nature of the disease and the inherent variability that exists in human patients. The first model of spontaneous OA was observed in the Dunkin-Hartley strain of Guinea Pigs (Silverstein *et al.*, 1958). Walton et al subsequently demonstrated during the 1970s that the STR/ort strain of mice had a particularly high incidence of OA in comparison to other strains studied (Walton *et al.*, 1977). Joint deterioration was observed from approximately 4 months of age, with the incidence and severity of OA increasing with age. Cartilage deterioration in this model is initially localised in the medial tibial plateau, with the severity of degradation ranging from fibrillation through to

erosional lesions that expose the subchondral bone beneath the articular cartilage (Mason *et al.*, 2001). As observed in the spontaneous guinea pig model, the incidence of OA is lower in female STR/ort mice and the initial onset of disease occurs much later in life from 12 months of age. It is unclear why male mice and guinea pigs, in comparison to their female counterparts, appear to have a predisposition to developing OA, as in humans the incidence of OA is roughly equal in men and women prior to the menopause and post-menopausally OA is more prevalent in women than men.

Larger species such as dogs also exhibit progressive OA like changes during aging (Lust *et al.*, 1972). With the most clinically relevant spontaneous models occurring in the non-human primates species such as the Rhesus macaque and Cynomolgus macaque (Billingham, 2000; Pritzker *et al.*, 1994). As a bipedal animal, joint mechanics and joint loading more closely represent the human joint, these animals also develop OA like changes in the knee joint during middle age that slowly progress mimicking the clinical picture in humans (Carlson *et al.*, 1994). However, the associated costs of using large animal species and the current UK ban issued under the Animals (Scientific Procedures) Act 1986 favours the use of small animal models.

1.5.2 Genetically modified OA models.

The advent of genetically modified mice allows the role of specific cytokines, MMPs, chemokines and other mediators in OA to be studied (Goldring, 1999). Transgenic mice have been designed as knockin species in which the gene encoding a specific mediator is expressed or as knockout species whereby the gene encoding a cytokine, MMP or growth factor believed to be

catabolic is deficient and the mediator is not expressed within the animal (Helminen *et al.*, 2002).

One of the earliest knockout mice developed was a mouse deficient in bone morphogenic protein (BMP) receptor type 1a. This model was designed to further our understanding of the role of BMP in cartilage formation (Rountree *et al.*, 2004), and resulted in a BMP deficiency only in the developing joints by the inclusion of a promoter that encodes the gene for a cartilage derived morphogenetic protein, Gdf5, thus targeting the BMP deletion to developing cartilaginous joints only (Young *et al.*, 2005). This knockout model successfully demonstrated that BMP signalling is necessary for normal joint functioning as these knockout mice developed early osteoarthritis within the BMP deficient joints (Rountree *et al.*, 2004).

A second transgenic model demonstrated that elderly male mice (18 months or older) deficient in IL-6 demonstrated severe cartilage erosion in both the tibia and femur in comparison to age matched wildtype male and female mice, and age matched female IL-$6^{-/-}$ mice (de Hooge *et al.*, 2005). In the IL-$6^{-/-}$ male mice there was evidence of subchondral bone sclerosis and proteoglycan and bone deposition in the ligaments of the joint. This model proposed a potentially cartilage protective role for IL-6 in elderly male mice that develop OA spontaneously.

Several other transgenic mice are available that encode mutations or deletions in the collagens of the articular cartilage (Young *et al.*, 2005). ColIXa1$^{-/-}$ mice deficient in type IX collagen develop early stage osteoarthritic changes from the age of 3 months where chondrocyte clustering is evident, by 9 months of age fibrillation is present with erosional lesions present (Hu *et al.*,

2006). A study performed to decipher the importance of the two aggrecanases, ADAMTS-4 and ADAMTS-5 demonstrated that transgenic mice deficient in ADAMTS-5 exhibited reduced cartilage erosion in response to antigen-induction of arthritis (AIA) in comparison to control wildtype mice (Stanton *et al.*, 2005).

1.5.3 Chemically and enzymatically induced OA models.

Chemically or enzymatically induced models of OA are designed to selectively degrade the matrix of the articular cartilage (Pritzker *et al.*, 1994). These models provide an advantage over the types of *in vivo* OA models as the timeframe from initiation to endstage cartilage destruction is shorter than the majority of other available models, although a drawback of these models is the pathological changes they induce may not be the most representative of the OA pathological process.

The collagenase induced model of OA is an example of an enzymatically induced model of OA routinely employed in mice. Intraarticular injections of collagenase results in weakening of the ligaments of the knee, which subsequently causes joint instability and OA-like changes to develop within the joint (van der Kraan *et al.*, 1990). Despite collagen forming the major constituent protein of articular cartilage, an injection of collagenase appears to have limited effect upon the cartilage itself. This model demonstrates similar changes to those observed in the spontaneous model of OA, with cartilage lesions that expose the subchondral bone, and osteophyte formation and sclerosis of the subchondral bone developing within 6 weeks of intraarticular injection of collagenase (van der Kraan *et al.*, 1990). The instability elicited by collagenase injections which is suspected to degrade the type I collagen present

in the tendons, ligaments and menisci of the joint, results in the formation of osteophytes which act as a stabilising mechanism in the affected joint from around day 7. By day 35 erosions have begun to form in the articular cartilage particularly in the tibial plateau (van Osch *et al.*, 1994). This model has been used successfully to model OA changes in the femorotibial compartment of the joint with associated patellar dislocation which has also be observed in the STR/ort mice where patella subluxation was suspected as the source of degenerative changes within the joint (Mason *et al.*, 2001; Walton *et al.*, 1977).

1.5.4 Surgically induced mechanical models of OA.

The final group of animal models of OA are those that result from surgically induced instability within the joint, this can occur via repeated loading of the joint or by inducing surgical instability to the joint typically by damaging either the meniscus or the ligaments that hold the joint in alignment (Bendele *et al.*, 2001). Repetitive loading of the joint has been used to induce osteoarthritic like changes in the weight bearing joints of larger species (Pritzker *et al.*, 1994). Radin et al demonstrated in sheep that repeated exercise on concrete surfaces resulted in osteoarthritic like changes in the weight bearing joints of sheep that were not observed in control animals (Pritzker *et al.*, 1994). Such a model indicates that repeated stress to a joint can initiate OA.

A number of different methods are used to surgically induce OA in a number of species, the two most routinely used are mensicectomy or menisical damage and surgical modification to the anterior cruciate ligament (Ameye *et al.*, 2006). The ACLT canine model has been the most widely employed, surgical damage is induced either through a carefully selected incision of the ligament or by a stab wound induced at random, either method results in

instability in the hind knee of the dog that consequently initiates osteoarthritic changes that ultimately result in the formation of lesions, similar to those seen in OA patients whose disease stems from joint trauma (Bendele *et al.*, 2001). Originally the canine model was believed to model cartilage repair in response to injury, as during the initial weeks following surgery the chondrocytes present in the ACLT knee elicit a repair response as demonstrated by an increase in proteoglycan synthesis (Brandt *et al.*, 2002). Studies terminated at 24 months after surgery indicated that the joint elicited a repair response with no evidence of further cartilage deterioration or disease progression (Marshall *et al.*, 1996). However, a study employing the same model over an extended 54 month period demonstrated that cartilage lesions were present as demonstrated by MRI and macroscopic pathological changes evident following sacrifice, indicating that this model is an accurate representation of progressive OA following joint injury. Previous studies terminated at 24 months after the initiation of the ACLT model suggested that the canine model was more a model of repair mechanisms within the joint in response to injury (Marshall *et al.*, 1996). The ACLT has been used successfully to mimic OA in both rats and mice (Hayami *et al.*, 2006; Kamekura *et al.*, 2005).

A second common method of inducing damage within the joint is to induce damage to the meniscus. Menisical tears induced in a canine model demonstrated that during the early stages the joint appears to elicit a reparative response as observed by the increase in chondrocyte numbers up to 4 weeks post surgery, 12 weeks after surgery cartilage deterioration was evident (Nishida *et al.*, 2005). In rabbits meniscectomy results in articular changes within 6 weeks (Bendele *et al.*, 2001). Mensical damage has been performed in both mice and

guinea pigs to mimic arthritic changes (Kamekura *et al.*, 2005; Sabatini *et al.*, 2005).

1.6 Current treatment strategies for OA.

Despite the advances made in recent decades to further our understanding of the pathological processes that occur within the joint, treatment options for OA remain limited. Currently the treatment choices available to OA patients largely provide symptomatic relief and are unable to alter disease progression, which in the long term limits their efficacy. The treatment options employed can be either non-pharmacological strategies or pharmacological therapies.

1.6.1 Non-Pharmacological strategies.

Such strategies are especially efficacious in patients with mild or moderate disease activity. The major options available are outlined in Table 1.5.

1.6.2. Pharmacological approaches.

Pharmaceutics employed in the treatment of OA reduce the symptomatic pain and stiffness the disease elicits, and are typically prescribed in combination with non-pharmacological approaches. Three broad groups of pharmacological options for OA exist; topical agents, intra-articular agents and orally administered systemic agents. The major therapies used in the treatment of OA are outlined in Table 1.6.

Table 1.5 Non-Pharmacological treatment strategies.

Strategy	Efficacy
Patient Education	Information provided allows patients to manage their condition and make informed decisions. Can also allay any concerns patients may have about disability as a result of their disease.
Weight Loss	For patients with high BMI or obesity, weight loss can dramatically reduce symptomatic pain.
Physical Aids	Supportive aids such as walking sticks and frames, crutches, orthotic lateral wedges or insoles, and knee braces can all support the joint and reduce mechanical loading providing symptomatic pain relief.
Exercise	Joint strengthening exercises can reduce pain and increase mobility, aerobic exercise improves joint function and in patients with high BMI can aid weight loss.
Thermal Applications	Moist heat pads (40°C - 45°C) applied directly to the joint for 30 mins have been reported by patients to provide symptomatic relief, although a study has yet to demonstrate such an effect. Other options include hot baths and ultra sound treatment and cold compresses for inflamed joints.

(Adapted from Lozada *et al.*, 2003)

Table 1.6 Pharmacological treatment strategies

STRATEGY	ADMINSTRATION ROUTE	EFFICACY
NSAIDs (Non Steroidal Anti Inflammatory Drugs)	Topically administered	Typically prescribed to treat short inflammatory flares, well tolerated with fewer adverse effects, can significantly reduce pain (Trnavsky *et al.*, 2004)
Capsaicin	Topically administered	Only effective in 1:8 OA patients, can be applied to any joint particularly beneficial in hand OA. Elicits some local side effects (Mason *et al.*, 2004)
Corticosteroid	Intra-articular administration	Reduces inflammation within the joint, alleviates pain in the short term (a week or less), can elicit transient synovitis and a minimal risk of infection is present (Hirsh *et al.*, 2002)
Hyaluronic Acid (HA)	Intra-articular administration	Provides lubrication for the articular cartilage and can provide pain relief up to 6 months after initiation of treatment. Elicits minimal side effects typically pain at injection site and an inflammatory reaction following administration (Moreland *et al.*, 2003)
Acetaminophen (paracetomol)	Orally administered non-opiod analgesic	Provides analgesia but elicits no effect on any inflammation, swelling, stiffness that maybe present. Is well tolerated, usually prescribed for patients with mild or moderate pain (Towheed, 2006).
Tramadol	Orally administered opoid analgesic	Opoid receptors are activated and inhibitory pain channels reduced by Tramadols atypical mode of action. Provides short term analgesia but does not elicit an anti-inflammatory effect. (Reig, 2002)
Non-selective NSAIDs (Ibuprofen, Naproxen, difclofenac)	Orally administered	Provide high levels of analgesia, and anti-inflammatory effects. Used for the short term treatment of OA due to the adverse side effects elicited, namely increased risk of gastro-intestinal and renal complications and in some cases cardiovascular complications (Steinmeyer *et al.*, 2006)
Selective NSAIDs (Celecoxib, Etoricoxib)	Orally administered	Cycloxgenase inhibitors (COX-2) selectively target the prostaglandins present at inflammatory sites. COX-2 inhibitors elicit a greater efficacy in relieving pain and other OA associated symptoms than the more traditional NSAIDs, whilst also reducing the gastrointestinal complications exhibited by other NSAIDs (Bingham *et al.*, 2007).
Nutraceuticals Glucosamine Sulphate	Orally administered	Glucosamine Sulphate is a naturally occurring glycosaminoglycan within cartilage. *In vivo* and *in vitro* it has been demonstrated to elicit anti-inflammatory properties and regulate cartilage metabolism, it may have the potential to rebuild damaged cartilage in vivo. Over a 6 week period it appears to reduce pain and increase mobility, studies over longer periods have demonstrated no notable improvement in joint function. No adverse side effects are elicited by Glucosamine (Towheed *et al.*, 2005)
Nutraceuticals Chondrotin Sulphate	Orally administered	A naturally occurring glycosaminoglycan present within articular cartilage. Large scale clinical trials have demonstrated that compared to placebo chondrotin sulphate is effective in reducing pain (Distler *et al.*, 2006)

1.6.3 Total Joint Replacement – The final outcome?

Due to the lack of disease modifying treatment options available for OA, a significant proportion of patients find that over time the pain, combined with a lack of function in the affected joint, can no longer be controlled by the treatment options available. In such cases joint replacement surgery is usually proposed if the patient is to retain mobility and quality of life. OA joint replacement surgery is usually performed in the large weight bearing joints, namely the knees and hips, once a patient is experiencing severe pain and a degree of functional loss in the joint making mobility difficult. Despite OA being a condition that primarily effects the ageing population, success rates for surgery are high with the majority of patients observing a dramatic clinical improvement in the replaced joint (Gill *et al.*, 1999).

However, joint replacement surgery is a costly procedure and like all invasive surgery carries a significant risk, hence the demand for therapeutics that have the ability to modify OA progression or even reverse the disease process is paramount (Pynsent *et al.*, 1996; Slover *et al.*, 2006).

1.5.4 Disease Modifying Agents in the Treatment of OA.

The implementation of disease-modifying and biological agents that inhibit immune and inflammatory responses in the treatment of RA has revolutionised the clinical picture for thousands of rheumatoid patients. The development of agents for OA that have the ability to either inhibit or modify the catabolic processes, or agents with the ability to enhance anabolic pathways within the joint could revolutionise OA therapy in the future.

Inhibition of the MMPs that drive cartilage catabolism within the joint is one of the most attractive targets for future OA therapy. First generation global

MMP inhibitors were developed that target the active site of the MMP that exhibits high sequence specificity throughout the matrixin family. Designed to chelate the zinc ion within the active site they prevent inactivation of the MMPs (Lindsey, 2006). Such early global inhibitors such as Marimstat, which was trialled in cancer patients, elicited reversible toxic side effects typically muscoskeletal effects such as tendonitis and inflammatory joint pain (Brown, 2000). Such side effects occur as a result of the lack of selectivity of Marimstat, such that it inhibits MMPs needed for normal physiological processes.

Second generation small molecule MMP inhibitors have been trialled in arthritis with varying degrees of success (Milner *et al.*, 2005). Tanomastat, a selective inhibitor of MMP-2, MMP-3, MMP-9 and MMP-13 was employed successfully in both canine and guinea pig models of OA. A subsequent clinical trial in OA patients demonstrated that the agent was well tolerated, but was subsequently withdrawn after safety issues in a cancer study employing Tanomastat (Leff *et al.*, 2003) A second agent, Trocade designed to selectively target the collagenases MMP-1, MMP-8 and MMP-13, and to a lesser extent the gelatinases MMP-2 and MMP-9 and the stromelysin MMP-3, has been used successfully to prevent cartilage degradation in the SRT/ORT *in vivo* model of OA (Lewis *et al.*, 1997). Trocade has never been trialled in OA patients, but a clinical trial in RA patients indicated a lack of efficacy in preventing cartilage deterioration (Hemmings *et al.*, 2001).

Despite the development of a number of MMP inhibitors, their use in the treatment of OA still remains a distant prospect, due to the lack of specificity and efficacy of such agents. The physiological necessity of MMPs in the body has also prompted safety fears and indeed the adverse side effects evoked by the

earlier agents, suggests that the development of an agent capable of inhibiting catabolism within the joint without eliciting toxic side effects may prove to be a significant challenge.

A second potential target for altering the catabolic/anabolic balance within the osteoarthritic joint is to target the cytokine and MMP profile present at the transcriptional level. As previously alluded to in section 1.3 a number of cytokines and MMPs have been highlighted as having a critical role in enhancing joint destruction, namely IL-1β , TNFα and four members of the MMP family, MMP-1, MMP-3, MMP-9 and MMP-13. Targeting the expression of these mediators at the transcriptional level could alter catabolism within the joint, with the NFκB cascade highlighted as a potential target for future therapies designed to treat OA. The pathway not only upregulates MMP expression, but is also stimulated by the two key inflammatory cytokines IL-1β and TNFα which can be subsequently expressed by the transcription factor resulting in enhanced catabolism. *In vitro* and *in vivo* studies employing a small molecule inhibitor of the IKK complex, have demonstrated that NFκB inhibition prevented collagen and aggrecan release in IL-1β stimulated cartilage explants and prevented joint destruction in a murine collagen-induced arthritic model (McIntyre *et al.*, 2003; Pattoli *et al.*, 2005). Such observations, whilst encouraging remain to be translated into a clinical therapeutic agent for the treatment of either OA or RA.

As previously described in 1.3.1, IL-1β is believed to be the pivotal cytokine in driving cartilage destruction within the osteoarthritic joint, consequently inhibition of this inflammatory cytokine is speculated to significantly reduce or possibly halt cartilage deterioration *in vivo*. As a result

of numerous studies a pharmacological agent designed to inhibit IL-1β has been developed; Diacerhein (Fidelix *et al.*, 2006).

1.7 Aims of the thesis.

Implicated in OA, the role of the transcription factor NFκB in disease pathology remains to be fully elucidated.

This thesis aims to examine the role the NFκB signal transduction pathway plays in the disease process by conducting a number of *in vitro* and *in vivo* studies, as an attempt to determine the potential of NFκB as a future therapeutic target for OA. To achieve this during the study I sought to address the following areas:

1) Characterise the major cell types involved in OA synovial pathology, determine their cytokine profile and demonstrate which, if any, are the critical cytokines implicated in OA synovitis.
2) Demonstrate *in vitro* the efficacy of NFκB inhibition in synovial derived models.
3) Examine the effect of NFκB inhibition upon cartilage deterioration *in vitro*
4) Determine the efficacy of small molecule inhibitors of NFκB upon joint destruction in a murine model of OA.

CHAPTER TWO

Materials & Methods

2.1 Reagents

2.1.1 Chemicals

All chemicals were purchased from Sigma-Aldrich (Dorset, UK) unless stated otherwise.

2.1.2 Tissue culture consumables & reagents

(i) All tissue culture flasks (T25's, T80's and T125's), petri-dishes and tissue culture plates (6 well, 12 well, 24 well, 48 well and 96 well) were supplied by Nalge, Nunc International, New York, USA.

(ii) Tissue culture media used for the growth of all cells throughout this study was Dulbecco's Modified Eagle's Media (D-MEM/F12) without L-Glutamine (Gibco-Invitrogen, Paisley, UK) supplemented with 2mM L-Glutamine (Invitrogen, Paisley, UK), 10units/ml Penicillin-Streptomycin (Invitrogen),1% insulin-transferrin-slenium (Invitrogen) and 10% fetal calf serum (FCS) (Biosera, Ringmer, East Sussex, UK) unless stated otherwise. FCS was heat-inactivated for 30 minutes at 56°C prior to use.

(iii) PBS used for tissue culture techniques was supplied by Gibco - Invitrogen

2.1.3 Recombinant Human Cytokines

Recombinant IL-1β and TNFα used for the stimulation of *in vitro* model systems was supplied by R & D Systems Europe, Abingdon, UK.

2.1.4 Distilled water (dH_2O)

dH_2O was obtained from a Millipore reverse osmosis system followed by filtration through two ion exchange resin columns using a Millipore Milli-Q system. dH_2O was used for the preparation of buffers, reagents and stains throughout this study.

2.2 Adenoviruses

The recombinant adenoviral vectors encoding porcine IκBα (AdvIκBα), green fluorescent protein (AdVGFP), the β-galactosidase gene (AdVβGal) and the functional adenovirus without an insert (AdV0) were a kind gift from Dr A Brynes, Dr M Wood and Dr R de Martin through collaboration with the Kennedy Institute, London, UK. The crude viral lysate used in the AdVIKK2dn studies was a kind gift of Prof M Feldmann of the Kennedy Institute, London, UK. All viruses used in this study were first generation, E1 and E3 deleted, serotype 5.

2.2.1 Adenoviral amplification and purification

The steps outlined in Figure 2.1 were performed to amplify the AdVIKK2dn lysate. The amplified viral lysate was purified by a standard double caesium chloride purification procedure to remove cellular contaminants and unpackaged viral particles as outlined in Figure 2.2. In order to determine the quantity of infectious adenoviral particles present in the purified stock virus, plaque assay assessment was performed following the steps outlined in Figure 2.3. Titration by plaque assay in 293 cells allows the plaques/holes caused by lytic infections to be counted determining the plaque forming units per millilitre (pfu/ml).

2.2.2 Adenoviral infectability studies

The efficacy of adenoviral infection across a range of multiplicity of infections (MOIs) was assessed by UV microscopy. OA-SF were plated into 12 well plates at a concentration of 2 x 10^5 in DMEM/F12 and left to adhere overnight. Following the overnight adherence period, the existing media was removed from the cells and replaced with 300μl of serum-free D-MEM/F12 and

a range of viral titres of AdVGFP were employed to infect OA-SF. At 48 hours post transfection OA-SF were visualised by UV microscopy, the expression of the green fluorescent protein determined by visual analysis.

Figure 2.1 Adenoviral amplification

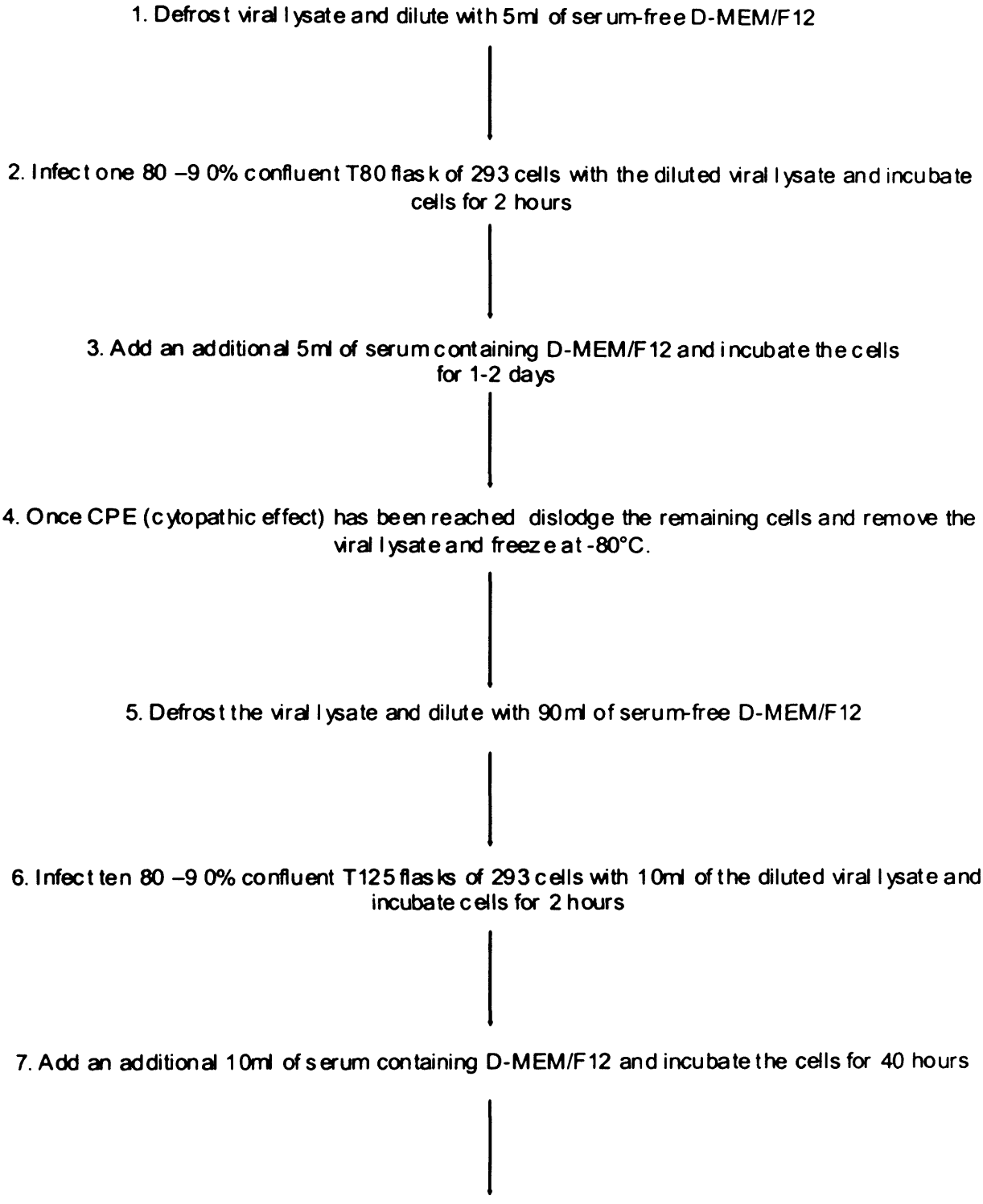

Figure 2.2 Caesium chloride purification of recombinant adenovirus

1. The viral lysate produced in step 8 of figure 2.1 is collected in 4 50ml centrifuge tubes and centrifuged at 200 x G

↓

2. Discard the supernatant, combine the 4 pellets and resuspend in 10ml of serum free D-MEM/F12, centrifuge at 200 x G

↓

3. Discard the supernatant,resuspend the pellet in 10ml of Tris-HCl pH 8

↓

4. Split the viral lysate into two 10ml cryogenic vials and freeze/thaw (-80°C) three times

↓

5. Place the viral lysate into a clean 50ml centrifuge tube and pass the lysate 4 times through a 19G needle to shear the chromatin

↓

6. Centrifuge the viral lysate at 400 x G for 5 minutes

↓

7. Discard the cell pellet. Note the volume of the supernatant and add 0.1M Tris-HCl pH 8 to a total volume of 11.4ml. Add 6.6ml of saturated CsCl and mix throughly

↓

8. Divide the viral supernatant into 2 ultra centrifuge tubes using a 19G syringe needle and 10ml syringe needle, top up the tube with 0.1M Tris-HCl pH 8

↓

9. Centrifuge tubes at 180,000 x G overnight (at least 8 hours) at 4°C

↓

10. Remove the tubes from the centrifuge and place into a clampstand

↓

11. Puncture the wall of the ultracentrifuge tube using a 19G needle and 5ml syringe several millimetres below the viral band. Carefully remove the viral band. Place a finger over the top of the ultra centrifuge tube and withdraw the needle. Insert a second needle and remove the contaminated viral containing media to below the puncture hole.

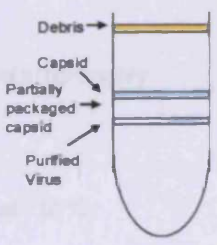

↓

Figure 2.2 continued

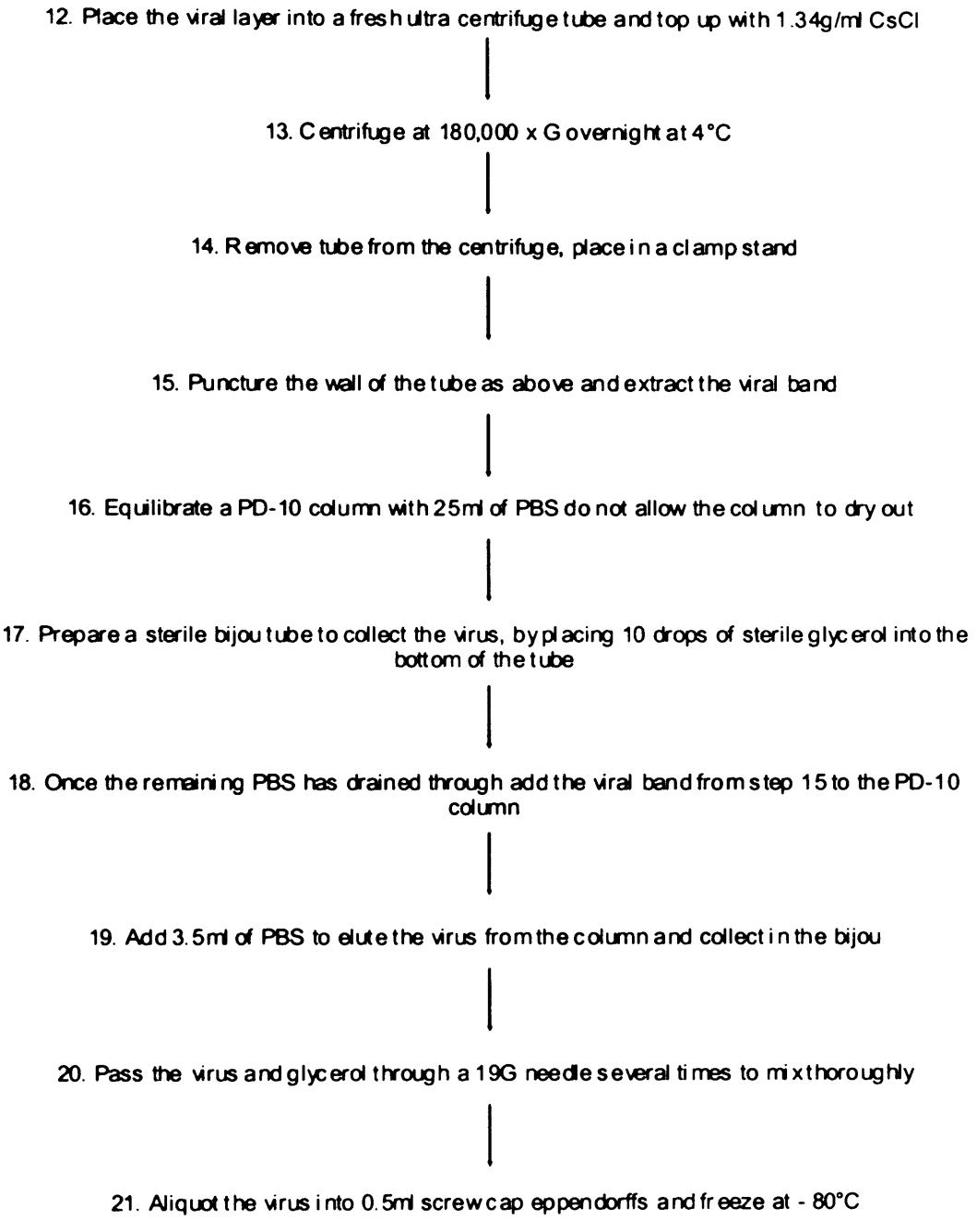

Figure 2.3 Plaque formation

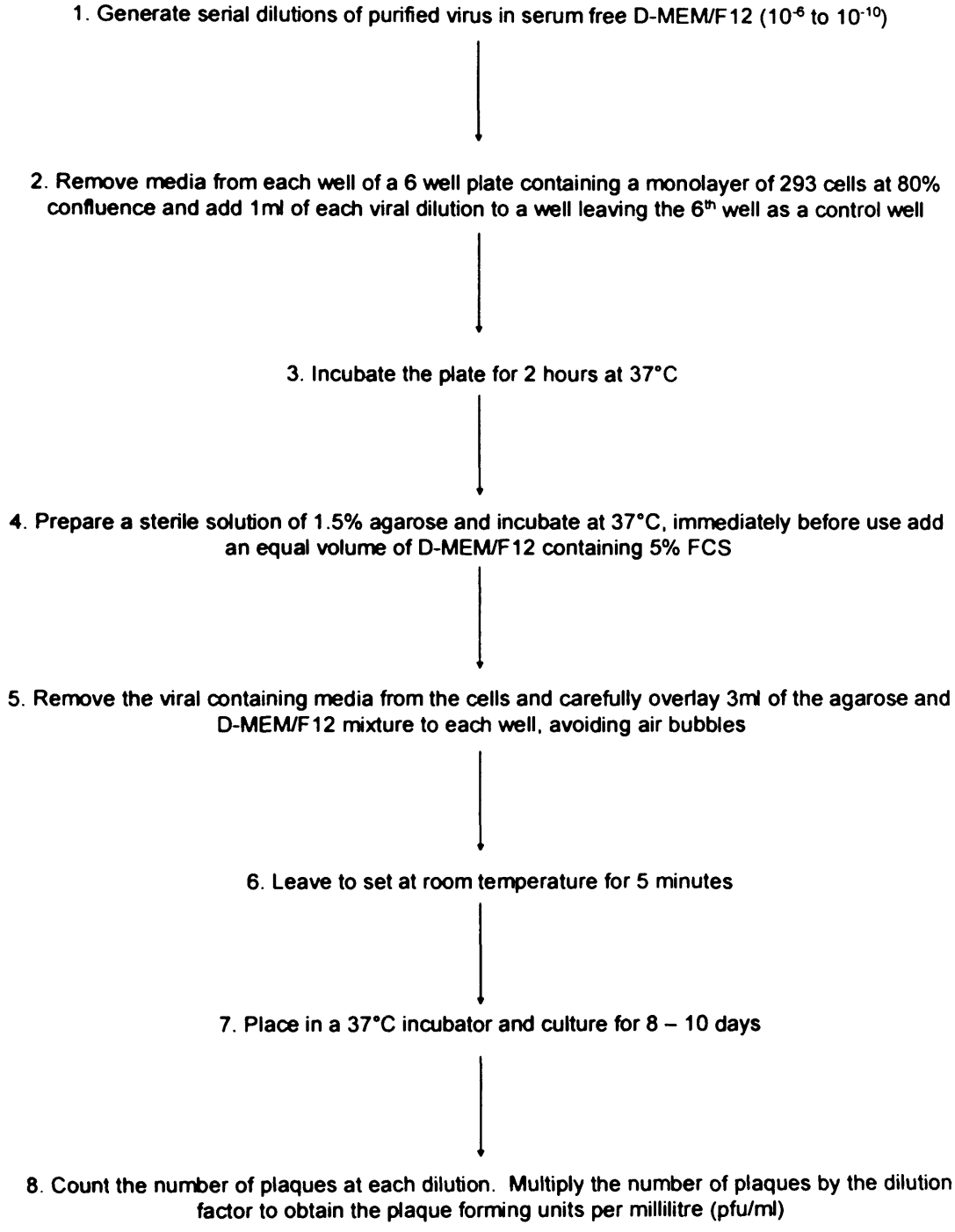

2.3 IL-1β and TNFα neutralising agents

Anti-Cytokine agents were used to inhibit the production of TNFα and IL-1β *in vitro*. Etanercept (Wyeth, Taplow, Maidenhead, Berkshire, UK), a soluble TNF-receptor Ig Fusion protein was a kind gift of the Rheumatology Outpatients Department, University Hospital of Wales, Cardiff, UK. Anti-IL-1β antibody was supplied by R & D Systems Europe, Abingdon, UK.

2.4 Small molecule NFκB inhibitors

RO100 and RO919, two pharmacological inhibitors of the IKK step of the NFκB signalling pathway, were a kind gift of Roche, Palo Alto, CA 94304, USA.

2.5 *In vitro* model systems

2.5.1 OA CoCulture Models (OA-COCUL)

2.5.1.1 Synovial membrane digestion method

Synovial tissue specimens were obtained from consenting patients diagnosed with end-stage OA who were undergoing synovectomy at the time of joint replacement surgery. Ethical approval was obtained from Bro-Taf Health Authority (Cardiff, Wales, UK) prior to the commencement of the study (024692 – Proteomic analysis of diseases of the human joint). Following extraction from the joint, synovium was stored at 4°C in PBS prior to digestion. Dissection scissors and forceps were used to cut the synovium into small fragments, before digestion with collagenase (1mg/ml) (Sigma-Aldrich) and DNAse (2000 Kunitz units) (Sigma-Aldrich) in a total volume of 10 – 20ml of

D-MEM/F12 (5% FCS). Tissue was digested at 37°C with mechanical shaking for 2 hours. An additional 10ml of D-MEM/F12 was added to the digested tissue after 2 hours, this was immediately passed through a 100μm filter (BD Biosciences, Cowley, Oxford, UK) to remove any large undigested tissue fragments. The filtered supernatant was centrifuged at 300 x g for 10 minutes. The supernatant was removed from the initial pellet, collected and centrifuged again at 300 x g for 10 minutes to produce a second pellet. The two pellets were combined and resuspended into 10ml of D-MEM/F12, and plated into 2 T25 flasks (5ml/flask). Synovial cells were cultured overnight before removing the non-adherent cells and replacing the media with fresh. Synovial cells were cultured thereafter in D-MEM/F12 with twice weekly media changes until confluence was reached.

2.5.1.2 Isolation and phenotypic characterisation of the cells present in OA-COCUL

Synovial tissue, digested as previously described in 2.5.1.1, generated a mixed cell population containing all the cell types present in osteoarthritic synovium. Cytospins were prepared from this resulting synovial coculture (OA-COCUL) using a Shandon cytospin centrifuge. OA-COCUL were centrifuged at 112.90 x g for 6 minutes. Following centrifugation the resulting specimen slides were airdried prior to fixation in 100% methanol (15 minutes). Specimens were stained for 15 minutes in May-Grunwald (diluted 1:2 from a stock 1 litre solution supplied by BDH Laboratories, Poole, Dorset, UK) and subsequently 15 minutes in Giemsa (diluted 1:10 from a stock 500ml solution supplied by BDH). Specimen slides were washed for 2 minutes in a phosphate buffer pH 6.8 solution prepared by dissolving 1 tablet (Merck, Darmstadt,

Germany) in 1 litre of dH_2O. Slides were air dried and mounted with DPX (Fluka – Sigma-Aldrich).

2.5.1.3 Characterisation of a $CD14^+$ population of cells isolated from OA-COCUL

Synovial tissue digestion, as described in 2.5.1.1, generated a mixed cell population containing all the cell types present in osteoarthritic synovium. The steps outlined in Figure 2.4 were performed to isolate the $CD14^+$ cells from the COCUL. population.

Depletion buffer used throughout was prepared by dissolving 74mg of EDTA (2mM) and 500mg of BSA (0.5%) in 100ml of sterile PBS. Depletion buffer was filtered prior to use. The MiniMACS separation unit, MACS multistand and MS columns were supplied by Miltenyi Biotec, Bergisch Gladbach, Germany and assembled and used according to the manufacturers guidelines.

Due to the diversity of synovial membranes the numbers of cells present in each population varied enormously between experiments, consequently the number of cells was different between experiments but was adjusted to be equal between the total, CD14 depleted and $CD14^+$ populations, typically between 0.3 x 10^6 and 1 x 10^6 cells. Cells were plated into 12 well plates and cultured for 48 hours before harvesting the supernatants.

Figure 2.4 Isolation of a CD14$^+$ population of cells from OA COCUL

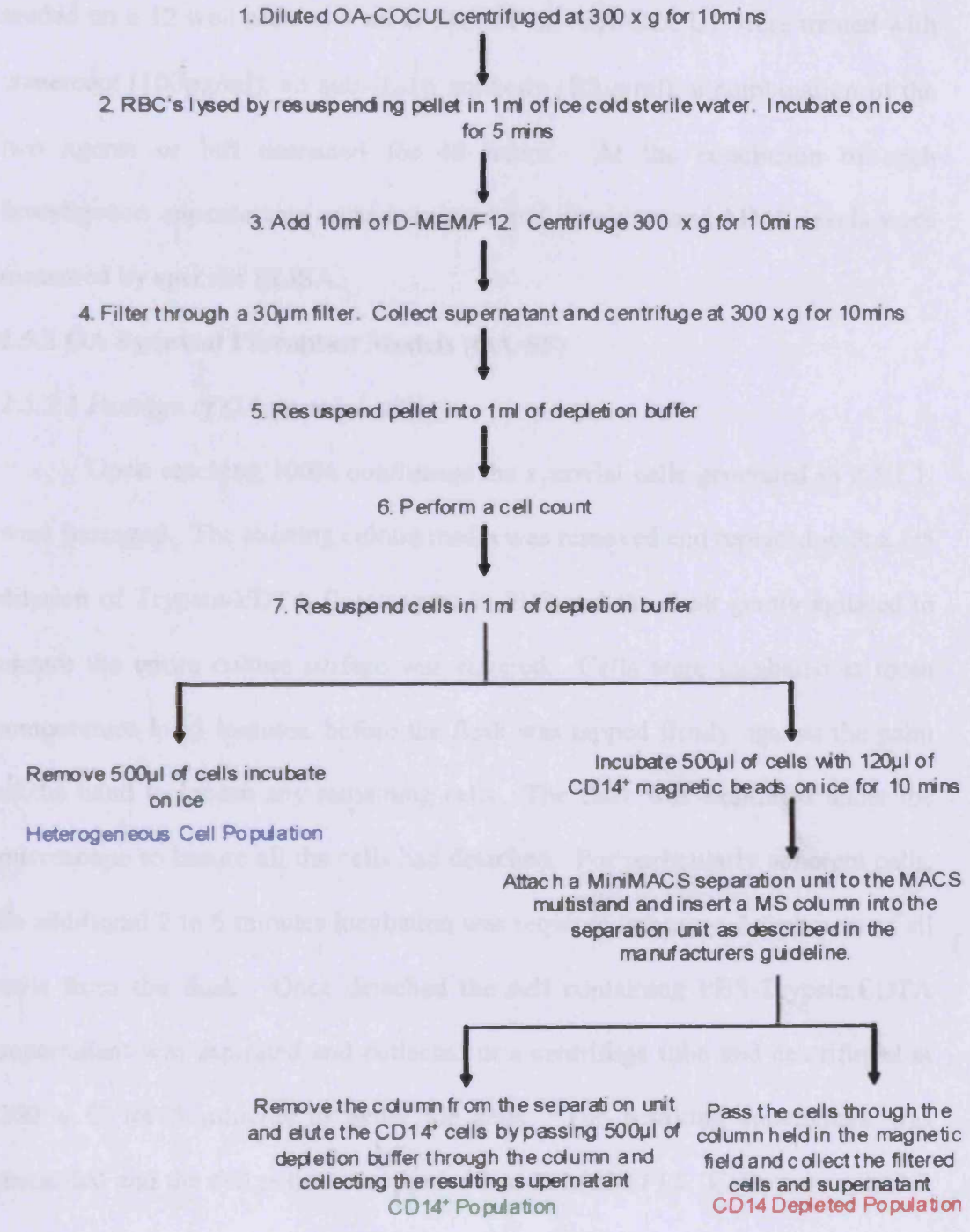

2.5.1.4 Neutralisation of TNFα and IL-1β in OA-COCUL

OA-COCUL were prepared as described in 2.5.1.1. 2 x 10^6 cells were seeded on a 12 well plate in 1 ml D-MEM/F12. OA-COCUL were treated with etanercept (100μg/ml), an anti-IL-1β antibody (10μg/ml), a combination of the two agents or left untreated for 48 hours. At the conclusion of each investigation supernatants were harvested and cytokine and MMP levels were measured by specific ELISA.

2.5.2 OA Synovial Fibroblast Models (OA-SF)

2.5.2.1 Passage of OA synovial cells

Upon reaching 100% confluence the synovial cells generated in 2.5.1.1. were passaged. The existing culture media was removed and replaced with a 1:5 dilution of Trypsin-EDTA (Invitrogen) in PBS and the flask gently agitated to ensure the entire culture surface was covered. Cells were incubated at room temperature for 5 minutes, before the flask was tapped firmly against the palm of the hand to loosen any remaining cells. The flask was examined under the microscope to ensure all the cells had detached. For particularly adherent cells, an additional 2 to 5 minutes incubation was required to ensure detachment of all cells from the flask. Once detached the cell containing PBS-Trypsin:EDTA supernatant was aspirated and collected in a centrifuge tube and centrifuged at 200 x G for 5 minutes to pellet the cells. The resulting supernatant was discarded and the cell pellet resuspended into D-MEM/F12. Cells were split 1:2 between each passage and typically took 7 – 14 days to reach confluence between passages, cells at passages 1 – 6 were cultured in T80 tissue culture flasks in a total volume of 20ml. By passage 3, synovial cells represented a

homogenous population of OA synovial fibroblasts (OA-SF). Studies employing OA-SF used cells between passage 4 and passage 6.

2.5.2.2 Inhibition of NFκB via overexpression of IκBα proteins

OA-SF were plated into 12 well plates at a concentration of 2 x 10^5. Following an overnight adherence period the existing media was removed and replaced with 300μl of serum free D-MEM/F12. AdV0 or AdVIκBα. were employed at an MOI of 30:1 to infect OA-SF. At 2 hours post infection, the viral containing media was removed and replaced with 1ml of fresh D-MEM/F12. OA-SF were stimulated at 24 hours post-infection with IL-1β (20ng/ml) or TNFα (20ng/ml), cells were left for an additional 24 hours before the supernatants were harvested and cytokine and MMP production quantified by specific ELISA.

2.5.2.3. Inhibition of NFκB via the IKK complex

2 x 10^5 OA-SF were plated into 12 well plates. Following an overnight adherence period the existing media was replaced with 1ml of fresh D-MEM/F12. OA-SF were either left untreated, treated with 1μl of DMSO or treated with a dose (1μM, 0.1μM, 0.03μM) of either RO100 or RO919 for 2 hours before the OA-SF were stimulated with 20ng/ml of IL-1β. Cells were cultured for an additional 24 hours before the supernatants were harvested and cytokine and MMP production quantified by specific ELISA.

2.5.2.4. alamarBlue® cell viability assay

Cell viability was assessed using an alamarBlue® cell viability assay (Biosource Europe, Nivelles, Belgium) according to the manufacturer's guidelines. Briefly the alamarBlue® assay incorporates a colorimetric indicator that allows detection of metabolically active cells. The viability of cells cultured

in culture media alone was compared to cells undergoing other treatment conditions during the same experiment. The viability of cells was expressed as a percentage using the following equation;

$$\frac{(\varepsilon ox\lambda_2)(A\lambda_1) - (\varepsilon ox\lambda_1)(A\lambda_2)}{(\varepsilon red\lambda_1)(A°\lambda_2) - (\varepsilon red\lambda_2)(A°\lambda_1)} \times 100$$

Where:

$(\varepsilon ox\lambda 2)$ = 117,216 (Molar extinction coefficient of oxidised alamarBlue® at 600nm)

$(A\lambda_1)$ = Absorbance of test wells at 570nm

$(\varepsilon ox\lambda_1)$ = 80,586 (Molar extinction coefficient of oxidised alamarBlue® at 570nm)

$(A\lambda_2)$ = Absorbance of test wells at 600nm

$(\varepsilon red\lambda_1)$ = 155,677 (Molar extinction coefficient of reduced alamarBlue® at 570nm)

$(A°\lambda_2)$ = Absorbance of control wells, containing alamarBlue® solution but no cells at 600nm (Blank)

$(\varepsilon red\lambda_2)$ = 14, 652 (Molar extinction coefficient of reduced alamarBlue® at 600nm)

$(A°\lambda_1)$ = Absorbance of control wells, containing alamarBlue® solution but no cells at 570nm (Blank)

2.5.3 OA Synovial Explants (OA-EXP)

2.5.3.1 Comparative efficacy of anti-cytokine strategies and IKK inhibitors in OA-EXP

OA-EXP were excised at random from synovial membrane specimens and weighed prior to experimental investigation. OA-EXP were dispensed into 1.5ml of D-MEM/F12 into 12 well plates and allowed to equilibrate for 18 hours. Supernatant samples taken at this time provided baseline measurements for each mediator prior to the initiation of treatment protocols. The baseline

value (100% mediator production) for each well was used as the reference point against which subsequent responses to individual treatment was compared. To accommodate the intra-variability present within each synovial sample, treatment conditions were conducted in triplicate or quadruplicate depending upon the size of the original synovial specimen and the mean calculated for each treatment strategy.

OA-EXP were either left untreated or were treated with a combination of etanercept and anti-IL-1β (at the doses stated in 2.5.1.4) or a 0.1μM dose of RO100 for 24 hours before the experiment was terminated and the supernatants were harvested and cytokine and MMP production quantified by specific ELISA.

2.5.4 *In vitro* model of early OA pathological changes

2.5.4.1 Effect of IL-1β on bovine cartilage explants

Bovine articular cartilage was obtained from 7 day old animals shortly after sacrifice. Cartilage explants were aseptically removed from the metacarpophalangeal joint using a scalpel. Care was taken to ensure that explants were of approximately equal size and no subchondral bone was present. Explants were cultured overnight in D-MEM/F12 to allow the cartilage to equilibrate prior to commencing experimental analysis.

OA-SF were seeded at 0.75 x 10^5 into 12 well plates. OA-SF were cultured for 48 hours allowing the cells to adhere and reach approximately 80% confluence prior to the addition of the cartilage explants. The combination of OA-SF and cartilage explants were either stimulated with an increasing dose of IL-1β (0.2ng, 2ng, 20ng) or were left unstimulated. Culture media was replaced on alternate days and the cultures retreated with IL-1β, at 10 days the study was

terminated. Cartilage explants were removed and fixed in NBFS for histological analysis whilst the viability of OA-SF was assessed using the alamarBlue® assay.

2.5.4.2 Inhibition of NFκB via IKK in the early stage model of OA pathology

Murine patellas were excised from the hind limbs of healthy wild type adult mice shortly after sacrifice using dissection forceps and a scalpel. Direct contact with the patella was avoided to minimise damage to the cartilage surface. Patellas were cultured overnight in D-MEM/F12 prior to commencing experimental analysis.

OA-SF were seeded at 0.75 x 10^5 into 12 well plates and cultured for 48 hours allowing the cells to adhere and reach approximately 80% confluence prior to the addition of the murine patellas. The OA-SF, cultured in combination with murine patellas, were either left untreated or treated with a dose range (1μM, 0.1μM, 0.03μM) of either RO100 or RO919 for 2 hours. After 2 hours cultures were stimulated with a 20ng dose of IL-1β. Culture media was removed every 48hours and replaced with fresh D-MEM/F12 before the cultures were retreated and restimulated as described previously. At 10 days the experiment was terminated, the murine patellas were removed and fixed in NBFS for histological analysis, whilst the viability of the OA-SF was assessed by the alamarBlue® assay.

2.6 Enzyme linked immunoabsorbent assay (ELISA)

2.6.1 ELISA Buffers

PBS used for wash buffers was supplied in tablet form by Oxoid, Basingstoke, UK. One tablet was dissolved per 100ml of dH_2O

2.6.1.1 Blocking Buffer

Blocking buffer used for IL-6, IL-8, IL-1β, TNFα and MMP-3 ELISAs contained PBS with 5mg/ml BSA. CCL2, CCL5, OSM, TNFR1, TIMP-1 and MMP-1 ELISAs used PBS containing 10mg/ml BSA.

2.6.1.2 Wash Buffer

Wash Buffer used in IL -6, IL-8, IL-1β, TNFα and MMP-3 ELISAs contained PBS with 0.1% Tween-20. CCL2, CCL5, OSM, TNFR1, TIMP-1 and MMP-1 ELISAs used PBS containing 0.05% Tween-20

2.6.1.3 Streptavidin

Streptavidin (Biosource Europe) was reconstituted at 1mg/ml in 1ml of PBS containing 400µl of glycerol (40%) and 0.1mg of thimerosal (0.01%).

2.6.1.4 Citrate Buffer

8.4g of citric acid (0.2M) was dissolved at room temperature in 200ml of dH_2O. The pH of the solution was adjusted to 3.95 by the addition of a potassium hydroxide solution.

2.6.1.5 Tetramethylbenzidine (TMB)

240mg of TMB was dissolved at a concentration of (0.1M) in 5ml of dimethyl sulphoxide (DMSO) and 5ml of ethanol, and stored at 4°C.

2.6.1.6 Developing Solution

Developing solution used for all ELISAs (except MMP-9 and MMP-13) was freshly prepared and contained 10ml of citrate buffer, 10µl of hydrogen peroxide (H_2O_2, 30% w/v) and 100µl of previously prepared TMB solution per 96 well ELISA plate.

2.6.2 Cytokine quantification by ELISA

2.6.2.1 Quantification of Interlukin-6 (IL-6)

IL-6 levels were measured using a specific Biosource Europe ELISA kit (Human IL-6 Cytoset-CHC1264) following the manufacturers protocol supplied with each kit.

Briefly 96 well ELISA plates (Nunc International) were coated with 100µl of specific capture antibody (10µl of IL-6 capture antibody diluted in 10mls of PBS) and incubated overnight at 4°C with mechanical shaking. Following incubation the antibody was discarded and the plate blocked at room temperature with 300µl of blocking buffer. After 2 hours the plates were washed 4 times with wash buffer. 100µl of diluted specific standards for the ELISA were added in duplicate (sensitivity range: 1000pg/ml – 15.625pg/ml). 100µl of each sample diluted in D-MEM/F12 was added at appropriate dilutions, for IL-6 dilutions between 1:5 and 1:2000 were typically performed. 50µl of detection antibody (4µl of detection antibody diluted in 5.5mls of D-MEM/F12) was added to each well and the plate was incubated for 2 hours at room temperature with mechanical shaking. After 4 washes with wash buffer, 100µl of purified streptavidin-horseradish peroxidase conjugate (Biosource Europe) was added at a dilution of 1:4000 and incubated at room temperature for 30 minutes with mechanical shaking. After 4 final washes, 100µl of developing buffer was added and the colour was developed at room temperature. The reaction was terminated by the addition of 50µl of 12.5% H_2SO_4. The optical density of the plates was measured at 450nm (0.1s).

2.6.2.2 Quantification of IL-1β

IL-1β levels were measured using a specific Biosource Europe ELISA kit (Human IL-1β Cytoset CHC1214) following the procedure outlined for IL-6

in 2.6.2.1, with the following modifications; appropriate dilutions for IL-1β were between 1:2 and 1:50 and streptavidin-horseradish peroxidase conjugate was added at a concentration of 1:2000.

2.6.2.3 Quantification of TNFα

TNFα levels were measured using a specific Biosource Europe ELISA kit (Human TNFα Cytoset CHC1754) following the procedure outlined for IL-6 in 2.6.2.1, with the following modifications; appropriate dilutions for TNFα were between 1:5 and 1:50 and streptavidin-horseradish peroxidase conjugate was added at a concentration of 1:1000.

2.6.2.4 Quantification of Oncostatin-M (OSM)

OSM levels were measured using a specific R & D Systems ELISA kit (Human OSM Duoset-DY295) following the manufacturers protocol supplied with each kit.

Briefly 96 well ELISA plates (Nunc International) were coated with 100µl of specific capture antibody (50µl of OSM capture antibody diluted in 10ml of PBS, final concentration 2.0µg/ml) and incubated overnight at 4°C with mechanical shaking. Following incubation the antibody was discarded and the plate blocked with blocking buffer for 1 hour at room temperature. Following 4 washes with wash buffer, diluted standards specific for the OSM ELISA were added in duplicate to the plate (sensitivity range 2000pg/ml – 31.5pg/ml). 100µl of samples at the appropriate dilution range (1:2 – 1:25) were added to the plate (diluted in PBS containing BSA at 10mg/ml). The plate was incubated at room temperature for 2 hours with mechanical shaking. Following 4 washes with wash buffer, 100µl of detection antibody was added to each well at a concentration of 30ng/ml and the plate incubated for 2 hours at room

temperature with mechanical shaking. Following 4 washes with wash buffer 100µl of streptavidin-horseradish peroxidase conjugate at a dilution of 1:200 was added to the plate and incubated for 30 minutes at room temperature with mechanical shaking. After 4 final washes, 100µl of developing buffer was added and the colour was developed at room temperature. The reaction was terminated by the addition of 50µl of 12.5% H_2SO_4. The optical density of the plates was measured at 450nm (0.1s).

2.6.3 Chemokine quantification by ELISA

2.6.3.1 Quantification of CXCL8

CXCL8 levels were measured using a specific Biosource Europe ELISA kit (Human CXCL8 Cytoset CHC1754) following the procedure outlined for IL-6 in 2.6.2.1, with the following modifications; appropriate dilutions for CXCL8 were between 1:5 and 1:2000 and streptavidin-horseradish peroxidase conjugate was added at a concentration of 1:8000.

2.6.3.2 Quantification of CCL2

CCL2 levels were measured using a specific R & D Systems ELISA kit (Human CCL2 Duoset-DY279) following the manufacturers protocol supplied with each kit following the procedure outlined for OSM in 2.6.2.4, with the following modifications; the capture and detection antibody concentrations were 1.0µg/ml and 100ng/ml respectively. The sensitivity range for CCL2 was 1035pg/ml – 16pg/ml with appropriate dilutions of samples for CCL2 between 1:5 and 1:100.

2.6.3.3 Quantification of CCL5

CCL5 levels were measured using a specific R & D Systems ELISA kit (Human CCL5 Duoset-DY278) following the manufacturers protocol supplied with each kit following the procedure outlined for OSM in 2.6.2.4, with the following

modifications; the capture and detection antibody concentrations were 1.0μg/ml and 100ng/ml respectively. The sensitivity range for CCL5 was 1035pg/ml – 16pg/ml with appropriate dilutions for samples for CCL5 between 1:5 and 1:50.

2.6.4 MMP and TIMP quantification by ELISA

2.6.4.1 Quantification of MMP-1

A specific sandwich ELISA was developed to measure MMP-1 using matched antibody pairs and recombinant human MMP-1 (R & D Systems Europe). All procedures were carried out at room temperature. Briefly 96 well ELISA plates (Nunc International) were coated with 100μl of monoclonal anti-human MMP-1 antibody (MAB901, R & D Systems Europe) at 1μg/ml diluted in PBS overnight with mechanical shaking. Following incubation the antibody was discarded and plates were blocked for 1 hour at room temperature with 300μl of 1% BSA/PBS. Plates were washed 4 times in PBS with 0.05% Tween-20 (pH 7.2 – 7.4) added. 100μl of diluted recombinant human MMP-1 (901-MP, R & D Systems Europe) standards (3.125 – 200ng/ml) were added in duplicate. 100μl of each sample diluted in 1% BSA/PBS (appropriate dilutions were between 1:2 – 1:100) were added accordingly and incubated for 1.5 hours at room temperature with mechanical shaking. After 4 washes 100μl of biotinylated anti-human MMP-1 antibody (BAF901, R & D Systems Europe) at 0.03μg/ml diluted in 1% BSA/PBS was added and incubated for 1 hour at room temperature with mechanical shaking. Following 4 washes, 100μl of purified streptavidin-horseradish peroxidase conjugate (Biosource Europe) at 1μg/ml was added and incubated for 30 minutes at room temperature with mechanical shaking. After 4 final washes, 100μl of developing solution was added and the colour was developed at room temperature. The reaction was terminated by the

addition of 50µl of 12.5% H_2SO_4. The optical density of the plates was measured at 450nm (0.1s) using a Wallac Victor 2 plate reader.

2.6.4.2 Quantification of MMP-3

MMP-3 levels were measured using a specific Biosource Europe ELISA kit (Human MMP-3 Cytoset CHC1544) following the procedure outlined for IL-6 in 2.6.2.1, with the following modifications; the sensitivity range for MMP-3 was 20ng/ml – 0.3125ng/ml. The appropriate dilutions for MMP-3 were routinely between 1:5 and 1:100 and streptavidin-horseradish peroxidase conjugate was added at a concentration of 1:1000.

2.6.4.3 Quantification of MMP-9

MMP-9 levels were quantified using specific R & D Quantikine ELISA kits (Human MMP-9 Immunoassay DMP-900) following the manufacturers protocol supplied with each kit.

Briefly, 96 well ELISA plates were supplied pre-coated with the relevant capture antibody and preblocked. 100µl of assay diluent was added to each well on the plate. Standards were prepared by adding 100µl of supplied standard + 900µl of calibrator and doubling dilutions thereafter (sensitivity range 10ng/ml – 0.156ng/ml), 50µl of the standards were added to the plate. 50µl of each sample diluted accordingly with calibrator diluent was added to the plate, for MMP-9 appropriate sample dilutions were 1:10. The plate was incubated for 2 hours at room temperature with mechanical shaking. Following 4 washes with the wash buffer provided with the kit, 200µl of MMP-9 conjugate was added to each well and the plate incubated at room temperature for 2 hours with mechanical shaking. After 4 washes 200µl of the substrate solution supplied with the kit was added to each well and the plate incubated for 30 minutes at room

temperature in the dark. After 30 minutes 50µl of stop solution supplied with the kit was added to each well to terminate the reaction. The optical density of the plates was measured at 450nm (0.1s).

2.6.4.4 Quantification of MMP-13

MMP-13 levels were quantified using specific R & D Quantikine ELISA kits (Human MMP-13 Immunoassay DMP-1300) following the procedure outlined for MMP-9 in 2.6.4.3, with the following modifications; the sensitivity range for MMP-13 was 5000pg/ml – 78.125pg/ml. The appropriate sample dilution for MMP-13 was 1:5.

2.6.4.5 Quantification of TIMP-1

TIMP-1 levels were measured using a specific R & D Systems ELISA kit (Human TIMP-1 Duoset-DY970) following the procedure outlined for OSM in 2.6.2.4, with the following modifications; the capture and detection antibody concentrations were 2.0µg/ml and 50ng/ml respectively. The sensitivity range for TIMP-1 was 1936pg/ml – 30.25pg/ml with appropriate dilutions for samples for TIMP-1 between 1:100 and 1:1000.

2.6.5 Cartilage Oligomeric Matrix Protein (COMP) quantification by ELISA

2.6.5.1 Quantification of soluble COMP

COMP levels were measured using a specific MD Biosciences (Zurich, Switzerland) ELISA kit (Animal COMP ELISA kit A-COMP.96) following the manufacturers protocol supplied with the kit.

Briefly 96 well ELISA plates were supplied pre-coated with the relevant capture antibody and preblocked. 50µl of each sample diluted accordingly (1:8 dilutions) with the sample buffer provided was added to the plate. COMP

calibrators (standards) were supplied ready prepared, 50µl of each calibrator was added in duplicate to the plate (sensitivity range 0.9 U/L – 0.055 U/L) prior to the addition of 50µl of polyclonal antibody. The plate was incubated for 2 hours at room temperature with mechanical shaking. Following 6 washes with the wash buffer provided with the kit, 50µl of conjugate was added to each well on the plate and incubated at room temperature for 1 hour with mechanical shaking. After 6 washes 100µl of enzyme substrate was added to each well on the plate and incubated for 15 minutes at room temperature. After 15 minutes 50µl of stop solution supplied with the kit was added to terminate the reaction. The optical density of the plate was measured at 450nm (0.1s).

2.7 Electrophoretic Mobility Shift Assays (EMSAs)

2.7.1 Cytosolic & Nuclear Extraction Buffers

Prior to extraction the following stock solutions were prepared:

(i) 2.38g of HEPES dissolved in 100ml of dH_2O (100mM, pH to 7.9 at 4°C)

(ii) 142mg of $MgCl_2$ dissolved in 100ml of dH_2O (15mM)

(iii) 745mg of KCl dissolved in 100ml of dH_2O (100mM)

(iv) 74mg of EDTA dissolved in 100ml of dH_2O (2mM).

(v) 298mg of HEPES dissolved in 100mls dH_2O (8mM, pH to 7.9 at 4°C)

(vi) 186mg of KCl dissolved in 100ml of dH_2O (25mM)

(vii) 3.7mg of EDTA dissolved in 100ml of dH_2O (0.1mM)

Buffer A (prepared fresh):

10ml of 100mM HEPES

10ml of 15mM $MgCl_2$

10ml of 100mM KCl

70ml of dH_2O

Immediately prior to use add:

0.5mM DTT

0.5mM PMSF

5μg/ml Aprotinin

5μg/ml Pepstatin A

30μg/ml Leupeptin

Buffer C (prepared fresh):

20ml of 100mM HEPES

10ml of 15mM $MgCl_2$

10ml of 100mM KCl

10ml of 2mM EDTA

25ml of Glycerol

2.45g of NaCl (0.42M final concentration)

25ml of dH_2O

Immediately prior to use add:

0.5mM DTT

0.5mM PMSF

5μg/ml Aprotinin

5μg/ml Pepstatin A

30μg/ml Leupeptin

Buffer D (prepared fresh):

80μl of 8mM HEPES

400μl of 25mM KCl

2μl of 0.1mM EDTA

0.5mM DTT

40µl of Glycerol

2.7.2 Isolation of nuclear extracts

OA-SF were dispensed at a concentration of 1 x 10^6 cells/well into 6 well plates. Cells were stimulated with IL-1β (20ng/ml) for 30 minutes before terminating the stimulation using ice cold PBS. Nuclear extracts were prepared as described previously by Dignam et al (Dignam *et al.*, 1983). Briefly, cells were detached using mechanical agitation, collected and centrifuged at 3000g. Cells were washed in Buffer A and centrifuged at 12,000g. OA-SF were incubated with 400µl of Buffer A + 0.125% IPEGAL (equivalent to the non-ionic surfactant Nonidet-P40) on ice for 5 minutes. OA-SF were centrifuged at 12,000g for 5mins and the resulting pellet resuspended in 100µl of Buffer C and incubated at 4°C with mechanical shaking for 60 minutes. OA-SF were centrifuged at 13,000g, before the supernatant was collected and 100µl of Buffer D added.

2.7.3 Protein quantification of nuclear extracts

The protein content of each nuclear extract was established using a BCA protein assay kit (Pierce, USA) according to the manufacturer's guidelines. Briefly 10µl of standards (2000µg/ml – 31µg/ml) prepared by performing doubling dilutions of a stock standard of 2mg/ml BSA dissolved in PBS. Doubling dilutions of samples were prepared and 10µl of each sample added to the plate. 200µl of prepared BCA solution (15mls BCA solution A + 0.3mls of BCA Solution B) was added to each well and the plate was incubated for 30 minutes at 37°C. The optical density of the plate was measured at 540nm (0.1s)

2.7.4 EMSA buffers & reagents

2.7.4.1 5 x TBE

5 x TBE was prepared by dissolving 54g of TRIS and 27.5g of boric acid in 980ml of dH_2O. 20ml of a 0.5M EDTA solution (18.6g in 100ml of dH_2O) was added and the solution mixed thoroughly.

2.7.4.2 4% Polyacrylamide Gel

Separating gels used for EMSA were comprised of 40% w/v acrylamide (5ml), 5 x TBE (10ml), dH_2O (35ml), TEMED (20µl) and ammonium persulfate (0.1g).

2.7.4.3 Running Buffer

A 0.5 x running buffer was used for the separation of protein-DNA complexes, comprised of 100ml of 5 x TBE and 900ml of dH_20.

2.7.4.4 Oligonucleotides

NFκB oligo (5'-AGT TGA GGG GAC TTT CCC AGG C-3', 3'-TCA ACT CCC CTG AAA GGG TCC G-5'), AP-1 consensus oligo (5'-CGC TTG ATG ACT CAG CCG GAA-3', 3'-GCG AAC TAC TGA GTC GGC CTT-5') and AP-1 mutant oligo (5'-CGC TTG ATG ACT TGG CCG GAA-3', 3'-GCG AAC TAC TGA ACC GGC CTT-5') (Promega, Southampton, UK)

2.7.5 NFκB EMSAs

4µg of each nuclear extract was incubated with 10x binding buffer (40% glycerol, 10mM EDTA, 50mM DTT, 100mM TRIS pH 7.5, 1M NaCl, 1mg/ml nuclease free BSA), 2µg of non-specific DNA competitor (polydIdC) and 1µl of radiolabelled ^{32}P oligo probe for NFκB at room temperature for 30 minutes. For the cold competitor and non-self EMSA, 25-fold excess of unlabelled NFκB oligo or 10-fold excess of AP-1 consensus oligo or 10-fold excess of AP-1 mutant oligo was added to the samples and incubated on ice for 30 minutes prior

to addition of radiolabelled probe. Protein-DNA complexes were resolved on a 4% polyacrylamide gel for 80 minutes and visualized by autoradiograph.

2.8 *In vivo* studies

2.8.1 General

All experiments were performed in strict accordance with the Animals (Scientific Procedures) 1986 Act. All procedures performed were conducted as detailed in the project licence 30/2361 and personal licence 30/7435.

2.8.2 Purchase of animals

Wild type C57/Blk6 mice were used for all *in vivo* studies and were purchased from Charles River, UK. Mice were allowed to settle for 4 – 7 days following delivery before commencement of experimental procedures. Mice were aged between 8 – 10 weeks at the start of each experiment and were male.

2.8.3 Housing of Mice

All mice were located at the Biomedical Services Unit at the Heath Park site of Cardiff University. Mice were kept in groups of between 6 – 9 animals per cage, and were provided a diet of standard mouse chow, with water *ad libitum*, in rooms with a temperature range of 18 - 22°C with 12 hour light-dark cycles. To minimise discomfort to the animals all mice were housed in solid bottomed cages as opposed to wire bottom cages.

2.8.4 Arthritis Induction

A monoiodoacetate (MIA) murine arthritis model was used as a model of OA. Prior to induction of arthritis baseline weight and knee diameter measurements were taken and venous tail bleeds performed. Mice were anaesthetised with isoflurane/oxygen and given a single intraarticular injection

of 3mg/ml MIA (Sigma Aldrich) into their right knee. MIA was dissolved in dH_2O. Mice were randomly assigned a treatment group, 6 animals were given 10µl of 3mg/ml MIA + 10µl of DMSO, 6 were given a 10µl of 3mg/ml MIA + 10µl of 5mM of RO100 and 6 were given a 10µl of 3mg/ml MIA + 10µl of 5mM of RO919. All injections were performed using 27 gauge needles to minimise trauma. The left contralateral knee did not receive any injections and was used as the normal control for the study.

2.8.5 Murine knee diameter assessment

Changes in the diameter of the right knee joint, as a result of inflammatory swelling, was assessed by measuring both the left and right knee joints using an analogue micrometer. Measurements were performed prior to induction of arthritis, at days 1, 2 and 3 post- induction, an additional two measurements were taken prior to termination of the experiment at day 14. The swelling associated with the induction of arthritis was expressed as the difference in diameters between the mean of the right (arthritic) knee readings and left (control).

2.8.6 Histological sections of murine knee joints

Mice from the 3 different treatment groups were sacrificed 14 days post-arthritis induction. In a supplementary experiment 3 additional mice from each treatment group were sacrificed at day 1 post-arthritis induction. Both the right (arthritic) knees and left (control) knees were removed intact, the skin removed and the joints histologically analysed as detailed in 2.9.5.

2.8.7 Determination of serum markers of cartilage degradation

Tail bleeds were performed from three mice from each treatment group at baseline, day 1, day 7 and day 14. The serum was isolated from whole blood

by centrifuging the freshly isolated blood samples at 300 x G for 5 minutes and extracting the serum using a pasteur pipette prior to the levels of COMP being quantified by specific ELISA.

2.9 Histology

2.9.1 Histological Buffers & Stains

The following stock solutions were routinely used for all histological staining procedures:

(i) Neutral Buffered Formalin Solution (NBFS)

Tissue specimens were fixed in NBFS fixative comprised of 100mls of 10x PBS, 100mls of 37% w/v formaldehyde and 800mls of dH_2O. The pH was adjusted to 7.0 by the addition of a potassium hydroxide solution.

(ii) Decalcification Buffer

Specimens were decalcified in a 10% formic acid solution, comprised of 100mls of formic acid (Fischer, Loughborough, Leicestershire, UK), 50mls of 37% w/v formaldehyde and 850mls of dH_2O.

(iii) Tris Buffered Saline (TBS)

TBS was prepared by dissolving 61g of TRIS (0.5M), 90g of NaCl (1.5M) in 1 litre of dH_2O. The pH of TBS was adjusted to pH 7.6 by the addition of HCl.

(iv) 100%, 90% & 70% Alcohols – ethanol used throughout

(v) Eosin (1%)

10g of Eosin (Fischer, UK) dissolved in 1 litre of dH_2O

(vi) Scotts Tap Water

3.5g of $NaHCO_3$ and 20g of $MgSO_4$ dissolved in 1 litre of dH_2O

(vii) Toluidine blue (0.125%)

1g of sodium acetate and 1.5g of sodium barbitone dissolved in 1 litre of dH_2O, add 1ml of HCl and adjust the pH to 5. Dissolve 1.25g of toluidine blue (Gurr – BDH Laboratories, Poole, Dorset, UK) in the solution and filter.

(vii) Fast Green (0.02%)

80mg of fast green (Sigma-Aldrich) dissolved in 400ml of dH_2O

(viii) Safranin-O (0.1%)

400mg of safranin-o (Sigma-Aldrich) dissolved in 400ml of dH_2O

(ix) 1% acetic acid

4mls of glacial acetic acid (Fischer, UK) diluted in 400ml of dH_2O

2.9.1.1 Shandon Tissue Processor Cycles

(i) Murine Knee Joints:

70% alcohol (30mins), 90% alcohol (1hour), 100% alcohol (1 hour), 100% alcohol (1 hour), 100% alcohol (1 hour), 100% alcohol (1 hour), 100% Alcohol (1 hour), xylene (1 hour @ 37° C), xylene (1 hour @ 37° C), xylene (1 hour @ 45° C), wax (1 hour @ 60° C), wax (1 hour @ 60° C), wax (1 hour @ 60° C), wax (1 hour @ 60° C).

(ii) Synovial Tissue:

70% alcohol (1 hour and 30mins), 90% alcohol (1hour and 30mins), 100% alcohol (1 hour), 100% alcohol (1 hour), 100% alcohol (1 hour), 100% alcohol (1 hour), 100% alcohol (1 hour), xylene (1hour and 30mins @ room temperature), xylene (2 hours @ 37° C), xylene (2 hours @ 45° C), wax (2 hours @ 60° C), wax (1hour and 30mins @ 60° C), wax (1hour and 30mins @ 60° C), wax (1hour and 30mins @ 60° C).

2.9.2 Histological characterisation of synovial membranes

Synovial membrane specimens were fixed in NBFS (as described in 2.9.1 (i)) overnight at 4°C. Tissues were placed in an automated Shandon Tissue Processor and taken through the serial dehydration cycles of ethanol and xylene (detailed in 2.9.1.2 (ii)) before being permeated with wax at 60°C. Tissue was then embedded in wax blocks using a Shandon Histocentre. Serial sections (7μM) thick were cut with a microtome and situated on microscope slides (Menzel-Glaser Superfrost Plus).

2.9.2.1 Haematoxylin & eosin staining procedure

Synovial membrane sections were stained with haemotoxylin & eosin to allow histological analysis. Briefly, sections were deparaffinised by immersing slides in 3 changes of xylene (5 minutes), then washing slides in descending alcohols (100%, 100%, 90%, 70% ethanol x 3 minute washes). Slides were hydrated by washing in running tap water for 5 minutes and then rinsing in distilled water for 10 seconds before staining sections for 90 seconds in Mayers haematoxylin (supplied as a ready to use solution by BDH Laboratories). Excess haematoxylin was removed from the sections by washing the slides in running tap water for 5 minutes before rinsing in distilled water for 10 seconds. Slides were immersed in Scott's tap water for 10 to 30 seconds to enhance the blue staining of the haematoxylin. Excess Scott's tap water was removed from the slides by washing the slides in running tap water for 5 minutes and rinsing in distilled water for 10 seconds, before staining for 90 seconds with eosin. Excess eosin was removed from the sections by washing in running tap water for 5 minutes before rinsing in distilled tap water for 10 seconds. Slides were then washed in ascending alcohols to dehydrate the slides (90% 1 min, 100%, 100%,

100% x 3 minute washes) and then placed into washes of xylene (5 minutes). Slides were mounted using Ralmounts (BDH, UK).

2.9.3 Histological characterisation of bovine cartilage explants

Bovine cartilage explants were fixed in NBFS (as described in 2.9.1 (i)) overnight at 4°C. Explants were placed in an automated Shandon Tissue Processor and taken through the serial dehydration cycles of ethanol and xylene (detailed in 2.9.1.2 (i)) before being permeated with wax at 60°C. Explants were then embedded in wax blocks using a Shandon Histocentre. Serial sections (7μM) thick were cut with a microtome and situated on microscope slides.

2.9.3.1 Safranin-O & Fast Green staining procedure

Bovine explant sections were stained with safranin-o & fast green to allow histological analysis. Briefly, sections were deparaffinsed by immersing slides in 3 changes of xylene (5 minutes), then washing slides in descending alcohols (100%, 100%, 90%, 70% x 3 minute washes). Slides were hydrated by washing in running tap water for 5 minutes and then rinsing in distilled water for 10 seconds before staining slides in Mayers haematoxylin for 90 seconds. Excess haematoxylin was removed from the sections by immersing slides in distilled water for 2 minutes. Haematoxylin staining was enhanced by immersing the sections in Scott's tap water for 1 minute to intensify the blue staining. Excess Scott's tap water was removed by washing slides in distilled water for 2 minutes prior to staining with fast green for 5 minutes. Excess fast green was removed from the slides by rinsing in 1% acetic acid for 10 seconds before staining in safranin-o for 5 minutes. Excess safranin-o was removed by washing the slides in 2 distilled water washes for 2 minutes each. Slides were

dehydrated by washing in ascending alcohols (90%, 100% x 1 minute washes) before immersing in xylene (1minute). Slides were mounted using Ralmounts.

2.9.3.2 Toluidine Blue staining procedure

Bovine explant sections were stained with toludine blue to allow histological analysis. Briefly, sections were deparaffanised in xylene (5minutes x 3 washes) and then washed in descending alcohols for 3 minutes per wash (100%, 100%, 90%, 70%). Slides were hydrated by washing in running tap water for 5 minutes and rinsed in distilled water for 10 seconds prior to staining in toluidine blue for 30 seconds. Excess toluidine blue was removed by washing in tap water (5 minutes) and rinsing in distilled water. Slides were blotted dry using absorbent paper and left to air dry for approximately 10 minutes. Slides were immersed in xylene (2 minutes x 2 washes) and then mounted using DPX mountant.

2.9.4 Histological characterisation of murine patellas

Murine patellas were fixed in NBFS (as described in 2.9.1 (i)) overnight at 4°C. Murine patellas were subsequently decalcified in 10% formic acid (as detailed in 2.9.1 (ii)) until completion as assessed by ammonium oxylate precipitation. Explants were placed in an automated Shandon Tissue Processor and taken through the serial dehydration cycles of ethanol and xylene (detailed in 2.9.1.2 (i)) before being permeated with wax at 60°C. Explants were then embedded in wax blocks using a Shandon Histocentre. Serial sections (7μM) thick were cut with a microtome and situated on microscope slides (Menzel-Glaser Superfrost Plus).

2.9.4.1 Safranin-O & Fast Green staining

Murine patella sections were stained with safranin-o & fast green as detailed in 2.9.3.1

2.9.4.2 Toluidine Blue staining

Murine patella sections were stained with toluidine blue as detailed in 2.9.3.2

2.9.5 Histological characterisation of murine knee joints

Murine knee joints were fixed in NBFS (as described in 2.9.1 (i)) overnight at 4°C. Murine knee joints were subsequently decalcified in 10% formic acid (as detailed in 2.9.1 (ii)) until completion as assessed by ammonium oxylate precipitation. Knee joints were placed in an automated Shandon Tissue Processor and taken through the serial dehydration cycles of ethanol and xylene (detailed in 2.9.1.2 (i)) before being permeated with wax at 60°C. Knee joints were then embedded in wax blocks using a Shandon Histocentre. Serial sections (10μM) thick were cut with a microtome in the sagittal plane and situated on microscope slides.

2.9.5.1 Safranin-O & Fast Green staining

Murine knee joint sections were stained with safranin-o & fast green as detailed in 2.9.3.1. Cartilage damage was assessed using the scoring system outlined in table 2.1.

Table 2.1 Joint scoring criteria

Criteria	No Changes	Mild Evidence	Moderate Evidence	Severe Evidence
Cartilage fibrillation	0	+	++	+++
Erosion of noncalcified cartilage	0	+	++	+++
Erosion of calcified cartilage	0	+	++	+++
Chondrocyte death	0	+	++	+++
Chondrocye clusters	0	+	++	+++
Loss of staining	0	+	++	+++
Erosion of bone	0	+	++	+++
Sclerosis of subchondral bone	0	+	++	+++
Osteophyte formation	0	+	++	+++
Synovial hyperplasia	0	+	++	+++
NonInflammatory exudates	0	+	++	+++
Synovial infiltration	0	+	++	+++

2.9.6 Immunhistochemistry

2.9.6.1 Anti-NITEGE staining

The presence of aggrecanase cleavage sites in murine patellas and knee joints were assessed using an anti-NITEGE antibody (IBEX Technologies, Montreal, Canada). All immunohistochemical procedures were performed upon sections mounted on superfrost plus slides. A R & D Systems Rabbit Cell & Tissue Staining Kit was used for all steps as indicated. Sections were deparaffinised by immersing slides in 3 changes of xylene (5 minutes), then washing slides in descending alcohols (100%, 100%, 90%, 70% x 3 minute washes). Slides were rehydrated by washing in running tap water for 5 minutes, washing in distilled water for 5 minutes and washing in TBS for 5 minutes. Sections were digested with proteinase-free chondroitinase ABC (0.25 U/ml

0.1M Tris-HCl, pH 8.0; Sigma) for 1 hour at 37°C to remove chondroitin sulphate from the PG (this allows the staining to become more intense). Slides were washed in TBS/Tween (0.1%) (3 washes x 3 minutes) and immersed into TBS before removing excess liquid from the slides and adding 120µl of peroxidase blocking reagent (5 minutes, room temperature, R & D Systems). Slides were rinsed with TBS prior to gentle washing in TBS (5 minutes). Sections were incubated with 120µl of serum blocking reagent G (15 minutes, room temperature, R & D Systems Europe). Slides were rinsed with TBS, prior to gentle washing in TBS (15 minutes). Sections were incubated with 120µl of rabbit serum (diluted 1:10, 15minutes, room temperature, Sigma). Serum was drained from the slides and the excess carefully removed prior to incubating sections with 120µl of avidin blocking reagent (15 minutes, room temperature, R & D Systems Europe). Slides were rinsed with TBS, drained and the excess removed prior to incubating sections with 120µl of biotin blocking reagent (15 minutes, room temperature, R & D Systems). Slides were rinsed with TBS, drained and the excess removed before incubating slides with 120µl of Rabbit Polyclonal Antibody 1320 NITEGE Specific Ab (diluted 1:500 in 1:10 Rabbit Serum; Sigma) for 18 hours at 4°C. After incubation slides were rinsed and washed in TBS (3 washes x 15 minutes). Slides were drained, and the excess TBS was carefully removed, prior to incubating with 120µl of biotinylated secondary antibody for 1 hour at room temperature (R & D Systems Europe). Slides were rinsed and washed in TBS (3 washes x 15 minutes). Slides were drained and the excess TBS removed prior to incubating sections with 120µl of HSS-HRP (high sensitivity streptavidin conjugated to horseradish peroxidase) for 30 minutes at room temperature (R & D Systems Europe) Slides were rinsed

and washed in TBS (3 washes x 2 minutes). Slides were drained and the excess TBS removed prior to incubating with 120µl of freshly prepared DAB Chromagen solution for 5 minutes at room temperature (R & D Systems). Slides were rinsed and washed in dH_2O for 5 minutes prior to staining with Mayers haematoxylin for 90 seconds. Excess haematoxylin was removed by washing the slides in running tap water for 5 minutes and rinsing in distilled water prior to enhancing the haematoxylin staining by immersing slides in Scott's tap water for 10 to 30 seconds. Slides were rinsed in dH_2O before dehydrating the slides by immersing slides in ascending alcohol washes (90% 1 minute, 100%, 100%, 100% 3 minutes) and xylene (2 x 5 minutes). Slides were mounted using Ralmounts.

2.10 Statistical analysis and presentation of results

All results were expressed as the mean ± SEM. All statistical differences determined in this study used the paired means student's t test. p values of $\leq$ 0.05 were considered significant, with values of $\leq$ 0.01 considered highly significant. The Mann-Whitney U test was used to determine statistical differences in the MIA induced experimental OA studies.

CHAPTER THREE

Neutralisation of IL-1β and TNFα in OA Synovial Cells

3.1 Introduction.

OA is a disease primarily characterised by cartilage deterioration that results in pathological changes to all tissues of the synovial joint as the disease progresses. As detailed in chapter one, both the initiation and perpetuation of the attrition of cartilage is believed to result from an imbalance between the levels of anabolic and catabolic cytokines within the joint (Malemud *et al.*, 2003). The synovial membrane within the joint is an abundant source of catabolic cytokines and MMPs that are speculated to activate chondrocytes promoting the destruction of cartilage (Martel-Pelletier *et al.*, 1999). Consequently the role of the synovium in OA pathology has been the focus of several studies.

IL-1β and TNFα have been highlighted as playing a prominent role in the progression of OA. Historically associated with cells of the immune system, within the osteoarthritic joint both IL-1β and TNFα are expressed by the resident articular chondrocytes and by synovial macrophages (Goldring, 1999). Both osteoarthritic articular cartilage and synovium exhibit elevated numbers of both IL-1 and TNF receptors in comparison to normal tissues further cementing the hypothesis that IL-1β and TNFα are intrinsic to cartilage deterioration (Alaaedine *et al.*, 1997; Sadouk *et al.*, 1995; Webb *et al.*, 1998). Numerous studies since the 1970s have examined the inflammatory status and the presence of IL-1β and TNFα within the synovial membrane.

A landmark study performed during the late 1970s demonstrated the ability of the synovial membrane to degrade cartilage *in vitro*. The investigation conducted by Fell et al established that cartilage explants, cultured in the

presence of synovial membrane explants, exhibited deterioration in response to an unknown mediator (Fell *et al.*, 1977). Subsequent studies have identified the mediator, derived from the synovial membrane and responsible for cartilage degradation, as IL-1 (Dingle *et al.*, 1979; Lin *et al.*, 1988). As macrophages are known to be potent inducers of IL-1β production, a number of later studies examined the presence of inflammation within the membrane which may demonstrate the cellular source of IL-1β from the synovium.

Early studies conducted on the synovial membrane of OA patients, concentrated on determining the presence or absence of inflammation within the tissue. During the early 1980s Goldenberg *et al.*, examined synovial membrane specimens extracted from end stage OA patients undergoing joint replacement surgery. Of the 15 patients studied, 3 individuals displayed inflammation characteristic of RA synovial membranes (Goldenberg *et al.*, 1982). Such observations demonstrated that the concept that OA as a non-inflammatory disease was not accurate for many patients. A later study by Revell *et al* elaborated upon the initial study by Goldenberg et al, examining the different cell populations present within the osteoarthritic synovial membrane using monoclonal antibodies (Revell *et al.*, 1988). Consistent with the earlier study, Revell *et al* observed that the synovial membrane of numerous OA patients was an inflammatory environment with the cellular infiltrate present typically comprised of macrophages and to a lesser extent T lymphocytes. Such studies have led to the acceptance in the field of rheumatology that end stage synovitis is characteristic of OA pathology during the latter stages. However, speculation still remained as to the presence and importance of synovitis during earlier stages of OA.

Myers *et al* demonstrated that approximately half of all OA patients displayed no evidence of synovial inflammation and that localised cartilage erosion within the joint did not correlate with synovitis (Myers *et al.*, 1990). However, a subsequent study by Benito *et al* contradicted the earlier observations of Myers *et al* and demonstrated that synovial membranes from early OA patients exhibited an enhanced inflammatory phenotype in comparison to the inflammation observed in end stage patients, as illustrated by cellular infiltrate into the lining layer of the synovial membrane (Benito *et al.*, 2005). This study also demonstrated elevated numbers of CD68+ macrophages within the synovial membrane of early stage OA patients. Such an increase in the presence of macrophages, and the IL-1β that they have the ability to produce, highlights the potential of macrophage derived IL-1β eliciting a catabolic effect within the joint that could result in cartilage deterioration and disease progression. An earlier study by Smith *et al* again highlighted the presence of synovitis in patients with early OA, but illustrated that IL-1β within the synovial membrane was upregulated in comparison to normal membranes (Smith *et al.*, 1992).

In light of the accumulating evidence which indicated that synovial inflammation was an important part of OA pathology, a number of studies assessed the cytokine profile from OA synovial membranes in comparison to synovial membranes from the typically inflammatory arthritic condition, RA. The spontaneous production of IL-1β and TNFα by RA and OA primary synovial cells was clarified during the late 1980s (Brennan *et al.*, 1989). This study demonstrated that RA synovial cells produce elevated levels of both IL-1β and TNFα in comparison to OA, but that the levels of infiltrating macrophages

in the synovium is approximately the same. Monoclonal antibody staining of synovial membranes concurred the observations of Brennan's earlier study, that IL-1β, TNFα and IL-6 are indeed present in osteoarthritic synovium but that the levels of these three inflammatory mediators are greater in RA synovial tissues than OA membranes (Farahat *et al.*, 1993). Both IL-1β and TNFα are known to induce production of MMPs, consequently the levels of MMPs derived from the synovium was examined. Yoshihara *et al* observed that whilst MMPs were present in osteoarthritic synovial fluid, the levels of MMPs, particularly MMP-1, -2, -3, -8 and -9 present in the synovial fluid from RA patients were significantly higher than in OA synovial fluid (Yoshihara *et al.*, 2000). Such studies indicate that both RA and OA synovial membranes exhibit a similar cytokine profile with the major difference between the two diseases being quantitative rather than qualitative.

During this study we sought to clarify the importance of OA synovial macrophages, and the TNFα and IL-1β they produce, in promoting the release of cytokines and MMPs, implicated in OA pathology.

The specific aims of this chapter were to:

- Determine the cellular composition and degree of inflammation typically present in synovial specimens derived from OA patients undergoing end stage total hip or knee joint replacement surgery.
- Develop a method of removing synovial macrophages from freshly digested OA synovial cocultures (OA-COCUL) and subsequently assess the effect removal of macrophages had upon the production of an array of mediators associated with OA pathology.

- Verify the importance of IL-1β and TNFα within the synovial membrane and determine if amelioration of one or both of these pro-inflammatory cytokines may be a useful target for future therapy for OA.

3.2 Results

3.2.1 Histological analysis of synovial specimens derived from OA patients revealed that inflammation within the membrane varies markedly.

Synovial specimens were extracted from patients at the time of joint replacement surgery, as described during chapter two, and fixed in NBFS prior to histological sectioning. Histological sections of synovial membranes stained with haemotoxylin and eosin demonstrated the heterogeneity of the disease (Figure 3.1). A number of OA patients exhibited no inflammation within the synovial membrane (Figure 3.1 a, b, c) whilst a notable proportion of OA patients exhibited synovial inflammation within the intimal layer (Figure 3.1 d, e, f). A healthy intimal layer with a typical depth of 1 -2 cells thick was evident (Figure 3.1 a), with adipose tissue a common feature of a non-inflammatory synovial membrane (Figure 3.1 b). Cellular infiltration of the intimal layer was evident in all 3 inflammatory images (Figure 3.1 d, e, f) , with the intimal layer increasing in depth to > 10 cells (Figure 3.1 f).

3.2.2 Cytospins of OA-COCUL demonstrated that synovial fibroblasts and macrophages were the major constituent cell type present in osteoarthritic synovium.

Cytospins of synovial cocultures (OA-COCUL) were prepared, as described during chapter two, and stained with May-Grunwald and Giemsa stain to allow morphological identification of the cell types present in OA synovial membranes (Figure 3.2 a). 10 fields of view at x 40 magnification were counted for each synovial specimen and the mean for each patient presented (Figure 3.2 b). It was observed that whilst the proportion of synovial fibroblasts to leukocytes varied between individual patients, the major constitutive cell type of the osteoarthritic synovium was fibroblasts

(87.9% ± 1.4, mean ± SEM) with synovial leukocytes, typically macrophages constituting the remainder of the cell types present (12.1% ± 1.4).

3.2.3 Removal of synovial macrophages from synovial membrane cultures resulted in downregulation of proinflammatory cytokines implicated in OA pathology.

Synovial macrophages were removed from the total OA-COCUL population using magnetic cell separation systems as outlined during chapter two. The total OA-COCUL and those depleted of synovial macrophages were cultured for 48 hours prior to the removal of the culture supernatants with IL-1β, TNFα and IL-6 production from the supernatants subsequently quantified by specific ELISA (Figure 3.3). The observations of this study demonstrated that the removal of synovial macrophages resulted in significant ($p \leq 0.01$) inhibition of IL-1β and TNFα (Figure 3.3 a & b). The levels of the inflammatory mediator IL-6 (Figure 3.3 c) were not significantly affected by the depletion of synovial macrophages.

3.2.4 Removal of synovial macrophages from synovial membrane cultures resulted in suppression of chemokines *in vitro*.

Synovial macrophages were removed from the total OA-COCUL population using magnetic cell separation systems as outlined in the materials and methods. The total OA-COCUL and those depleted of synovial macrophages were cultured for 48 hours prior to the removal of the culture supernatants with IL-8, CCL2 and CCL5 production from the supernatants subsequently quantified by specific ELISA (Figure 3.4). The observations of this study demonstrated that the removal of synovial macrophages resulted in significant ($p \leq 0.05$) suppression of IL-8 (Figure 3.4 a) and a highly significant reduction in CCL2 levels ($p \leq 0.01$) (Figure 3.4 b). The levels of a

third chemokine CCL5 (Figure 3.4 c) were not significantly affected by the removal of synovial macrophages from OA-COCUL's.

3.2.5 Removal of synovial macrophages from synovial membrane cultures resulted in inhibition of destructive MMPs *in vitro*.

Synovial macrophages were removed from the total OA-COCUL population using magnetic cell separation systems as outlined in chapter two. The total OA-COCUL and those depleted of synovial macrophages were cultured for 48 hours prior to the removal of the culture supernatants with MMP-1 and MMP-3 production from the supernatants subsequently quantified by specific ELISA (Figure 3.5 a & b). The observations of this study demonstrated that the removal of synovial macrophages resulted in significant ($p \leq 0.05$) inhibition of both MMP-1 and MMP-3.

3.2.6 The quantification of spontaneous cytokine production from OA-COCUL revealed that cytokine release varied between OA patients.

The spontaneous production of a range of cytokines was established by specific ELISA (Table 3.1). The mean value for each cytokine measured is presented alongside the minimum, maximum and median values level for each mediator. OA-COCUL spontaneously produce TNFα at 10 fold the levels of IL-1β, however both are produced by synovial cultures in the ng/ml range (mean; 11 and 2 respectively). Whilst IL-6 in this system was produced at considerably higher levels than IL-1β or TNFα production.

3.2.7 The heterogeneous distribution of chemokine production from OA-COCUL.

The spontaneous production of a range of chemokines was established by specific ELISA (Table 3.2). The mean value for each chemokine measured is presented alongside the minimum, maximum and median values level for each

mediator. OA-COCUL spontaneously produce chemokines at much lower levels than cytokines or MMPs, with the chemokines IL-8, CCL2 and CCL5 levels measured in the pg/ml range. Levels of CCL5 from OA-COCULs were on the threshold of detection.

3.2.8 The spontaneous MMP production from OA-COCUL was heterogeneous between OA patients.

The spontaneous production of a number of different MMPs by OA-COCUL was established by specific ELISA (Table 3.3). The mean value for each MMP measured is presented alongside the minimum, maximum and median values level for each mediator. The collagenase MMP-1, and the stromeolysin MMP-3, were produced at extremely high levels by OA-COCUL (mean; 1,372 and 4,334 respectively), however MMP-9 and MMP-13, both strongly implicated in OA were produced at almost 100 fold less than the two aforementioned MMPs.

3.2.9 Neutralisation of IL-1β and TNFα significantly inhibited IL-6 in OA-COCUL.

IL-1β and TNFα were neutralised in the OA-COCUL using a specific anti-IL-1β antibody (10μg/ml) and etanercept (100μg/ml) (Figure 3.6). Anti-IL-1β repressed levels of IL-1β by 99.5% (Figure 3.6 a), whilst TNFα levels were downregulated by 89.6% by treatment with etanercept (Figure 3.6 b). Anti-IL-1β did not significantly affect TNFα production with no significant reduction in IL-1β levels elicited by etanercept. Combination therapy with both etanercept and anti-IL-1β antibody evoked a greater reduction in cytokine and MMP production, than the two agents used alone. Both anti-IL-1β and etanercept significantly ($p \leq 0.05$) inhibited the induction of IL-6 (Figure 3.6 c), in combination the two agents elicited an enhanced inhibitory effect.

3.2.10 Neutralisation of IL-1β and TNFα significantly inhibited IL-8 and CCL2, but not CCL5 in OA-COCUL.

IL-1β and TNFα were neutralised in the OA-COCUL using a specific anti-IL-1β antibody (10μg/ml) and etanercept (100μg/ml) (Figure 3.7). IL-8 (Figure 3.7 a) levels were significantly ($p \leq 0.05$) suppressed by neutralisation of TNFα in the OA-COCUL system. Inhibition of IL-8 was enhanced when the two agents were employed in combination, although this effect was not significant. CCL2 and CCL5 production was not inhibited by IL-1β and TNFα neutralization (Figure 3.7 c).

3.2.11 Neutralisation of IL-1β and TNFα significantly inhibited MMP-1 and MMP-3, but not MMP-9, MMP-13 or TIMP-1 in OA-COCUL.

IL-1β and TNFα were neutralised in the OA-COCUL using a specific anti-IL-1β antibody (10μg/ml) and etanercept (100μg/ml) (Figure 3.8). MMP-1 (Figure 3.8 a), MMP-3 (Figure 3.8 b) and MMP-9 (Figure 3.8 c) levels were significantly ($p \leq 0.05$) inhibited by the two agents in combination, however MMP-13 (Figure 3.8 d) levels were not significantly down regulated by combination therapy. The effect combination therapy elicited upon TIMP-1 (Figure 3.8 e) was negligible.

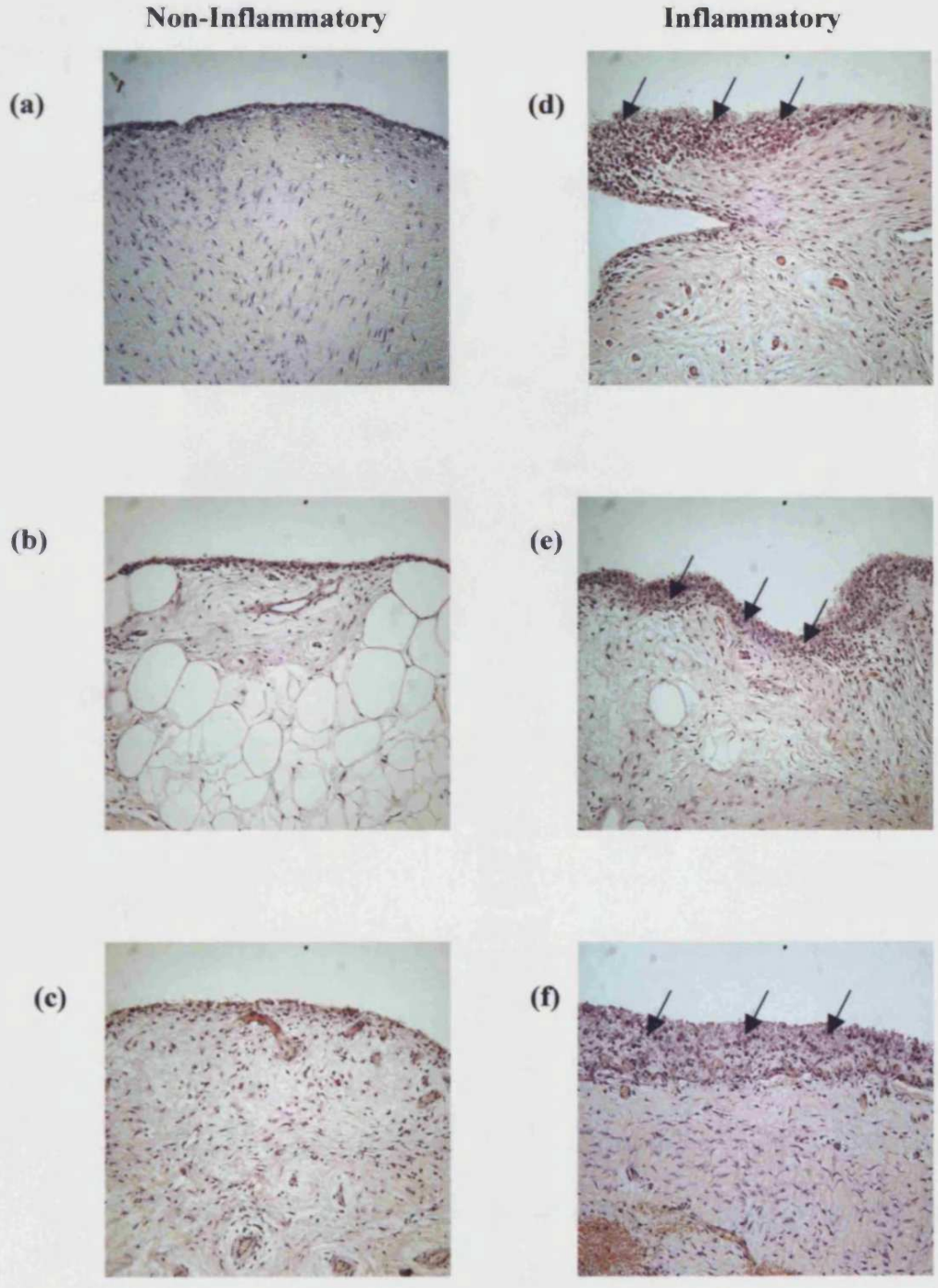

Figure 3.1 Histological determination of synovial inflammation
Synovial explants were removed at random from synovial membrane specimens derived from endstage patients, prior to fixation and histological processing. 7μM serial sections from the synovial explants were stained with haemotoxylin and eosin (a – f). Patients exhibiting a non-inflammatory phenotype are illustrated in (a – c), with synovial specimens displaying an inflammatory phenotype depicted in (d – f). Arrows highlight areas of synovial inflammation. Magnification x 200

(a)

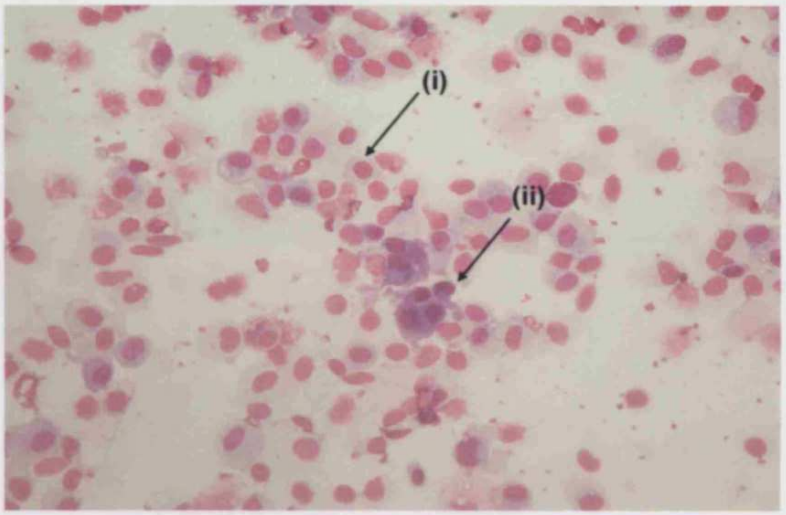

(b)

Patient	OA-SF (%)	Leukocyte (%)
1	98.1	1.9
2	84.9	15.1
3	88.9	11.1
4	85.6	14.4
5	88.4	11.6
6	82.4	17.6
7	87.9	12.1
8	89.2	10.8
9	87.8	12.2
10	85.3	14.7
Mean	**87.9**	**12.1**

Figure 3.2 Histological analysis of the cell types present within the synovial membrane

Cytospins were prepared from freshly digested synovium as described in 2.5.1.2. and stained with Giemsa and May-Grunwald stains to allow morphological identification (a). The major constituent cell types present in freshly digested synovial cocultures are identified as (i) synovial fibroblasts (OA-SF) and (ii) leukocytes (primarily macrophages). The percentage of OA-SF in comparison to synovial leukocytes was established by counting the numbers of OA-SF and leukocytes present in 10 fields of view at x 400 magnification (b). 10 cytospins from 10 randomly selected OA synovial specimens were counted and the mean cellular composition was established as percentage OA-SF and percentage leukocytes.

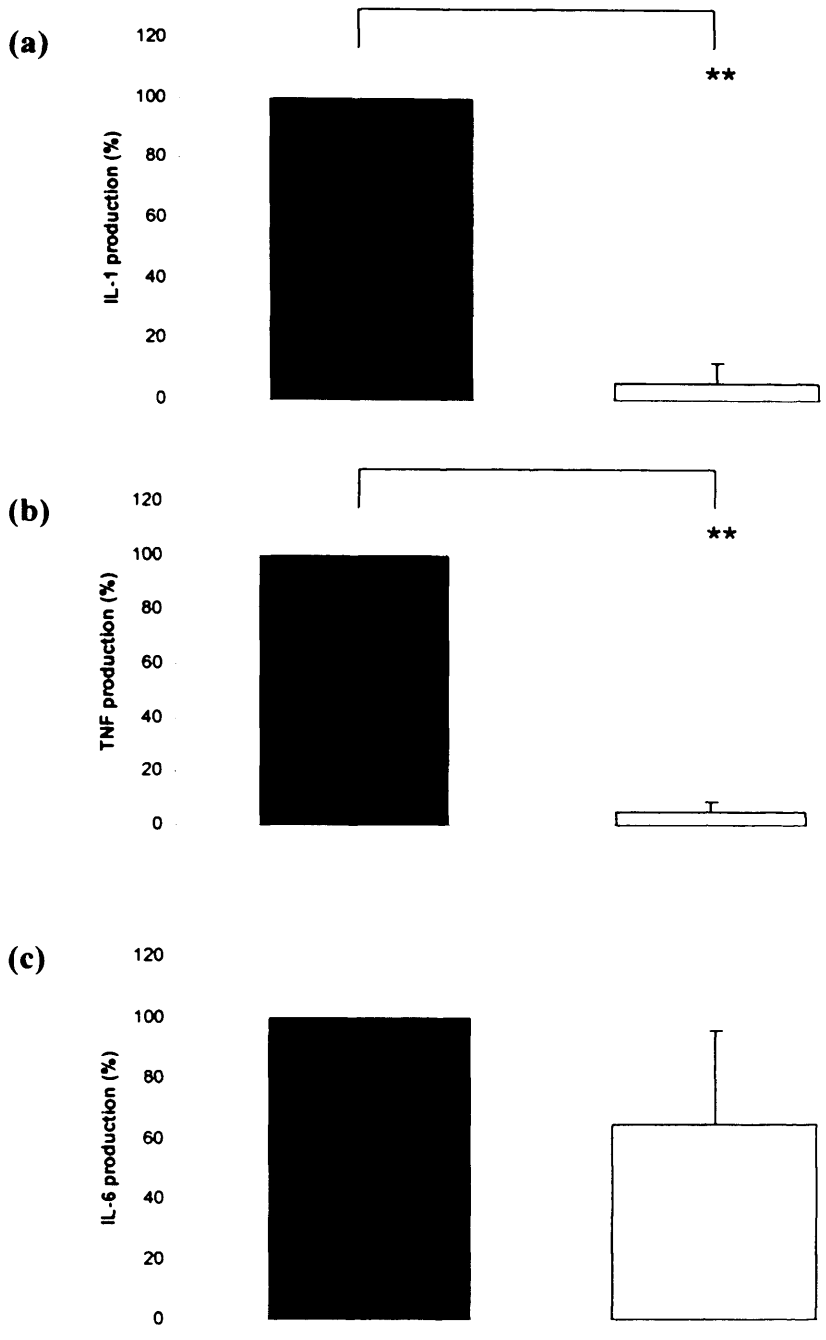

Figure 3.3 The effect of depleting synovial macrophages from OA-COCULs upon spontaneous cytokine production.

OA-COCULs were generated from freshly digested synovium as described in 2.5.1.1 prior to the removal of synovial macrophages as detailed in 2.5.1.3. Total OA-COCUL and those depleted of $CD14^+$ cells (synovial macrophages) were plated at equal cell densities and cultured for 48 hours prior to the removal of the culture supernatants. The spontaneous production of IL-1β, TNFα and IL-6 from the two cell populations was quantified by specific ELISA. The mean ± SEM for each cell population expressed as a percentage of the total OA-COCUL ($n = 4$, ** $p \leq 0.01$). Closed bars denote total OA-COCUL, open bars denote OA-COCUL depleted of $CD14^+$ cells.

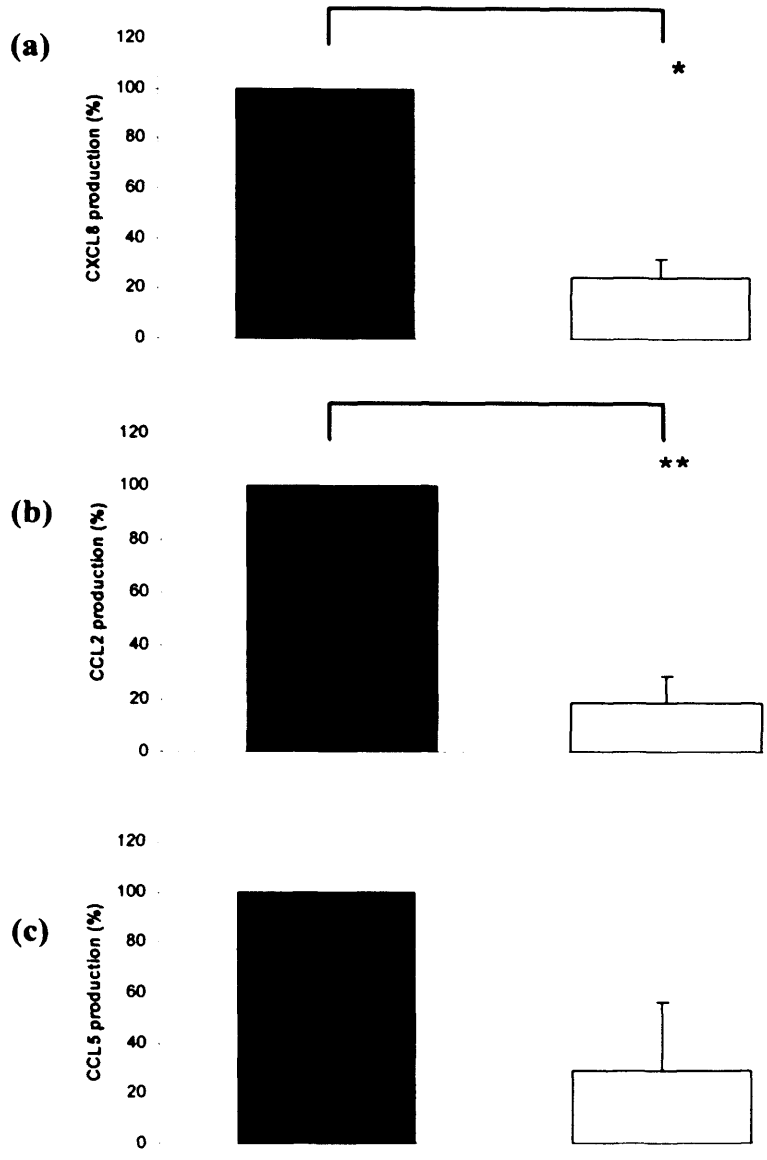

Figure 3.4 The effect of depleting synovial macrophages from OA-COCULs upon spontaneous chemokine production.

OA-COCULS were generated from freshly digested synovium as described in 2.5.1.1 prior to the removal of synovial macrophages as detailed in 2.5.1.3. Total OA-COCUL and those depleted of $CD14^+$ cells (synovial macrophages) were plated at equal cell densities and cultured for 48 hours prior to the removal of the culture supernatants. The spontaneous production of CXCL8, CCL2 and CCL5 from the two cell populations was quantified by specific ELISA. Data represent the mean ± SEM for each cell population expressed as a percentage of the total OA-COCUL (n = 4 patients, * $p \leq 0.05$, ** $p \leq 0.01$). Closed bars denote total OA-COCUL, open bars denote OA-COCUL depleted of $CD14^+$ cells.

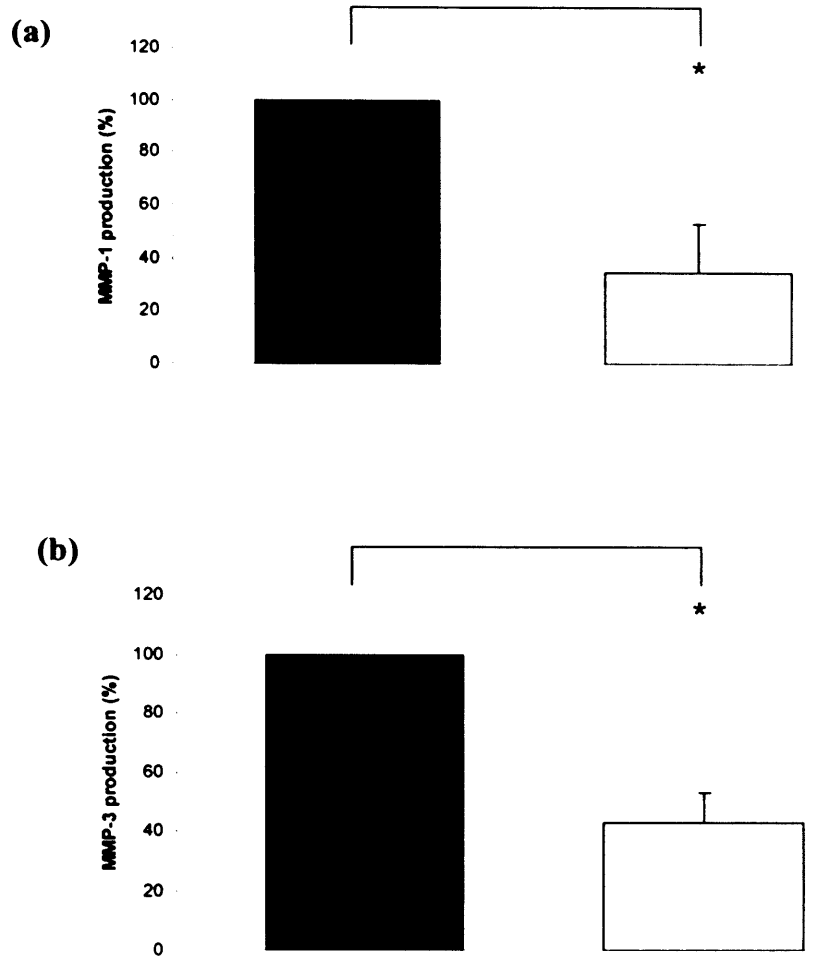

Figure 3.5 The effect of depleting synovial macrophages from OA-COCULs upon spontaneous MMP production.

OA-COCUL were generated from freshly digested synovium as described in 2.5.1.1 prior to the removal of synovial macrophages as detailed in 2.5.1.3. Total OA-COCUL and those depleted of $CD14^+$ cells (synovial macrophages) were plated at equal cell densities and cultured for 48 hours prior to the removal of the culture supernatants. The spontaneous production of MMP-1 and MMP-3 from the two cell populations was quantified by specific ELISA. Data represent the mean ± SEM for each cell population expressed as a percentage of the total OA-COCUL (n = 4 patients, * $p \leq 0.05$). Closed bars denote total OA-COCUL, open bars denote OA-COCUL depleted of $CD14^+$ cells.

	Mean	*Max*	*Min*	*Median*	*Sample Size*
TNFα	11	33	0.1	6	9
IL-1β	2	8	0.01	1	9
IL-6	1254	2667	83	1327	9
OSM	5	18	2	3	6

Table 3.1 Quantification of spontaneous cytokine production from OA-COCUL

OA-COCULs were generated from synovial specimens as described in 2.5.1.1, prior to culturing for 48 hours. Following the culture period supernatants were removed and the spontaneous production of IL-1β, TNFα, IL-6 and OSM was quantified by specific ELISA. The range, mean and median for each mediator was presented as determined for n=9 synovial specimens for IL-1β, TNFα, IL-6 and n=6 for OSM. Values presented as ng/ml.

	Mean	*Max*	*Min*	*Median*	*Sample Size*
CCL2	54,058	104,813	2,668	45,804	9
CCL5	161	308	26	143	5
CXCL8	325,625	785,234	89,981	158,181	7

Table 3.2 Quantification of spontaneous chemokine production from OA-COCUL

OA-COCULs were generated from synovial specimens as described in 2.5.1.1, prior to culturing for 48 hours. Following the culture period supernatants were removed and the spontaneous production of CCL2, CCL5, and CXCL8 was quantified by specific ELISA. The range, mean and median for each mediator was presented as determined for n=9 synovial specimens for CCL2, n=7 for IL-8 and n=5 for CCL5. Values presented as pg/ml.

	Mean	*Max*	*Min*	*Median*	*Sample Size*
MMP-1	1,372	3,935	247	916	9
MMP-3	4,334	10,820	392	2,867	9
MMP-9	24	50	3	25	6
MMP-13	4	9	0.2	3	7
TIMP-1	204	398	11	211	9

Table 3.3 Quantification of spontaneous MMP production from OA-COCUL

OA-COCULs were generated from synovial specimens as described in 2.5.1.1, prior to culturing for 48 hours. Following the culture period supernatants were removed and the spontaneous production of MMP-1, MMP-3, MMP-9, MMP-13 and TIMP-1 was quantified by specific ELISA. The range, mean and median for each mediator was presented as determined for n=9 synovial specimens for MMP-1, MMP-3, TIMP-1, n=7 for MMP-13 and n=6 for MMP-9. Values presented as ng/ml.

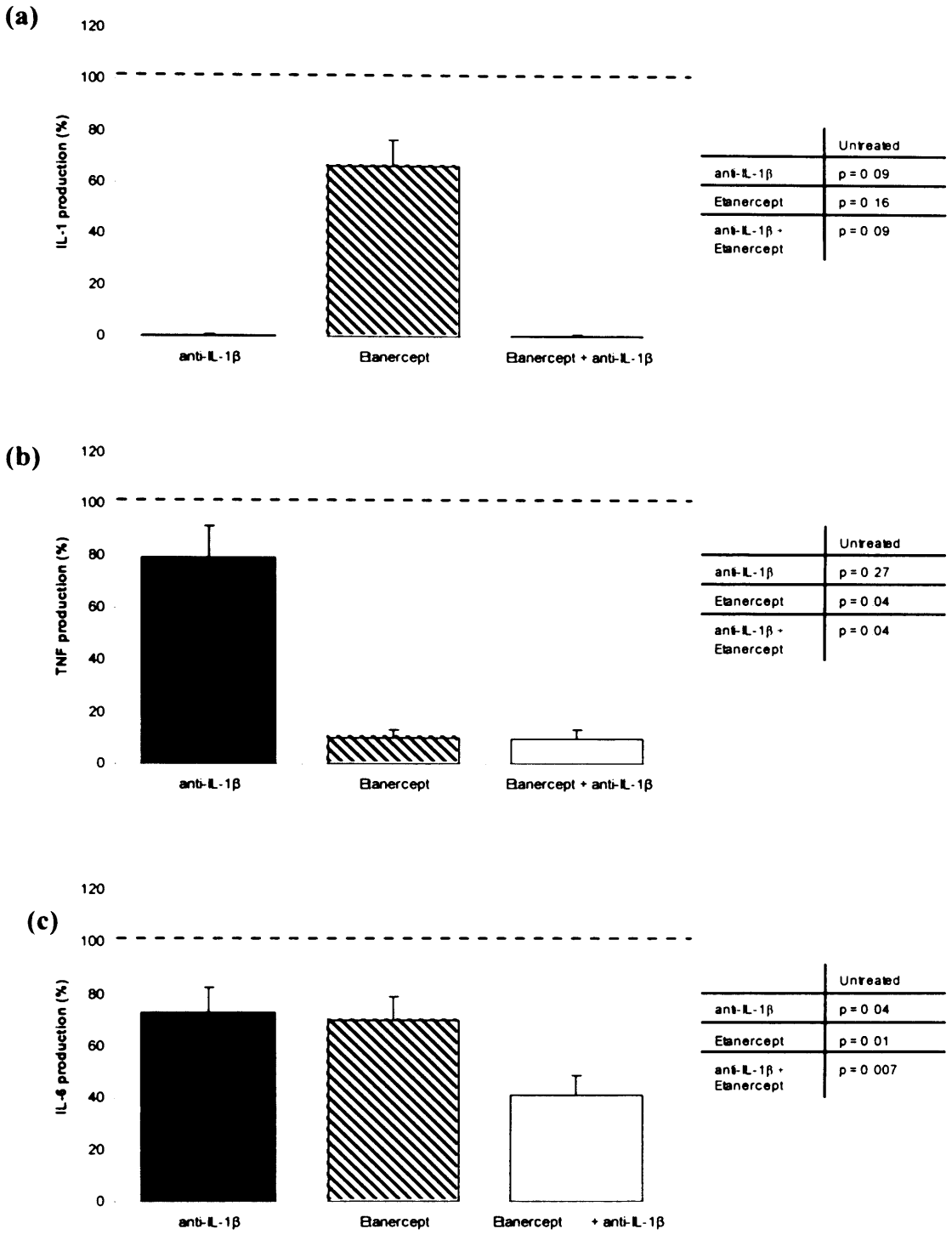

Figure 3.6 The effect of anti-cytokine strategies upon cytokine production in OA-COCUL

OA-COCUL were generated as described previously in 2.5.1.1 prior to plating. Etanercept and anti-IL-1β were employed as detailed in 2.5.1.4 to neutralise the spontaneous IL-1β and TNFα present in the OA-COCUL model. Following treatment, cells were cultured for 48 hours prior to harvesting of the supernatants. The levels of IL-1β, TNFα and IL-6 were quantified by specific ELISA. Data presented as percentage production in comparison to untreated cells, indicated as 100% by the dashed line. p values for each treatment strategy in comparison to untreated cells is presented for each individual cytokine

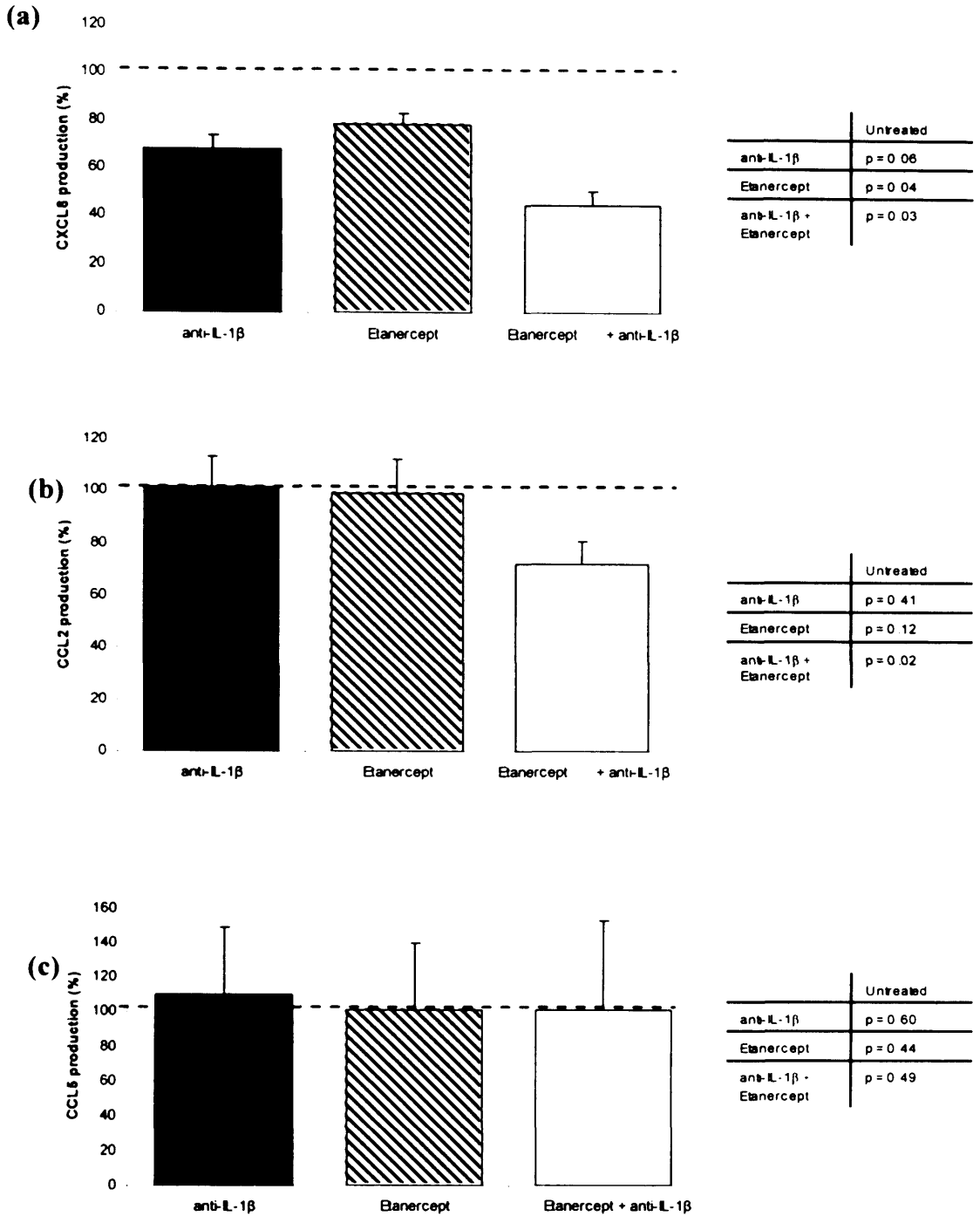

Figure 3.7 The effect of anti-cytokine strategies upon chemokine production in OA-COCUL

OA-COCUL were generated as described previously in 2.5.1.1 prior to plating. Etanercept and anti-IL-1β were employed as detailed in 2.5.1.4 to neutralise the spontaneous IL-1β and TNFα present in the OA-COCUL model. Following treatment, cells were cultured for 48 hours prior to harvesting of the supernatants. The levels of CXCL8, CCL2 and CCL5 were quantified by specific ELISA. Data presented as percentage production in comparison to untreated cells, indicated as 100% by the dashed line. p values for each treatment strategy in comparison to untreated cells is presented for each individual cytokine

(a)

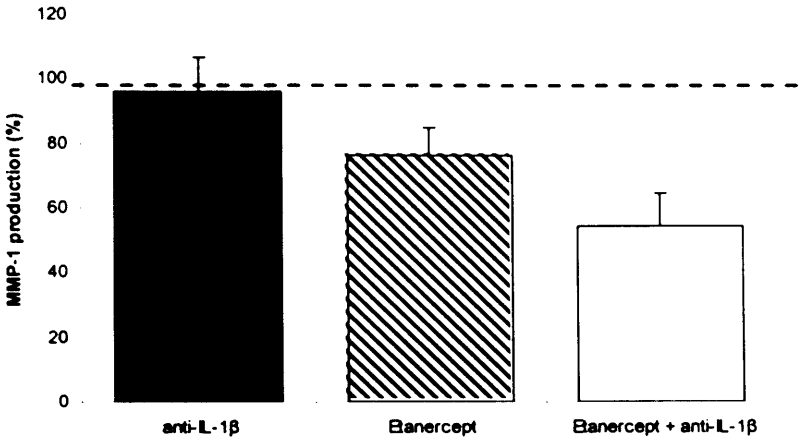

	Untreated
anti-IL-1β	p = 0 97
Etanercept	p = 0 03
anti-IL-1β + Etanercept	p = 0 02

(b)

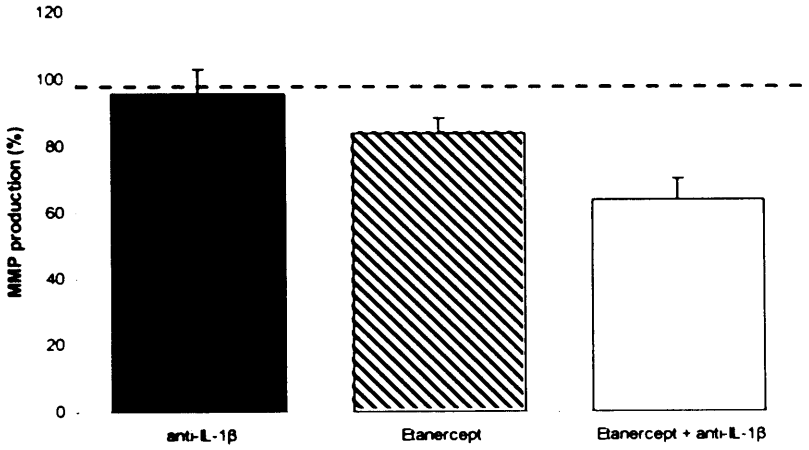

	Untreated
anti-IL-1β	p = 0 13
Etanercept	p = 0 09
anti-IL-1β + Etanercept	p = 0 02

(c)

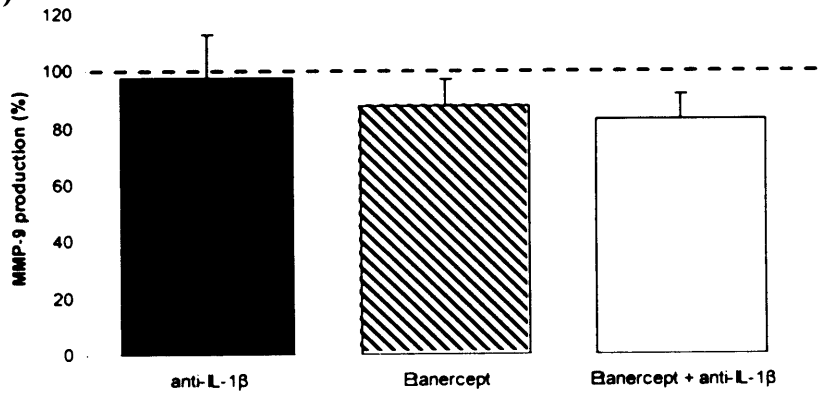

	Untreated
anti-IL-1β	p = 0 92
Etanercept	p = 0 22
anti-IL-1β + Etanercept	p = 0 04

Figure 3.8 Continued overleaf.

(d)

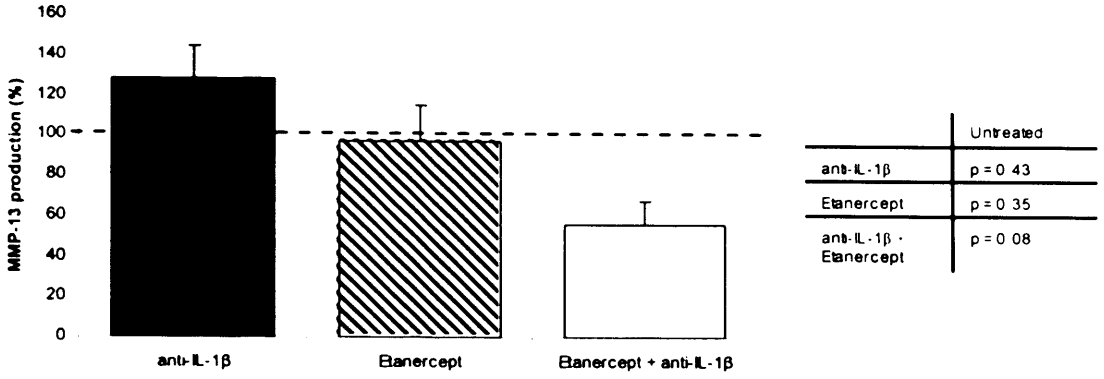

(e)

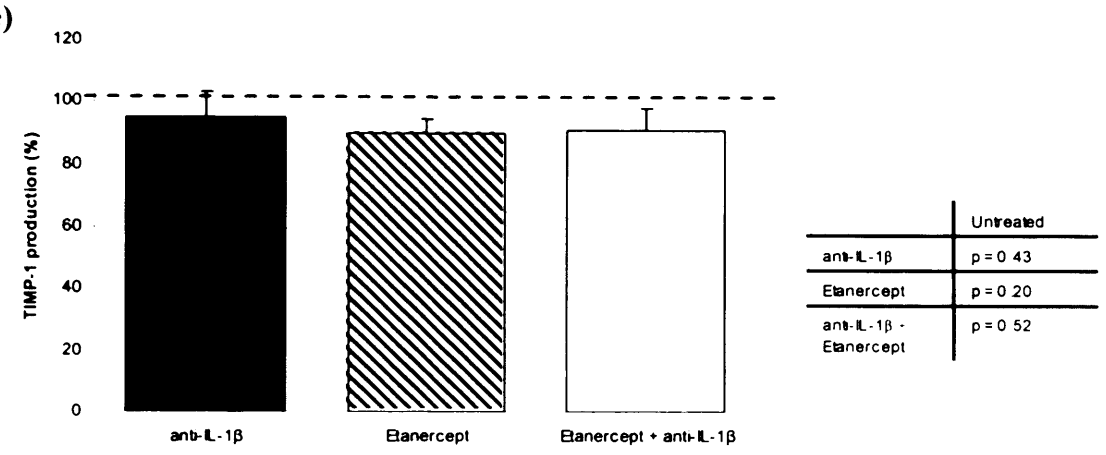

Figure 3.8 The effect of anti-cytokine strategies upon MMP production in OA-COCUL

OA-COCUL were generated as described previously in 2.5.1.1 prior to plating. Etanercept and anti-IL-1β were employed as detailed in 2.5.1.4 to neutralise the spontaneous IL-1β and TNFα present in the OA-COCUL model. Following treatment, cells were cultured for 48 hours prior to harvesting of the supernatants. The levels of MMP-1, MMP-3, MMP-9, MMP-13 and TIMP-1 were quantified by specific ELISA. Data presented as percentage production in comparison to untreated cells, indicated as 100% by the dashed line. p values for each treatment strategy in comparison to untreated cells is presented for each individual cytokine

3.3 Discussion.

Mounting evidence suggests that OA is not simply a degenerative, 'wear and tear' disease and that there is a significant inflammatory element to the disease in many cases. It is widely accepted that an array of cytokines, chemokines and MMPs are involved in the pathology of OA, with IL-1β and TNFα underpinning this process. We assessed the importance of both inflammation and IL-1β and TNFα in synovial pathology during chapter 3.

It is acknowledged that the inflammation within the osteoarthritic synovium varies markedly. In order to clarify the cohorts of patients used during our study we histologically determined the degree of inflammation present within the membrane using haemotoxylin and eosin staining. In accordance with previous studies the degree of synovial inflammation in the initimal layer was diverse. Cohorts of patients had a synovial membrane exhibiting a normal phenotype, whilst others displayed an inflammatory phenotype similar to that of an RA specimen. In consideration of the differences that exist between OA patients we sought to determine the composition of a 'typical' synovial membrane.

Historically, it has been demonstrated that the cells of the immune system, and in particular the circulating macrophages are an abundant source of IL-1β and TNFα. We conducted a study to determine the percentage of macrophages typically found within osteoarthritic synovial tissue to determine if macrophage derived IL-1β and TNFα would be sufficient to elicit a pathological response within the joint. Cytospins of freshly digested synovial membrane cultures (OA-COCUL) demonstrated that whilst the numbers of leukocytes in comparison to fibroblasts varied marginally, overall the ratio of leukocytes,

predominantly macrophages, to synovial fibroblast-like cells was 1:10. The study conducted by Brennan *et al.*, quantified the number of $CD14^+$ synovial macrophages present in OA synovial samples by flow cytometry, and demonstrated that the numbers of $CD14^+$ cells was slightly greater than in our study. However, the variation in Brennan's study (26% ± 9) was greater than the variation observed in our study (12% ± 4), in combination with the differences between cytospin analysis and flow cytometry, the two studies provide comparable results (Brennan *et al.*, 1989). In reflection it may have been beneficial to determine the cellular composition of the OA-COCUL using flow cytometry and staining the different populations present with antibodies specific for the surface markers they express. Typically the macrophages present could have been identified by their expression of the markers CD14 or CD68, whilst the fibroblast-like cells should be negative for these surface markers but stain positive with a CD90w antibody used routinley to identify fibroblasts. Brennan also examined the numbers of infiltrating T lymphocytes present in OA synovial cultures and established that the levels of T cells in OA are greatly reduced in comparison to RA synovial cultures (1:3 ratio). Subsequent studies also demonstrated the presence of a significant T cell infiltrate in the synovial membrane of several OA patients (Haynes *et al.*, 2002; Nakamura *et al.*, 1999). IL-1β and TNFα production from activated T cells was not examined during our study. To assess the importance of activated T cells in OA pathology it may have been beneficial to examine the numbers of T cells present within synovial specimens, and examine the effect removal of T cells has upon OA-COCULs.

We attempted to determine the importance of synovial macrophages in promoting the spontaneous production of an array of mediators associated with

pathology. Isolating differential subsets of cells from a mixed population present in the synovium has posed a significant challenge for many years. The advent of magnetic cell separation systems based upon the expression of specific cell surface markers resolved this technical difficulty. The MACS cell separation system was previously used for the successful isolation of $CD14^+$ monocytes/macrophages from whole blood (Obermaier *et al.*, 2003; Thivierge *et al.*, 2006). Using the same technology we developed a method of extracting $CD14^+$ macrophages from the freshly digested OA-COCUL. The removal of macrophages from the remaining synovial cell types allowed us to evaluate the importance of macrophages in perpetuating an inflammatory cytokine profile within the OA synovium. In the absence of macrophages, the levels of the IL-1β and TNFα were almost totally abrogated, as expected. Both MMP-1 and MMP-3, which have a role in the destruction of cartilage within the joint, were significantly downregulated in the absence of macrophages suggesting that either the macrophages themselves are responsible for the production of these two destructive enzymes or alternatively, that the IL-1β and TNFα produced by the macrophages induced production of the MMPs from the remaining synovial cell types. The chemokines CXCL8 and CCL2 which have a prominent role in RA pathology (Vergunst *et al.*, 2005) were significantly reduced in the absence of synovial macrophages.

Previous studies illustrated that IL-6 production is induced by IL-1β and TNFα, we would therefore anticipate a reduction in the levels of IL-6 would occur in the absence of synovial macrophages (Vanden Berghe *et al.*, 2000). However, we observed that depletion of macrophages reduced the levels of IL-6 produced by OA-COCUL by approximately 40%. IL-6 levels are not

dramatically reduced by depletion of $CD14^+$ cells for a number of reasons. Firstly the synovial fibroblasts present produce IL-6 and as fibroblasts constitute the majority of cells present in OA-COCULs, the removal of macrophages does not elicit a great effect on the level of IL-6 present. Secondly OA-COCULs depleted of macrophages were cultured in the presence of 10% FCS. FCS is routinely used to stimulate IL-6 production in stromal cells, and the sIL-6R present in FCS can stimulate the fibroblasts to release IL-6 (Nakao *et al.*, 2002). Hence the effect of synovial macrophage removal upon IL-6 production may prove to be greater if synovial cells were cultured in serum-free media. However a drawback of using serum-free media so early after synovial digestion is that the cells are very fragile and a lack of serum in the system may result in enhanced apoptosis.

Whilst the removal of synovial macrophages from freshly digested synovial cell cultures proved effective in demonstrating that macrophages and the cytokines they produce are intrinsic to synovial pathology, a number of technical difficulties were highlighted with this method. Firstly, for effective extraction a high cell number was required at the start of the study ($> 2 \times 10^6$), many of the synovial specimens were not large enough to be effectively depleted of macrophages. Consequently we are positively selecting for large synovial specimens which may prove to phenotypically different to smaller synovial specimens. Secondly, the process of depletion of macrophages from the synovium is harsh, and consequently some of the downregulation in cytokines, chemokines and MMPs observed in cocultures depleted of macrophages may result from increased apoptosis as a result of the cell separation process. Thirdly, and possibly most importantly because of the differences in size of the

synovial specimens between patients and the percentage of the different cell types present within the membrane, it was impossible to plate the depleted and total cell populations at the same cell density between experiments. As a result only percentage production of each mediator from different experiments was compared. Retrospectively it may have been advantageous to examine the production of the mediators from the isolated synovial macrophages. Such an investigation would have clarified if the reduction in mediator levels produced by cells depleted of synovial macrophages was a consequence of the macrophages themselves or the proinflammatory cytokines IL-1β and TNFα they produce. However, the isolation of synovial macrophages employed magnetically labelled $CD14^+$ beads that attach to the CD14 receptor present on synovial macrophages and monocytes. As the CD14 receptor is responsible for LPS stimulation, the binding of magnetically labelled beads could potentially have activated the macrophages and consequently, may have altered the phenotype of the cells, and therefore the production of mediators from these cells can not be accurately assessed (Labeta *et al.*, 1993).

In light of these drawbacks, we opted to determine the importance of IL-1β and TNFα within the synovial membrane by a neutralisation strategy. An anti-IL-1β antibody was employed to repress the IL-1β present within the system, whilst etanercept, an anti-TNFα therapy used clinically for the treatment of RA, was employed in the OA-COCUL to neutralise the TNFα present. As expected, anti-IL-1β and etanercept neutralised each cytokine respectively. Neutralisation of IL-1β alone significantly inhibited the levels of IL-6 but elicited no inhibitory effect on the levels of the other mediators examined. Neutralisation of TNFα elicited a more potent effect than IL-1β alone with

significant downregulation in the levels of IL-6, CXCL8, CCL2 and MMP-1. Combined IL-1β and TNFα neutralisation elicited a significantly enhanced effect, repressing the levels of IL-6, CXCL8, CCL2, MMP-1 and MMP-3. Our observations are in accordance with a previous study conducted by Kobayshi *et al* in which the activity of IL-1β and TNFα in OA cartilage explants was neutralized using recombinant IL-1β receptor agonist (IL-1RA) and PEGlyated soluble TNF receptor I (sTNFRI) respectively showed marked reduction in MMP-1 and MMP-3 gene expression and reduced cartilage depletion (Kobayshi *et al.*, 2005). A subsequent clinical study conducted by Chevalier et al concluded that targeting IL-1β by intraarticular administration of IL-1RA could provide a viable target for therapy in OA (Chevalier *et al.*, 2005). Currently, there are no published studies that have targeted TNFα for the treatment of OA, although anti-TNFα agents such as infliximab and etanercept have revolutionized the management of RA (Bathon *et al.*, 2000; Klareskog *et al.*, 2004).

Whilst the neutralisation of IL-1β and TNFα, suppressed the production of the majority of mediators examined, the effect elicited was not as dramatic as expected. It is possible that the apparent lack of efficacy elicited by IL-1β and TNFα neutralisation upon the levels of cytokines, chemokines and MMPs examined in the study may result from a 'masking effect'. Residual mediators generated prior to dosing with anti-IL-1β and Etanercept, may elevate the levels of each mediator tested, despite the efficacy of IL-1β and TNFα neutralisation within the model. Consequently the inclusion of an overnight equilibration period prior to the commencement of the study that would allow accurate

determination of baseline levels of each mediator prior to cytokine neutralisation may resolve this issue.

The observations of this study demonstrate that IL-1β and TNFα act synergistically and that a treatment strategy that targets both cytokines maybe more beneficial than targeting either cytokine alone in the treatment of OA. TNFα inhibitors, etanercept and infliximab are widely used in the treatment of RA and psoriatic arthritis patients (Bansback *et al.*, 2005). Etanercept is a human soluble p75 receptor that binds to soluble TNFα thus preventing the cytokine from eliciting an inflammatory response (Scott *et al.*, 2005), whilst infliximab is a chimeric monoclonal antibody to TNFα that again binds to the TNFα present within the joint (Bansback *et al.*, 2005). Both agents are administered under the care of a rheumatologist with etanercept typically given as subcutaneous injections whilst infliximab is administered intravenously, of the two agents etanercept is favoured as subcutaneous administration is less time consuming (Nuijten *et al.*, 2001). Both agents can improve the clinical signs and symptoms of both RA and psoriatic arthritis within a matter of weeks of starting treatment, however there are two major drawbacks with TNFα inhibition. Firstly, inhibition of TNFα results in an increased risk of infection, with *Mycobacterium tuberculosis* infection a specific problem, the longterm suppression of TNFα is also associated with an increased risk of cancer (Bansback *et al.*, 2005). The second drawback is the significant cost of the TNFα inhibitors and the continued monitoring patients require during treatment (Spalding *et al.*, 2006).

The development of disease modifying therapeutics for OA remains the ultimate clinical goal. Whilst both IL-1β and TNFα remain an attractive target

for disease modulation, the adverse effects and cost associated with the use of TNFα inhibitors for the treatment of RA have demonstrated that if these two cytokine pathways are to be targeted for the treatment of OA, a novel strategy that does not elicit such severe effects would need to be sought (Abramson *et al.*, 2006). In light of such observations, NFκB inhibition within the joint has been suggested as an attractive target for OA therapy, as both cytokines are known to be potent inducers of the transcription factor. Consequently the role of this transcription factor in response to IL-1β and TNFα stimulation in OA pathology will be assessed in the next chapter.

CHAPTER FOUR

The effect of NFκB inhibition upon pathogenic mediators released by OA-SF *in vitro*

4.1 Introduction.

A number of cytokines and matrix metalloproteinases (MMPs) have been identified as playing a central role in the pathophysiology of OA, (discussed in chapter one). With a role in inflammation, NFκB has been highlighted as a potential target for new therapeutic strategies, consequently in recent years the role of the transcription factor in arthritis has been the focus of a number of studies (Berenbaum , 2004). Diacerhein and glucosamine, two agents employed in the treatment of OA, elicit an inhibitory effect upon NFκB activation (Largo *et al.*, 2003; Mendes *et al* 2002). Small molecule inhibitors and viral gene transfer are two methods which have been used with varying degrees of success to modulate NFκB signalling *in vitro* and *in vivo* (Friedman *et al.*, 2002; Schreiber *et al.*, 2005).

Viral vectors have been employed as a tool in vaccination and to modify gene expression for nearly half a century and have been successfully employed in *in vitro*, *in vivo* and *ex vivo* studies (Graham *et al.*, 1995). Of the 5 viral vector systems routinely used to modify gene expression, adenoviruses are particularly attractive as they can infect both dividing and non-dividing cells, possess a readily manipulated genome and can be amplified to high viral titers (Barnett *et al.*, 2002). Structurally, each adenoviral virion forms a nonenveloped capsid with a linear double stranded DNA genome approximately 36kb in size. In humans, 51 adenoviral serotypes exist, serotypes Ad2 and Ad5 are the most extensively studied (Osten *et al.*, 2007). Adenoviruses contain transcription sites, referred to as either early or late transcription units dependent upon when during the viral infection process they are activated. Six early transcription sites: E1A, E1B E2A, E2B, E3 and E4, activated during the initial stages of viral

infection, are responsible for the replication of the adenoviral genome within the host cell (Goncalves *et al.*, 2006; He *et al.*, 1998). The gene of interest is routinely inserted into the E1 and E3 regions or into the region between E4 and the end of the genome (Chroboczek *et al.*, 1992; Graham *et al.*, 1995). Replacement of the E1 region by the inserted gene renders the virus replication deficient (Graham *et al.*, 1977), whilst insertion of the target gene into the E3 region deletes non-essential processes, such as the production of viral proteins employed during the evasion of host immunity. Infection of host cells with the recombinant adenovirus results in the inserted gene of interest being expressed in the nucleus of the cell, however as the adenovirus does not integrate into the host cell chromosomes, the effect of the inserted gene is relatively transient and hence repeated administration is typically required (Glick & Pasternak, 1998).

First generation adenoviruses with deletions in the E1 and E3 regions have proved to be relatively toxic *in vivo*, a reduction in toxicity was observed when deletions in the E2 and E4 regions of the adenoviral genome were included (Gorziglia *et al.*, 1999; Ji *et al.*, 1999). However, helper dependent adenoviruses, deleted for all viral genes, may prove to be the most successful, as toxicity is reduced significantly, whilst expression of the transgene of interest is increased markedly (Thomas *et al.*, 2003).

Adenoviral gene transfer studies have routinely been used as 'proof of concept' approaches to determine if modulation of signalling cascades or the overexpression of specific genes can alter pathology. Targeting the NFκB signalling pathway through the overexpression of the inhibitory protein IκBα resulted in downregulation of a host of mediators associated with activation of endothelial cells, such mediators have also been associated with inflammation

and disease pathology in a number of different disease processes (Wrighton *et al.*, 1996). A subsequent study demonstrated that targeting the NFκB signalling pathway in the same fashion resulted in inhibition of TNFα production by human macrophages, inhibition of TNFα in RA has since revolutionised treatment for the disease (Foxwell *et al.*, 1998). Synovial cells derived from rheumatoid patients have been successfully transfected with an adenovirus that overexpresses the inhibitory IκBα protein, resulting in downregulation of a range of mediators associated with inflammation and joint destruction (Bondeson *et al.*, 1999). Such observations have been strengthened by a later study employing an adenovirus encoding IKK2 in RA synovial fibroblasts. This study demonstrated that inflammatory cytokine and destructive MMP levels from RA-SF could be reduced by transfection with the IKK2 encoding adenovirus (Andreakos *et al.*, 2003).

Alternatively, specific cytokines and mediators associated with disease pathology can be targeted. Adenoviral gene transfer of TGFβ and BMP anatagonists were employed successfully to demonstrate the critical role of these two mediators in OA pathology (Scharstuhl *et al.*, 2003). Studies performed in both rabbits and mice with experimentally induced arthritis demonstrated that adenoviral gene transfer of IL-10, a cytokine expressed by T cells and macrophages, resulted in a reduction in cartilage matrix degradation, synovitis and other arthritic-associated effects *in vivo* (Keravala *et al.*, 2006; Lechman *et al.*, 1999; Ma *et al.*, 1998).

Adenoviral gene transfer has yet to be employed as a routine clinical option in humans, the greatest success story to date has been gene therapy for cystic fibrosis patients. The identification of the mutated CFTR gene in cystic

fibrosis patients in 1989 led to intensive research being focused on gene therapy as a potential therapeutic strategy (Flotte *et al.*, 1999). Adenoviral vectors were employed as a vehicle to deliver the CTFR gene to the lungs of rats with a degree of success (Riordan, 1999; Wagner *et al.*, 1997). However, clinical studies employing viral mediated transfer of the CFTR gene have highlighted that the principle of gene therapy for cystic fibrosis patients as a realistic concept, yet current strategies employing adenoviral gene transfer have proved inefficient with no significant clinical improvement reported (Joseph *et al.*, 2001; Rosenecker *et al.*, 2006).

Despite the advances of viral gene transfer and clinical trials employing adenoviral vectors in cystic fibrosis sufferers, adenoviral vectors remain problematic due to the lack of efficiency in expression of the gene of interest during *in vitro* studies and immune responses to the viral vector during *in vivo* studies. Clinical trials employing adenoviruses have been relatively unsuccessful and in one study the death of a participant was due to the intravenous dose of adenovirus received eliciting an acute inflammatory response that eventually led to multiple organ failure (Thomas *et al.*, 2003). Such a severe reaction to administered adenoviruses has been reported to occur in response to the capsid proteins of the virus (Schnell *et al.*, 2001). Currently adenoviral gene transfer remains a useful tool for *in vitro* studies, but remains to be employed successfully *in vivo*.

Consequently during recent years, drug development has focused on the design of small molecule inhibitors as a method of modifying disease pathology for a whole host of disease (Fantini *et al.*, 2006). Small molecule inhibitors typically target cell surface receptors, enzymes involved with pathology and

proteins that form a protein-protein interaction (Gadek *et al.*, 2003). Of the three targets, inhibiting enzymes has proved the most successful in the treatment of OA, as NSAIDS, agents able to block to prostaglandin synthesis, have been used successfully in the clinic for over 4 decades to treat the symptoms of OA (Gadek *et al.*, 2003; Paulus *et al.*, 1973).

Developing small molecule inhibitors that can bind to a cell surface receptor and prevent binding of the natural peptide or hormone has the potential to modulate pathology for an array of conditions. An example of an agonist of a cell surface receptor is Losartan, an angiotensin II receptor antagonist that has been used successfully in the treatment of renal disease (Timmermans *et al.*, 1993). The third class of small molecule inhibitors, those that target protein-protein interactions are still in their relative infancy, but recent advances have highlighted that of the three classes, modulation of protein-protein interactions may prove to be the most successful. It was speculated that small molecule inhibitors would be unable to successfully target large protein-protein interactions due to the difference in size, however, advances in structural studies of protein-protein interactions have led to a greater selectivity in targeting small molecule inhibitors successfully (Ockey *et al.*, 2002; Toogood 2002). Aggrestat and Integrilin, are examples of two small molecule inhibitors that target protein-protein interactions that have been employed for the treatment of patients undergoing transluminal coronary angioplasty (Quinn *et al.*,1999).

Modulation of cell signalling by small molecule protein kinase inhibitors is one of the most attractive targets in the search for new pharmacological agents. Protein kinases within signal transduction cascades are responsible for protein phosphorylation, inhibitors are typically directed towards the ATP-

binding site on the kinase. However as many peptides utilise ATP, inhibitors need to specifically discriminate between the kinase ATP binding site they are directed against and an abundance of similar sites (Bogoyevitch *et al.*, 2005; Fischer, 2004). Inhibition of the NFκB signalling pathway has been highlighted as an attractive target for OA due to the involvement of IL-1β and TNFα, two potent inducers of NFκB signalling. Indeed Ibuprofen and Aspirin both routinely prescribed to alleviate the pain associated with OA are inhibitors NFκB signalling via the IKK and both the IKK and IκB proteins respectively (Kopp *et al.*, 1994; Palayoor *et al.*, 1999; Yin *et al.*, 1998). A major step in the pathway that has been targeted by small molecule inhibitors are the IKK peptides, with IKK2 a particularly attractive target (Roshak *et al.*, 2002). Many inhibitors of the IKK complex are under development with SPC839 an IKK2 specific inhibitor demonstrated to be efficacious as a small molecule inhibitor in an animal model of arthritis (Roshak *et al.*, 2002; Siebenlist *et al.*, 1994).

Other IKK inhibitors that have been trialled in rodent models of inflammatory arthritis include ML102B trialled in both murine and rat models with a degree of success, BMS-345541 employed in the murine CIA model of arthritis demonstrated an anti-inflammatory effect and TPCA-1 reduced the severity of disease when administered in the murine CIA model (Izmailova *et al.*, 2007; McIntyre *et al.*, 2003; Podolin *et al* 2005; Schopf *et al.*, 2006). A fourth inhibitor, DHMEQ, inhibits the nuclear translocation of activated NFκB and has demonstrated an anti-inflammatory effect in both *in vitro* and *in vivo* models of RA (Wakamatsu *et al.*, 2005). Despite such promising results, small molecule inhibitors of the NFκB signalling pathway have yet to be used successfully in the clinical treatment of either RA or OA.

Few studies have previously examined the efficacy of NFκB inhibition as a potential therapeutic target for OA. We studied the validity of NFκB inhibition as a therapeutic intervention for OA using adenoviral gene transfer and two small molecule pharmacological inhibitors. We determined whether this signalling cascade played an important role in the OA disease process using adenoviruses, and subsequently employed two small molecule inhibitors of the NFκB signalling cascade and assessed their efficacy *in vitro*.

The specific aims of this chapter were to:

- Establish the efficacy of transfection of OA-SF with an adenovirus encoding the inhibitory subunit IκBα and thereby assess the importance of NFκB in pathogenic responses driven by IL-1β stimulation.
- Employ small molecule inhibitors of NFκB signalling *in vitro* using OA-SF to determine their ability to prevent nuclear NFκB activation in these cells.
- Determine the toxicity that inhibition of NFκB by small molecule inhibitors induces in OA-SF
- Assess the ability of small molecule inhibitors to down regulate the production of pathogenic mediators in response to IL-1β stimulation in OA-SF.

4.2 Results

4.2.1 IL-1β differentially induced a range of cytokines and MMPs.

IL-1β was employed to stimulate OA-SF at a pre-determined concentration (20 ng/ml). Its potency with regard to the generation of pathogenic mediators and MMPs was determined (Figure 4.1). IL-1β elicited significant ($p \leq 0.01$) upregulation of IL-6 (Figure 4.1 a) but no significant effect upon TIMP-1 (Figure 4.1 b), MMP-1 (Figure 4.1 c) and MMP-3 (Figure 4.1 d) levels compared to control unstimulated cells.

4.2.2 Differential induction of a range of cytokines and MMPs by TNFα.

TNFα was employed to stimulate OA-SF at a pre-determined concentration (20 ng/ml). TNFα elicited significant ($p \leq 0.01$) upregulation of IL-6 (Figure 4.2 a) and MMP-1 (Figure 4.2 c) in comparison to control unstimulated cells. TNFα stimulation did not elicit a significant effect upon the levels of TIMP-1 (Figure 4.2 b) or MMP-3 (Figure 4.2 d) in comparison to control unstimulated cells.

4.2.3 OA-SF can be effectively infected using adenoviral gene transfer.

An adenovirus encoding the green fluorescent protein, AdVGFP was employed to determine the MOI required to infect > 90% of OA-SF. Approximately 30% of OA-SF infected with AdVGFP at an MOI of 10:1 expressed the green fluorescent protein when visualised by UV microscopy (Figure 4.3 a). At an increased MOI of 30:1 approximately 90% of OA-SF infected expressed the green fluorescent protein, suggesting that adenoviral gene transfer at 30:1 ensures expression of the inserted transgene in >90% of OA-SF (Figure 4.3 b).

4.2.4 Efficacy of adenoviral gene transfer of the inhibitory subunit IκBα in response to IL-1β stimulation in OA-SF.

In order to assess the inhibitory efficacy of adenoviral gene transfer of the IκBα subunit in OA-SF following IL-1β stimulation, an adenovirus encoding the inhibitory protein IκBα (AdVIκBα) was compared against a control vehicle-only adenovirus (AdV0) (Figure 4.4). In response to IL-1β stimulation the levels of IL-6, TIMP-1, MMP-1 and MMP-3 were not significantly reduced by AdVIκBα transfection in comparison to AdV0 infected OA-SF (Figure 4.4 a, b, c, d).

4.2.5 Efficacy of adenoviral gene transfer of the inhibitory subunit IκBα in response to TNFα stimulation in OA-SF.

In order to assess the inhibitory efficacy of adenoviral gene transfer of the IκBα subunit in OA-SF following TNFα stimulation, an adenovirus encoding the inhibitory protein IκBα (AdVIκBα) was compared against a control vehicle-only adenovirus (AdV0) (Figure 4.5). In response to TNFα stimulation the levels of IL-6, TIMP-1, MMP-1 and MMP-3 were not significantly repressed by AdVIκBα transfection compared to AdV0 infected OA-SF (Figure 4.5 a, b, c, d).

4.2.6 IL-1β induction of IL-6, MMP-1, MMP-3 but not TIMP-1 can be inhibited by preventing NFκB activation.

The levels of IL-6, MMP-1, MMP-3 and TIMP-1 produced by AdVIκBα infected, IL-1β stimulated OA-SF were compared to uninfected, IL-1β stimulated OA-SF (Figure 4.6). The data, expressed as a percentage, illustrated that inhibition of NFκB signalling via overexpression of IκBα resulted in

significant inhibition ($p \leq 0.05$) of IL-6 representing a 68% reduction in comparison to uninfected IL-1β stimulated cells (Figure 4.6 a). The cartilage protective mediator, TIMP-1 was not significantly affected by AdVIκBα but was modestly downregulated (18%) (Figure 4.6 b), whilst the destructive enzymes, MMP-1 and MMP-3 were significantly repressed by 65% ($p \leq 0.01$) and 59% ($p \leq 0.05$) respectively following AdVIκBα infection (Figure 4.6 c & d).

4.2.7 An adenovirus encoding IKK2dn demonstrated limited efficacy in inhibiting NFκB activation in OA-SF

An adenovirus encoding the IκB kinase2 (IKK2) subunit, a critical protein involved in NFκB signal transduction, was employed across an MOI range (50:1 – 500:1) and compared with uninfected OA-SF and OA-SF infected with a control adenovirus encoding the β-galactosidase gene (Figure 4.7). It was observed that only at a dose of 500:1 was NFκB activation inhibited in OA-SF by AdvIKK2dn (Figure 4.7 a). Densitometric analysis demonstrated OA-SF infected with the 3 lower MOIs of AdVIKK2dn (50:1, 100:1, 250:1) and subsequently stimulated with TNFα elicited an upregulation in NFκB activation in comparison to uninfected OA-SF (Figure 4.7 b). Only at an MOI of 500:1 did AdVIKK2dn elicit a marked downregulation in nuclear NFκB activation. However, cell viability data from OA-SF infected with AdVIKK2dn at an MOI of 500:1 demonstrated that viability was markedly reduced (< 50%), suggesting that the effect upon nuclear activation at this dose was probably a consequence of toxicity (Figure 4.7 c).

4.2.8 A micromolar dose range of both RO100 and RO919 dose dependently inhibit NFκB activation without affecting cell viability

Both RO100 and RO919 (0.03, 0.1, 1μM) were employed to modulate IL-1β (20ng/ml) induced NFκB activation in OA-SF (Figure 4.8). EMSAs conducted on the nuclear extracts of treated OA-SF showed dose dependent inhibition of NFκB activation (Figure 4.8 a). Densitometric analysis demonstrated a significant ($p \leq 0.05$) reduction in NFκB nuclear signalling at the 1μM dose (Figure 4.8 b). Binding specificity was confirmed by competition assays against unlabelled oligonucleotides of identical NFκB sequence and using unrelated AP-1 consensus or mutant sequences. Cell viability at the three doses employed were assessed in OA-SF using the alamarBlue® assay. Across the dose range cell viability remained >95% for both RO100 and RO919 (Figure 4.8 c).

4.2.9 IL-1β induction of MMP-3 but not TIMP-1 in OA-SF can be inhibited by preventing NFκB activation

Both RO100 and RO919 were initially employed across a dose range (0.03, 0.1, 1μM) to determine the dose required to inhibit the cartilage destructive regulator for MMP-3 but not its natural mediator TIMP-1 (Figure 4.9). Both RO100 and RO919 elicit a significant ($p \leq 0.05$) dose dependent inhibition of IL-1β induced MMP-3 with the greatest effect observed at the 1μM dose, suggesting that IL-1β induction of MMP-3 is NFκB dependent across the dose range (Figure 4.9 a & b). In contrast neither the 0.1μM nor 0.03μM dose affected TIMP-1 production in this system. However at the 1μM dose the levels of TIMP-1 were significantly affected ($p \leq 0.05$) and were reduced to pre-IL-1β

stimulation levels. It would therefore appear that IL-1β induced TIMP-1 can only be regulated by NFκB inhibition at high doses that result in significant inhibition of IL-1β induced NFκB nuclear activation.

4.2.10 IL-1β induction of IL-6, MMP-1 and MMP-3 in OA-SF can be inhibited by preventing NFκB activation.

As a consequence of the study conducted in 4.2.9 which examined the effect of a micromolar dose range of both RO100 and RO919 upon the cartilage destructive mediator MMP-3 and the cartilage protective mediator TIMP-1, a 0.1μM dose was used for further investigation. The induction of IL-6 was significantly ($p \leq 0.05$) repressed with a 73% reduction in IL-6 levels from OA-SF treated with RO100 (Figure 4.10 a) and a 56% reduction when treated with RO919 (Figure 4.10 b). Induction of MMP-3 was also significantly ($p \leq 0.05$) inhibited with an 80% drop in MMP-3 levels from OA-SF treated with RO100 and a 72% reduction from RO919 treated OA-SF. The effect upon the induction of MMP-1 was more pronounced with a highly significant reduction ($p \leq 0.01$) when treated with RO100 (80%) and RO919 (66%). Neither inhibitor elicited a notable effect upon the induction of TIMP-1.

4.2.11 Synovial explants treated with either anti-cytokine therapeutics or an NFκB inhibitor produced significantly lower levels of IL-6 and MMP-1.

Synovial explants treated with a combination of etanercept and anti-IL-1β or a 0.1μM dose of RO100 elicited a significant ($p \leq 0.01$) reduction in IL-6 (Figure 4.11 a). Neither treatment strategy elicited a notable effect upon the production of TIMP-1 in comparison to untreated explants (Figure 4.11 b). Whilst MMP-1 production was significantly ($p \leq 0.05$) inhibited by both a

combination of etanercept and anti-IL-1β or a 0.1μM dose of RO100 (Figure 4.11 c), neither treatment strategy elicited a significant effect upon MMP-3 production (Figure 4.11 d). Thus, we have demonstrated a cytokine signalling cascade dependent on IL-1β and TNFα activation of NFκB can be targeted to inhibit a range of critical mediators in OA, in both single cell systems and in a physiological relevant *ex vivo* model.

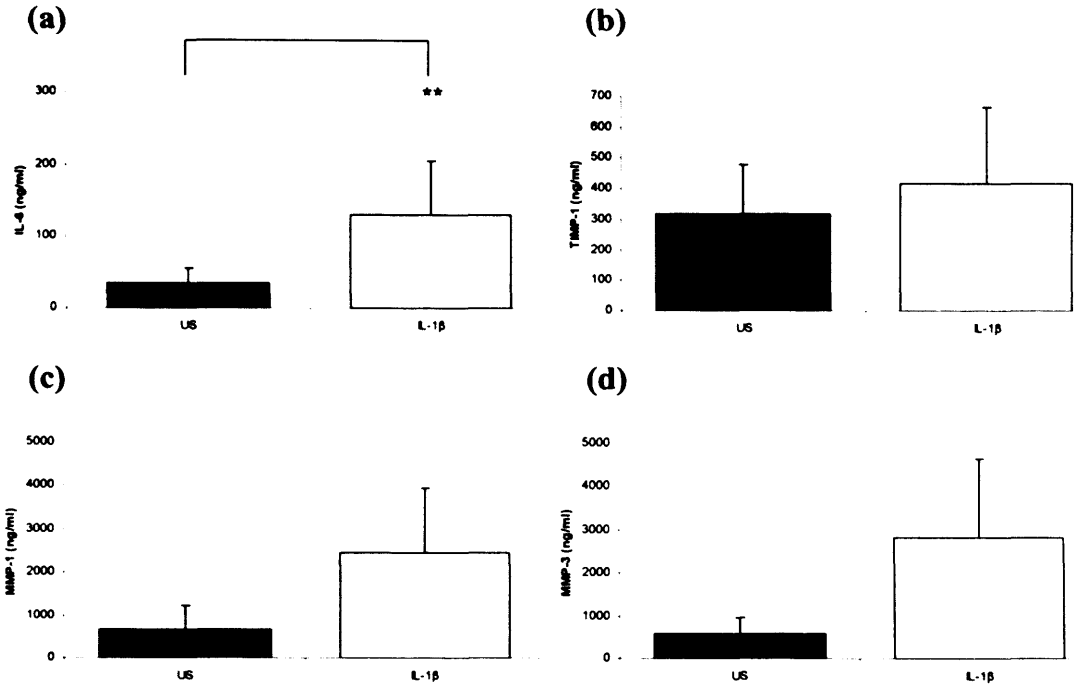

Figure 4.1 The effect of IL-1β stimulation upon cytokine and MMP production from OA-SF.

OA-SF were cultured on 12 well plates as previously described. Following a 36 hour adherence period the cells were either left unstimulated (US) or stimulated with IL-1β (20ng/ml). At 24 hours post stimulation supernatants were harvested and analysed by specific ELISA to determine the levels of IL-6, MMP-1, MMP-3 and TIMP-1. Results are given as the mean ± SEM of 4 independent experiments expressed as ng/ml. ** $p \leq 0.01$ as determined by the students two tailed paired means T test.

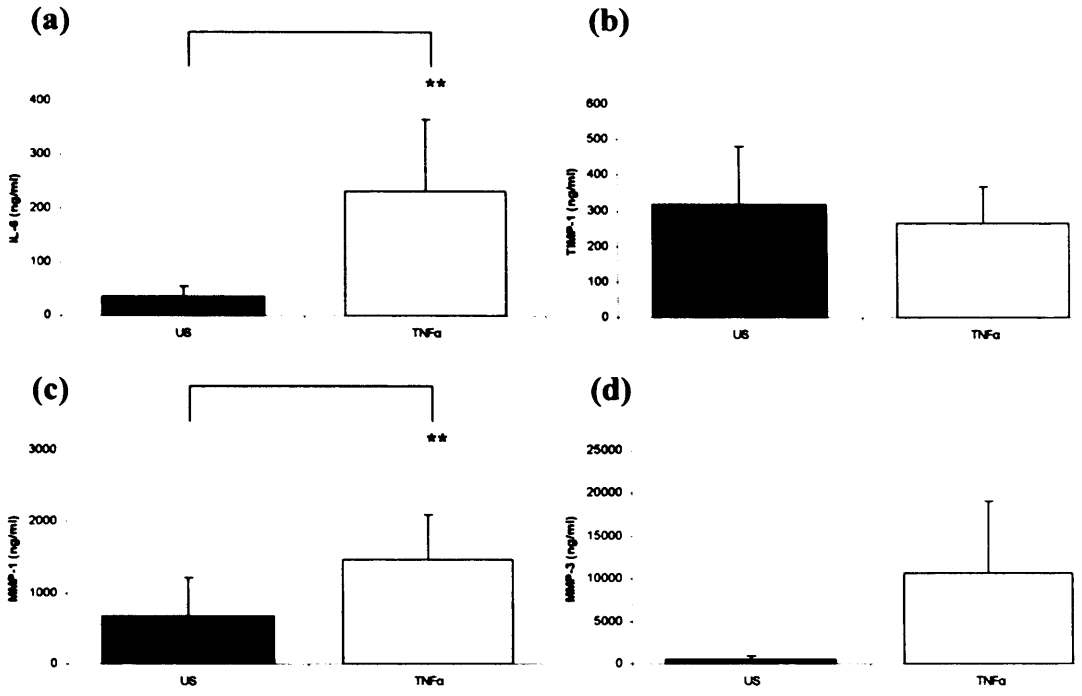

Figure 4.2 The effect of TNFα stimulation upon cytokine and MMP production from OA-SF.

OA-SF were cultured on 12 well plates as previously described. Following a 36 hour adherence period the cells were either left unstimulated (US) or stimulated with TNFα (20ng/ml). At 24 hours post stimulation supernatants were harvested and analysed by specific ELISA to determine the levels of IL-6, MMP-1, MMP-3 and TIMP-1. Results are given as the mean ± SEM of 4 independent experiments expressed as ng/ml. ** $p \leq 0.01$ as determined by the students two tailed paired means T test.

(a)

(b)

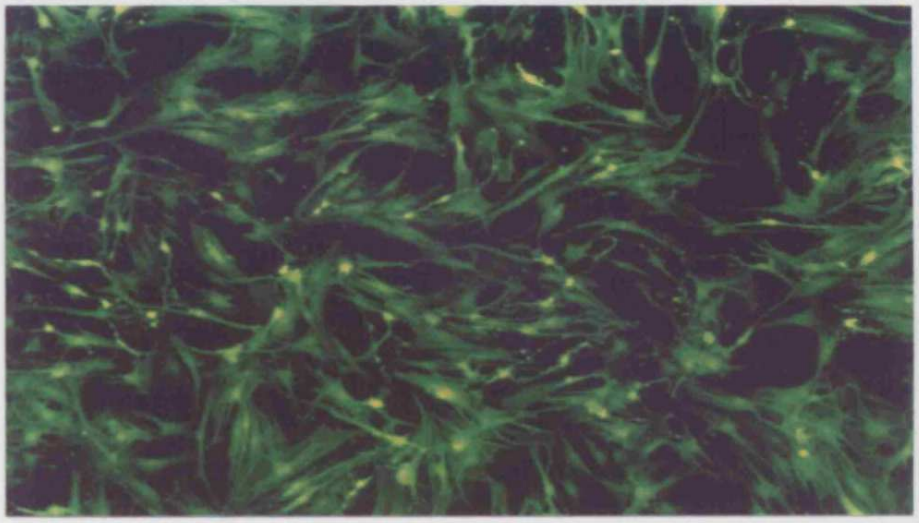

Figure 4.3 Efficiency of adenoviral gene transfer.
OA-SF transfected with an adenovirus encoding green fluorescent protein, AdVGFP, at an MOI of 10:1 (a) and 30:1 (b), were visualised using UV microscopy at 48 hours post-transfection. The efficacy of adenoviral gene transfer of OA-SF was quantified visually by calculating the overall percentage of cells expressing the AdVGFP transgene. Magnification x 200

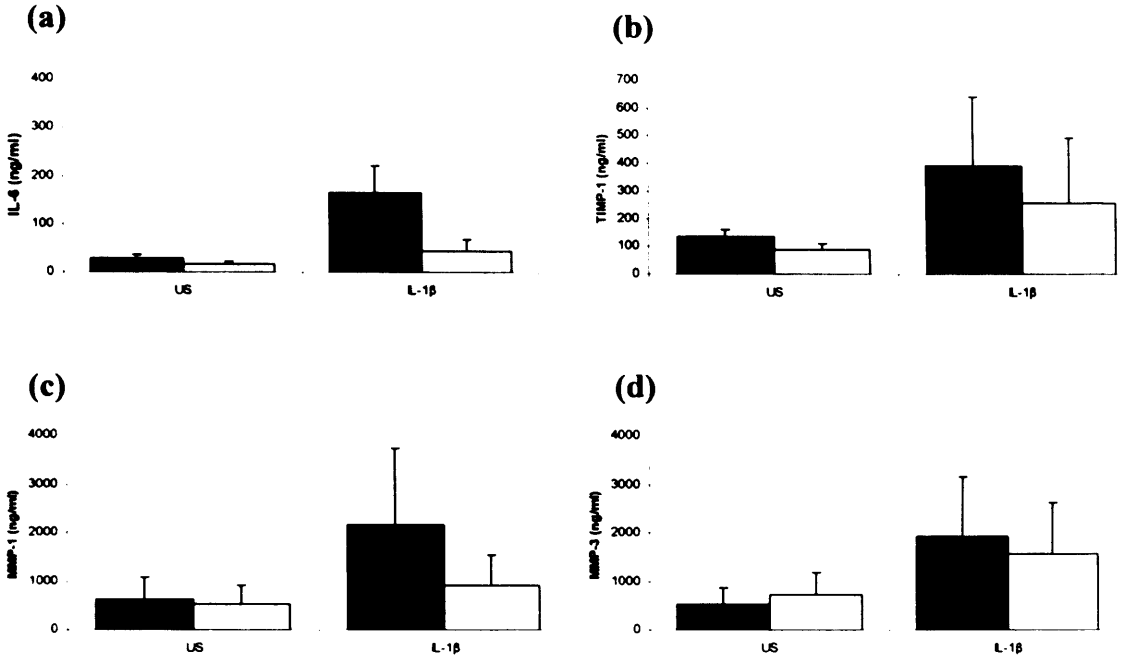

Fig 4.4 Effect of overexpression of the inhibitory protein IκBα upon cytokine and MMP production induced by IL-1β.

OA-SF were infected with either AdV0 or AdVIκBα for 2 hours as described in chapter two. Viral supernatants were removed and the cells left for 22 hours to allow gene expression. Cells were then either left unstimulated (US) or stimulated with IL-1β (20ng/ml) for 24 hours. The resulting supernatants were harvested and IL-6, MMP-1, MMP-3 and TIMP-1 levels were specifically quantified by ELISA. The effect of an adenovirus transferring the IκBα protein (AdVIκBα) was compared to a vehicle-only adenovirus (AdV0). Closed bars denotes AdV0 infected cells , open bars denote AdVIκBα infected cells.

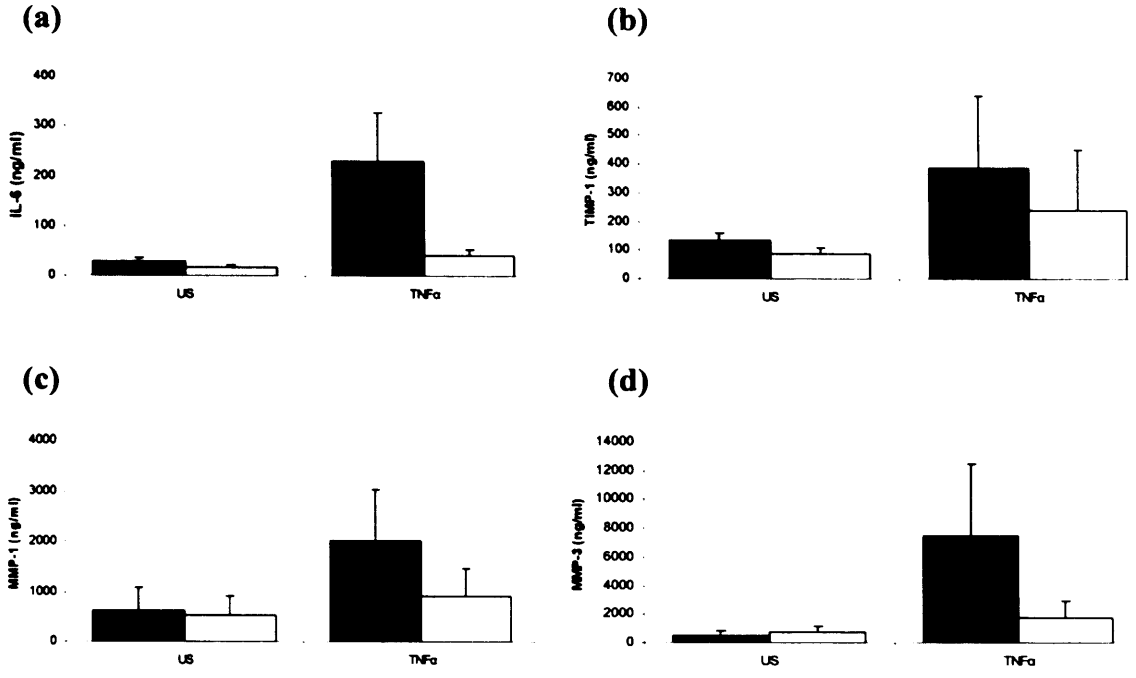

Fig 4.5 Effect of overexpression of the inhibitory protein IκBα upon cytokine and MMP production induced by TNFα.

OA-SF were infected with either AdV0 or AdVIκBα for 2 hours as described in chapter two. Viral supernatants were removed and the cells left for 22 hours to allow gene expression. Cells were then either left unstimulated (US) or stimulated with TNFα (20ng/ml) for 24 hours. The resulting supernatants were harvested and IL-6, MMP-1, MMP-3 and TIMP-1 levels were specifically quantified by ELISA. The effect of an adenovirus transferring the IκBα protein (AdVIκBα) was compared to a vehicle-only adenovirus (AdV0). Closed bars denotes AdV0 infected cells, open bars denote AdVIκBα infected OA-SF.

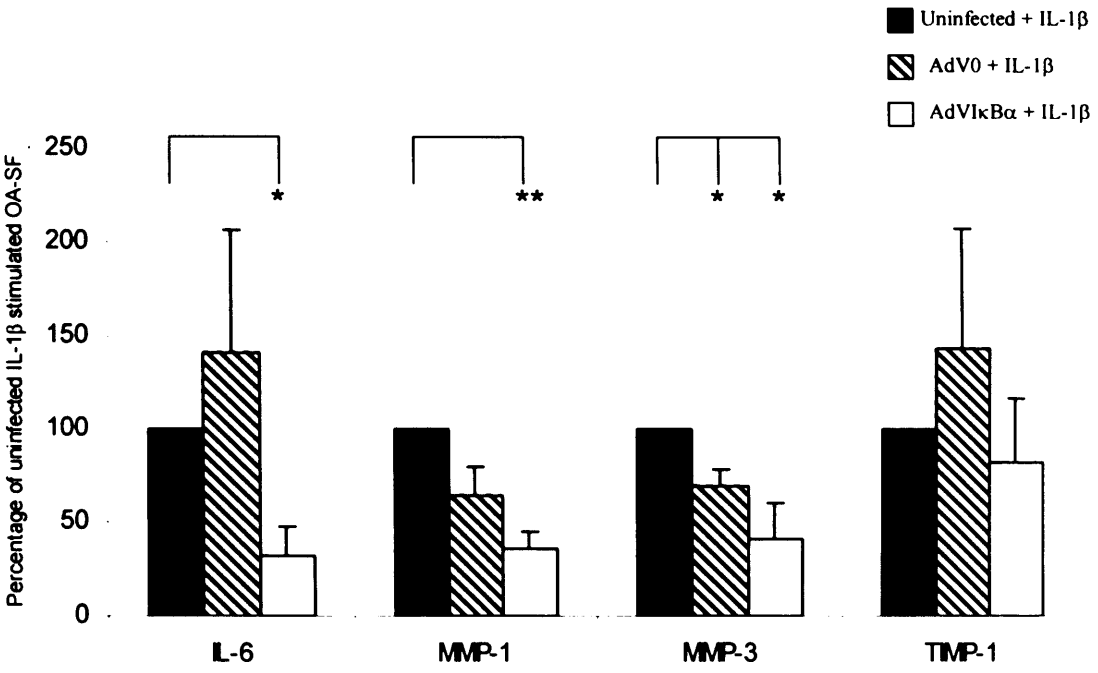

Fig 4.6 The effect of inhibiting NFκB signalling by overexpression of the inhibitory protein IκBα

OA-SF were infected with either AdV0 or AdVIκBα for two hours, as described in the materials and methods. Viral supernatant was removed and cells left for 22 hours to allow gene expression. Cells were then stimulated with IL-1β (20ng/ml) for 24 hours, the resulting supernatants were harvested and IL-6, MMP-1, MMP-3 and TIMP-1 levels were specifically quantified by ELISA. Results are expressed as the mean percentage of 4 independent experiments, with 100% representing the production of mediators from uninfected, IL-1β stimulated OA-SF. Error bars represent SEM. A paired T test was conducted on the percentage data, with the uninfected IL-1β stimulated levels of each cytokine given as follows (ng/ml mean ± SEM), IL-6 (131 ± 13.46), MMP-1 (3013 ± 1296.63), MMP-3 (239 ± 217.66), TIMP-1 (184 ± 59.80) * denotes $p \leq 0.05$, ** $p \leq 0.01$ versus uninfected IL-1β stimulated OA-SF.

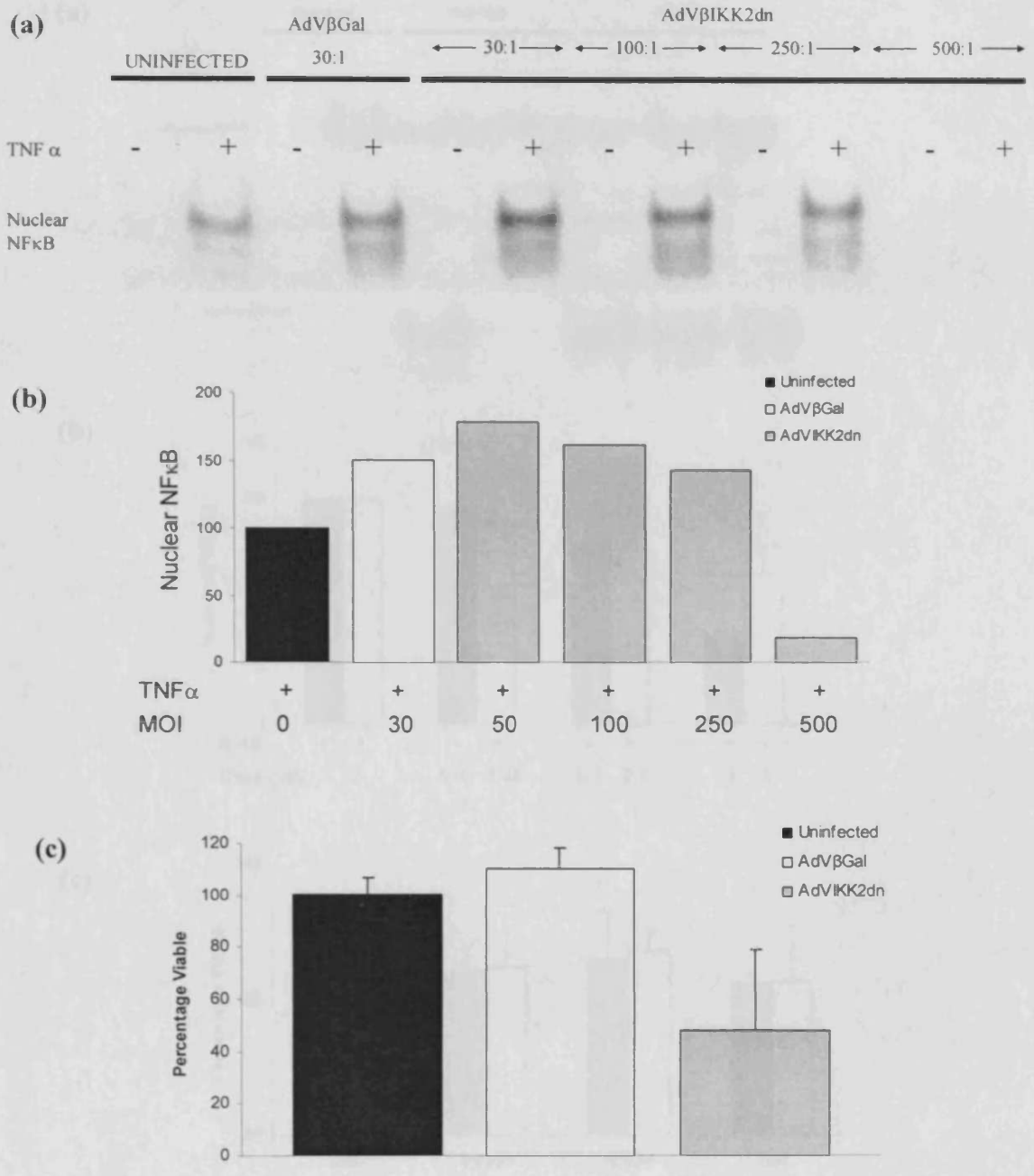

Figure 4.7 Modulation of NFκB signalling by an adenovirus encoding the IKK protein

Nuclear extracts were generated from OA-SF infected with AdVβGal (MOI 30:1) or AdVIKK2dn (MOI 50:1 – 500:1) for 2 hours before stimulation with TNFα (20ng/ml) for 30 minutes. The extracts were analysed by EMSA (a) note only the nuclear-protein DNA complexes are shown. Densitometric analysis (b) was conducted on the EMSA illustrated using NIH image software with the results given as the mean ± SEM expressed as a percentage of the nuclear NFκB. An almarBlue® cell viability assay was conducted on two cell lines treated with an MOI range of AdVIKK2dn (c). The mean of the two cell lines is expressed as a percentage (error bars represent SEM).

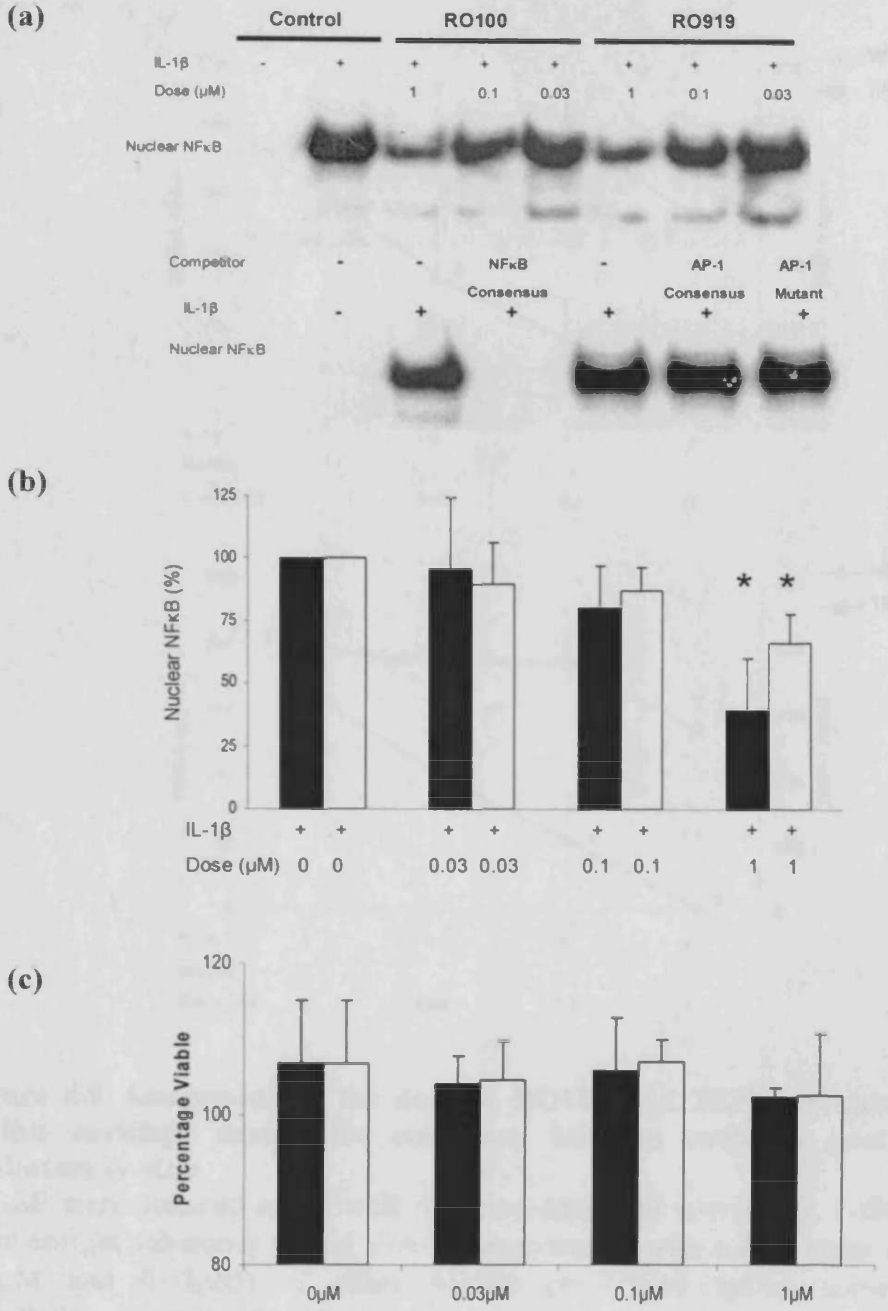

Figure 4.8 The effect of an administered dose range of RO100 and RO919 upon IL-1β induced NFκB activation.

Nuclear extracts were generated from OA-SF treated with the doses of RO100 and RO919 indicated for two hours before stimulation with IL-1β (20ng/ml) for 30 minutes. The extracts were analysed by EMSA (a) note only the nuclear-protein DNA complexes are shown. Densitometric analysis (b) was conducted on EMSAs derived from 4 individual OA patients using NIH image software with the results given as the mean ± SEM, expressed as a percentage of nuclear NFκB. OA-SF were cultured on 12 well plates as described previously. Following an overnight adherence period, OA-SF were treated with a dose range of RO100 (closed bars) and RO919 (open bars) (1μM, 0.1μM, 0.03μM) before subsequent stimulation with IL-1β (20ng/ml). Cell viability was assessed at 24 hours post stimulation (c). The data is presented as the percentage viable of control untreated, IL-1β stimulated cells.

(a)

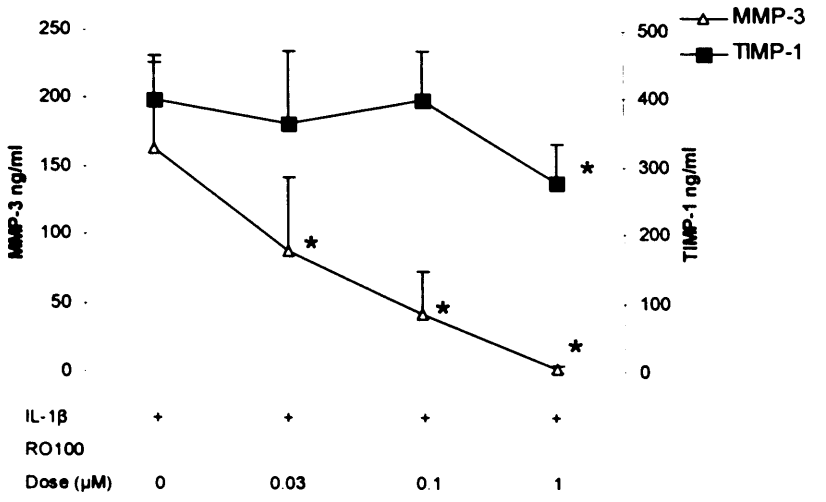

(b)

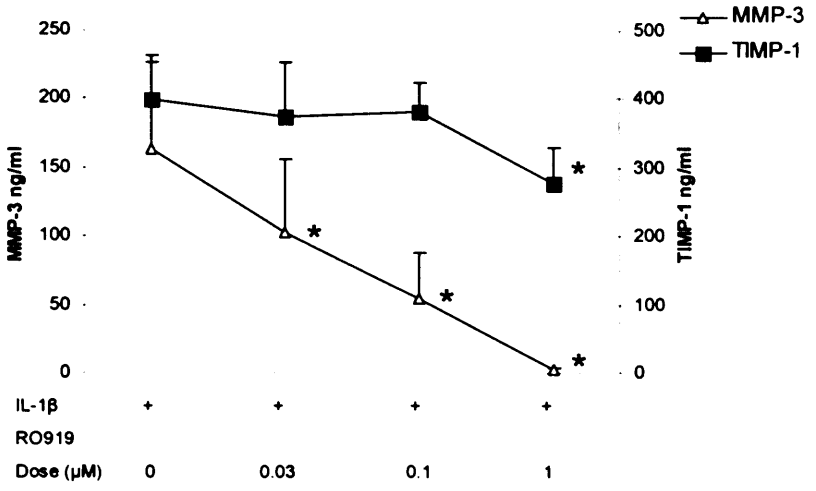

Figure 4.9 Assessment of the dose of RO100 and RO919 required to inhibit cartilage destructive mediators but not cartilage protective mediators *in vitro*.

OA-SF were cultured on 12 well plates as described previously. Following an overnight adherence period, OA-SF were treated with a dose range (1μm, 0.1μM and 0.03μM) of either RO100 or RO919 before subsequent stimulation with IL-1β (20ng/ml). Supernatants were harvested 24 hours after stimulation and analysed by specific ELISA to determine the levels of MMP-3 and TIMP-1 present as a result of each treatment condition. Results are given as the mean ± SEM of 5 independent experiments expressed as ng/ml. The MMP-3 axis and TIMP-1 axis are different to incorporate the different physiological levels expressed *in vitro*. * $p \leq 0.05$ versus untreated IL-1β stimulated OA-SF determined using a two tailed paired means student's t test.

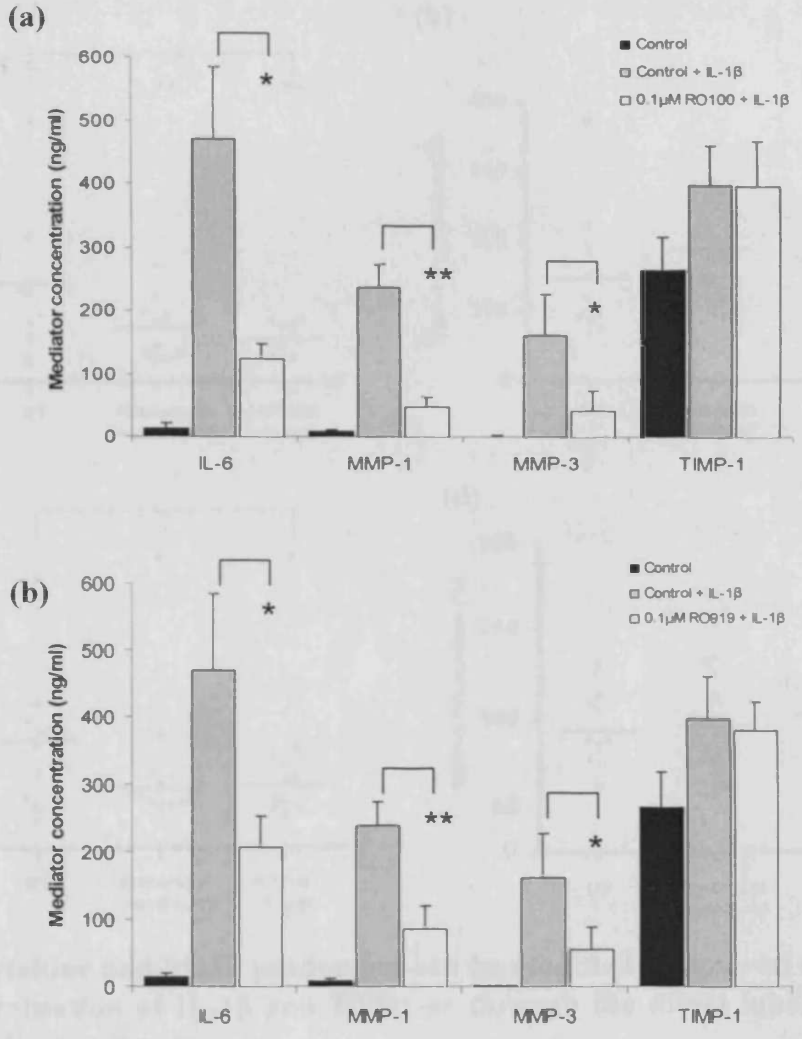

Figure 4.10 Effect of NFκB inhibition upon the release of pathogenic mediators in response to IL-1β stimulation in the OA-SF model
OA-SF, derived from 5 individual patients, were treated with a 0.1μM dose of RO100 and RO919 for 2 hours prior to IL-1β stimulation (20ng/ml), at 24 hours post stimulation supernatants were harvested and the levels of IL-6, MMP-1, MMP-3 and TIMP-1 quantified by specific ELISA. Data represent mean ± SEM of each treatment condition expressed in ng/ml. * $p \leq 0.05$ and ** $p \leq 0.01$ versus carrier + IL-1β.

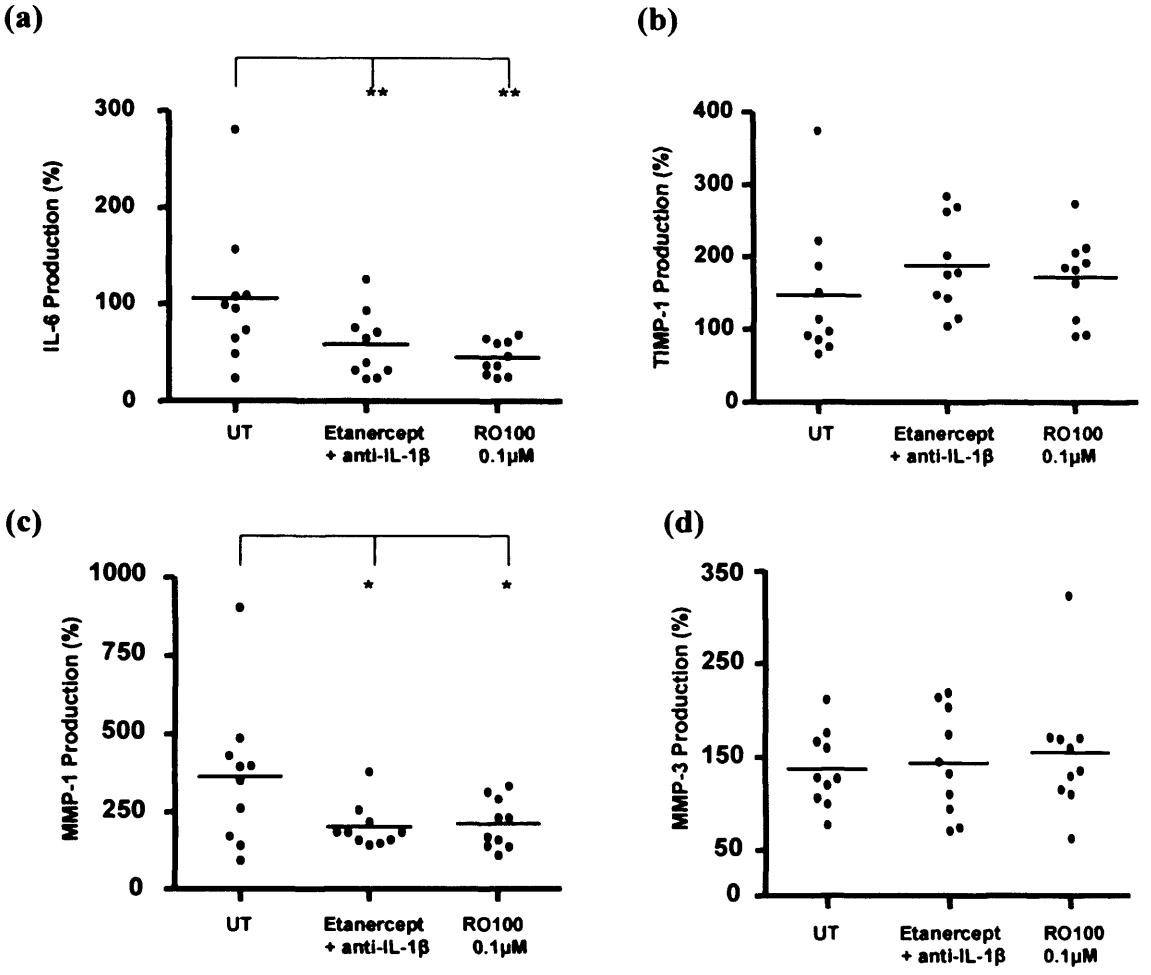

Figure 4.11 Cytokine and MMP production can be modified in synovial explants either by neutralisation of IL-1β and TNFα or through the direct inhibition of the NFκB signalling pathway

Synovial explants were prepared as described previously in the materials and methods, each explant was left to equilibrate for 18 hours to provide a baseline value to compare against. The baseline value provides the 100% value against which the explant is compared following treatment, after 18 hours each explant was either left untreated (UT) or treated with a combination of Etanercept and anti-IL-1β (10μg/ml and 100μg/ml respectively) or a 0.1μM dose of RO100 for 24 hours before the supernatants were harvested and IL-6, MMP-1, MMP-3 and TIMP-1 production established by ELISA and adjusted for weight. To accommodate the intra-variability present within each synovial sample, treatment conditions were conducted in triplicate or quadruplicate depending upon the size of the original synovial specimen and the mean calculated for each treatment strategy. Results are expressed as a percentage, with the mean of each treatment condition indicated by the solid horizontal line. Data represents 10 independent experiments, derived from 10 individual patients. * $p \leq 0.05$ and ** $p \leq 0.01$ versus untreated explants, as determined by using both a two tailed paired t test and the nonparametric Wilcoxon match pairs test.

4.3 Discussion.

Mounting evidence suggests that IL-1β and TNFα are critical in the initiation and perpetuation of cartilage destruction in OA (Fernades *et al.*, 2002). The OA-COCUL system used in chapter three demonstrated that IL-6, MMP-1, and MMP-3 production was downregulated when TNFα and IL-1β were neutralised. Consequently the levels of these three mediators were measured following NFκB inhibition as a representative readout of OA pathology throughout the studies conducted during chapter 4.

Initial studies conducted in order to determine the effect of IL-1β and TNFα upon IL-6, MMP-1, MMP-3 and TIMP-1, demonstrated that TNFα induced greater levels of IL-6 and MMP-3 than IL-1β, whilst the levels of TIMP-1 and MMP-1 were enhanced in response to IL-1β stimulation in comparison to TNFα. Whilst this effect was not significant, due to the large inter-patient variability, each individual experiment demonstrated increased cytokine and MMP production following stimulation. However, when OA-SF are infected with AdVIκBα the differential induction of IL-6, MMP-1, MMP-3 and TIMP-1 in response to IL-1β and TNFα was altered, with both IL-1β and TNFα eliciting a similar stimulatory effect upon the production of IL-6, MMP-1, MMP-3 and TIMP-1. In light of the literature that suggests IL-1β plays the primary role in cartilage destruction within the joint (Goldring *et al.*, 2004), and due to the observations of our own study whereby both IL-1β and TNFα upregulate cytokine and MMP release from OA-SF, IL-1β was used to stimulate cells in subsequent studies employing pharmacological agents, unless indicated otherwise.

Adenoviral gene transfer has been successfully employed as an *in vitro* tool to modulate a number of signalling pathways in a range of cell types including epithelial cells, dendritic cells, and chondrocytes (Arai *et al.*, 2004; Foxwell *et al.*, 2001; Wrighton *et al.*, 1996). Studies conducted to determine the adenoviral MOI required to efficiently transfect OA-SF with >95% efficiency, were in agreement with previous studies in RA-SF whereby an MOI of 30:1 was sufficient to elicit expression of the GFP transgene in >95% of RA-SF infected with AdVGFP (Andreakos *et al.*, 2003). An adenovirus encoding the inhibitory protein IκBα was employed in subsequent studies to modulate NFκB signalling. During the original construction of the AdVIκBα vector, a reporter gene was not incorporated alongside the gene of interest. Currently constructed adenoviruses would typically include a reporter gene which allows the transfection process to be assessed and determine if problems with efficacy are due to infection of the cells. Having verified that > 95% of OA-SF could be transfected at an MOI of 30:1 with AdVGFP, we employed AdVIκBα at an MOI of 30:1 to modulate NFκB signalling *in vitro*. Previous studies have successfully employed the AdVIκBα virus to modulate activation of the transcription factor (Bondeson *et al.*, 1999; Foxwell *et al.*, 1998).

Adenoviral gene transfer of IκBα proteins enabled the signalling cascade to be blocked at the final step prior to nuclear activation. Transfection of OA-SF with AdVIκBα resulted in the cells overexpressing the inhibitory protein, hence upon stimulation of the cell the excess of IκBα present within the cytoplasm of the cell ensured that an IκBα protein was available to retain the transcription factor latently within the cytoplasm. An empty vehicle only adenovirus (AdV0) was employed to ensure that any alteration in signalling was due to

overexpression of the gene of interest and not due to the adenovirus itself. Targeting the NFκB signalling cascade in this approach resulted in significant inhibition in the induction of IL-6 and MMP-3 and highly significant inhibition of MMP-1 in comparison to uninfected IL-1β stimulated cells. This study demonstrated that NFκB could be effectively targeted *in vitro* resulting in modulation of the pathogenic mediators released by OA-SF.

In light of the promising results observed with overexpression of the IκBα proteins, a second adenovirus was employed to determine if the NFκB signalling cascade could be targeted further upstream. This study was designed to demonstrate if universal NFκB inhibition was a realistic target by assessing the importance of inhibition of different proteins that constitute the NFκB signalling cascade. Such studies would also highlight proteins within the pathway that may provide an attractive target for future therapies designed for the treatment of OA. We employed an adenovirus encoding a dominant negative form of IKK2, a protein that forms part of the IκB kinase complex, responsible for the phosphorylation of the IκB proteins which results in the nuclear activation of NFκB. Unlike AdVIκBα, which was supplied as a purified ready to use adenovirus, AdVIKK2dn was supplied by the Kennedy Institute as a crude viral lysate requiring amplification and titration. Following amplification, caesium-chloride gradient purification and determination of the MOI by plaque assay, AdVIKK2dn was employed across an MOI range to determine the dose required to effectively downregulate nuclear NFκB activation. It was observed that only at the highest MOI employed, 500:1, was inhibition of NFκB evident. This observation was in agreement with a previous study whereby transfection of RA-SF using an identical AdVIKK2dn required

an MOI of 500:1 (Andreakos *et al.*, 2003). However, cell viability studies conducted on OA-SF transfected with AdVIKK2dn demonstrated that an MOI of 500:1 resulted in toxicity as, > 50% of cells were viable. Visual examination by microscopy of the cells demonstrated that the cells were evidently not healthy and had become detached from the tissue culture plates. Such a toxic effect at the only MOI that appears to elicit a functional effect in inhibiting NFκB activation raises questions about the true efficacy of the adenovirus. It is apparent that the inhibition of NFκB activation corresponds to toxicity, the lack of downregulation observed in nuclear activation at the previous MOI of 250:1 suggests that whilst the adenovirus was able to infect the cells due to the toxicity it can elicit, it appears unable to express a functional AdVIKK2dn protein. During the construction and amplification of adenoviral constructs there are many steps at which a problem can arise. It is probable that the insert had not been cloned in correctly or during recombination events the inserted gene may have been deleted. The study by Andreakos *et al.*, indicated that the virus was functional as a consequence of its ability to reduce the levels of IL-1β, IL-6, IL-8 and MMP-1, -3 and -13, however an MTT assay was used to assess the toxicity of the adenovirus at 500:1, it was stated that the effects seen were not due to toxicity although the viability data was not presented. Our own study contradicts that of Andreakos *et al*, with the adenovirus demonstrated to be toxic.

Despite the initial success we demonstrated with AdVIκBα, subsequent studies employing AdVIKK2dn highlighted the major drawbacks of using adenoviral gene transfer. Firstly, the adenoviruses used were first generation E1, E3 deleted vectors, previous studies demonstrated that these early vectors

can potentially elicit an immunogenic response (Lusky *et al.*, 1998). Second generation adenoviruses possess a greater number of deletions and in some cases the entire genome encoding viral proteins is deleted which significantly reduces the cellular immune response to transfection with the adenovirus (Thomas *et al.*, 2003). The SEM values observed for the AdVIκBα studies were large, such an effect is likely to result from the variability observed when different cell lines are transfected due to a lack of stability of AdVIκBα upon transfection. The expression of transgenes delivered by first generation adenoviruses is a transient effect and as such longterm inhibition of NFκB signalling would require repeated administration of AdVIκBα. Recently constructed adenoviruses with the entire viral genome deleted, HAd, have demonstrated prolonged expression of the transgene that could overcome this disadvantage (Parks *et al.*, 1999). In light of the drawbacks highlighted, we opted to use novel pharmacological agents designed to inhibit NFκB signalling in an attempt to find a more robust and reproducible method of modulating NFκB signalling *in vitro*.

Two pharmacological inhibitors of the NFκB signalling pathway that specifically target the IKK stage of the pathway, namely RO100 and RO919, were used to modify NFκB signalling. Across a micromolar dose range (1μM, 0.1μM, 0.03μM) both RO100 and RO919 elicited a dose dependent effect upon nuclear activation of NFκB. The inclusion of cold competitors demonstrated that our 2 IKK inhibitors were specific for the NFκB transcription factor. At the highest dose inhibition of nuclear activation of the transcription factor was significant as demonstrated by densitometric analysis. However at the lower dose, 0.1μM, a small but notable reduction in NFκB activation was evident.

Indeed, a diminutive reduction in nuclear NFκB activation at the 0.1μM dose of either RO100 or RO919 resulted in significant inhibition of IL-6, MMP-1 and MMP-3 in IL-1β stimulated OA-SF. Such observations suggest that the production of these three mediators, that are so important in the acceleration of the disease process, is tightly regulated by NFκB activation. Our study is strengthened by the observations from a previous study conducted by Wakamatsu et al who demonstrated that a small molecule inhibitor of NFκB suppressed TNFα induced IL-6, CCL2, CCL5 and MMP-3 production in RA fibroblast like synoviocytes (Wakamatsu *et al.*, 2005).

RO100 and RO919 at doses up to 1μM did not elicit a suppressive effect upon the production of TIMP-1 from OA-SF. Whilst TIMP-1 is upregulated by IL-1β stimulation, as observed in our own study and previous studies in astrocytes and hepatic cells (Wilczynska *et al.*, 2006; Zhang *et al.*, 2006), it would appear that TIMP-1 is only partially regulated by NFκB. At the two lower doses (0.1μM & 0.03μM) neither inhibitor elicited downregulation in the levels of TIMP-1 produced by IL-1β stimulated OA-SF, a 1μM dose of either inhibitor however resulted in a significant downregulation in the levels of IL-1β induced TIMP-1. Such observations suggest that either, as previously eluded to, the regulation of TIMP-1 is modestly controlled by IL-1β induced NFκB activation, or that at doses of 1μM or greater the IKK inhibitors elicit non-specific effects that result in the downregulation of TIMP-1 without significantly affecting cell viability. If the latter is the case then the dramatic repression observed in MMP-3 production at the 1μM dose is likely to result from non-specific, unknown effects.

To determine the ability of the small molecule inhibitors to penetrate the extracellular matrix of the synovial membrane, we employed a robust *ex vivo* model of the synovium using OA synovial explants. In this model we employed etanercept and anti-IL-1β, previously used with potent success in the inhibition of IL-6, MMP-1, and MMP-3 in the OA-COCUL model employed during chapter 3, as a comparison to RO100. Both RO100 and etanercept, in combination with anti-IL-1β, at the doses tested, significantly reduced IL-6 and MMP-1 production without significantly affecting TIMP-1 or MMP-3. There are a number of possible explanations for this, firstly several signalling pathways induce MMP expression and it would appear that MMP-3 production in the more robust OA-EXP model is not primarily dependent upon NFκB signalling. Secondly, MMP-3 is most active early in OA affecting proteoglycan depletion in cartilage, OA-EXP were derived from end-stage OA patients where MMP-3 levels are relatively low (Bau *et al.*, 2002) thus IKK inhibitors appear unable to further downregulate the production of this enzyme.

In summary the observations of these studies support the view that NFκB is an integral signalling pathway implicated in the pathology of OA. Our studies have demonstrated that the inhibition of the transcription factor can be achieved by targeting different steps within the pathway and by different methods. Such inhibition results in downregulation of a host of mediators associated with disease pathology but does not evoke a deleterious effect upon mediators eliciting a protective effect within the joint such as TIMP-1. *In vitro* inhibition of the NFκB signalling pathway does not result in any toxicity in the OA-SF model used. Together these observations highlight a viable therapeutic target for the modulation of OA pathology. However, as OA is primarily a disease

driven by cartilage destruction, the ability of this process to be modified by NFκB inhibition requires elucidation. Consequently to assess the efficacy of the IKK inhibitors in modifying OA pathology, we employed both RO100 and RO919 in a crude *in vitro* model of OA to determine their ability to modulate cartilage destruction, the observations of which will be discussed during chapter five.

CHAPTER FIVE

The effect of NFκB inhibition upon IL-1β induced cartilage deterioration *in vitro*

5.1 Introduction.

The central pathological feature of OA is the initiation and subsequent erosion of the articular cartilage surface. As previously described, the extracellular matrix of cartilage constitutes a collagen type II scaffold filled with aggregates of proteoglycan. The initiation, deterioration and finally complete erosion of articular cartilage is a result of a number of aggrecanases and MMPs acting in a choreographed fashion, with two major phases of degradation apparent (Bau *et al.*, 2002; Billinghurst *et al.*, 1997; Fosang *et al.*, 1996). Firstly, the proteoglycans present within the matrix are proteolytically cleaved by both aggrecanases and MMPs resulting in the depletion of aggrecan from cartilage. During the second phase, the extracellular collagen II scaffold is degraded by a number of MMPs, enhancing cartilage erosion (Mankin *et al.*, 1970; Nagase *et al.*, 2003).

During the early stages of OA one of the first observed changes within articular cartilage is a reduction in the levels of aggrecan. Aggrecan, a large matrix protein, is the most abundant proteoglycan of articular cartilage. A 2000 amino acid protein core forms the backbone of the aggrecan molecule to which glycoasminoglycans bind at specific locations (Doege *et al.*, 1991). The structure of aggrecan predisposes the protein to cleavage by both aggrecanases and MMPs. Three globular domains are located along the backbone of aggrecan; the G1 and G2 domains are located at the N terminal domain of the molecule, with G3 located at the C terminal domain (Paulsson *et al.*, 1987; Schwartz *et al.*, 1999) (see fig 5.1a). The G1 domain provides the binding site of hyaluronan to the aggrecan backbone, the interaction between aggrecan and

hyaluronan is stabilised by a link protein molecule binding (Dudhia, 2005; Hascall *et al.*, 1974). The G2 domain whilst sharing a similar structural homology to the G1 domain is unable to bind hyaluronan, consequently its exact role remains to be defined (Doege *et al.*, 1990: Doege *et al.*, 1991). Adjacent to the G2 domain the CS1 and CS2 attachment regions are located. The CS1 region allows attachment of keratan sulphate chains, with chondroitin sulphate chains binding to the aggrecan backbone in both the CS1 and CS2 regions. Attachment of the negatively charged keratan sulphate and chondroitin sulphate chains provides cartilage with the ability to dissipate mechanical loads (Dudhia *et al.*, 2005; Poole, 1986). The G3 domain is situated at the C terminal of the aggrecan molecule, its exact role remains to be fully elucidated although it is speculated to play a role in translocation of newly synthesised aggrecan (Domowicz *et al.*, 2000; Dudhia *et al.*, 1996). The interglobular domain (IGD) is located between the G1 and G2 domains of the aggrecan backbone and is short stiff protein sequence (Paulsson *et al.*, 1987). Such rigidity in the IGD domain is speculated to be associated with the proteolytic cleavage of the domain that results in the aggrecan degradation. Two major cleavage sites are present within the IGD domain, the first is cleaved by the aggrecanases and the second by the MMPs (Fosang *et al.*, 1996; Little *et al.*, 1999). Cleavage by either results in the loss of the chondroitin and keratan GAG side chains, consequently resulting in a reduction in the ability of cartilage to reversibly deform under mechanical strain (Ratcliffe *et al.*, 1986; Tyler, 1985).

Figure 5.1 Aggrecan.

(a)

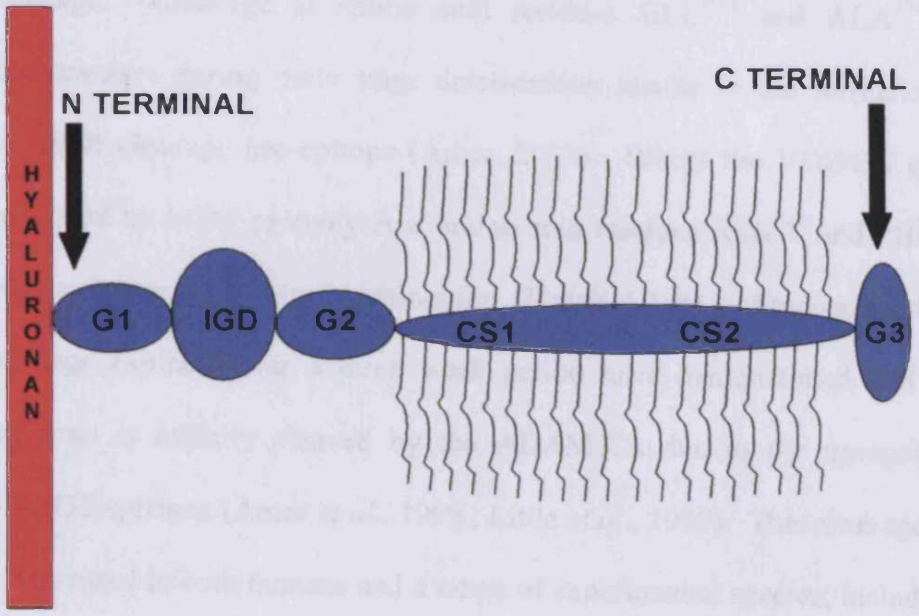

(b)

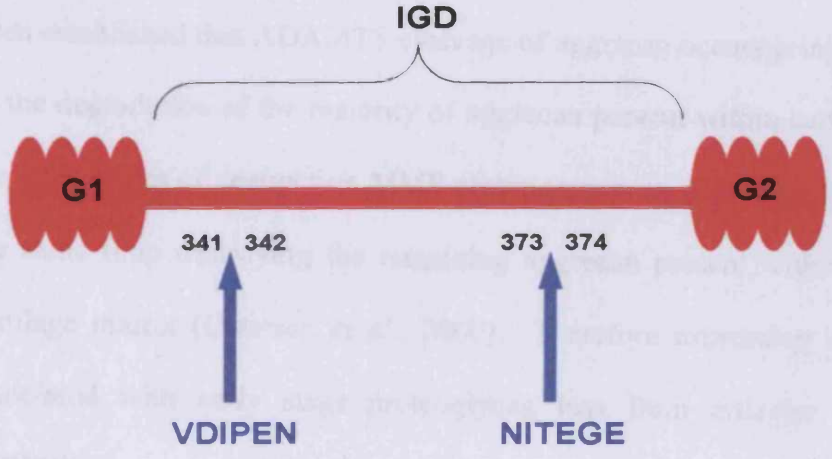

Figure 5.1 (a) Schematic of the structure of an aggrecan molecule indicating the N & C terminals and G1, G2, IGD and G3 domains and the CS1 and CS2 GAG attachment sites. (b) Schematic of the IGD cleavage sites for MMPs (VDIPEN) and ADAMTSs (NITEGE)

Proteolytic cleavage of the IGD domain occurs at one of two amino acid sequences, resulting in the formation of neo-epitopes characteristic of damaged cartilage. Cleavage at amino acid residues GLU^{373} and ALA^{374} by the aggrecanases during early stage deterioration results in the formation of the NITEGE cleavage neo-epitope (Arner, 2002). Whilst the VDIPEN epitope is generated by MMP proteolysis at amino acid residues ASN^{341} and PHE^{342} and occurs during later stage deterioration (Figure 5.1 b). Studies conducted in cartilage explants over a three week period have demonstrated that *in vitro* aggrecan is initially cleaved by the ADAMTSs due to the upregulation of NITEGE epitopes (Arner *et al.*, 1999 ; Little *et al.*, 1999). This cleavage epitope is expressed in both humans and a range of experimental species, including both rats and mice (Lark *et al.*, 1997; Singer *et al.*, 1997). However, after three weeks in culture MMP cleavage is predominant as demonstrated by the presence of VDIPEN cleavage epitopes (Little *et al.*, 2002). Consequently it has now been established that ADAMTS cleavage of aggrecan occurs primarily, resulting in the degradation of the majority of aggrecan present within cartilage. During the later stages of destruction MMP cleavage occurs, degrading collagen and at the same time destroying the remaining aggrecan present within the articular cartilage matrix (Caterson *et al.*, 2000). Therefore expression of NITEGE is associated with early stage proteoglycan loss from articular cartilage and VDIPEN expression with later stage catabolism of cartilage.

The catabolism of aggrecan has been demonstrated to be upregulated by pro-inflammatory cytokines within the joint, namely TNFα, IL-1α and IL-1β (Arner *et al.*, 1998; Stabellini *et al.*, 2003; Sztrolovics *et al.*, 2002; Tortorella *et al.*, 2001). Both ADAMTS4 (aggrecanase-1) and ADAMTS5 (aggrecanase-2)

play a key role in this early stage aggrecan degradatation (Porter *et al.*, 2005; Tortorella *et al.*, 2001). A number of models have been developed which mimic the initiation of OA and the progressive loss of aggrecan from the cartilage. Cartilage explants cultured in combination with pro-inflammatory cytokines appear to provide an accurate representation of early OA changes (Caterson *et al.*, 2000; Ratcliffe *et al.*, 1986). Such models allow chondrocytes to be retained within the cartilage extracellular matrix, and allow changes in the matrix architecture in response to cytokine stimulation to be assessed *in vitro.* However, few studies have investigated the interactions that occur between the synovium and the cartilage that result in cartilage catabolism. We sought to resolve this issue by developing an *in vitro* model, which allowed us to study the interactions between OA synovium and cartilage, and delineate the NFκB driven mechanisms that result in early stage pathological changes.

The aims of this chapter were:

- To develop an *in vitro* model of pathological changes observed during early OA.
- To examine the role of OA-SF in inducing cartilage depletion in OA in response to IL-1β stimulation.
- To determine the effect NFκB inhibition had upon early stage proteoglycan depletion in articular cartilage, by examining the presence of NITEGE cleavage neoepitopes.

5.2 Results

5.2.1 Proteoglycan depletion was not evident in healthy cartilage explants.

Bovine cartilage explants were extracted from the metacarpophalangeal joint of calves, as described in chapter two, and immediately fixed in NBFS to preserve morphology and prevent biochemical degradation, prior to histological sectioning (Figure 5.2). Bovine explant sections stained with both safranin-o/fast green, employed in the histological analysis of early stage changes (Figure 5.2 a), and toluidine blue, employed to examine later stage histological changes (Figure 5.2 b), demonstrated consistent staining of the proteoglycans throughout all zones of the cartilage.

5.2.2 Histological assessment of proteoglycan depletion induced by IL-1β demonstrated that proteoglycan loss was enhanced when bovine cartilage explants were cultured in the presence of OA-SF.

IL-1β was added to bovine explants at concentrations ranging from 0.2 to 20ng/ml in the presence or absence of OA-SF (Figure 5.3). Explants cultured in the absence of IL-1β stimulation demonstrated no reduction in proteoglycans as observed histologically by safranin-o/fast green staining (Figure 5.3 a & b). Treatment with IL-1β at a concentration of 0.2ng/ml elicited a minimal reduction in staining intensity in the surface zone of the articular cartilage (Figure 5.3 c & d). However stimulation at the higher concentrations of IL-1β elicited a notable reduction in staining of the articular cartilage (Figure 5.3 e, f, g & h). Explants treated with the two highest doses of IL-1β exhibited enhanced proteoglycan loss when cultured in combination with OA-SF.

5.2.3 Quantification of proteoglycan depletion induced by IL-1β

demonstrated that bovine cartilage explants cultured in the presence of OA-SF exhibited enhanced proteoglycan loss.

IL-1β induced proteoglycan loss in bovine explants was quantified by measuring the loss of safranin-o/fast green staining in each section (Figure 5.4). A significantly deeper zone ($p \leq 0.05$, mean ± SEM) of proteoglycan loss was observed in explants cultured in the presence of OA-SF (107μm ± 5.13) than explants cultured in the absence of OA-SF (67μm ± 7.09) at the maximal dose of IL-1β (20ng/ml). A similar effect was seen at the 2ng/ml dose of IL-1β, with explants cultured in the presence of OA-SF demonstrating an increased zone of proteoglycan loss (43μm ± 6.01) over explants cultured in the absence of OA-SF (13μm ± 1.16). The differences observed in proteoglycan loss indicated that cartilage depletion was mediated via the stimulatory effect of IL-1β upon the OA-SF, rather than IL-1β eliciting a direct effect upon the cartilage. However, the bovine explants used were representative of immature cartilage, consequently for further studies we employed murine patellas from adult mice as a source of mature cartilage.

5.2.4 Proteoglycan depletion was not observed in patellas extracted from adult wildtype mice

Murine patellas were extracted from the hind limbs of adult wildtype mice, fixed immediately in NBFS and decalcified in formic acid prior to histological processing. Safranin-o/fast green and toluidine blue staining was performed to examine the sections histologically (Figure 5.5 a & b). The proteoglycans present in the articular cartilage of murine patellas were uniformly stained with both histological stains demonstrating that adult, wildtype mice

displayed no evidence of cartilage breakdown prior to *in vitro* experimental investigations.

5.2.5 Both early and late stage proteoglycan depletion was induced by IL 1β *in vitro.*

A 20ng/ml dose of IL-1β was used to induce proteoglycan loss in murine patellas cultured with OA-SF in this and subsequent studies (Figure 5.6). Safranin-o/fast green staining was used to determine the early stage pathological changes IL-1β induced at 2 days (Figure 5.6 a & b), whilst toluidine blue was used at 10 days to histologically assess the later stage changes induced by IL-1β (Figure 5.6 c & d). IL-1β at both 2 and 10 days induced proteoglycan loss in murine patellas cultured in combination with OA-SF.

5.2.6 Early and late stage proteoglycan depletion was significantly increased by treatment with IL-1β.

IL-1β induced proteoglycan loss in the murine patellas was quantified by measuring the loss of safranin-o/fast green and toluidine blue staining in each section (Figure 5.7). A significantly ($p < 0.01$) increased zone of proteoglycan depletion was evident in patellas treated with IL-1β (127μm ± 10.81) in comparison to untreated patellas (10μm ± 1.25) stained with safranin-o after a 48hour culture period (Figure 5.7 a). This significant ($p < 0.01$), effect was repeated following a 10 day culture period when sections were stained with toluidine blue, patellas cultured in the presence of IL-1β demonstrated an increased zone of depletion (111μm ± 4.28) in comparison to untreated patellas (2μm ± 1.37) (Figure 5.7 b). These observations demonstrated that it was possible to both initiate and model early and more advanced cartilage deterioration *in vitro*.

5.2.7 Histological assessment of proteoglycan loss in response to NFκB inhibition *in vitro.*

The IKK inhibitors, RO100 and RO919 were employed to modulate IL-1β (20ng/ml) induced proteoglycan depletion (Figure 5.8). Histological observations demonstrated that patellas treated with IL-1β (Figure 5.8 a) exhibited an enhanced loss of safranin-o/fast green staining following a 48 hour culture period in comparison to patellas treated with either RO100 (Figure 5.8 b) or RO919 (Figure 5.8 c). An almost identical effect was observed following a 10 day culture period with patellas treated with IL-1β (Figure 5.8 d) displaying extensive loss of proteoglycans as demonstrated by the loss of toluidine blue staining in comparison to RO100 (Figure 5.8 e) and RO919 (Figure 5.8 f) treated patellas.

5.2.8 Quantification of proteoglycan loss following NFκB inhibition *in vitro.*

A significantly ($p \leq 0.05$) reduced zone of proteoglycan depletion was evident in patellas treated with RO100 (70μm ± 9.96), RO919 elicited an enhanced significant ($p \leq 0.01$) inhibitory effect in treated patellas (1.5μm ± 1.12) when compared to untreated patellas (127μm ± 10.81) following a 48 hour culture period (Figure 5.9 a). An increased culture period of 10 days resulted in both RO100 and RO919 eliciting a significant ($p \leq 0.01$) protective effect, with a reduced zone of proteoglycan loss evident (RO100; 35μm ± 2.98, RO919; 0.6μm ± 0.67) when compared to untreated patellas (111μm ± 4.68) (Figure 5.9 b).

5.2.9 Histological visualisation of the aggrecanase cleavage neoepitope

NITEGE in response to IL-1β.

Aggrecanase cleavage induced by IL-1β resulted in the formation of NITEGE neoepitopes in the intermediate and radial zones. The presence of these neoepitopes was assessed immunohistochemically using an anti-NITEGE antibody, visualised using DAB Chromagen which stained the NITEGE neoepitopes brown (Figure 5.10). Expression of NITEGE was enhanced during early cartilage degradation but was not evident during more advanced cartilage deterioration. Patellas treated with IL-1β demonstrated a greater number of chondrocytes staining for the NITEGE cleavage neoepitope (Figure 5.10 b) in comparison to patellas treated with RO100 or RO919 (Figure 5.10 c & d).

5.2.10 Quantification of the expression of the aggrecanase cleavage neoepitope NITEGE following treatment with RO100 and RO919.

Four fields of view at x 40 magnification were counted for each treatment strategy and the total NITEGE expression displayed as a percentage (Figure 5.11). Immunohistochemical analysis revealed that a 1μM dose of RO100 significantly ($p \leq 0.05$) reduced NITEGE expression in response to IL-1β (12.2 ± 4.01). Treatment with a 1μM dose of RO919 exhibited greater potency in this respect, with a greater reduction in NITEGE expression (1.6 ± 0.91, $p \leq 0.01$) in comparison to untreated, IL-1β stimulated patellas (32.4 ± 3.05) following a 48 hour culture period. These observations suggest that inhibition of NFκB *in vitro* can reduce aggrecanase cleavage, an intrinsic process involved in the depletion of proteoglycans from articular cartilage.

(a)

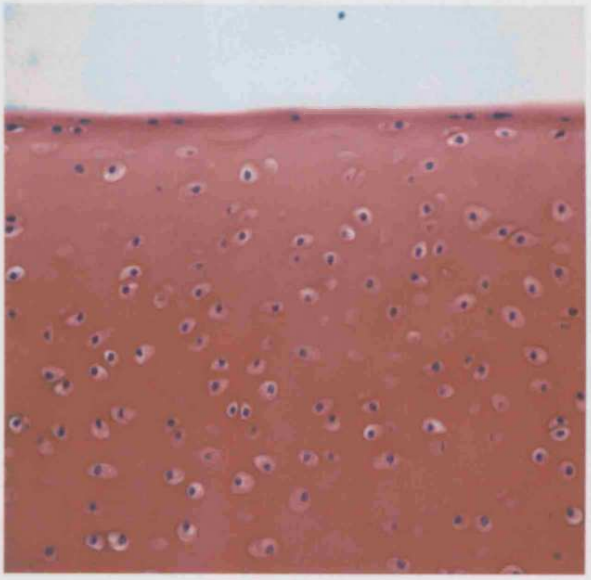

(b)

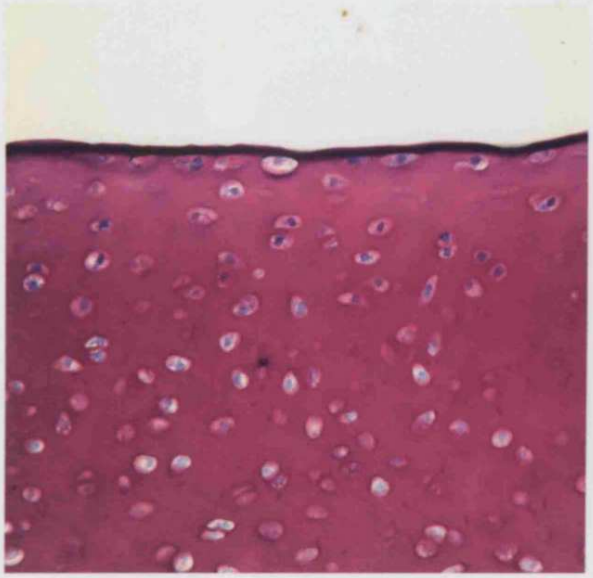

Figure 5.2 Histological staining of the proteoglycans present in articular cartilage.
Cartilage explants (a & b) were derived from freshly slaughtered 7 day old calves. Explants were fixed prior to sectioning. Histological sections were stained with safranin-o/fast green (a) and toluidine blue (b). Magnification x 400.

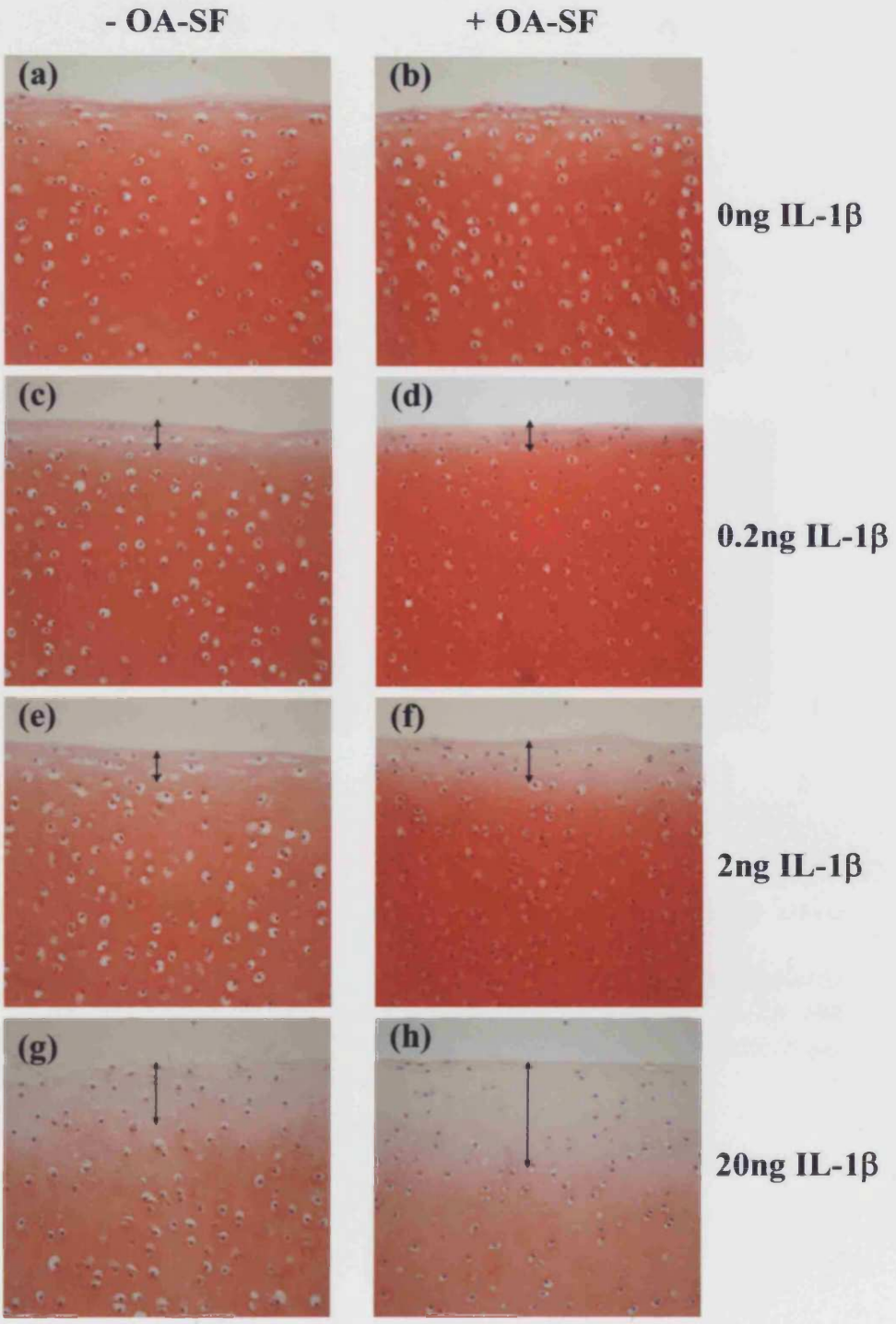

Figure 5.3. Representative histological images demonstrating proteoglycan depletion from bovine cartilage explants in the presence or absence of OA-SF.

Bovine cartilage explants were cultured for a 10 day period in the absence (a, c, e, g) or presence (b, d, f, h) of human OA-SF and were treated with an increasing doses of IL-1β (a & b untreated, c & d 0.2ng/ml IL-1β, e & f 2ng/ml IL-1β, g & h 20ng/ml IL-1β). Sections were stained with safranin-o/fast green, loss of red staining is indicative of proteoglycan depletion. Magnification x 200 (n = 2, 5 fields of view measured for each section..

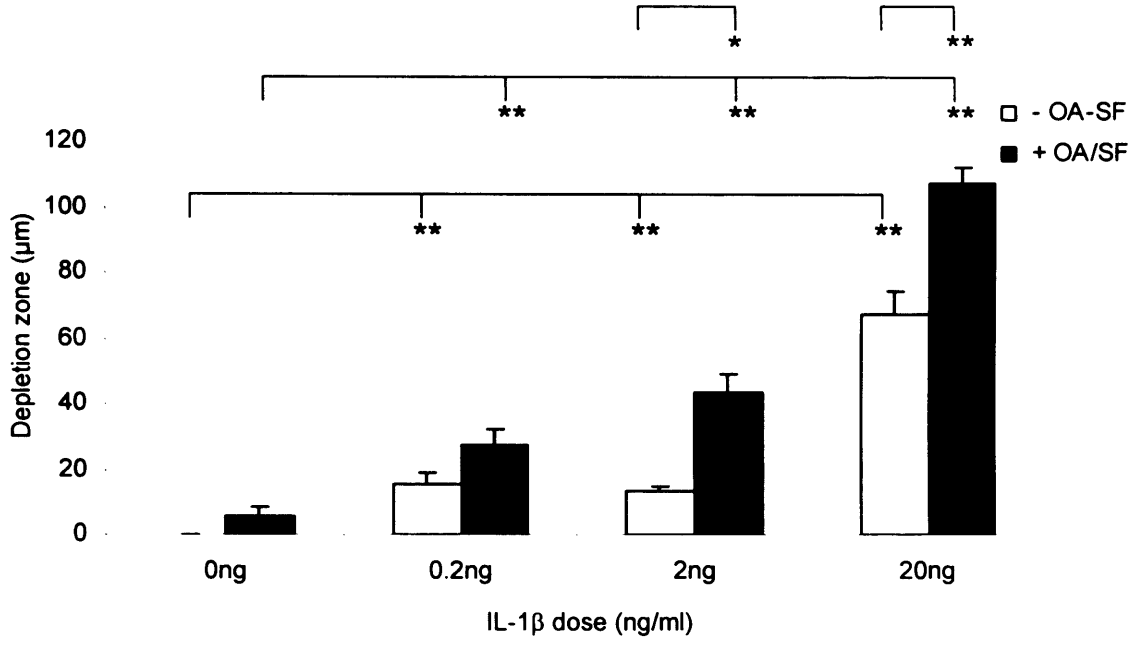

Figure 5.4 Proteoglycan depletion induced by IL-1β is enhanced when bovine explants are cultured in the presence of OA-SF.
Following staining with safranin-o/fast green the depth of proteoglycan depletion present in bovine explants cultured in the presence or absence of OA-SF and subsequently treated with an increasing dose range of IL-1β was measured in µm using a graticule. (* $p \leq 0.05$, ** $p \leq 0.01$)

(a)

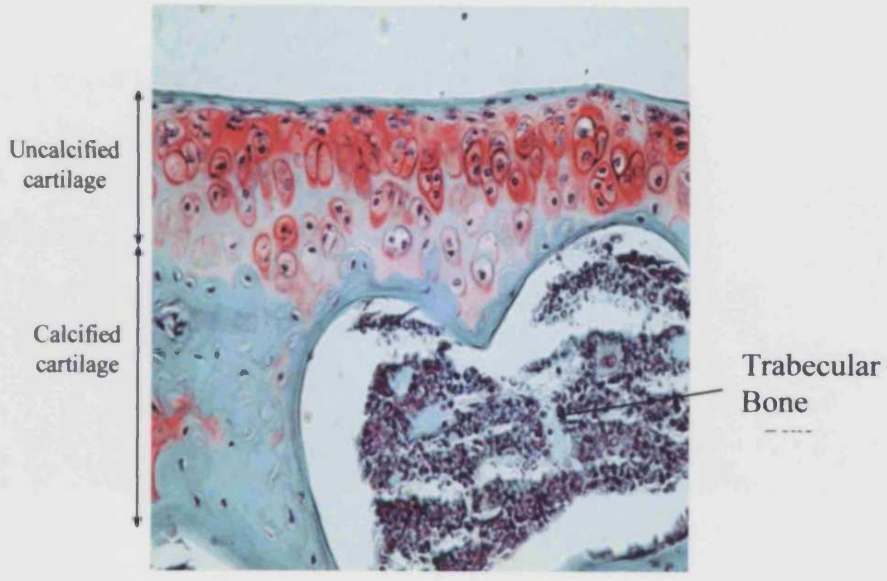

(b)

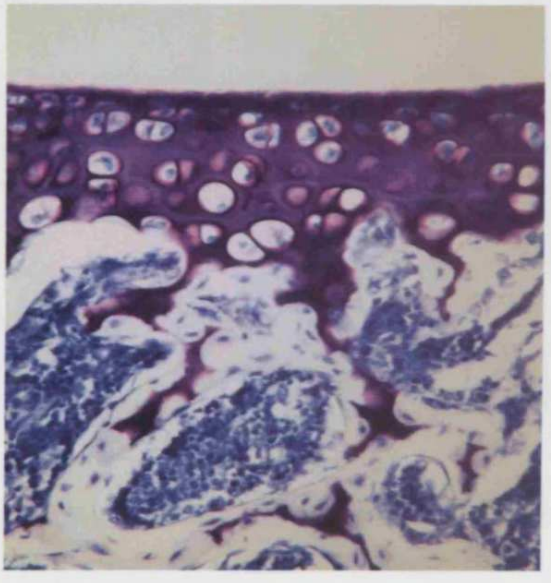

5.5 Histological staining of the proteoglycans in articular cartilage.
Murine patellas were derived from freshly sacrificed adult wild type BalbC mice. Patellas were fixed and subsequently decalcified prior to sectioning. Histological sections were stained with safranin-o/fast green (a) and toluidine blue (b). Staining was uniform throughout all zones of the articular cartilage. Magnification x 40.

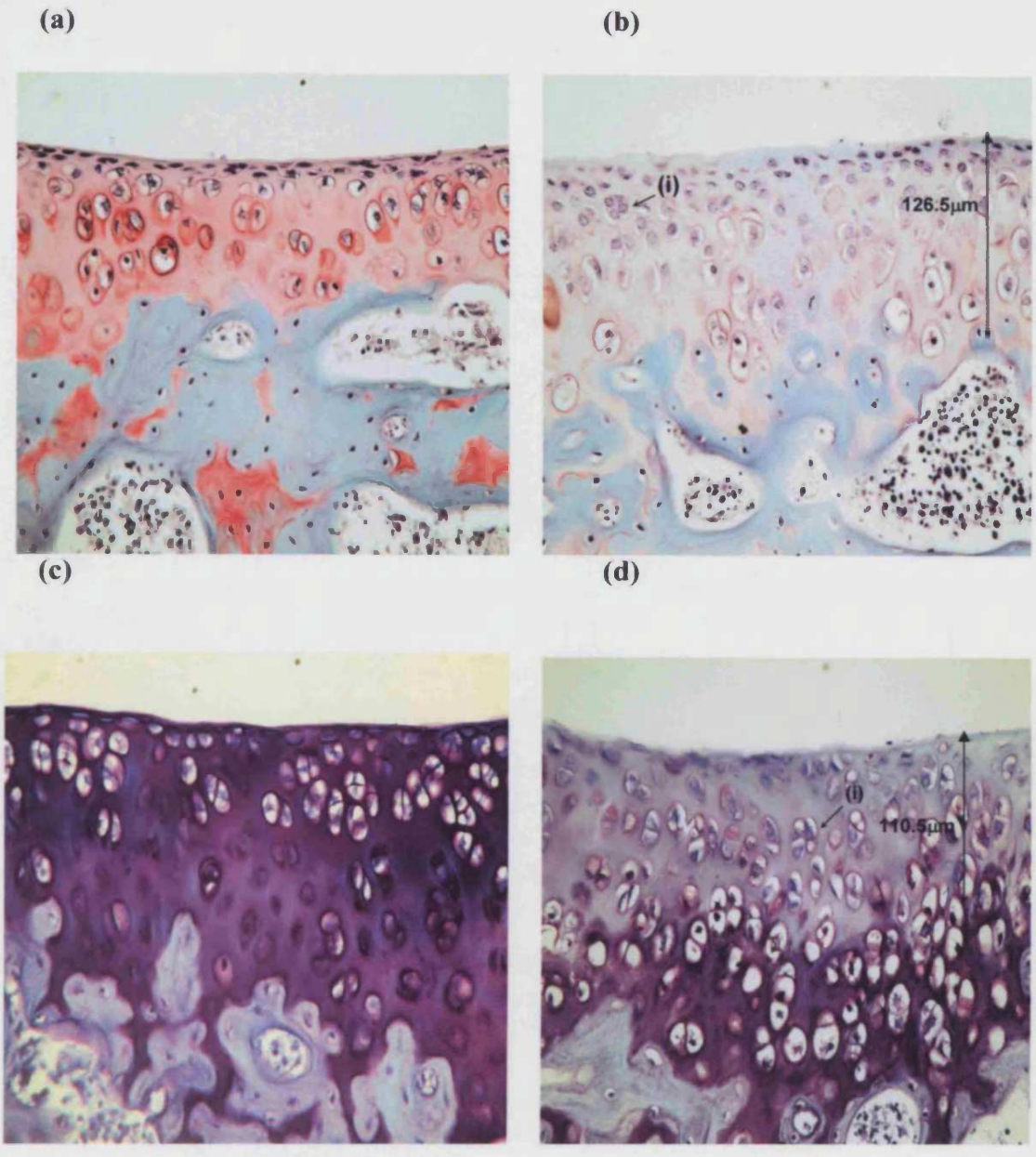

Figure 5.6 Histological representation of IL-1β induced proteoglycan depletion in murine patellas.

Murine patellas were cultured in combination with OA-SF in the absence (a & c) or presence (b & d) of a 20ng/ml dose of IL-1β. Histological sections were stained with either safranin-o/fast green following 2 days in culture (a & b) or toluidine blue following a 10 day culture period (c & d). (i) represents chondrocyte clustering within the patellas . Magnification x 400. n= 2, 5 fields of view examined per section.

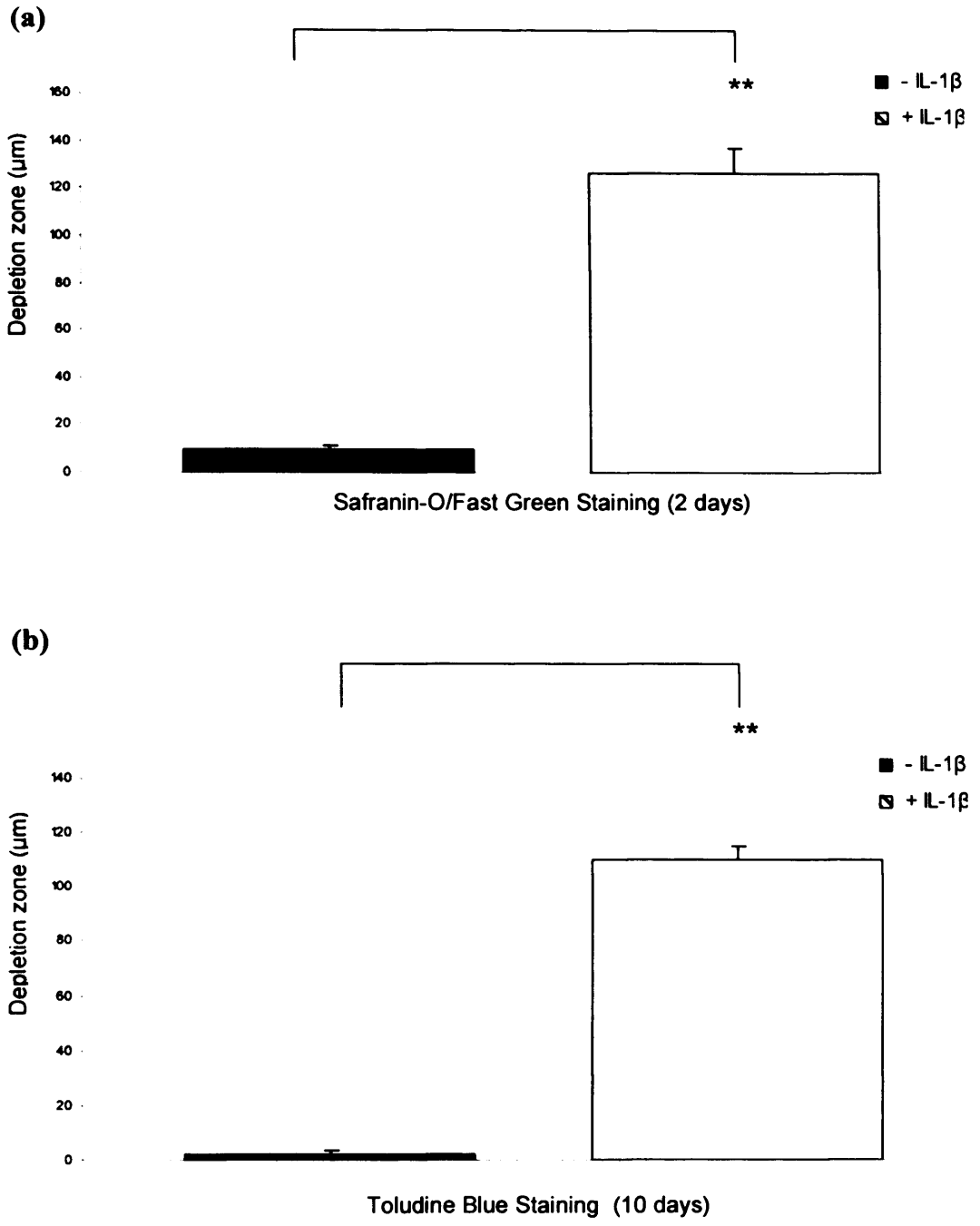

Figure 5.7 Quantification of proteoglycan depletion induced by IL-1β in murine patellas.

Histological sections of murine patellas cultured for 2 days and 10 days were stained with safranin-o/fast green (a) and toluidine blue (b) respectively. The depth of proteoglycan depletion present in murine patellas cultured in the presence or absence of a 20ng/ml dose of IL-1β was measured in μm using a graticule. (** $p \leq 0.01$)

Figure 5.8 Histological determination of the effect of NFκB inhibition upon IL-1β induced proteoglycan depletion.

Murine patellas cultured in combination with OA-SF were treated with a 1μM dose of RO100 or RO919 and subsequently stimulated with a 20ng/ml dose of IL-1β. Patellas were cultured for a 2 or 10 day culture period. Sections from patellas cultured for 2 days were stained with safranin-o/fast green (a, b, c), sections from 10 day cultures were stained with toluidine blue (d, e, f). Magnification x 400. n=2, 5 fields of view counted per section.

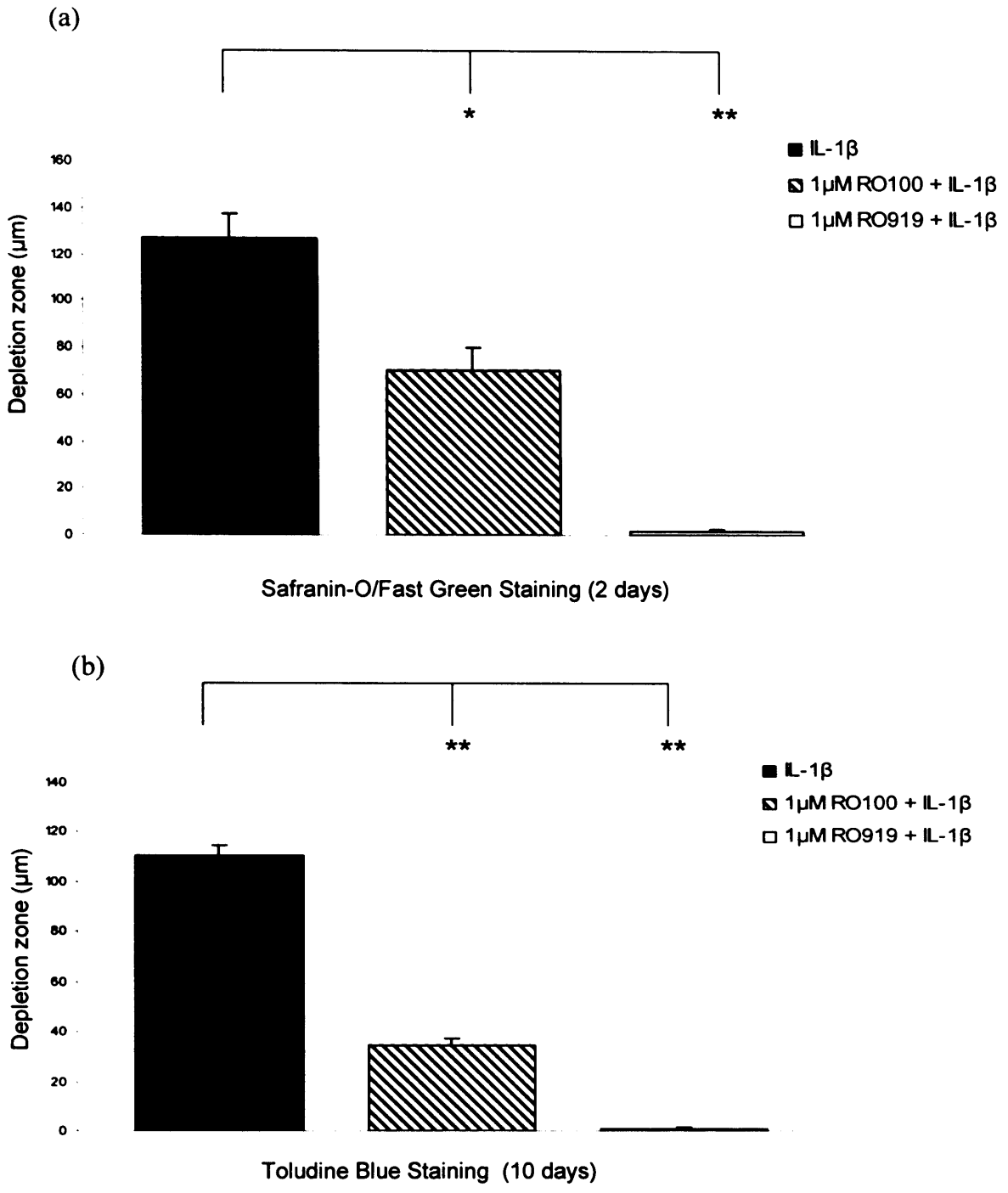

Figure 5.9 Quantification of depth of IL-1β induced proteoglycan depletion following NFκB inhibition.

Graphical representation of histological section of murine patellas cultured for 2 days and 10 days were stained with safranin-o/fast green (a) and toluidine Blue (b) respectively. The depth of proteoglycan depletion induced by IL-1β and treated with either RO100 or RO919 was measured in μm using a graticule. (* $p \leq 0.05$, ** $p \leq 0.01$).

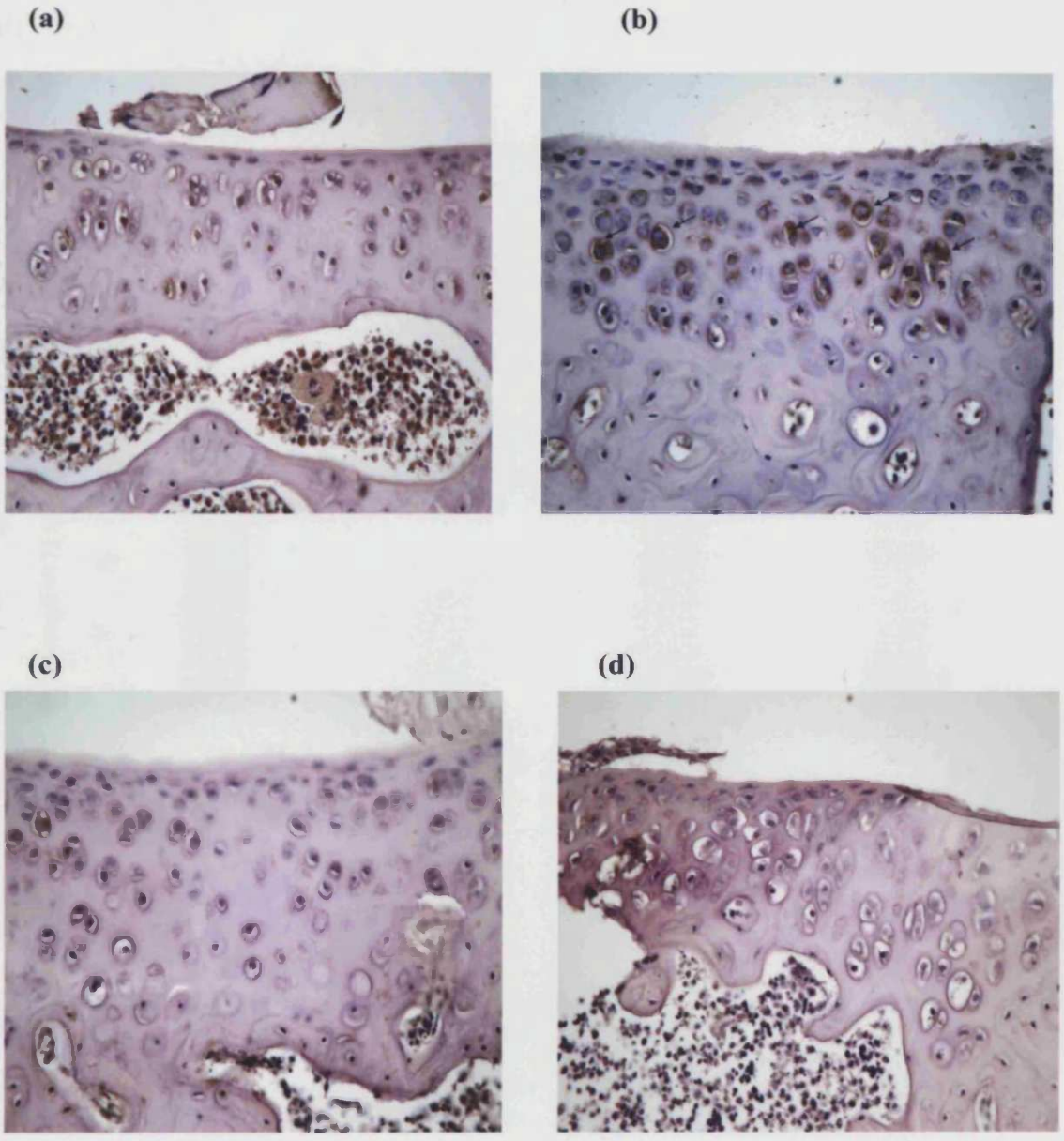

5.10 The effect of NFκB inhibition upon IL-1β induced aggrecanase cleavage.
The effect of NFκB inhibition upon IL-1β induced aggrecanase cleavage was assessed immunohistochemically using an anti-NITEGE antibody. Murine patellas were either left unstimulated (a) or stimulated with a 20ng/ml dose of IL-1β (b, c, d) prior to treatment with either a 1μM dose of RO100 (c) or RO919 (d). Arrows indicate the NITEGE epitopes visualised by the brown staining typically located in the intermediate and radial zones. Magnification x 400.

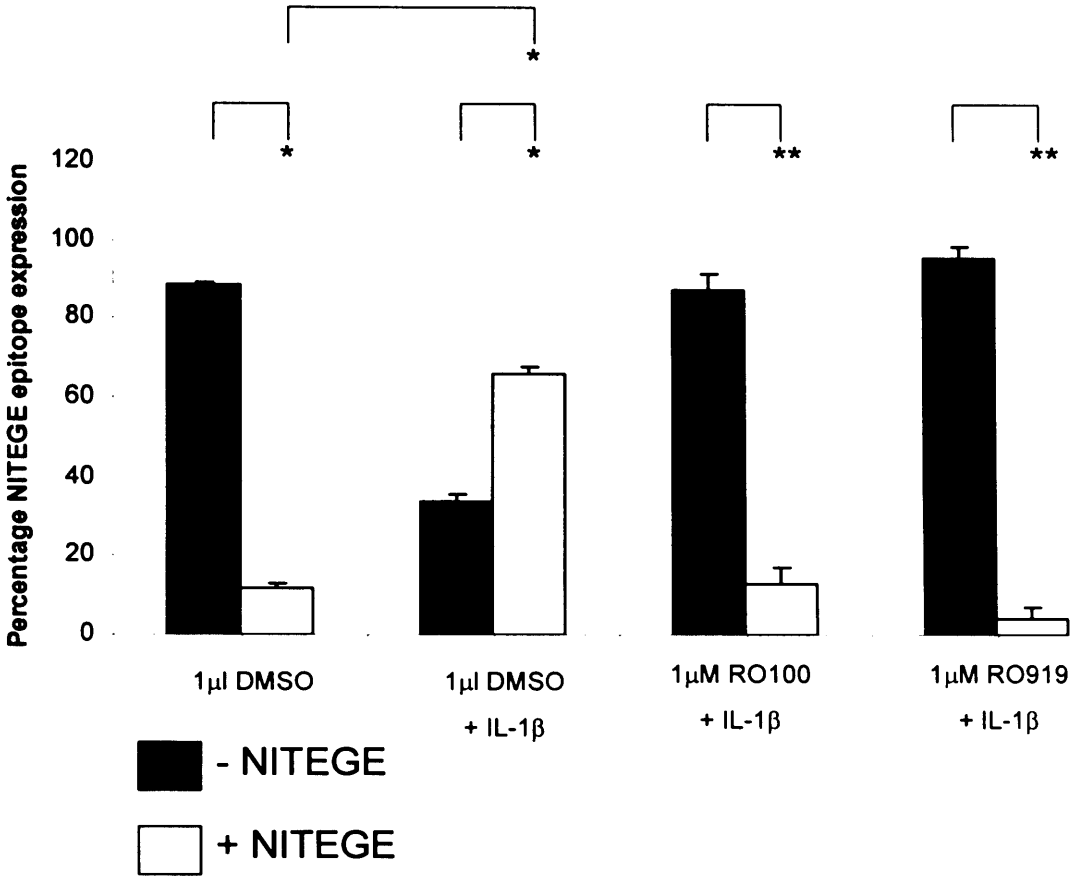

Figure 5.11 Percentage of NITEGE neoepitope expression following NFκB inhibition.

Sections stained immunohistochemically with an anti-NITEGE antibody were examined microscopically and the percentage of cells expressing the NITEGE epitope (stained brown) was calculated by counting the number of stained and unstained cells present in 4 fields of view for each treatment group (x 400 magnification.) (* $p \leq 0.05$, ** ≤ 0.01) $n = 2$

5.3 Discussion.

Several cytokines and MMPs associated with OA pathology were successfully downregulated by 2 inhibitors of NFκB in the synovial membrane models employed in the previous chapter. However, as OA is primarily a disease driven by cartilage degradation, preventing cartilage breakdown remains the ultimate goal in the search for new therapeutic agents. Consequently the efficacy of these inhibitors in modulating IL-1β induced cartilage catabolism *in vitro* was assessed during chapter 5.

Initial studies employed cartilage sourced at random from the metacarpophalangeal joints of 7 day old calves. Bovine cartilage was selected as the cartilage of choice in this initial model for two reasons; firstly due to a lack of specialised equipment within the department, namely a biopsy punch, which are routinely used for preparing cartilage discs of equal size, the cartilage was extracted from the joint using a sterile scalpel (Wilson *et al.*, 2006). It was therefore necessary that the cartilage was still relatively pliable. With age cartilage becomes increasingly rigid and brittle, thus it would be difficult to cut explants from adult cartilage with a scalpel. Secondly bovine cartilage is routinely used as a source of articular cartilage as it is readily available from local abattoirs shortly after death (6 hours or less) and provides a source of 'normal' healthy articular cartilage with no visual abnormalities. Bovine cartilage explants derived from this source have been effectively utilised in a number of different studies modelling OA and articular cartilage changes (Bonassar *et al.*, 1996; Chan *et al.*, 2006; Sandy *et al.*, 1991). Previous studies have demonstrated that bovine explants can be cultured in either serum free media or serum containing media, successfully for a 24 day period (Sandy *et al.*,

1991, Shingleton *et al.*, 2006, Wilson *et al.*, 2006). Culture conditions were optimised to ensure both cartilage explants and OA-SF could be successfully cultured for a 10 day period without adversely affecting OA-SF viability.

Two histological stains were used routinely throughout the studies performed during this chapter, namely safranin-o/fast green and toluidine blue. Safranin-o is a metachromatic dye that is transformed to an orthochromatic dye when sections are permanently mounted, such as those used during this study. Chondroitin-6 sulphate and keratan sulphate that form the GAG chains of proteoglycan aggregates are stained stoichometrically at a 1:1 ratio with safranin-o (Rosenberg, 1971). Fast green is typically used as a counter dye, staining the underlying subchondral bone and soft tissues present, whilst haematoxylin is used as a nuclear stain. Safranin-o does not stain the collagen present within articular cartilage and hence is only a measure of proteoglycan loss. Toluidine blue is a second stain used to stain the glycosaminoglycans present within articular cartilage. Toluidine blue stains cartilage in both the orthochromatic phase and metachromatic phase, with staining of the cartilage in the orthochromatic phase directly proportional to glycosaminoglycans present within the cartilage (Shepard *et al.*, 1976). Thus safranin-o/fast green is used as a stain that determines the initial degradative events that occur, whilst toluidine blue is used to determine more progressive changes within the cartilage matrix.

Numerous studies have demonstrated that direct IL-1 stimulation of cartilage *in vitro* results in matrix degradation (Bonassar *et al.*, 1997; Hughes *et al.*, 1995; Kozaci *et al.*, 2005; Sztrolovics *et al.*, 2002; Wilson *et al.*, 2006). Recombinant human IL-1β was employed in this system to stimulate cartilage depletion *in vitro*. IL-1β has previously been demonstrated in chapter 4 to

induce the release of MMPs, responsible for cartilage destruction, from human OA-SF, thus allowing us to model the effect IL-1β induced synovial cytokine and MMP release had upon cartilage depletion *in vitro*. The IL-1β induced release of cartilage destructive mediators, such as MMP-1 and MMP-3 from the OA-SF resulted in enhanced proteoglycan loss and increased cartilage destruction *in vitro*. Bovine explants cultured in the absence of OA-SF but stimulated with IL-1β, demonstrated a degree of proteoglycan loss when stained with safranin-o/fast green. Such observations suggest some cross reactivity between human recombinant IL-1β and bovine cartilage explants. However the notable difference in proteoglycan loss, especially at the maximal dose of IL-1β employed demonstrated that it is the OA-SF and the mediators they release in response to IL-1β stimulation that markedly increased proteoglycan depletion within this model. Whilst this model effectively demonstrated that OA-SF stimulated with IL-1β enhanced proteoglycan loss from articular cartilage, a number of notable drawbacks were noted from the cartilage explants employed.

Firstly, the bovine cartilage explants were derived from skeletally immature animals and hence are more representative of juvenile than adult cartilage. In humans and several experimental species, juvenile and adult articular cartilage differ markedly in both their morphological appearance and their biochemistry (Meachim *et al.*, 2001). The numbers of chondrocytes present in articular cartilage declines gradually from birth over an individual's lifetime, such a decline in the number of chondrocytes is believed to result in a reduced capacity to elicit a successful repair response (Leutert, 1980). The proteoglycans present within articular cartilage help to maintain tensile strength, studies in bovine cartilage have demonstrated that ageing cartilage produces

proteoglycan aggregates that are smaller than the original aggregates or aggregates produced by juvenile cartilage, consequently such an alteration in proteoglycan can weaken the cartilage matrix (Thonar *et al.*, 1986). It has also been demonstrated that the capacity for chondrocytes to synthesise and metabolise decreases with age (Bolton, 1999; Martin *et al.*, 2000). Consequently the ability for chondrocytes to repair damage is reduced in adult ageing cartilage (Martin *et al.*, 2002). These factors taken together, indicate that juvenile cartilage, may have an increased capacity to withstand degradation than adult cartilage. It is speculated that the changes that occur in ageing adult cartilage increases the risk of OA developing and hence employing healthy adult cartilage maybe more representative of the changes that occur during the initiation of OA (Martin *et al.*, 2002). This hypothesis was strengthened by the differences observed in proteoglycan loss from adult murine patellas and juvenile bovine explants. A 20ng dose of IL-1β elicited extensive proteoglycan depletion in adult cartilage, as observed in the murine patellas, this loss was notably reduced in the bovine explants. Such an effect may be due to inherent differences between species but is more likely to result from the age differences between the two cartilage sources, with the juvenile chondrocytes present in bovine explants able to accommodate the degradative changes that occur with greater success than mature chondrocytes.

Secondly, a number of studies have demonstrated morphological differences in the structure of articular cartilage between species. A study by Stockwell in 1971 demonstrated that chondrocyte density varied markedly between humans and a number of experimental species (Stockwell, 1971). A subsequent study by Kaab *et a,* in 1998 examined the structural arrangement of

collagen fibres between different species using scanning electron microscopy (Kaab *et al.*, 1998). This study demonstrated that of 6 experimental species, porcine cartilage exhibited the same leaf-like collagen fibril arrangement that is evident in humans. Bovine collagen fibrils were arranged in a columnar fashion. As collagen is the matrix protein responsible for providing articular cartilage with its intrinsic strength, such differences in the arrangement of fibrillar collagen may result in differences in the rate of degradation during the latter stages.

A third complication with using bovine explants is that histological orientation is difficult. Due to the nature of extraction the explants are not full depth sections and both the subchondral bone and calcified cartilage are missing. Bovine explants lack the definitive strata seen in adult articular cartilage, consequently determining which surface is the superficial zone can be problematic. The extraction method itself is severe and in some cases damage is evident which may elicit a repair response.

In light of the drawbacks highlighted we sought to resolve these issues by modifying the *in vitro* joint model, replacing the bovine explants with murine patellas, extracted from adult wildtype mice which have been employed successfully in studies by other groups (van Beuningen *et al.*, 1993). Using murine patellas from adult mice avoided the problems associated with the use of juvenile cartilage, and due to the extraction method, required no specialised equipment. The extraction of murine patellas is far less rigorous, with the patella dissected from the joint with a small degree of ligament remaining ensuring the patella itself does not come into contact with either the scalpel or forceps and hence the potential for damage to the cartilage surface is minimised. The issue

of orientation is resolved as the patella itself possesses an articular cartilage surface with a degree of underlying subchondral bone. Like the bovine explants used previously the question of species differences and how these findings may relate to human cartilage remains questionable. Mouse articular cartilage also demonstrates structural differences in comparison to human cartilage, but is an adult source of healthy cartilage that is easily accessible (Hughes *et al.*, 2005). Accessibility to human adult healthy cartilage is extremely limited and consequently there is no is easy resolution to this problem. However as we have used a murine model of OA in chapter 6, using murine patellas in this model provides data on how cartilage degradation can be modified through the inhibition of NFκB *in vitro* and allows comparison with the effect of NFκB inhibition *in vivo* in chapter 6.

Having previously demonstrated that NFκB inhibition may be a useful therapeutic target in OA, we treated patellas cultured in combination with OA-SF, with the two IKK inhibitors to assess histologically their efficacy in preventing cartilage deterioration *in vitro*. Of the two inhibitors, RO100 elicited the more potent effect in the chapter 4 studies, with both eliciting a significant inhibitory effect upon the induction of cartilage destructive mediators, namely MMP-1 and MMP-3. Throughout the studies performed during this chapter, an increased dose of 1μM of both RO100 and RO919 is required to significantly modify IL-1β induced proteoglycan depletion, and in contrast to the chapter 4 studies, RO919 elicits the greater inhibitory effect. Such an effect may be due to an enhanced ability for RO919 in comparison to RO100 to inhibit ADAMTS-4 and ADAMTS-5 release from the OA-SF, quantifying the levels of these two aggrecanases released by the OA-SF would resolve this question. However as

the differences in inhibition of MMPs in the OA-SF does not vary enormously between the two agents, it is perhaps more likely that the articular cartilage itself is targeted by the inhibitors. Due to the structural differences that exist between RO100 and RO919 it is possible that uptake of RO919 by the chondrocytes occurs more readily than that of RO100. RO919 may reduce proteoglycan depletion either as a consequence of increasing the chondrocytes capacity to repair or more likely by reducing the release of MMPs and ADAMTSs from chondrocytes in response to IL-1β stimulation.

It has been demonstrated that IL-1 stimulation of articular cartilage results in the formation of the aggrecanase cleavage neo-epitope NITEGE (Fosang *et al.*, 2000). *In vivo* and *in vitro* murine studies have demonstrated that ADAMTS-5 is the predominant aggrecanase in mice responsible for the formation of NITEGE epitopes within the cartilage and that IL-1β upregulates ADAMTS-5 increasing expression of NITEGE (Stanton *et al.*, 2005). As expected a 20ng/ml dose of IL-1β increased NITEGE expression as observed by immunohistochemical staining of the cartilage sections following a 2 day culture period. Patellas treated with RO100 demonstrated a significant reduction ($p \leq 0.05$) in NITEGE expression in comparison to IL-1β treated patellas, this effect was more pronounced in patellas treated with RO919 ($p \leq 0.01$). A study by van Meurs examined the expression and localisation of NITEGE epitopes in comparison to the MMP induced VDIPEN epitopes (Singer *et al.*, 1997; van Meurs *et al.*, 1999). It was evident from this study that NITEGE eptiopes are produced during the early stages of cartilage deterioration and during the advanced stages of cartilage erosion their expression is minimal, but the expression of VDIPEN epitopes is enhanced (van Meurs *et al.*, 1999). These

observations are in agreement with the observations of our own study, whereby at 10 days NITEGE epitopes are absent in the IL-1β treated and RO100 and RO919 treated patellas, suggesting that the aggrecanase cleavage process is complete at 10 days and that cartilage deterioration is advanced. van Meurs also demonstrated that the expression of the NITEGE neoepitope was localised to the superficial and intermediate zones of the articular cartilage, we observed a similar staining pattern in our study. At 10 days we would expect to observe enhanced expression of the MMP induced VDIPEN epitope in patellas treated with IL-1β, with reduced expression of the cleavage epitope in those patellas treated with RO100 and RO919. However, a commercially available antibody for the VDIPEN cleavage neo-epitope is currently unavailable and consequently we have been unable to assess if such an effect occurs.

In conclusion, the results from chapter 4 and chapter 5 suggest that NFκB can be effectively targeted *in vitro*. Inhibition of the transcription factor resulted in a reduction of pathogenic mediators released by OA-SF as demonstrated in chapter 4. These findings have been advanced by the observations in chapter 5 that proteoglycan depletion from the surface zone of the articular cartilage can be reduced by treatment of the *in vitro* model of early stage cartilage pathology with a 1μM dose of either RO100 or RO919. A reduction in the expression of the NITEGE neoepitope in patellas treated with the 2 IKK inhibitors would suggest that NFκB inhibition *in vitro* targets aggrecanase cleavage. Whether this effect is a chondrocyte or OA-SF derived process remains to be determined. In light of such observations NFκB modulation presents as an attractive target for the development of future therapeutics for OA. To further assess the efficacy of the 2 IKK inhibitors in

modulating OA pathology, we employed both RO100 and RO919 in an *in vivo* murine model of OA. These experiments will be presented and discussed in the next chapter.

CHAPTER SIX

Efficacy of NFκB inhibition *in vivo*

6.1 Introduction.

Current treatment strategies for OA are limited to agents that provide symptomatic pain relief typically analgesics such as acetaminophen and NSAIDS. Diacerhein is the first and only agent prescribed for OA that is able to modulate disease pathology. Unlike the NSAID agents which target prostaglandin formation and reduce inflammation within the joint, relieving pain, diacerhein elicits its therapeutic effect by inhibiting the synthesis of IL-1β within the joint (Pelletier *et al.*, 2006). *In vitro* studies have demonstrated that diacerhein inhibits IL-1β activation of the transcription factor NFκB by preventing degradation of the inhibitory IκB proteins (Domagala *et al.*, 2006; Mendes *et al.*, 2002; Martin *et al.*, 2003). Such inhibition of IL-1β activation results in down regulation of the production of MMP-1, -3, -9 and -13 from articular chondrocytes (Tamura *et al.*, 2001). *In vivo* studies have demonstrated in canine and murine models of experimental OA, that diacerhein elicits a cartilage protective effect, slowing the progression of OA and reducing GAG loss from the articular cartilage (Brandt *et al.*, 1997; Moore *et al.*, 1998; Smith *et al.*, 1999). Clinically diacerhein has been licensed for the treatment of OA in France since 1994, where it appears from radiographic assessment of the joint to slow disease progression and joint space narrowing (Dougadas *et al.*, 2001; Fidelix *et al.*, 2006; Pham *et al.*, 2004). The success of a diacerhein, an agent with the capacity to inhibit NFκB signalling within the joint, highlights the true potential of modulation of this signalling pathway for OA therapy.

The ultimate goal for OA is to find a therapeutic agent that can modify disease activity or even reverse the catabolic destruction of the joint, whilst the

search for such an agent continues the development of *in vivo* OA animal models provides a tool in which potential therapeutics can be assessed to determine their efficacy in modifying or even preventing joint deterioration.

The IKK inhibitors, RO100 and RO919 used in chapters 4 and 5, have effectively inhibited activation of the NFκB transcription factor *in vitro* and demonstrated, in response to IL-1β stimulation, the production of a range of mediators associated with pathological processes within the joint can be suppressed. To fully assess their efficacy, we sought to trial both RO100 and RO919 in an animal model of OA to establish their ability to modify arthritic changes *in vivo*.

As discussed during chapter one, an array of animal models of OA have been reported in the literature. Although each has its benefits, they are generally slow to yield data, with disease progression slow and insidious. Osteoarthritic like changes can be established quickly in chemically induced models of OA, making them a popular choice for pilot studies designed to test the efficacy of novel agents with the potential to modulate OA activity.

The monosodium iodoacetate (MIA) model of OA is an example of a chemically induced model that has been used in a number of species including mice, rats and chickens. The MIA model is different to many of the other available models as it accurately models the pain associated with the disease, a symptom of the disease overlooked by many other models (Fernihough *et al.*, 2004; Kobayshi *et al.*, 2003). MIA is administered intraarticularly into the joint where it inhibits glyceraldehyde-3-phosphate dehydrogenase activity which results in inhibition of cellular metabolism in the chondrocytes, leading to cell death (Dunham *et al.*, 1992). The MIA induced model of OA in rats

demonstrated that depletion of proteoglycans from the articular cartilage and erosion of the cartilage surface was evident by day 15 post injection (0.3mg MIA) (Guingamp *et al.*, 1997). An extended study over a 56 day period demonstrated that in rats treated with a single intraarticular injection of 1mg/ml MIA, gross lesions in the articular cartilage were present by 28 days and that by day 56 evidence of osteoclastogenesis and subchondral bone remodelling was present (Guzman *et al.*, 2003). The MIA model has been employed in mice where the pathology of induced arthritis follows a similar but less severe pattern. A study by van der Kraan established that cartilage fibrillation occurred between day 7 and day 21 post MIA injection, with progressive fibrillation of the surface up to day 64 (Van der Kraan *et al.*, 1989). Chondrocyte death was observed from day 1, with a greater reduction in chondrocyte survival from day 3. Evidence of osteophyte formation was apparent at day 7, with enhanced bone remodelling by day 21, although sclerosis of the subchondral bone was not observed.

Pathological changes in experimental models of OA in the smaller rodent species are routinely assessed by histological examination of the joint post sacrifice. Histological stains such as safranin-O/fast green, toluidine blue and haemotoxylin & eosin are widely used to determine cartilage erosion, subchondral bone remodelling and sclerosis, the presence of osteophytes and increased inflammatory exudate within the joint. Evidence of biochemical cartilage deterioration is routinely examined by immunohistochemistry with the presence of NITEGE and VDIPEN epitopes a popular choice to examine the destruction of cartilage mediated by aggrecanases and MMPs respectively.

A novel marker of arthritis observed in the MIA induced OA model in rats is the weight bearing ability of animals upon the affected joint. Animals with MIA induced in one hind limb have an altered weight bearing pattern as they avoid using the affected joint (Bove *et al.*, 2003). The alteration in weight bearing can be used as a method of assessing the efficacy of analgesics and other treatment strategies in this model.

The presence of clinically relevant serum biomarkers that provide a reliable and reproducible indication of osteoarthritic activity and progression is a contentious issue. Cartilage oligomeric matrix protein (COMP) is a noncollagenous protein, produced by the articular cartilage, synovial membrane and tendons of the joint. COMP structurally consists of 5 protein subunits that adjoin at the base of the molecule exhibiting a bouquet like structure (Morgelin *et al.*, 1992). COMP has been demonstrated to be released during cartilage breakdown and has been highlighted as a potential marker of cartilage deterioration that could be measured in serum samples (Saxne *et al.*, 1992). COMP levels have been assessed in the serum taken from animal models of both OA and RA, these studies demonstrate that the elevated levels of COMP correlated with arthritic changes within the joint (Larsson *et al.*, 2002).

During chapters 4 and 5 we demonstrated the efficacy of NFκB inhibition in mediating the release of inflammatory and destructive mediators from the synovial tissue and their ability to prevent IL-1β induced cartilage deterioration. However the ability of the 2 IKK inhibitors to modulate OA pathology *in vivo* needed to be tested. The MIA murine model of experimental OA was employed as the model of choice, in which to test the validity of NFκB inhibition as a target for therapy in OA.

The aims of this chapter were:

- To establish an MIA-induced model of experimental OA in C57Bl/6 mice.
- To characterise the pathological changes that a single intraarticular injection of MIA could induce over a 14 day period by histological techniques.
- To determine the efficacy of both RO100 and RO919 in modulating osteoarthritic changes induced by MIA injection within the joint.
- To quantify the serum levels of COMP over the 14 day time course of the MIA model to determine the rate of cartilage deterioration *in vivo*.

6.2 Results

6.2.1 Murine knee diameter was notably increased following MIA-induction of experimental OA.

The left and right knee diameter for each mouse was measured prior to the initiation of MIA induced arthritis (day 0), thereafter the MIA injected and control knees were measured and compared at days 1, 2 and 3 (Figure 6.1). Following MIA injection, the arthritic knee was significantly ($p \leq 0.01$) swollen in comparison to the control knee for each mouse in the first three days post-arthritis induction. At three days post arthritis induction the swelling present in the arthritic knee subsided and both arthritic and control knees were of a comparable diameter for the remainder of the study (data not shown).

6.2.2 Histological evidence of arthritic changes was evident from day 1 through to day 14 following the induction of experimental OA.

MIA injected knee joints and the corresponding normal knee joints were extracted from sacrificed mice at day 1 and day 14 post arthritis induction, immediately fixed in NBFS and subsequently decalcified prior to histological sectioning. Murine knee joint sections were stained with safranin-o/fast green allowing assessment of morphological arthritic changes in response to MIA injection (Figure 6.2). At day 1 post-MIA injection, mild inflammatory infiltration of the synovial membrane was noted compared with the non-injected normal joint (Figure 6.2 a & b). No morphological changes were evident in the articular cartilage at this early time point. By day 14, injected arthritic knees exhibited articular cartilage changes with a reduction in safranin-o/fast green staining and increased chondrocyte death in the patellofemoral region, in

comparison to normal joints (Figure 6.2 c & d). By day 14 mild synovial inflammation was still evident in the synovial membrane.

6.2.3 Several morphological changes are observed in MIA induced arthritic joints over a 14 day period.

A scoring system was applied (as detailed in the materials and methods, Table 2.1) that had previously been used to assess arthritis severity in a number of murine models. The combined arthritis score was assessed against a number of parameters that were determined histologically, namely cartilage fibrillation, chondrocyte death, loss of safranin-o/fast green staining, synovial hyperplasia, synovial infiltration and inflammatory exudate. Frequently observed changes in the MIA injected arthritic joints at 14 days post arthritis induction are illustrated (Figure 6.3). Synovial inflammation was typically observed following MIA injection which was not observed in the normal joint (Figure 6.3 a & b). Arthritic changes frequently observed following MIA injection included chondrocyte death, with empty lacunae present in the superficial and intermediate zone of articular cartilage (as indicated). A reduction in safranin-o/fast green staining in comparison to normal knees (Figure 6.3 c & d) was routinely observed. Fibrillation and roughening of the articular surface was frequently observed in the MIA injected knees but was not evident in normal knees (Figure 6.3 e & f).

6.2.4 Quantification of arthritis severity following MIA injection demonstrated significant pathological changes at day 1 and day 14 in MIA injected joints.

Histological sections stained with safranin-o/fast green from arthritic and control knees at both day 1 and day 14 were scored blinded using the scoring

system outlined in the materials and methods (Table 2.1). The mean score for arthritic and normal knees was quantified (Figure 6.4). At day 1 post arthritis induction, MIA injected knees demonstrated arthritic changes that were significantly ($p \leq 0.01$) different to normal knees (Figure 6.4 a). At day 14, MIA injected knees also demonstrated pathological changes that were significantly ($p \leq 0.01$) different to normal knees (Figure 6.4 b). Several of the normal knees at day 14 exhibited minimal changes that could be scored, such observations in the normal joints are likely to result from potentially altered joint loading, or maybe due to unassociated effects.

6.2.5 Serum COMP levels were suppressed at day 1 following the initiation of MIA induced experimental OA.

COMP has been highlighted as a biomarker of cartilage deterioration. Serum samples taken from mice at 3 time points during MIA induced arthritis. COMP was determined in each sample by ELISA. At day 1 post MIA injection, the levels of COMP present within the serum were significantly ($p \leq 0.05$) reduced in comparison to normal animals that had not received an injection of MIA (Figure 6.5). At days 7 and 14 following MIA injection no significant difference in COMP levels was evident in serum samples taken from normal animals and those that had received an injection of MIA.

6.2.6 Treatment with either RO100 or RO919 did not elicit an observable effect upon knee swelling in response to MIA injection.

The knee diameter of MIA injected joints of mice treated with either RO100 or RO919 were compared to untreated knees at days 1, 2 and 3 (Figure 6.6). Neither agent elicited a notable effect upon knee joint swelling.

6.2.7 NFκB inhibition did not modulate pathological changes in the MIA experimental model of OA at day 1 post-MIA injection.

Histological sections stained with safranin-o/fast green from untreated, RO100 treated and RO919 treated arthritic knees at day 1 post injection were scored blinded using the scoring system outlined in the materials and methods (Table 2.1). The mean score for each treatment strategy was determined (Figure 6.7). At day 1, arthritic changes in untreated knees were more pronounced than the changes observed in RO100 and RO919 treated knees. However this effect was not significant (Figure 6.7 a & b).

6.2.8 Neither RO100 or RO919 modified arthritic changes within MIA injected joints at 14 days post arthritis induction.

Safranin-o/fast green stained histological sections from untreated, RO100 treated and RO919 treated MIA injected knees at day 14 post arthritis induction were scored blinded using the scoring system outlined in the materials and methods (Table 2.1). The mean score for each treatment strategy was determined (Figure 6.8). Neither RO100 nor RO919 elicited a notable effect upon pathological changes induced by MIA injection in comparison to untreated knees (a). As observed at day 1, at day 14 post injection individual scores for each mouse varied both within and between each treatment group (b).

6.2.9 Pathological changes induced by MIA injection were observed in all mice regardless of treatment regime.

Histological sections stained with safranin-o/fast green from untreated, RO100 treated and RO919 treated, arthritic knees at day 14 post arthritis induction were examined for observable pathological changes in response to MIA injection (Figure 6.9). Pathological changes were observed in all mice at

day 14 post-MIA injection. The most frequently observed changes in untreated, RO100 treated and RO919 treated mice were loss of safranin-O/fast green staining and chondrocyte death in the superficial and intermediate zones (Figure 6.9 a, b & c). Evidence of fractures and fibrillation (Figure 6.9 d), synovial hyperplasia (Figure 6.9 e) and the formation of osteophytes at the patella margins (Figure 6.9 f) were evident in all mice injected with MIA.

6.2.10 NFκB inhibition did not affect COMP levels in the serum of MIA induced osteoarthritic mice.

The presence of COMP in serum samples taken from untreated, RO100 treated and RO919 treated mice at 3 time points in the duration of the MIA-induced model of OA was quantified by specific ELISA (Figure 6.10). No quantifiable difference was apparent in the serum levels of COMP in mice treated with either RO100 or RO919 at day 1 post MIA injection in comparison to untreated mice (Figure 6.10 a). At days 7 and 14 post MIA injection, no difference was observed in serum COMP levels between treated and untreated mice (Figure 6.10 b & c).

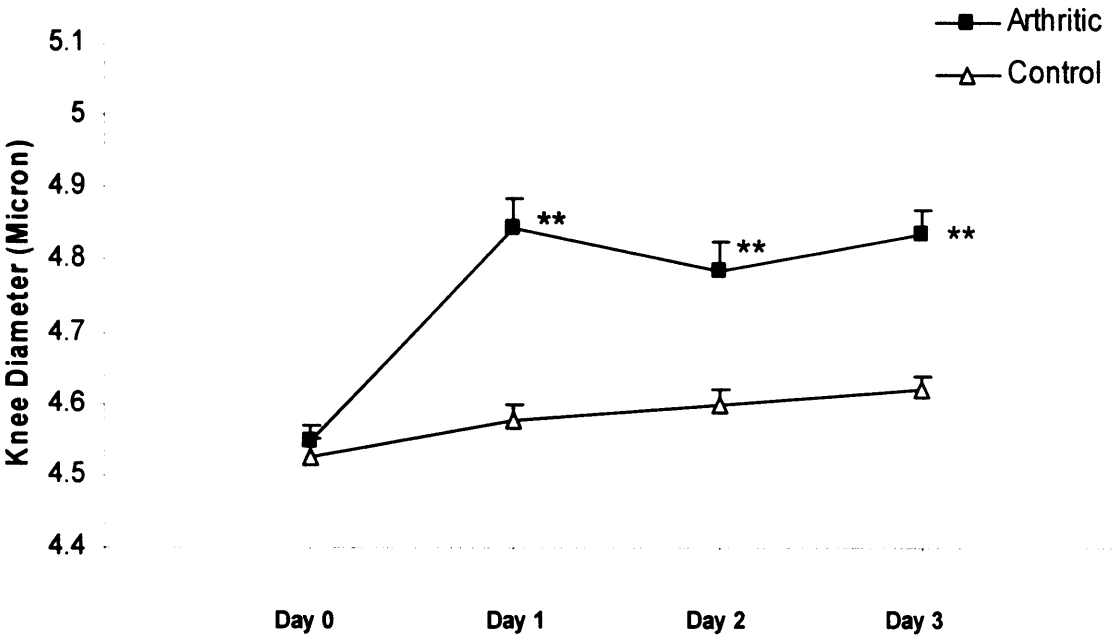

Figure 6.1 Assessment of knee swelling in response to MIA injection.

The knee diameter of both normal and MIA injected knees was measured using an analogue micrometer at day 0, prior to the initiation of arthritis and at days 1, 2 and 3 post MIA injection to determine the degree of inflammation intraarticular injection of MIA induced. (** $p \leq 0.01$, $n = 36$).

Day 1

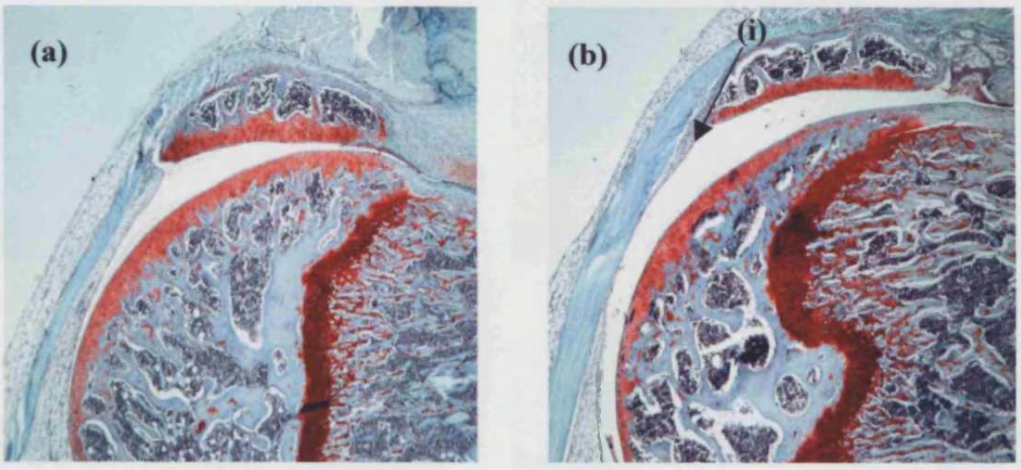

Day 14

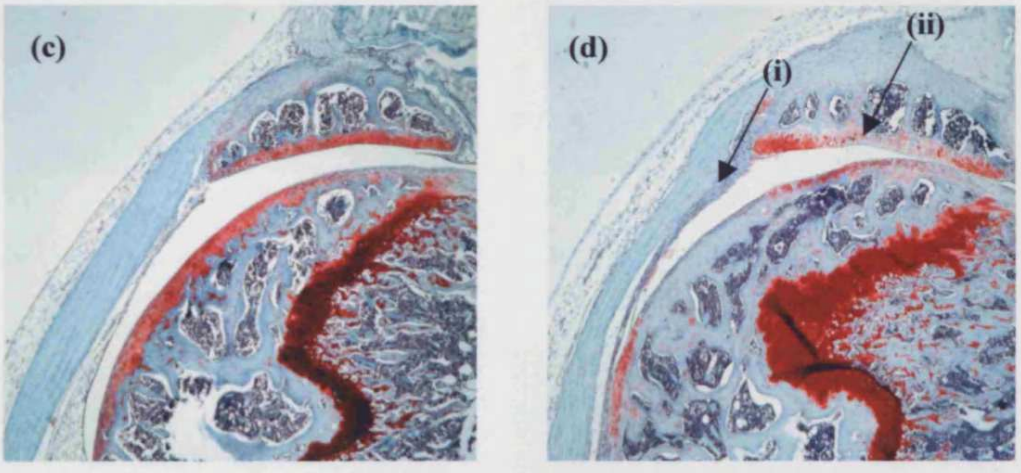

Figure 6.2 Representative histological sections of normal and arthritic knees

Normal knee joints (a & c) were extracted along with the MIA injected knee joints (b & d) from mice sacrificed at day 1 (a & b) and day 14 (c & d) post MIA injection. Murine knee joints were fixed in NBFS and decalcified in 10% formic acid prior to sectioning. Histological sections were stained with safranin-o/fast green. Original magnification x 40. Arrows indicate areas of synovial inflammation (i) and cartilage depletion (ii).

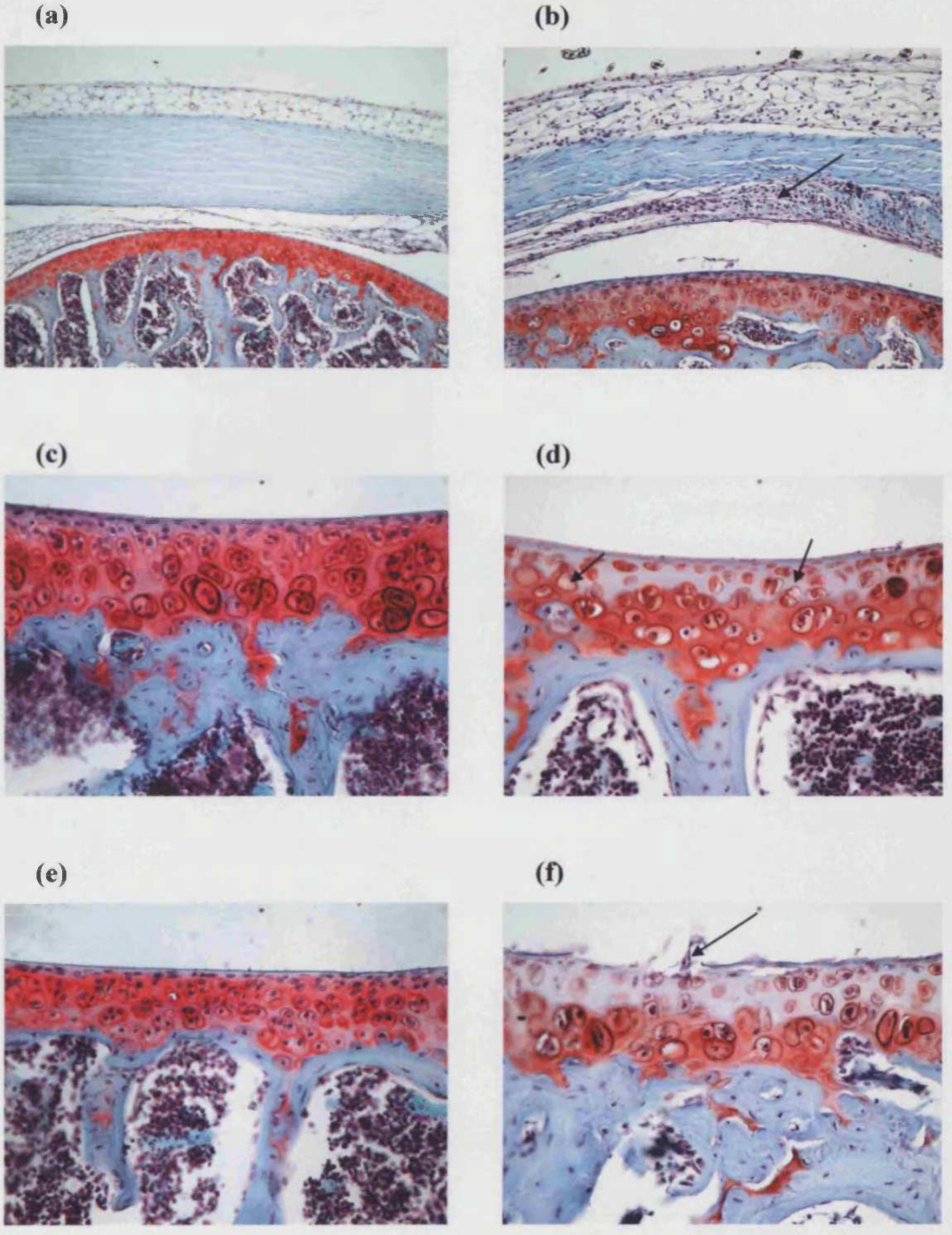

Figure 6.3 Representative histological examples of pathological changes present in MIA injected murine knees.

MIA injected knee joints were sectioned and stained with safranin-O/fast green to allow histological scoring of disease severity. Representative histological examples of the scoring criterion are illustrated, with normal knees (a, c, e) compared to MIA injected knees (b, d, f). Arrows indicate pathological changes observed at 14 days post MIA injection, typically synovial inflammation (b), evidence of chondrocyte death as determined by the presence of empty lacunae (d), and fibrillation and roughening of the surface of the articular cartilage (f). Magnification x 100 (a & b), x 400 (c, d, e & f).

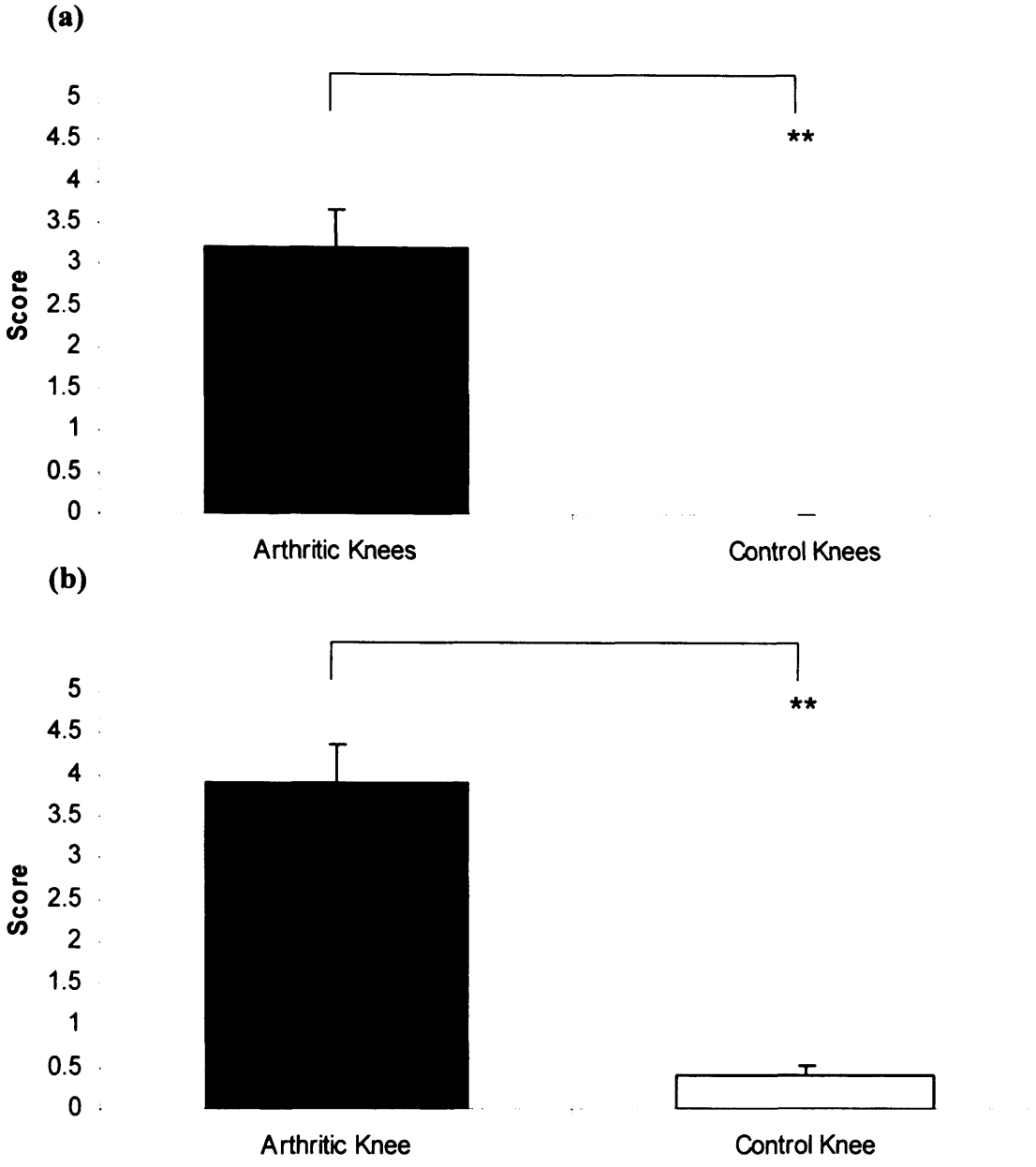

Figure 6.4 Quantification of arthritis scores for MIA injected and normal knees.

MIA injected and normal knees were scored blinded at day 1 (a) and day 14 (b) post-arthritis induction. The mean score for arthritic and normal joints at the two time points is displayed. n = 6 at day 1, n = 34 at day 14. Error bars represent SEM. (** $p \leq 0.01$)

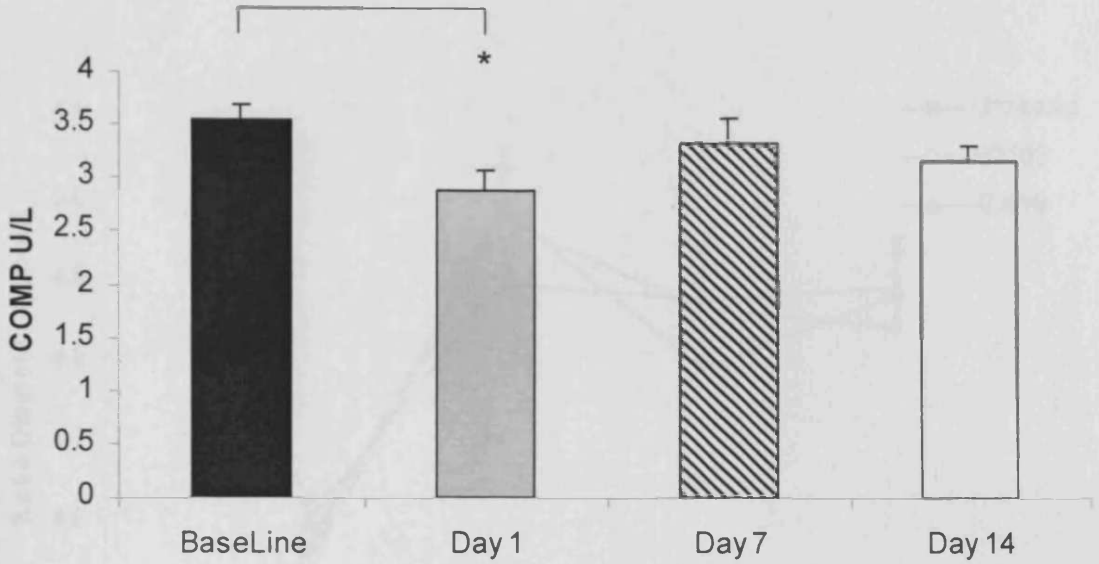

Figure 6.5 Quantification of serum COMP levels during the course of MIA induced experimental OA.

Serum samples taken at 4 time points during the duration of the MIA induced OA model were assessed for the presence of the cartilage biomarker COMP using a specific ELISA kit. The mean COMP production for each time point is displayed, error bars represent SEM. (* $p \leq 0.05$, n = 8 at baseline, day 7 and day 14, n = 3 at day 1).

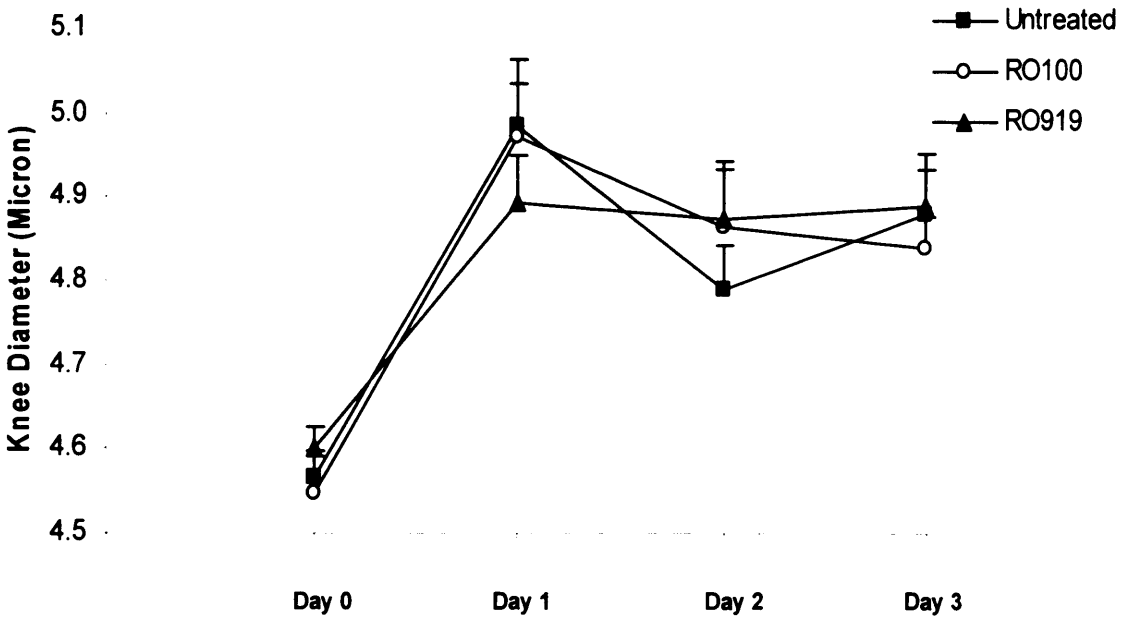

Figure 6.6 Assessment of knee swelling in untreated, RO100 treated or RO919 treated knees in response to MIA injection.

The knee diameter of untreated, RO100 treated and RO919 treated MIA injected knees was measured using an analogue micrometer at day 0, prior to the initiation of arthritis and at days 1, 2 and 3 post MIA injection to determine the degree of inflammation intraarticular injection of MIA induced. Error bars represent SEM, n = 12 for each treatment group.

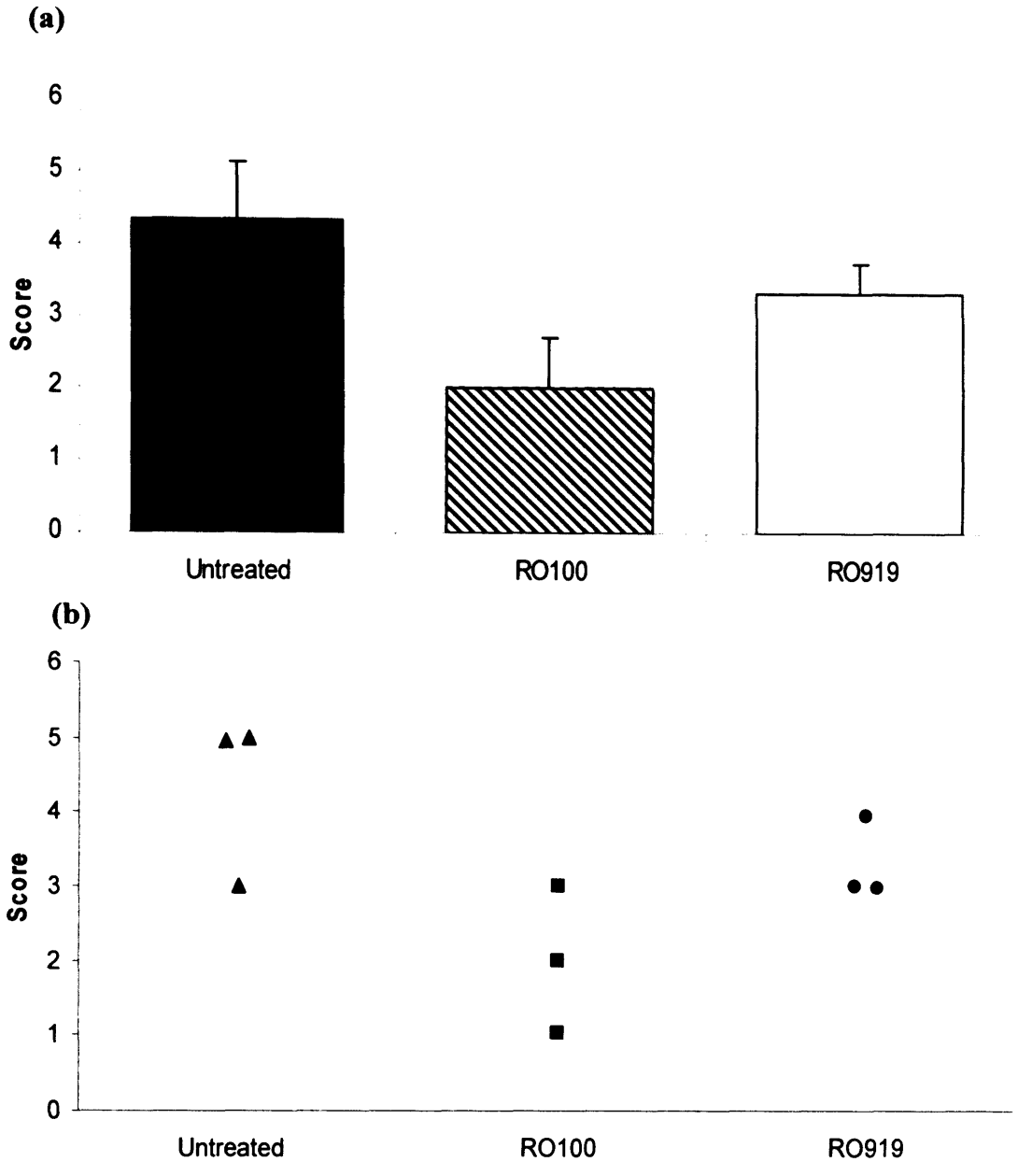

Figure 6.7 Quantification of arthritis score for RO100 and RO919 treated MIA injected knees at day 1 post-injection.

Untreated, RO100 treated and RO919 treated knees were scored blinded at day 1 post MIA injection. The mean for each treatment strategy is displayed (a) alongside the indivdual scores for each mouse (b). n = 3 for each treatment group, error bars represent SEM.

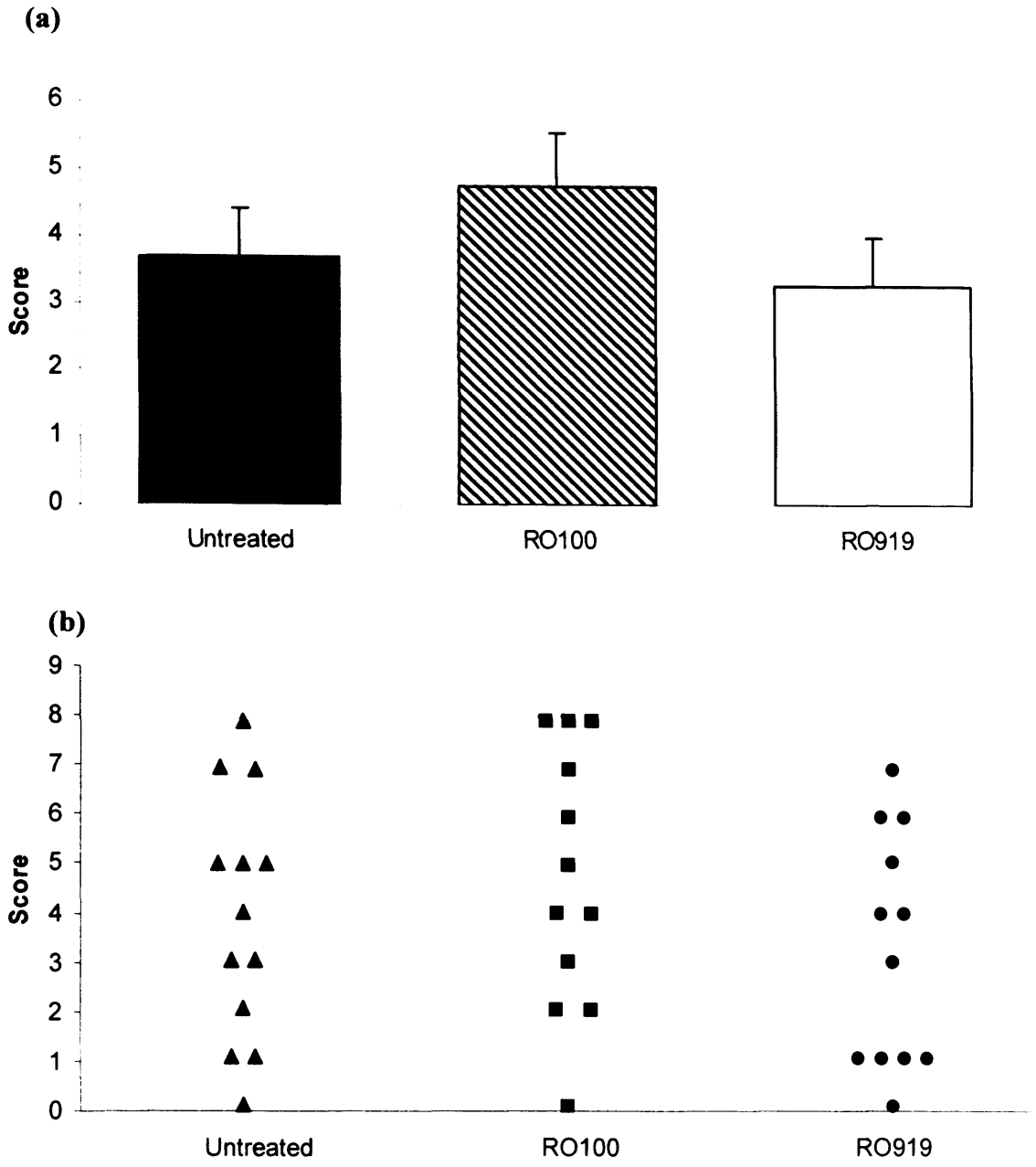

Figure 6.8 Quantification of arthritis score for RO100 and RO919 treated MIA injected knees at day 14 post-injection.

Untreated, RO100 treated and RO919 treated knees were scored blinded at day 14 post MIA injection. The mean for each treatment strategy is displayed (a) alongside the indivdual scores for each mouse (b). n = 12 for each treatment group, error bars represent SEM.

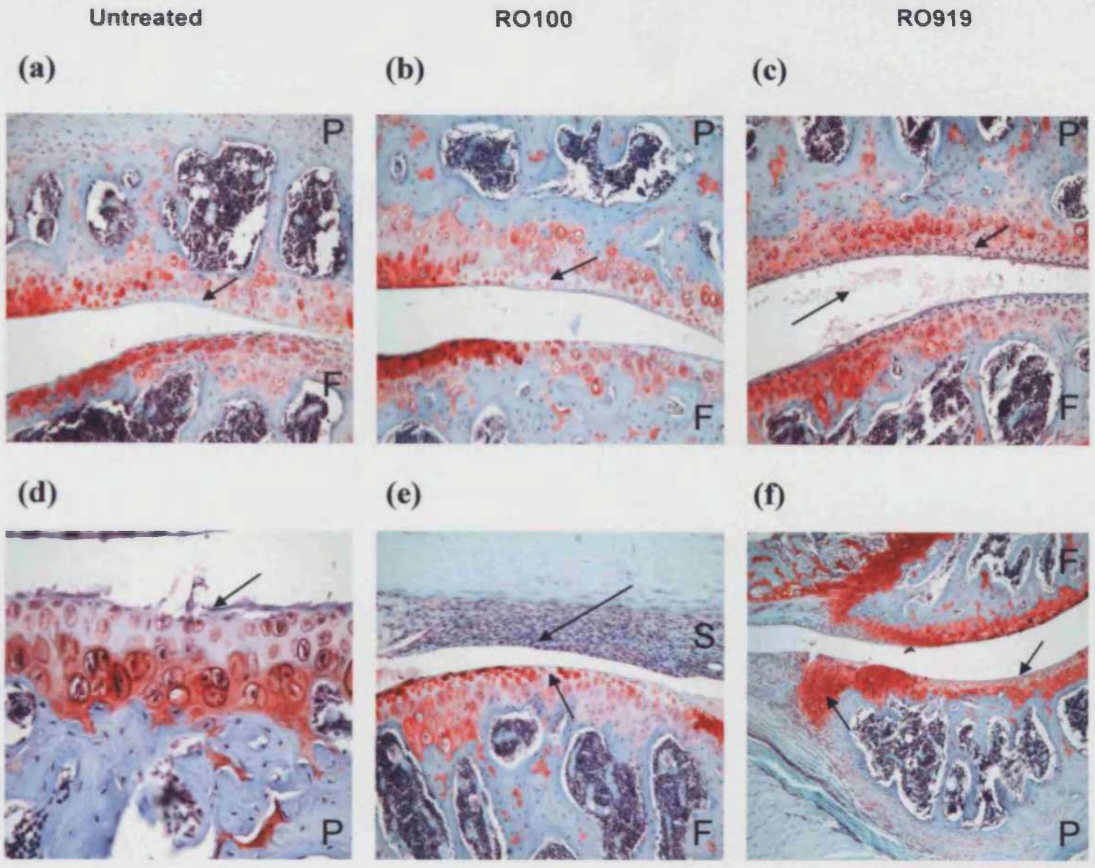

Figure 6.9 Representative histological sections of untreated, RO100 treated and RO919 treated arthritic joints at day 14 post-MIA injection

MIA injected knee joints (a – f) were extracted from mice sacrificed at 14 days post MIA injection. Murine knee joints were fixed in NBFS and decalcified in formic acid prior to sectioning. Histological sections were stained with safranin-o/fast green to allow identification of pathological changes. Loss of safranin-o staining is evident in the articular cartilage as indicated by the arrows (a, b, c, d, e and f), evidence of fractures and fibrillation (d), synovial inflammation (e) and osteophyte formation (f) are also indicated. F = Femur, P= Patella, S= Synovium. Original magnification x 100 (f) x 200, (a, b, c, e) and x 400 (d).

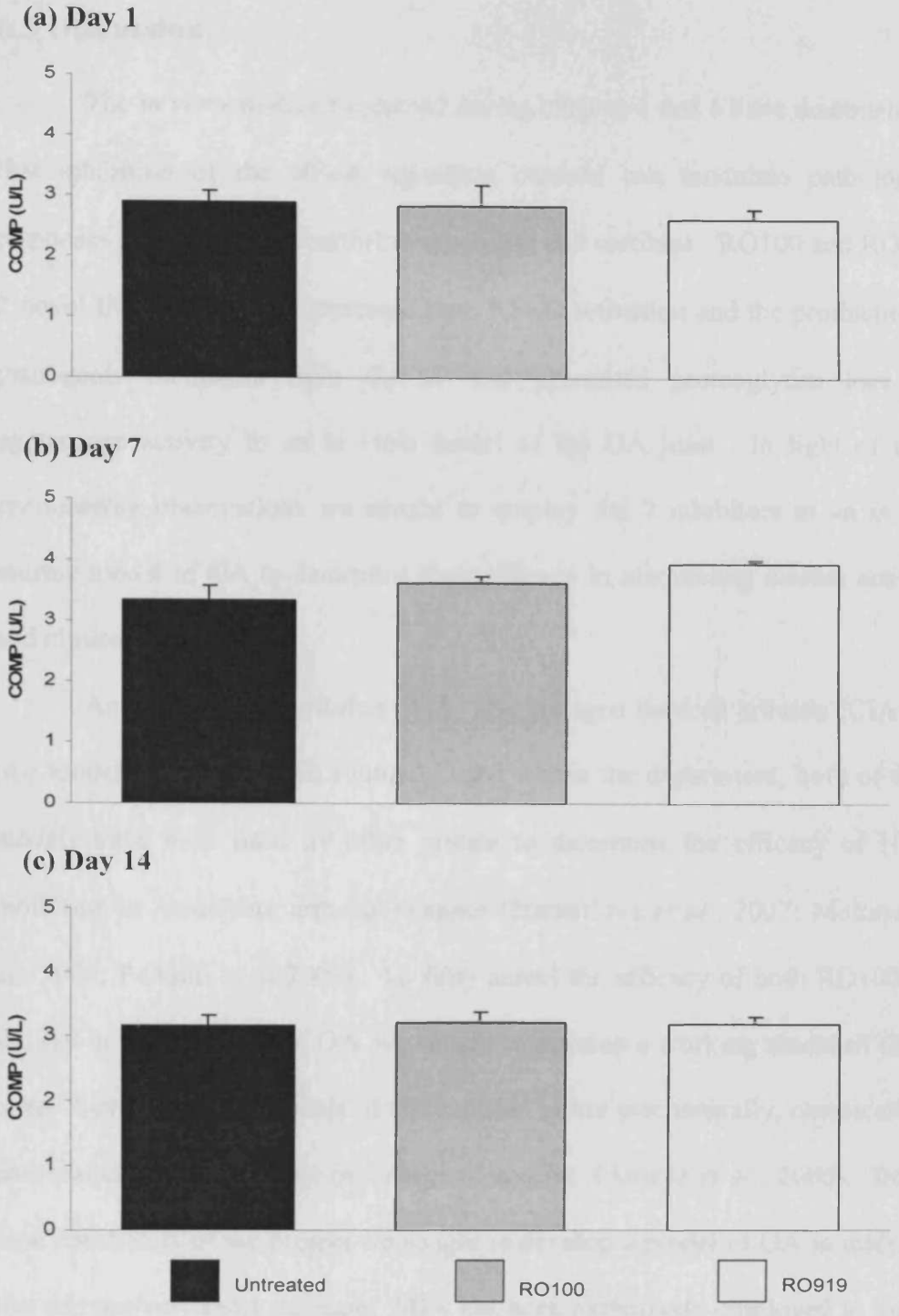

Figure 6.10 Quantification of serum COMP levels in response to the different treatment strategies employed during the course of MIA induced experimental OA.

Serum samples were taken from three animals from each treatment group at day 1 (a), day 7 (b) and day 14 (c) and the levels of COMP quantified using a specific ELISA kit. The mean COMP production for each time point and treatment strategy is displayed, error bars represent SEM.

6.3 Discussion.

The *in vitro* studies conducted during chapter 4 and 5 have demonstrated that inhibition of the NFκB signalling cascade can modulate pathological responses in both the osteoarthritic synovium and cartilage. RO100 and RO919, 2 novel IKK inhibitors, suppressed both NFκB activation and the production of pathogenic mediators from OA-SF and prevented proteoglycan loss and aggrecanse activity in an *in vitro* model of the OA joint. In light of these encouraging observations we sought to employ the 2 inhibitors in an *in vivo* murine model of OA to determine their efficacy in modulating disease activity, and clinical outcome.

Antigen induced arthritis (AIA) and collagen induced arthritis (CIA) are two models of RA that are routinely used within the department, both of these models have been used by other groups to determine the efficacy of NFκB inhibition in modifying arthritic changes (Izamailova *et al.*, 2007; McIntyre *et al.*, 2003; Podolin *et al* 2005). To fully assess the efficacy of both RO100 and RO919 in the treatment of OA, we sought to develop a working model of OA in mice. Several animal models of OA induced either mechanically, chemically or enzymatically are available in a range of species. (Ameye *et al.*, 2006). Due to time constraints of the project we sought to develop a model of OA in mice that was of relatively short duration. MIA has been extensively employed to induce osteoarthritic like changes in a number of species, most commonly the MIA model is employed in rats to induce OA and model the pain associated with the disease (Guzman *et al.*, 2003; Ivanavicius *et al.*, 2007; Kobayshi *et al.*, 2003). The MIA model was developed by Kalbhen during the 1980's to induce OA changes in the knee joints of hens and rats over a 2 – 4 month period (Kalbhen,

1987). Subsequent studies have demonstrated that MIA inhibits the oxidative pathways of the chondrocytes resident within the articular cartilage (Dunham *et al.*, 1992; Dunham *et al.*, 1993). Such inhibition of cellular metabolism results in increased cell death leading to the deterioration of articular cartilage.

A study conducted by Guingamp *et al* demonstrated that with an increasing dose of MIA, the histological changes within the articular cartilage and subchondral bone became more severe (Guingamp *et al.*, 1997). At day 15 a 0.1mg dose of MIA induced loss of proteoglycans from the articular cartilage as demonstrated by the reduction in safranin-o/fast green staining, whilst a 0.3mg dose resulted in erosions that extended to reveal the underlying subchondral bone with a degree of subchondral bone sclerosis. By day 30 in this study macroscopic evidence of cartilage lesions was evident following sacrifice. Three separate studies have employed MIA to induce osteoarthritic like changes in mice (van der Kraan *et al.*, 1989; van der Kraan *et al.*, 1992; van Osch *et al.*, 1994). Mice treated with doses of MIA ranging between 0.1% – 1%, exhibited a notably reduced severity of arthritis at day 15 in comparison to the aforementioned study by Guingamp *et al.* All three studies sacrificed mice at several time points during the 64 day study which demonstrated changes within both the articular cartilage and synovial membrane at day 7 and day 21. By day 64, all the constitutive tissues of the joint demonstrated changes associated with the pathology of OA.

Time constraints prevented us from conducting the study for a 64 day period. In light of the literature and the efficacy of both RO100 and RO919 in preventing early stage changes within the joint, we chose to sacrifice mice at day 14 post-MIA injection. Whilst a 14 day period would be too short to model

advanced OA, it was feasible that early stage changes could be successfully modelled.

MIA was injected intraarticularly into the knee (stifle) joint of the right hind limb of each mouse in accordance with previous studies, with the left hind knee acting as the contralateral control, normal joint (van der Kraan *et al.*, 1989; van der Kraan *et al.*, 1992; van Osch *et al.*, 1994). Histological sections from both the arthritic and normal knees stained with safranin-o/fast green at days 1 and 14 post-MIA demonstrated that a 3mg/ml intraarticular injection of MIA induced pathological changes representative of OA at both day 1 and day 14 in comparison to the contralateral healthy knee.

Throughout the duration of both the antigen induced arthritis (AIA) and collagen induced arthritis (CIA) model, inflammation is a significant clinical feature, consequently swelling of the affected joint(s) is an important measurable parameter that directly relates to disease severity (Nowell *et al.*, 2003; Richards *et al.*, 1999). Whilst the MIA model has not been reported as an inflammatory model, we noted a degree of inflammatory pathology in the arthritic joint that was greater than that seen in the normal knee. During the first three days post MIA injection the arthritic knee was significantly larger in comparison to the control knee as determined by measuring the diameter of the knee. After three days swelling resolved with knee diameters in the MIA injected joint comparable with normal non-injected knees. These observations were in agreement with the previous study in which knee swelling and inflammation were considered mild (van der Kraan *et al.*, 1989). Having demonstrated that we could effectively model OA in mice we treated MIA injected mice with the two IKK inhibitors and assessed disease outcome histologically.

The IKK inhibitors, RO100 and RO919, employed throughout this thesis were developed by Roche for oral administration as a therapeutic agent for OA. Consequently treating the mice orally with RO100 and RO919 would have been preferential. However there are disadvantages to oral administration, whilst the oral gavage method ensures that an exact dose can be administered it is uncomfortable to the animal and is typically performed under anaesthesia. In an animal as small as a mouse it can be inherently difficult to perform the gavage technique correctly, so administration of therapeutics in the drinking water is the favoured route of administration. A major drawback to dosing animals via the drinking water is that it is difficult to determine whether each animal receives a reproducible dose of therapeutic and that this is identical on each day. The efficacy of each inhibitor would therefore be problematic to extrapolate. To overcome the problems with bioavability and targeting by injection we opted to administer agents intraarticularly as a single dose. As arthritis was induced by a single intraarticular injection of MIA into the hind knee at day 0, to prevent further discomfort to the animals by repeatedly injecting the same joint, we administered a 5mM dose of either RO100 or RO919.

Histological sections scored for signs of synovial inflammation and cartilage deterioration at day 1 post-MIA injection using the scoring system outlined in van der Kraan's earliest study (van der Kraan *et al.*, 1989, outlined in Table 2.1), demonstrated that whilst the arthritis score of untreated mice was higher than that of RO100 or RO919 treated mice this effect was not significant. This was an interesting observation as arthritic joint scores at day 1 post MIA induction are predominantly a consequence of synovial membrane changes within the joint rather than cartilage destruction. The studies conducted during

chapter 4 demonstrated that of the 2 inhibitors RO100 was more efficacious in inhibiting the production of pathogenic mediators from OA-SF than RO919, whilst in chapter 5 we observed the opposite effect with RO919 proving the more effective agent of the two in preventing proteoglycan loss from cartilage *in vitro*. It would appear from the histological scores at day 1 that RO100 was more effective at targeting pathological changes within the synovium than RO919. However, due to the small number of mice examined at day 1, caution must be exercised at drawing such a conclusion. To determine if this effect was real we would need to conduct further studies to increase the number of animals assessed.

In light of the disappointing results demonstrated by the two inhibitors in improving clinical score in response to MIA injection, we sought to quantify the levels of COMP present in the serum of untreated, RO100 treated and RO919 treated mice. Numerous studies have demonstrated that during cartilage deterioration COMP is released into the joint space and subsequently the circulation as a product of breakdown which has been highlighted as a potential marker of disease severity of both RA and OA (Sharif *et al.*, 2004; Skoumal *et al.*, 2003; Wislowska *et al.*, 2005). We observed that at day 1, day 7 and day 14 post-MIA injection, there was no observable difference in the production of COMP by RO100 or RO919 treated mice in comparison to untreated mice. Several studies in humans have demonstrated that exercise, running in particular, significantly elevates the serum levels of COMP (Andersson *et al.*, 2006; Kersting *et al.*, 2005; Neidhart *et al.*, 2000). Serum samples were taken from mice during the morning, as mice are predominantly nocturnal. The animals had been active for a number of hours and it is possible that the COMP

detected was in response to activity. In light of this it may have proved beneficial to extract serum samples from mice following a period of inactivity to see if a detectable difference in COMP levels was measurable.

It is likely that both RO100 and RO919 elicit limited efficacy in modulating disease activity in this model. Firstly, both inhibitors have been developed for repeated oral administration and therefore a single dose given intraarticularly may not be sufficient to improve pathological changes within the joint. Ideally we would have administered both inhibitors orally, initially as a single dose and subsequently as a repetitive dosing strategy to ascertain if longterm suppression of NFκB within the joint is required to prevent joint deterioration. Secondly, due to the limited quantity of both RO100 and RO919 available experiments employing a range of doses of to determine the optimal dose of either inhibitor were not conducted. With unlimited supplies of the two agents it would have been beneficial to perform dosing experiments to optimise the dose required to modulate OA pathology. Thirdly, we have not ascertained the pharmacological properties of the agents. It is unclear if either RO100 or RO919 can penetrate the cartilage and modulate disease activity or how rapidly it is cleared from the joint. Fourthly, we selected a single concentration of MIA following a review of the literature to induce experimental OA in mice. It may have been beneficial to employ a range of concentrations to examine the importance of MIA concentration in inducing pathological changes.

A major drawback proposed with inhibiting the NFκB signalling cascade is the potential severe adverse effects that this could elicit due to the importance of NFκB in normal cellular function, apoptosis and inflammatory response

(Fraser, 2006). Mice were observed frequently for the duration of the study and displayed no obvious adverse effects or weight-loss.

In summary, the observations of this study suggest that the two IKK inhibitors do not have the capacity to modulate osteoarthritic disease activity. However, following the promising results demonstrated during our *in vitro* studies that NFκB inhibition can modulate pathological processes associated with OA, it may prove beneficial to expand upon our pilot *in vivo* studies. Our initial study not only employed two IKK inhibitors that had not been used previously *in vivo* but also developed and utilised an experimental model of OA that was novel to Cardiff. In light of these factors, the modifications that have been suggested previously may demonstrate that our 2 IKK inhibitors do indeed have the capacity to modify joint pathology *in vivo*. Or alternatively they may clarify why, despite the encouraging results demonstrated *in vitro*, both RO100 and RO919 do not elicit a protective effect . In light of the questions raised by the studies performed during chapter 6 it is impossible to determine if NFκB is truly a valid target for therapy until further studies have resolved these issues.

CHAPTER SEVEN

Final Discussion

7.1 IL-1β and TNFα drive synovial pathology

The cytokines IL-1β and TNFα have a primary role in immunity driving inflammatory responses within the body (Oberholzer *et al.*, 2000; Warren, 1990). The cytokines have been implicated in the pathology of an array of clinical diseases from cancer, whereby TNFα and IL-1β promote tumour progression and invasiveness (Apte, 2006; Balkwill, 2006; Szlosarek *et al.*, 2006), through to Crohns disease where TNFα and IL-1β are secreted by the intestinal macrophages and drive the inflammatory response during active disease (Kurtovic *et al.*, 2004; Schreiber *et al.*, 1999). Within the sphere of rheumatology, IL-1β and TNFα have been demonstrated to be of pivotal importance in RA (Arend *et al.*, 1995). TNFα has been established as the predominant cytokine in RA driving the early stage inflammatory changes, with IL-1β implicated in the deterioration of articular cartilage and promoting inflammation within the joint during the later stages (van den Berg *et al.*, 1999). TNFα is speculated to drive the disease process through its induction of IL-1β which results in the destruction of articular cartilage. Consequently TNFα inhibitors have been developed to suppress TNFα within the joint, which results in a substantial reduction in TNFα induced IL-1β production and consequently an improved clinical perspective for RA patients (Furst *et al.*, 2005).

Following the success of anticytokine strategies for the treatment of RA, attention in OA research has focused on determining the cytokine signalling network within the osteoarthritic joint that underpins the classic destruction of the articular cartilage and with progression, involves all four constitutive tissues of the joints. As OA is a disease driven primarily by cartilage destruction, it is

perhaps unsurprising that IL-1β has been implicated in the pathology of the disease and is speculated to be the pivotal cytokine with TNFα postulated to play a secondary role (Malemud, 2004; Martel-Pelletier, 1999). Biologically significant levels of IL-1β, in the ng/ml range, have been demonstrated in synovial fluid of osteoarthritic patients (Hopkins *et al.*, 1988), with increased numbers of IL-1 receptors evident in osteoarthritic cartilage and synovial membranes in comparison to normal tissues (Martel-Pelletier, 1992; Sadouk *et al.*, 1995). Osteoarthritic chondrocytes express greater numbers of TNF receptors than are expressed by normal chondrocytes (Westacott *et al.*, 1994) and are upregulated by IL-1β and IL-6 present within the osteoarthritic joint (Webb *et al.*, 1998). A study performed by Pelletier et al demonstrated that OA synovial membrane explants produced substantially greater levels of IL-1β in comparison to the levels of TNFα produced, consequently the upregulation of MMPs is believed to be in response to the IL-1β present (Pelletier *et al.*, 1995). Whilst the initiating trigger that results in osteoarthritic changes within the joint is largely unknown, it is understood that the homeostatic balance that exists between anabolism and catabolism within the joint, shifts in favour of catabolism with increased levels of MMPs, ADAMTS and inflammatory mediators such as IL-6, resulting in progressive joint destruction (Martel-Pelletier *et al.*, 2005).

The studies described in chapter 3 focused on the synovial membrane and the pathological processes it drives within the joint. Initial studies sought to determine the 'typical' cellular composition and inflammatory phenotype of the synovium derived from endstage OA patients. Characterisation of the synovial membrane revealed that as expected inflammation within the membrane varied

markedly between patients, with some individuals exhibiting no evidence of inflammation whilst others displayed highly inflamed membranes. Subsequent cellular analysis of the tissue demonstrated that the membrane was predominantly comprised of fibroblast-like synoviocytes and macrophages. Synovial macrophages are the primary source of IL-1β and TNFα within the synovium and are postulated to drive catabolic processes and the production of an array of mediators within the joint. In order to clarify the importance of the synovial macrophage in driving joint pathology, we developed a technique to remove macrophages from the remainder of the cell population. Our studies effectively demonstrated that in the absence of synovial $CD14^+$ macrophages the levels of IL-1β and TNFα were minimal, clarifying the importance of synovial macrophages as a source of catabolic IL-1β and TNFα within the joint. Furthermore in the absence of synovial macrophages the levels of a range of MMPs and inflammatory cytokines and chemokines are suppressed. A subsequent study conducted demonstrated that neutralisation of the spontaneous IL-1β and TNFα present within OA-COCUL inhibited the release of an array of mediators implicated in the pathology of OA. In summary, the studies described during chapter 3 demonstrated the importance of synovial macrophages and the inflammatory cytokines they produce, in the induction of a host of other catabolic mediators responsible for perpetuating a destructive environment within the joint.

7.2 The importance of the NFκB signalling pathway in OA.

Both IL-1β and TNFα, through their association with their respective cell surface receptors, induce the NFκB signalling cascade in many different cell

types, resulting in the transcription of an array of genes, including those implicated in the pathology, namely IL-6, MMP-1, and MMP-3 (Amos *et al.*, 2006; Vincenti *et al.*, 2002). The NFκB pathway is comprised of several constitutive steps that convert a signal, initiated by a cytokine or stress at a surface receptor, through to the production of a protein via the activation of the transcription factor (Beinke *et al.*, 2004). Several steps within the pathway have been highlighted as potential therapeutic targets, where inhibition in a specific cell type could result in the suppression of pathological mediators associated with disease-specific processes (Calzado *et al.*, 2007). Inhibitors of the IKK proteins (Agou *et al.*, 2004; May *et al.*, 2000) and the proteosome (Adams, 2002; Sanchez-Serrano I *et al.*, 2006) have been developed as potential targets for therapy.

The NFκB signalling cascade has been the focus of much attention within the sphere of rheumatology. Several studies have employed novel pre-clinical trial inhibitors of NFκB both *in vitro* and *in vivo* (Izamailova *et al.*, 2007; Podolin *et al.*, 2005; Schopf *et al.*, 2006). The findings of these studies have demonstrated that inhibition of the NFκB signalling cascade is a valid target for therapy. Following the studies described in chapter 3, which demonstrated that neutralisation of IL-1β and TNFα was an attractive target for OA therapy, we sought to study the role of the NFκB signalling cascade in response to IL-1β stimulation within OA.

The studies described in chapter 4 sought to determine the role of the transcription factor, NFκB, in the IL-1β induced production of pathological cytokines and MMPs. We demonstrated that OA-SF could be efficiently transfected with an adenovirus encoding the inhibitory subunit IκBα, resulting

in suppression of the levels of IL-6, MMP-1 and MMP-3 released by OA-SF in response to IL-1β. Subsequent studies employed two novel inhibitors of the NFκB signalling cascade that targeted the IKK subunit, namely RO100 and RO919. Our findings demonstrated that NFκB activation could be significantly inhibited by a 1μM dose of both RO100 and RO919 in OA-SF and that levels of MMP-1, MMP-3 and IL-6 production were significantly inhibited by a 0.1μM dose of either RO100 or RO919 in response to IL-1β. A physiologically relevant *ex vivo* model of OA demonstrated that both IL-6 and MMP-1 levels were suppressed by RO100 and the inhibition of these two mediators in this system was comparable to the efficacy elicited by the anti-cytokine neutralising strategies employed during chapter 3. Cell viability studies demonstrated that neither RO100 nor RO919 elicited a toxic effect in OA-SF at the doses employed. This study suggests that the IL-1β induced NFκB signalling cascade in OA-SF is involved in the production of mediators associated with pathology namely, MMP-1, MMP-3 and IL-6, and can be effectively targeted by two small molecule inhibitors of IKK.

Following the success of the chapter 4, we sought to establish the role of the transcription factor in cartilage deterioration as described in chapter 5. We developed a representative *in vitro* model of the joint, in which we could induce early pathological changes within the articular cartilage, culturing human OA-SF in combination with adult healthy articular cartilage derived from murine patellas. In response to IL-1β stimulation, the cartilage present in the joint model exhibited an enhanced loss of proteoglycans when cultured in combination with OA-SF. The increased expression of the aggrecanase cleavage neoepitope, NITEGE further illustrated the pathological changes that

IL-1β can induce *in vitro*. The two IKK inhibitors were employed successfully in the OA-JC model, demonstrating that both RO100 and RO919 reduced the loss of proteoglycans from the articular cartilage and reduced aggrecanase cleavage within the intermediate and radial zones.

In summary, our observations of the *in vitro* studies performed during chapters 4 and 5 highlighted the efficacy of both RO100 and RO919 in preventing pathological responses within the synovium and articular cartilage, and validate the hypothesis that modulation of the signalling pathway maybe a valid therapeutic target for OA.

7.3 NFκB inhibition within the synovial joint.

The advent of animal models that replicate the osteoarthritic process have transformed our understanding of the disease process (Bendele, 2001; Van den Berg, 2001). Pharmacological agents have also been trialled in animal models of OA to determine efficacy in improving the clinical symptoms of OA. Of all the agents trialled, the only true success story for OA is the agent diacerhein, which in initial *in vivo* studies demonstrated that it had the ability to modify structural changes within the osteoarthritic joint (Moore *et al.*, 1998; Smith *et al.*, 1999). As a consequence of this study diacerhein has been employed in the treatment of OA patients, whereby it has been demonstrated to slow structural progression of the disease as indicated by reduced joint space narrowing assessed radiographically (Dougados *et al.*, 2001; Felidix *et al.*, 2006, Mazieres *et al.*, 2006) and is speculated to be the first real agent developed for the treatment of OA with a disease modifying capacity.

The studies conducted during chapter 6 were designed to assess the ability of both RO100 and RO919 as novel therapeutic agents developed for the treatment of OA. It was speculated, as a result of the encouraging observations from both chapter 4 and 5, where the two agents clearly altered pathology *in vitro,* that the 2 agents would be able to modulate osteoarthritic changes within the joint. Following a review of the literature, we developed a successful murine model of experimental OA, in which early stage osteoarthritic changes could be modelled over 14 days as determined by histological analysis of the joints. However, the results of our *in vivo* study were disappointing. At day 1 post-MIA injection neither agent elicited a significantly different arthritis score than untreated mice, by day 14 post MIA injection all three treatment groups demonstrated comparable arthritis scores. The levels of COMP were measured and indicated that the presence of COMP in the serum remained relatively consistent for the duration of the model and was not affected by either inhibitor. As outlined during chapter 6, it is probable that the lack of efficacy of either inhibitor in improving joint pathology within the MIA experimental model of OA is due to a lack of optimisation of the treatment strategy.

7.4 Conclusions and future perspectives.

During the course of this thesis, we have demonstrated that the IL-1β activation of the transcription factor NFκB is involved in the expression of MMP-1, MMP-3 and IL-6. During chapter 3 we determined the importance of IL-1β and TNFα derived from synovial macrophages in the pathology of OA. The removal of synovial macrophages from the OA-COCULs highlighted their critical role in perpetuating a catabolic environment within the tissue and the

joint, however, the role of other cells implicated with the release of IL-1β and TNFα was not examined. It has been suggested that T cells have a role in the pathogenesis of OA, consequently it may prove beneficial to deplete any T cells present in OA-COCUL using antiCD3$^+$ magnetic beads to ascertain their role in driving pathology (Haynes *et al.*, 2002, Nakamura *et al.*, 1999). Whilst we examined the effect removal of synovial macrophages had upon mediator release in OA-COCUL we could have improved this study further by examining the mediators that the macrophages themselves release. Whilst it is evident that the IL-1β and TNFα they release is critical, inducing an array of cytokines, chemokines and MMPs, it would have been interesting to determine the contribution the macrophages themselves make to the levels of catabolic cytokines and MMPs within the joint. Such a study would indicate if targeting the synovial macrophages and inhibiting the cytokines and MMPs they release, could be a potential therapeutic target for further study.

The inflammation present within the synovial membrane varied markedly between OA patients, with patients falling into two major cohorts, those with an inflammatory phenotype and those exhibiting little or no inflammation within the synovial membrane. In respect of the two different groups of patients, it would be interesting to examine the patient's clinical history and compare this with their synovial membrane histology. Such a study would allow us to assess if synovial inflammation is characteristic of specific clinical features, and allow assessment of disease progression in comparison to synovial inflammation. The effect different therapeutic agents prescribed for OA had upon synovial inflammation could also be determined to assess if certain agents provided greater benefit in preventing inflammation within the

membrane. Blood samples taken from patients at the time of joint replacement surgery would have allowed us to quantify the levels of biomarkers of cartilage deterioration such as COMP, MMPs and ADAMTSs. The profiles of biomarkers of cartilage deterioration for each patient could have been compared with their synovial membrane histology to determine if there was an association between inflammation and cartilage deterioration.

Inhibition of the signalling cascade via 2 novel inhibitors of the IKK step of the pathway, suppresses NFκB activation in OA-SF. Whilst we demonstrated that NFκB activation could be prevented in response to IL-1β stimulation and that the inhibition observed was specific for the transcription factor, through the inclusion of cold competitors, we did not demonstrate experimentally the specific step in the pathway at which the two inhibitors act. Both RO100 and RO919 have been designed by Roche as inhibitors of the IKK subunit, western blotting for both the IKK1 and IKK2 proteins amongst others within the cascade would have allowed us to determine if the 2 inhibitors are IKK specific. Whilst we examined the effect the 2 inhibitors had upon early stage changes, it would be useful to determine their efficacy in preventing later stage changes, as the majority of patients with OA do not present clinically until their disease is fully established and progressing. The effect both RO100 and RO919 have upon MMP induced cartilage deterioration and the formation of VDIPEN neoepitopes could be assessed immunohistochemically. It is likely that the 2 inhibitors elicit their protective effect by preventing deterioration rather than eliciting a repair response within the cartilage, determining if the 2 inhibitors can provide any benefit in established disease would determine if they are a valid candidate for therapy.

Such encouraging results from the *in vitro* studies led to the trial of the 2 IKK inhibitors in a murine model of experimental OA. As discussed previously, the results of this pilot study demonstrated that the initial observations suggested that the 2 agents provided no clinical benefit and did not modify the structural changes associated with OA pathology. However, the *in vivo* studies have highlighted a number of issues that need resolving before a firm conclusion can be drawn regarding the efficacy of the 2 agents for the treatment. A single dose of the 2 inhibitors was selected which appeared to have no effect upon MIA induced arthritis pathology, consequently optimisation of the dose of both RO100 and RO919 is required to determine if at a greater dose, the 2 agents elicit a protective effect. Both RO100 and RO919 were developed for oral administration. It would be beneficial to dose the animals via the drinking water, to establish if the agent can elicit therapeutic benefit via oral administration. Repeated dosing of animals is a third experimental modification required, we established that a single dose of either inhibitor does not elicit a protective effect. It is probable that for the 2 agents to provide a protective effect, the activation of NFκB within the joint needs to be suppressed for the duration of the study, and as such repeated dosing of the animals is required. Whilst the animals demonstrated no observable toxic effects following intraarticular administration of either inhibitor, in future studies with repeated oral administration of the 2 inhibitors, the effect these agents had upon the animals would require closer monitoring, for example, the assessment of liver enzymes to ensure that the agents do not elicit a toxic effect *in vivo*. Such experimental modifications would allow us to determine if the two agents have any true potential to modulate OA progression, and consequently demonstrate if

the NFκB signalling cascade is a viable target for future therapeutic intervention in OA.

REFERENCES

Abramson SB, Yazici Y. Biologics in development for rheumatoid arthritis: relevance to osteoarthritis. Adv Drug Deliv Rev. 2006; **58(2)**:212-25 *(Review)*.

Adams J. Development of the proteasome inhibitor PS-341. Oncologist. 2002; **7(1)**:9-16 *(Review)*

.

Aderem A, Underhill DM. Mechanisms of phagocytosis in macrophages. Annu Rev Immunol. 1999; **17**:593-623. *(Review)*.

Aderka D, Maor Y, Novick D, Engelmann H, KahnY, Levo Y, Wallach D, Revel M. Interleukin-6 inhibits the proliferation of B-chronic lymphocytic leukemia cells that is induced by tumor necrosis factor-alpha or -beta. Blood. 1993; **81(8)**:2076 – 84

Agou F, Courtois G, Chiaravalli J, Baleux F, Coic YM, Traincard F, Israel A, Veron M. Inhibition of NF-kappa B activation by peptides targeting NF-kappa B essential modulator (nemo) oligomerization. J Biol Chem. 2004; **279(52)**:54248-57.

Aigner T, Hemmel M, Neureiter D, Gebhard PM, Zeiler G, Kirchner T, McKenna L. Apoptotic cell death is not a widespread phenomenon in normal aging and osteoarthritis human articular knee cartilage: a study of proliferation, programmed cell death (apoptosis), and viability of chondrocytes in normal and osteoarthritic human knee cartilage. Arthritis Rheum. 2001; **44(6)**:1304-12.

Aigner T, Sachse A, Gebhard PM, Roach HI. Osteoarthritis: pathobiology-targets and ways for therapeutic intervention. Adv Drug Deliv Rev. 2006; **58(2)**:128-49 *(Review)*.

Aigner T, Soeder S, Haag J. IL-1beta and BMPs--interactive players of cartilage matrix degradation and regeneration. Eur Cell Mater. 2006; **12:49**-56; discussion 56. *(Review)*.

Alaaeddine N, Olee T, Hashimoto S, Creighton-Achermann L, Lotz M. Production of the chemokine RANTES by articular chondrocytes and role in cartilage degradation. Arthritis Rheum. 2001;**44(7)**:1633 – 1643.

Alaaeddine N, Di Battista JA, Pelletier JP, Cloutier JM, Kiansa K, Dupuis M, Martel-Pelletier J. Osteoarthritic synovial fibroblasts possess an increased level of tumor necrosis factor-receptor 55 (TNF-R55) that mediates biological activation by TNF-alpha. J Rheumatol. 1997; **24(10)**:1985 – 94

Alexander HR, Billingsley KG, Block MI, Fraker DL. D-factor/leukaemia inhibitory factor: evidence for its role as a mediator in acute and chronic inflammatory disease. Cytokine. 1994; **6(6)**:589-96 *(Review)*.

Altman RD, Lozada CJ. Clinical features: Osteoarthritis and related disorders. In *Rheumatology* (Ed Hochberg MC, Silman AJ, Smolen JS, Weinblatt ME, Weisman MH). pp 1793 – 1800.Elsevier 2003.

Altman R, Asch E, Bloch D, Bole G, Borenstein D, Brandt K, Christy W, Cooke TD, Greenwald R, Hochberg M, et al. Development of criteria for the classification and reporting of osteoarthritis. Classification of osteoarthritis of the knee. Diagnostic and Therapeutic Criteria Committee of the American Rheumatism Association. Arthritis Rheum. 1986; **29(8)**:1039-49.

Ameye LG, Young MF. Animal models of osteoarthritis: lessons learned while seeking the "Holy Grail". Curr Opin Rheumatol. 2006; **18(5)**:537-47 *(Review)*.

Amos N, Lauder S, Evans A, Feldmann M, Bondeson J. Adenoviral gene transfer into osteoarthritis synovial cells using the endogenous inhibitor IkappaBalpha reveals that most, but not all, inflammatory and destructive mediators are NFkappaB dependent. Rheumatology (Oxford). 2006; **45(10)**:1201 – 9.

Anderson-MacKenzie JM, Quasnichka HL, Starr RL, Lewis EJ, Billingham ME, Bailey AJ. Fundamental subchondral bone changes in spontaneous knee osteoarthritis. Int J Biochem Cell Biol. 2005; **37(1)**:224-36.

Andersson ML, Thorstensson CA, Roos EM, Petersson IF, Heinegard D, Saxne T. Serum levels of cartilage oligomeric matrix protein (COMP) increase temporarily after physical exercise in patients with knee osteoarthritis. BMC Musculoskelet Disord. 2006;**7**:98.

Andreakos E, Smith C, Kiriakidis S, Monaco C, de Martin R, Brennan FM, Paleolog E, Feldmann M, Foxwell BM. Heterogeneous requirement of IkappaB kinase 2 for inflammatory cytokine and matrix metalloproteinase production in rheumatoid arthritis: implications for therapy. Arthritis Rheum. 2003; **48(7)**:1901-12.

Apte RN, Dotan S, Elkabets M, White MR, Reich E, Carmi Y, Song X, Dvozkin T, Krelin Y, Voronov E. The involvement of IL-1 in tumorigenesis, tumor invasiveness, metastasis and tumor-host interactions. Cancer Metastasis Rev. 2006; **25(3)**:387-408 *(Review)*.

Arai M, Anderson D, Kurdi Y, Annis-Freeman B, Shields K, Collins-Racie LA, Corcoran C, DiBlasio-Smith E, Pittman DD, Dorner AJ, Morris E, LaVallie ER. Effect of adenovirus-mediated overexpression of bovine ADAMTS-4 and human ADAMTS-5 in primary bovine articular chondrocyte pellet culture system. Osteoarthritis Cartilage. 2004; **12(8)**:599-613.

Archer CW, Francis-West P. The chondrocyte. Int J Biochem Cell Biol. 2003; **35(4)**:401-4 *(Review)*.

Arden N, Nevitt MC. Osteoarthritis: epidemiology. Best Pract Res Clin Rheumatol. 2006; **20(1)**:3-25 *(Review)*.

Arend WP, Dayer JM. Inhibition of the production and effects of interleukin-1 and tumor necrosis factor alpha in rheumatoid arthritis. Arthritis Rheum. 1995; **38(2)**:151 – 60.

Arend WP, Malyak M, Guthridge CJ, Gabay C. Interleukin-1 receptor antagonist: role in biology. Annu Rev Immunol. 1998; **16**:27-55 *(Review)*.

Arner EC, Hughes CE, Decicco CP, Caterson B, Tortorella MD. Cytokine-induced cartilage proteoglycan degradation is mediated by aggrecanase. Osteoarthritis Cartilage. 1998; **6(3)**:214-28.

Arner EC, Pratta MA, Decicco CP, Xue CB, Newton RC, Trzaskos JM, Magolda RL, Tortorella MD. Aggrecanase. A target for the design of inhibitors of cartilage degradation. Ann N Y Acad Sci. 1999; **878**:92-107.

Arner EC. Aggrecanase-mediated cartilage degradation. Curr Opin Pharmacol. 2002; **2(3)**:322-9 *(Review)*.

Athanasou NA, Quinn J. Immunocytochemical analysis of human synovial lining cells: phenotypic relation to other marrow derived cells. Ann Reum Dis. 1991; **50(5)**: 311 – 5

Baeuerle PA, Henkel T. Function and activation of NF-kappa B in the immune system. Annu Rev Immunol. 1994; **12**:141-79 *(Review)*.

Baker AH, Edwards DR, Murphy G. Metalloproteinase inhibitors: biological actions and therapeutic opportunities. J Cell Sci. 2002; **115(Pt 19)**:3719-27 *(Review)*.

Baldwin AS Jr. The NF-kappa B and I kappa B proteins: new discoveries and insights. Annu Rev Immunol. 1996;**14**: 649 – 81 *(Review)*.

Balkwill F. TNF-alpha in promotion and progression of cancer. Cancer Metastasis Rev. 2006; **25(3)**:409-16 *(Review)*.

Bansback NJ, Regier DA, Ara R, Brennan A, Shojania K, Esdaile JM, Anis AH, Marra CA. An overview of economic evaluations for drugs used in rheumatoid arthritis: focus on tumour necrosis factor-alpha antagonists. Drugs. 2005; **65(4)**:473-96 *(Review)*.

Barnett BG, Crews CJ, Douglas JT. Targeted adenoviral vectors. Biochim Biophys Acta. 2002; **1575(1-3)**:1-14 *(Review)*.

Bathon JM, Martin RW, Fleischmann RM et al. A comparison of Etanercept and Methotrexate in patients with early Rheumatoid Arthritis. New Eng J Med. 2000;**343 (22)**:1586 – 1593

Bau B, Gebhard PM, Haag J, Knorr T, Bartnik E, Aigner T. Relative messenger RNA expression profiling of collagenases and aggrecanases in human articular chondrocytes in vivo and in vitro. Arthritis Rheum. 2002; **46(10)**:2648-57.

Beinke S, Ley SC. Functions of NF-kappaB1 and NF-kappaB2 in immune cell biology. Biochem J. 2004; **382(Pt 2)**:393-409 *(Review)*.

Bell MC, Carroll GJ. Leukaemia inhibitory factor (LIF) suppresses proteoglycan synthesis in porcine and caprine cartilage explants. Cytokine. 1995;**7(2)**:137-41

Bendele A. Animal models of rheumatoid arthritis. J Musculoskelet Neuronal Interact. 2001; **1(4)**:377-85.

Benedek TG. A history of the understanding of cartilage. Osteoarthritis Cartilage. 2006; **14(3)**:203-9 *(Review)*.

Benedek TG. When did "osteo-arthritis" become osteoarthritis? J Rheumatol. 1999; **26(6)**:1374-6.

Benito MJ, Veale DJ, FitzGerald O, van den Berg WB, Bresnihan B. Synovial tissue inflammation in early and late osteoarthritis. Ann Rheum Dis. 2005; **64(9)**:1263-7.

Berenbaum F. Signaling transduction: target in osteoarthritis. Curr Opin Rheumatol. 2004; **16(5)**:616 – 622.

Billingham MEJ. Advantages afforded by the use of animal models for evaluation of potential disease modifying osteoarthritis drugs (DMOADS). In *Osteoarthritis* (ed Brandt KD, Doherty M, Lohmander LS). pp. 429 – 438. Oxford University Press 2000.

Billinghurst RC, Dahlberg L, Ionescu M, Reiner A, Bourne R, Rorabeck C, Mitchell P, Hambor J, Diekmann O, Tschesche H, Chen J, Van Wart H, Poole AR. Enhanced cleavage of type II collagen by collagenases in osteoarthritic articular cartilage. J Clin Invest. 1997; **99(7)**:1534-45.

Bingham CO 3rd, Sebba AI, Rubin BR, Ruoff GE, Kremer J, Bird S, Smugar SS, Fitzgerald BJ, O'brien K, Tershakovec AM. Efficacy and safety of etoricoxib 30 mg and celecoxib 200 mg in the treatment of osteoarthritis in two identically designed, randomized, placebo-controlled, non-inferiority studies. Rheumatology (Oxford). 2007; **46(3)**:496-507.

Birchfield PC. Osteoarthritis overview. Geriatr Nurs. 2001; **22(3)**:124-30; quiz 130-1 *(Review)*.

Black RA. Tumor necrosis factor-alpha converting enzyme. Int J Biochem Cell Biol. 2002; **34(1)**:1-5 *(Review)*.

Black RA, Kronheim SR, Cantrell M, Deeley MC, March CJ, Prickett KS, Wignall J, Conlon PJ, Cosman D, Hopp TP, Mochizuki DY. Generation of biologically active interleukin-1β by proteolytic cleavage of the inactive precursor. J Biol Chem. 1988; **263(19)**:9437 – 9442

Bobinac D, Spanjol J, Zoricic S, Maric I. Changes in articular cartilage and subchondral bone histomorphometry in osteoarthritic knee joints in humans. Bone. 2003; **32(3)**:284-90.

Bode W, Fernandez-Catalan C, Grams F, Gomis-Ruth FX, Nagase H, Tschesche H, Maskos K. Insights into MMP-TIMP interactions. Ann N Y Acad Sci. 1999; **878**:73-91 *(Review)*.

Bode W. Structural basis of matrix metalloproteinase function. Biochem Soc Symp. 2003; **(70)**:1-14 *(Review)*.

Bogoyevitch MA, Barr RK, Ketterman AJ. Peptide inhibitors of protein kinases-discovery, characterisation and use. Biochim Biophys Acta. 2005; **1754(1-2)**:79-99 *(Review)*.

Bolton MC, Dudhia J, Bayliss MT. Age-related changes in the synthesis of link protein and aggrecan in human articular cartilage: implications for aggregate stability. Biochem J. 1999; **337 (Pt 1)**:77-82.

Bonassar LJ, Sandy JD, Lark MW, Plaas AH, Frank EH, Grodzinsky AJ. Inhibition of cartilage degradation and changes in physical properties induced by IL-1beta and retinoic acid using matrix metalloproteinase inhibitors. Arch Biochem Biophys. 1997; **344(2)**:404-12.

Bonassar LJ, Stinn JL, Paguio CG, Frank EH, Moore VL, Lark MW, Sandy JD, Hollander AP, Poole AR, Grodzinsky AJ. Activation and inhibition of endogenous matrix metalloproteinases in articular cartilage: effects on composition and biophysical properties. Arch Biochem Biophys. 1996; **333(2)**:359-67.

Bondeson J, Browne KA, Brennan FM, Foxwell BM, Feldmann M. Selective regulation of cytokine induction by adenoviral gene transfer of IkappaBalpha into human macrophages: lipopolysaccharide-induced, but not zymosan-induced, proinflammatory cytokines are inhibited, but IL-10 is nuclear factor-kappaB independent. J Immunol. 1999; **162(5)**:2939-45.

Bondeson J, Foxwell B, Brennan F, Feldmann M. Defining therapeutic targets by using adenovirus: blocking NF-kappaB inhibits both inflammatory and destructive mechanisms in rheumatoid synovium but spares anti-inflammatory mediators. Proc Natl Acad Sci U S A. 1999; **96(10)**:5668-73.

Bonizzi G, Karin M. The two NF-kappaB activation pathways and their role in innate and adaptive immunity. Trends Immunol. 2004;**25(6)**:280-8. *(Review)*.

Bora FW Jr, Miller G. Joint physiology, cartilage metabolism, and the etiology of osteoarthritis. Hand Clin. 1987;**3(3)**:325-36 *(Review)*.

Bove SE, Calcaterra SL, Brooker RM, Huber CM, Guzman RE, Juneau PL, Schrier DJ, Kilgore KS. Weight bearing as a measure of disease progression and efficacy of anti-inflammatory compounds in a model of monosodium

iodoacetate-induced osteoarthritis. Osteoarthritis Cartilage. 2003; **11(11)**:821-30.

Bramono DS, Richmond JC, Weitzel PP, Kaplan DL, Altman GH. Matrix metalloproteinases and their clinical applications in orthopaedics. Clin Orthop Relat Res. 2004; **(428)**:272-85 *(Review)*.

Brandt KD, Mazzuca SA, Katz BP, Lane KA, Buckwalter KA, Yocum DE, Wolfe F, Schnitzer TJ, Moreland LW, Manzi S, Bradley JD, Sharma L, Oddis CV, Hugenberg ST, Heck LW. Effects of doxycycline on progression of osteoarthritis: results of a randomized, placebo-controlled, double-blind trial. Arthritis Rheum. 2005; **52(7)**:2015-25.

Brandt KD, Smith G, Kang SY, Myers S, O'Connor B, Albrecht M. Effects of diacerhein in an accelerated canine model of osteoarthritis. Osteoarthritis Cartilage. 1997; **5(6)**:438-49.

Brandt KD. Animal models of osteoarthritis. Biorheology. 2002; **39(1-2)**:221-35 *(Review)*.

Brennan FM, Chantry D, Jackson AM, Maini RN, Feldmann M. Cytokine production in culture by cells isolated from the synovial membrane. J Autoimmun. 1989; **2 Suppl**:177-86.

Brown PD. Ongoing trials with matrix metalloproteinase inhibitors. Expert Opin Investig Drugs. 2000; **9(9)**:2167-77.

Buckwalter, J. A., and Mankin, H. J., (1997). Instructional course lectures, the American Academy of Orthopaedic Surgeons – Articular Cartilage. Part I: tissue design and chondrocyte-matrix interactions. The Journal of Bone and Joint Surgery. **79**; 600 – 611

Buckwalter JA, Pita JC, Muller FJ, Nessler J. Structural differences between two populations of articular cartilage proteoglycan aggregates. J Orthop Res. 1994; **12(1)**: 144-8

Bullough PG. The role of joint architecture in the etiology of arthritis. Osteoarthritis Cartilage. 2004; **12 Suppl A**:S2-9 *(Review)*.

Burrage PS, Mix KS, Brinckerhoff CE. Matrix metalloproteinases: role in arthritis. Front Biosci. 2006; **11**:529-43 *(Review)*.

Calzado MA, Bacher S, Schmitz ML. NF-kappaB inhibitors for the treatment of inflammatory diseases and cancer. Curr Med Chem. 2007; **14(3)**:367-76 *(Review)*.

Carlson CS, Loeser RF, Jayo MJ, Weaver DS, Adams MR, Jerome CP. Osteoarthritis in Cynomolgue macaques: a primate model on naturally occurring disease. J Orth Res. 1994; **12**: 331 -9.

Caron JP, Fernandes JC, Martel-Pelletier J, Tardif G, Mineau F, Geng C, Pelletier JP. Chondroprotective effect of intraarticular injections of interleukin-1 receptor antagonist in experimental osteoarthritis. Suppression of collagenase-1 expression. Arthritis Rheum. 1996; **39(9)**:1535-44.

Carroll GJ, Bell MC. Leukaemia inhibitory factor stimulates proteoglycan resorption in porcine articular cartilage. Rheumatol Intl. 1993; **13(1)**:5 – 8

Carswell EA, Old LJ, Kassel RL, Green S, Fiore N, Williamson B. An endotoxin-induced serum factor that causes necrosis of tumors. Proc Natl Acad Sci USA. 1975; **72(9)**:3666 - 70

Caterson B, Flannery CR, Hughes CE, Little CB. Mechanisms involved in cartilage proteoglycan catabolism. Matrix Biol. 2000; **19(4)**:333-44 *(Review)*.

Chabaud M, Garnero P, Dayer JM, Guerne PA, Fossiez F, Miossec P. Contribution of interleukin 17 to synovium matrix destruction in rheumatoid arthritis. Cytokine. 2000; **12(7)**:1092 – 9.

Chakraborti S, Mandal M, Das S, Mandal A, Chakraborti T. Regulation of matrix metalloproteinases: an overview. Mol Cell Biochem. 2003; **253(1-2)**:269-85 *(Review)*.

Chan PS, Caron JP, Orth MW. Short-term gene expression changes in cartilage explants stimulated with interleukin beta plus glucosamine and chondroitin sulfate. J Rheumatol. 2006; **33(7)**:1329-40.

Chevalier X, Giraudeau B, Conrozier T, Marliere J, Kiefer P, Goupille P. Safety study of intraarticular injection of interleukin 1 receptor antagonist in patients with painful knee osteoarthritis: a multicenter study. J Rheumatol. 2005; **32(7)**:1317-23.

Chroboczek J, Bieber F, Jacrot B. The sequence of the genome of adenovirus type 5 and its comparison with the genome of adenovirus type 2. Virology. 1992; **186(1)**:280-5.

Clark JM, Huber JD. The structure of the human subchondral plate. J Bone Joint Surg Br. 1990; **72(5)**:866-73.

Clark JM. The organisation of collagen fibrils in the superficial zones of articular cartilage. J Anat. 1990; **171**:117-30.

Clarke IC. Articular cartilage: a review and scanning electron microscope study. 1. The interterritorial fibrillar architecture. J Bone Joint Surg Br. 1971; **53(4)**:732-50.

Cooper C, Egger P, Coggon D, Hart DJ, Masud T, Cicuttini F, Doyle DV, Spector TD. Generalized osteoarthritis in women: pattern of joint involvement and approaches to definition for epidemiological studies. J Rheumatol. 1996; **23(11)**: 1938 – 42

Cooper C, Cushnaghan J, Kirwan JR, Dieppe PA, Rogers J, McAlindon T, McCrae F. Radiographic assessment of the knee joint in osteoarthritis. Ann Rheum Dis. 1992; **51(3)**:80 – 2

Das S, Mandal M, Chakraborti T, Mandal A, Chakraborti S. Structure and evolutionary aspects of matrix metalloproteinases: a brief overview. Mol Cell Biochem. 2003; **253(1-2)**:31-40 *(Review)*.

de Hooge AS, van de Loo FA, Arntz OJ, van den Berg WB. Involvement of IL-6, apart from its role in immunity, in mediating a chronic response during experimental arthritis. Am J Pathol. 2000; **157(6)**:2081 – 91

de Hooge AS, van de Loo FA, Bennik MB, Arntz OJ, de Hooge P, van den Berg WB. Male IL-6 gene knock out mice developed more advanced osteoarthritis upon aging. Osteoarthritis Cartilage. 2005; **13(1)**:66 -73.

Desgeorges A, Gabay C, Silacci P, Novick D, Roux-Lombard P, Grau G, Dayer JM, Vischer T, Guerne PA. Concentrations and origins of soluble interleukin 6 receptor-alpha in serum and synovial fluid. J Rheumatol. 1997; **24(8)**:1510 – 6

Dignam JD, Lebovitz RM, Roeder AG. Accurate transcription initiation by RNA polymerase II in a soluble extract from isolated mammalian nuclei. Nuc Acid Res. 1983;**11(5)**: 1475 – 89.

Dinarello CA. Biologic basis for interleukin-1 in disease. Blood. 1996; **87(6)**:2095-147. *(Review)*.

Dinarello CA. The interleukin-1 family: 10 years of discovery. FASEB J. 1994; **8(15)**:1314-25 *(Review)*.

Dingle JT, SaklatvalaJ, Hembry R, Tyler J, Fell HB, JubbR. A cartilage catabolic factor from synovium. Biochem J. 1979; **184(1)**:177-80.

Distler J, Anguelouch A. Evidence-based practice: review of clinical evidence on the efficacy of glucosamine and chondroitin in the treatment of osteoarthritis. J Am Acad Nurse Pract. 2006; **18(10)**:487-93 *(Review)*.

Doege K, Sasaki M, Yamada Y. Related Articles, Links Rat and human cartilage proteoglycan (aggrecan) gene structure. Biochem Soc Trans. 1990; **18(2)**:200-2.

Doege KJ, Sasaki M, Kimura T, Yamada Y. Complete coding sequence and deduced primary structure of the human cartilage large aggregating proteoglycan, aggrecan. Human-specific repeats, and additional alternatively spliced forms. J Biol Chem. 1991; **266(2)**:894-902.

Domagala F, Martin G, Bogdanowicz P, Ficheux H, Pujol JP. Inhibition of interleukin-1beta-induced activation of MEK/ERK pathway and DNA binding

of NF-kappaB and AP-1: potential mechanism for Diacerein effects in osteoarthritis. Biorheology. 2006; **43(3-4)**:577-87.

Domowicz MS, Pirok EW 3rd, Novak TE, Schwartz NB. Role of the C-terminal G3 domain in sorting and secretion of aggrecan core protein and ubiquitin-mediated degradation of accumulated mutant precursors. J Biol Chem. 2000; **275(45)**:35098-105.

Dougados M, Nguyen M, Berdah L, Mazieres B, Vignon E, Lequesne M; ECHODIAH Investigators Study Group. Evaluation of the structure-modifying effects of diacerein in hip osteoarthritis: ECHODIAH, a three-year, placebo-controlled trial. Evaluation of the Chondromodulating Effect of Diacerein in OA of the Hip. Arthritis Rheum. 2001; **44(11)**:2539-47.

Dreier R, Grassel S, Fuchs S, Schaumburger J, Bruckner P. Pro-MMP-9 is a specific macrophage product and is activated by osteoarthritic chondrocytes via MMP-3 or a MT1-MMP/MMP-13 cascade. Exp Cell Res. 2004; **297(2)**:303-12.

Dudhia J, Davidson CM, Wells TM, Vynios DH, Hardingham TE, Bayliss MT. Age-related changes in the content of the C-terminal region of aggrecan in human articular cartilage. Biochem J. 1996; **313 (Pt 3)**:933-40.

Dudhia J. Aggrecan, aging and assembly in articular cartilage. Cell Mol Life Sci. 2005; **62(19-20)**:2241-56 *(Review)*.

Duffy MJ, Lynn DJ, Lloyd AT, O'Shea CM. The ADAMs family of proteins: from basic studies to potential clinical applications. Thromb Haemost. 2003; **89(4)**:622-31 *(Review)*.

Dunham J, Hoedt-Schmidt S, Kalbhen DA. Prolonged effect of iodoacetate on articular cartilage and its modification by an anti-rheumatic drug. Int J Exp Pathol. 1993; **74(3)**:283-9.

Dunham J, Hoedt-Schmidt S, Kalbhen DA. Structural and metabolic changes in articular cartilage induced by iodoacetate. Int J Exp Pathol. 1992; **73(4)**:455-64.

Eckstein F, Milz S, Anetzberger H, Putz R. Thickness of the subchondral mineralised tissue zone (SMZ) in normal male and female and pathological human patellae. J Anat. 1998; **192**: 81 – 90.

Eckstein F, Muller-Gerbl M, Putz R. Distribution of subchondral bone density and cartilage thickness in the human patella. J Anat. 1992; **180**: 425 - 33

Edwards JC. Synovial intimal fibroblasts. Ann Rheum Dis. 1995; **54(5)**:395-7 *(Review)*.

Edwards JC. The nature and origins of synovium: experimental approaches to the study of synoviocyte differentiation. J Anat. 1994; **184 (Pt 3)**:493-501 *(Review)*.

Edwards JC. The origin of type A synovial lining cells. Immunobiology. 1982; **161(3-4)**:227 – 31.

Edwards JC. Synovial physiology in the context of osteoarthritis. In *Osteoarthritis* (ed Brandt KD, Doherty M, Lohmander LS). pp. 167 – 175. Oxford University Press 2000.

Ehrlich GE. Osteoarthritis beginning with inflammation. Definitions and correlations. JAMA. 1975; **232(2)**:157-9.

Eyre D. Collagen of articular cartilage. Arthritis Res. 2002; **4(1)**:30-5 *(Review)*.

Eyre DR, Weis MA, Wu JJ. Articular cartilage collagen: an irreplaceable framework? Eur Cell Mater. 2006; **12**:57-63 *(Review)*.

Eyre DR, McDevitt CA, Billingham ME, Muir H. Biosynthesis of collagen and other matrix proteins by articular cartilage in experimental osteoarthrosis. Biochem J. 1980; **188(3)**: 823 - 37

Fantini MC, Becker C, Kiesslich R, Neurath MF. Drug insight: novel small molecules and drugs for immunosuppression. Nat Clin Pract Gastroenterol Hepatol. 2006; **3(11)**:633-44 *(Review)*.

Farahat MN, Yanni G, Poston R, Panayi GS. Cytokine expression in synovial membranes of patients with rheumatoid arthritis and osteoarthritis. Ann Rheum Dis. 1993; **52(12)**:870-5.

Fell HB, Jubb RW. The effect of synovial tissue on the breakdown of articular cartilage in organ culture. Arthritis Rheum. 1977; **20(7)**:1359 – 71.

Fenton MJ, Vermeulen MW, Clark BD, Webb AC, Auron PE. Human pro-IL-1 beta gene expression in monocytic cells is regulated by two distinct pathways. J Immunol. 1988; **140(7)**:2267 -73

Fernandes JC, Martel-Pelletier J, Lascau-Coman V, Moldovan F, Jovanovic D, Raynauld JP, Pelletier JP. Collagenase-1 and collagenase-3 synthesis in normal and early experimental osteoarthritic canine cartilage: an immunohistochemical study. J Rheumatol. 1998; **25(8)**:1585-94.

Fernandes JC, Martel-Pelletier J, Pelletier JP. The role of cytokines in osteoarthritis pathophysiology. Biorheology. 2002; **39(1-2)**:237-46 *(Review)*.

Fernihough J, Gentry C, Malcangio M, Fox A, Rediske J, Pellas T, Kidd B, Bevan S, Winter J. Pain related behaviour in two models of osteoarthritis in the rat knee. Pain. 2004; **112(1-2)**:83-93.

Fidelix TS, Soares BG, Trevisani VF. Diacerein for osteoarthritis. Cochrane Database Syst Rev. 2006; **(1)**:CD005117. *(Review)*.

Fiers W. Tumor necrosis factor. Characterization at the molecular, cellular and in vivo level. FEBS Lett. 1991; **285(2)**:199-212 *(Review)*

Fiorito S, Magrini L, Adrey J, Mailhe D, Brouty-Boye D. Inflammatory status and cartilage regenerative potential of synovial fibroblasts from patients with chondropathy. Rheumatology. 2005;**44(2)**:164 – 171.

Fischer PM. The design of drug candidate molecules as selective inhibitors of therapeutically relevant protein kinases. Curr Med Chem. 2004; **11(12)**:1563-83 *(Review)*.

Flotte TR. Gene therapy for cystic fibrosis. Curr Opin Mol Ther. 1999; **1(4)**:510-6. *(Review)*.

Forsyth CB, Cole A, Murphy G, Bienias JL, Im HJ, Loeser RF Jr. Increased matrix metalloproteinase-13 production with aging by human articular chondrocytes in response to catabolic stimuli. J Gerontol A Biol Sci Med Sci. 2005;**60(9)**:1118-24.

Fosang AJ, Last K, Maciewicz RA. Aggrecan is degraded by matrix metalloproteinases in human arthritis. Evidence that matrix metalloproteinase and aggrecanase activities can be independent. J Clin Invest. 1996; 98(10):2292-9.

Fosang AJ, Last K, Stanton H, Weeks DB, Campbell IK, Hardingham TE, Hembry RM. Generation and novel distribution of matrix metalloproteinase-derived aggrecan fragments in porcine cartilage explants. J Biol Chem. 2000; **275(42)**:33027-37.

Foxwell B, Browne K, Bondeson J, Clarke C, de Martin R, Brennan F, Feldmann M. Efficient adenoviral infection with IkappaB alpha reveals that macrophage tumor necrosis factor alpha production in rheumatoid arthritis is NF-kappaB dependent. Proc Natl Acad Sci U S A. 1998; **95(14)**:8211-5.

Foxwell BM, Yoshimura S, Bondeson J, Brennan FM, Feldmann M. High efficiency gene transfer is an efficient way of defining therapeutic targets: a functional genomics approach. Ann Rheum Dis. 2001; **60 Suppl 3:iii13-7**.

Fraser CC. Exploring the positive and negative consequences of NF-kappaB inhibition for the treatment of human disease. Cell Cycle. 2006; **5(11)**:1160-3 *(Review)*.

Friedman JM, Horwitz MS. Inhibition of tumor necrosis factor alpha-induced NF-kappa B activation by the adenovirus E3-10.4/14.5K complex. J Virol. 2002; **76(11)**:5515-21.

Furst DE, Breedveld FC, Kalden JR, Smolen JS, Burmester GR, Bijlsma JW, Dougados M, Emery P, Keystone EC, Klareskog L, Mease PJ. Updated consensus statement on biological agents, specifically tumour necrosis factor {alpha} (TNF{alpha}) blocking agents and interleukin-1 receptor antagonist

(IL-1ra), for the treatment of rheumatic diseases, 2005. Ann Rheum Dis. 2005; **64 Suppl 4**:iv2-14. *(Review)*.

Gadek TR, Nicholas JB. Small molecule antagonists of proteins. Biochem Pharmacol. 2003; **65(1)**:1-8 *(Review)*.

Ghosh S, May MJ, Kopp EB. NF-kappa B and Rel proteins: evolutionarily conserved mediators of immune responses. Annu Rev Immunol. 1998; **16**:225-60 *(Review)*.

Gill GS, Joshi AB, Mills DM. Total condylar knee arthroplasty. 16- to 21-year results. Clin Orthop Relat Res. 1999; **(367)**:210-5.

Glick BR, Pasternack JJ. Human Gene Therapy. In Molecular Biotechnology 2nd Edition. pp 555 – 90. American Society for Microbiology 1998

Goldenberg DL, Egan MS, Cohen AS. Inflammatory synovitis in degenerative joint disease. J Rheumatol. 1982; **9(2)**:204-9.

Goldring MB, Berenbaum F. The regulation of chondrocyte function by proinflammatory mediators: prostaglandins and nitric oxide. Clin Orthop Relat Res. 2004; **(427 Suppl)**:S37-46 *(Review)*.

Goldring MB, Birkhead J, Sandell LJ, Kimura T, Krane SM. Interleukin 1 suppresses expression of cartilage-specific types II and IX collagens and increases types I and III collagens in human chondrocytes. J Clin Invest. 1988; **82(6)**:2026-37.

Goldring MB. The role of cytokines as inflammatory mediators in osteoarthritis: lessons from animal models. Connect Tissue Res. 1999; **40(1)**:1-11 *(Review)*.

Goldring SR, Goldring MB. The role of cytokines in cartilage matrix degeneration in osteoarthritis. Clin Orthop Relat Res. 2004; **(427 Suppl)**:S27-36 *(Review)*.

Goncalves MA, de Vries AA. Adenovirus: from foe to friend. Rev Med Virol. 2006; **16(3)**:167-86 *(Review)*.

Gorziglia MI, Lapcevich C, Roy S, Kang Q, Kadan M, Wu V, Pechan P, Kaleko M. Generation of an adenovirus vector lacking E1, e2a, E3, and all of E4 except open reading frame 3. J Virol. 1999; **73(7)**:6048-55.

Grabowski PS, Wright PK, Van t'Hof RJ, Helfrich MH, Ohshima H, Ralston SH. Immunolocalization of inducible nitric oxide synthase in synovium and cartilage in rheumatoid arthritis and osteoarthritis. Br J Rheumatol. 1997; **36(6)**: 651 – 5.

Graham FL, Prevec L. Methods for construction of adenovirus vectors. Mol Biotechnol. 1995; **3(3)**:207-20.

Graham FL, Smiley J, Russell WC, Nairn R. Characteristics of a human cell line transformed by DNA from human adenovirus type 5. J Gen Virol. 1977; **36(1)**:59-74.

Grushko G, Schneiderman R, Maroudas A. Some biochemical and biophysical parameters for the study of the pathogenesis of osteoarthritis: a comparison between the processes of ageing and degeneration in human hip cartilage. Connect Tissue Res. 1989; **19(2-4)**:149-76.

Guingamp C, Gegout-Pottie P, Philippe L, Terlain B, Netter P, Gillet P. Mono-iodoacetate-induced experimental osteoarthritis: a dose-response study of loss of mobility, morphology, and biochemistry. Arthritis Rheum. 1997; **40(9)**:1670-9.

Gunja-Smith Z, Nagase H, Woessner JF Jr. Purification of the neutral proteoglycan-degrading metalloproteinase from human articular cartilage tissue and its identification as stromelysin matrix metalloproteinase-3. Biochem J. 1989; **258(1)**:115-9.

Guzman RE, Evans MG, Bove S, Morenko B, Kilgore K. Mono-iodoacetate-induced histologic changes in subchondral bone and articular cartilage of rat femorotibial joints: an animal model of osteoarthritis. Toxicol Pathol. 2003; **31(6)**:619-24.

Hascall VC, Heinegard D. Aggregation of cartilage proteoglycans. I. The role of hyaluronic acid. J Biol Chem. 1974; **249(13)**:4232-41.

Hayami T, Pickarski M, Zhuo Y, Wesolowski GA, Rodan GA, Duong le T. Characterization of articular cartilage and subchondral bone changes in the rat anterior cruciate ligament transection and meniscectomized models of osteoarthritis. Bone. 2006; **38(2)**:234-43.

Hayden MS, Ghosh S. Signaling to NF-kappaB. Genes Dev. 2004; **18(18)**:2195-224 *(Review)*.

Haynes MK, Hume EL, Smith JB. Phenotypic characterization of inflammatory cells from osteoarthritic synovium and synovial fluids. Clin Immunol. 2002; **105(3)**:315-25.

He TC, Zhou S, da Costa LT, Yu J, Kinzler KW, Vogelstein B. A simplified system for generating recombinant adenoviruses. Proc Natl Acad Sci U S A. 1998; **95(5)**:2509-14.

Helminen HJ, Saamanen AM, Salminen H, Hyttinen MM. Transgenic mouse models for studying the role of cartilage macromolecules in osteoarthritis. Rheumatology (Oxford). 2002; **41(8)**:848-56 *(Review)*.

Hemmings FJ, Farhan M, Rowland J, Banken L, Jain R. Tolerability and pharmacokinetics of the collagenase-selective inhibitor Trocade in patients with rheumatoid arthritis. Rheumatology (Oxford). 2001; **40(5)**:537-43.

Hill CL, Gale DG, Chaisson CE, Skinner K, Kazis L, Gale ME, Felson DT. Knee effusions, popliteal cysts, and synovial thickening: association with knee pain in osteoarthritis. J Rheumatol. 2001; **28(6)**:1330-7.

Hirota K, Akahoshi T, Endo H, Kondo H, Kashiwazaki S. Production of interleukin 8 by cultured synovial cells in response to interleukin 1 and tumor necrosis factor. Rheumatol Intl. 1992; **12(1)**:13 -6

Hirsh MJ, Lozada CJ. Medical management of osteoarthritis. Hospital Physcian. 2002;**57-66**.

Hollander AP, Heathfield TF, Webber C, Iwata Y, Bourne R, Rorabeck C, Poole AR. Increased damage to type II collagen in osteoarthritic articular cartilage detected by a new immunoassay. J Clin Invest. 1994; **94(3)**: 1722 – 32

Hopkins SJ, Humphreys M, Jayson MI. Cytokines in synovial fluid. I. The presence of biologically active and immunoreactive IL-1. Clin Exp Immunol. 1988; **72(3)**:422-7.

Hu K, Xu L, Cao L, Flahiff CM, Brussiau J, Ho K, Setton LA, Youn I, Guilak F, Olsen BR, Li Y. Pathogenesis of osteoarthritis-like changes in the joints of mice deficient in type IX collagen. Arthritis Rheum. 2006; **54(9)**:2891-900.

Huang W, Li WQ, Dehnade F, Zafarullah M. Tissue inhibitor of metalloproteinases-4 (TIMP-4) gene expression is increased in human osteoarthritic femoral head cartilage. J Cell Biochem. 2002; **85(2)**:295-303.

Hughes LC, Archer CW, ap Gwynn I. The ultrastructure of mouse articular cartilage: collagen orientation and implications for tissue functionality. A polarised light and scanning electron microscope study and review. Eur Cell Mater. 2005; **9**:68-84.

Hui W, Cawston T, Rowan AD. Transforming growth factor beta 1 and insulin-like growth factor 1 block collagen degradation induced by oncostatin M in combination with tumour necrosis factor alpha from bovine cartilage. Ann Rheum Dis. 2003; **62(2)**:172-4.

Hui W, Rowan AD, Cawston T. Insulin-like growth factor 1 blocks collagen release and down regulates matrix metalloproteinase-1, -3, -8, and -13 mRNA expression in bovine nasal cartilage stimulated with oncostatin M in combination with interleukin 1alpha. Ann Rheum Dis. 2001; **60(3)**:254-61.

Hui W, Rowan AD, Cawston T. Modulation of the expression of matrix metalloproteinase and tissue inhibitors of metalloproteinases by TGF-beta1 and IGF-1 in primary human articular and bovine nasal chondrocytes stimulated with TNF-alpha. Cytokine. 2001; **16(1)**:31-5.

Hui W, Rowan AD, Richards CD, Cawston TE. Oncostatin M in combination with tumor necrosis factor alpha induces cartilage damage and matrix metalloproteinase expression in vitro and in vivo. Arthritis Rheum. 2003; **48(12)**:3404-18.

Idriss HT, Naismith JH. TNF alpha and the TNF receptor superfamily: structure-function relationship(s). Microsc Res Tech. 2000; **50(3)**:184-95 *(Review)*.

Irlenbusch U, Schaller T. Investigations in generalized osteoarthritis. Part 1: genetic study of Heberden's nodes. Osteoarthritis Cartilage. 2006; **14(5)**:423-7.

Ito A, Mukaiyama A, Itoh Y, Nagase H, Thogersen IB, Enghild JJ, Sasaguri Y, Mori Y. Degradation of interleukin 1beta by matrix metalloproteinases. J Biol Chem. 1996; **271(25)**:14657-60.

Ivanavicius SP, Ball AD, Heapy CG, Westwood FR, Murray F, Read SJ. Structural pathology in a rodent model of osteoarthritis is associated with neuropathic pain: increased expression of ATF-3 and pharmacological characterisation. Pain. 2007; **128(3)**:272-82.

Iwanaga T, Shikichi M, Kitamura H, Yanase H, Nozawa-Inoue K. Morphology and functional roles of synoviocytes in the joint. Arch Histol Cytol. 2000; **63(1)**:17-31 *(Review)*.

Izmailova ES, Paz N, Alencar H, Chun M, Schopf L, Hepperle M, Lane JH, Harriman G, Xu Y, Ocain T, Weissleder R, Mahmood U, Healy AM, Jaffee B. Use of molecular imaging to quantify response to IKK-2 inhibitor treatment in murine arthritis. Arthritis Rheum. 2007; **56(1)**:117-28.

Ji L, Bouvet M, Price RE, Roth JA, Fang B. Reduced toxicity, attenuated immunogenicity and efficient mediation of human p53 gene expression in vivo by an adenovirus vector with deleted E1-E3 and inactivated E4 by GAL4-TATA promoter replacement. Gene Ther. 1999; **6(3)**:393-402.

Jones GC, Riley GP. ADAMTS proteinases: a multi-domain, multi-functional family with roles in extracellular matrix turnover and arthritis. Arthritis Res Ther. 2005; **7(4)**:160-9 *(Review)*.

Jones EY, Stuart DI, Walker NPC. Struture of tumour necrosis factor. Nature. 1989; **389**: 225 – 228

Joseph PM, O'Sullivan BP, Lapey A, Dorkin H, Oren J, Balfour R, Perricone MA, Rosenberg M, Wadsworth SC, Smith AE, St George JA, Meeker DP. Aerosol and lobar administration of a recombinant adenovirus to individuals with cystic fibrosis. I. Methods, safety, and clinical implications. Hum Gene Ther. 2001; **12(11)**:1369-82.

Kaab MJ, Gwynn IA, Notzli HP. Collagen fibre arrangement in the tibial plateau articular cartilage of man and other mammalian species. J Anat. 1998; **193 (Pt 1)**:23-34.

Kalbhen DA. Chemical model of osteoarthritis--a pharmacological evaluation. J Rheumatol. 1987; **14 Spec No**:130-1.

Kallen KJ. The role of transsignalling via the agonistic soluble IL-6 receptor in human diseases. Biochim Biophys Acta. 2002; **1592(3)**:323-43 *(Review)*.

Kamekura S, Hoshi K, Shimoaka T, Chung U, Chikuda H, Yamada T, Uchida M, Ogata N, Seichi A, Nakamura K, Kawaguchi H. Osteoarthritis development in novel experimental mouse models induced by knee joint instability. Osteoarthritis Cartilage. 2005; **13(7)**:632-41.

Karin M, Yamamoto Y, Wang QM. The IKK NF-kappa B system: a treasure trove for drug development. Nat Rev Drug Discov. 2004; **3(1)**:17-26 *(Review)*.

Karin M, Ben-Neriah Y. Phosphorylation meets ubiquitination: the control of NF-[kappa]B activity. Annu Rev Immunol. 2000; **18**:621 – 663.

Kellgren JH, Lawrence JS. Osteo-arthrosis and disk degeneration in an urban population. Ann Rheum Dis. 1958; **17(4)**:388-97.

Keravala A, Lechman ER, Nash J, Mi Z, Robbins PD. Human, viral or mutant human IL-10 expressed after local adenovirus-mediated gene transfer are equally effective in ameliorating disease pathology in a rabbit knee model of antigen-induced arthritis. Arthritis Res Ther. 2006; **8(4)**:R91.

Kersting UG, Stubendorff JJ, Schmidt MC, Bruggemann GP. Changes in knee cartilage volume and serum COMP concentration after running exercise. Osteoarthritis Cartilage. 2005; **13(10)**:925-34.

Kishimoto T, Taga T, Akira S. Cytokine signal transduction. 1994; **76(2)**:253 – 62

Klareskog L, van der Heijde D, de Jager JP et al. Therapeutic effect of the combination of etanercept and methtrexate compared with each treatment alone in patients with rheumatoid arthritis: double blind randomised controlled trial. Lancet 2004;**363**:675 – 81

Knudson CB, Knudson W. Cartilage proteoglycans. Semin Cell Dev Biol. 2001; **12(2)**:69-78 *(Review)*.

Kobayashi K, Imaizumi R, Sumichika H, Tanaka H, Goda M, Fukunari A, Komatsu H. Sodium iodoacetate-induced experimental osteoarthritis and associated pain model in rats. J Vet Med Sci. 2003; **65(11)**:1195-9.

Kobayashi M, Squires GR, Mousa A, Tanzer M, Zukor DJ, Antoniou J, Feige U, Poole AR. Role of interleukin-1 and tumor necrosis factor alpha in matrix

degradation of human osteoarthritic cartilage. Arthritis Rheum. 2005; **52(1)**:128-35.

Kontogiorgis CA, Papaioannou P, Hadjipavlou-Litina DJ. Matrix metalloproteinase inhibitors: a review on pharmacophore mapping and (Q)SARs results. Curr Med Chem. 2005; **12(3)**:339-55 *(Review)*.

Kopp E, Ghosh S. Inhibition of NF-kappa B by sodium salicylate and aspirin. Science. 1994; **265(5174)**:956-9.

Kozaci DL, Oktay G. et al. Effects of Interleukin 1 (IL-1) induced matrix breakdown on chondrocyte morphology in bovine nasal cartilage explants. Turk J Vet Anim Sci. 2005;**29**:951-7.

Kurtovic J, Segal I. Recent advances in biological therapy for inflammatory bowel disease. Trop Gastroenterol. 2004; **25(1)**:9 – 14.

Labeta MO, Durieux JJ, Spagnoli G, Fernandez N, Wijdenes J, Herrmann R. CD14 and tolerance to lipopolysaccharide: biochemical and functional analysis. Immunology. 1993; **80(3)**:415-23.

Lajeunesse D. The role of bone in the treatment of osteoarthritis. Osteoarthritis Cartilage. 2004; **12 Suppl A**:S34-8 *(Review)*.

Largo R, Alvarez-Soria MA, Diez-Ortego I, Calvo E, Sanchez-Pernaute O, Egido J, Herrero-Beaumont G. Glucosamine inhibits IL-1beta-induced NFkappaB activation in human osteoarthritic chondrocytes. Osteoarthritis Cartilage. 2003; **11(4)**:290-8.

Lark MW, Bayne EK, Flanagan J, Harper CF, Hoerrner LA, Hutchinson NI, Singer II, Donatelli SA, Weidner JR, Williams HR, Mumford RA, Lohmander LS. Aggrecan degradation in human cartilage. Evidence for both matrix metalloproteinase and aggrecanase activity in normal, osteoarthritic, and rheumatoid joints. J Clin Invest. 1997; **100(1)**:93-106.

Larsson E, Erlandsson Harris H, Lorentzen JC, Larsson A, Mansson B, Klareskog L, Saxne T. Serum concentrations of cartilage oligomeric matrix protein, fibrinogen and hyaluronan distinguish inflammation and cartilage destruction in experimental arthritis in rats. Rheumatology (Oxford). 2002; **41(9)**:996-1000.

Last RJ. Some anatomical details of the knee joint. J Bone Joint Surg. 1948; **30B**:683-8.

Lechman ER, Jaffurs D, Ghivizzani SC, Gambotto A, Kovesdi I, Mi Z, Evans CH, Robbins PD. Direct adenoviral gene transfer of viral IL-10 to rabbit knees with experimental arthritis ameliorates disease in both injected and contralateral control knees. J Immunol. 1999; **163(4)**:2202-8.

Leeman MF, Curran S, Murray GI. The structure, regulation, and function of human matrix metalloproteinase-13. Crit Rev Biochem Mol Biol. 2002; **37(3)**:149-66. *(Review)*.

Leff RL, Elias I, Ionescu M, Reiner A, Poole AR. Molecular changes in human osteoarthritic cartilage after 3 weeks of oral administration of BAY 12-9566, a matrix metalloproteinase inhibitor. J Rheumatol. 2003; **30(3)**:544 – 9.

Lemaitre V, D'Armiento J. Matrix metalloproteinases in development and disease. Birth Defects Res C Embryo Today. 2006; **78(1)**:1-10 *(Review)*.

Leutert G. Morphological aging changes in human articular cartilage. Mech Ageing Dev. 1980; **14(3-4)**:469-75.

Lewis EJ, Bishop J, Bottomley KM, Bradshaw D, Brewster M, Broadhurst MJ, Brown PA, Budd JM, Elliott L, Greenham AK, Johnson WH, Nixon JS, Rose F, Sutton B, Wilson K. Ro 32-3555, an orally active collagenase inhibitor, prevents cartilage breakdown in vitro and in vivo. Br J Pharmacol. 1997; **121(3)**:540-6.

Li Q, Lu Q, Bottero V, Estepa G, Morrison L, Mercurio F, Verma IM. Enhanced NF-kappaB activation and cellular function in macrophages lacking IkappaB kinase 1 (IKK1). Proc Natl Acad Sci U S A. 2005; **102(35)**:12425-30.

Liang KC, Lee CW, Lin WN, Lin CC, Wu CB, Luo SF, Yang CM. Interleukin-1beta induces MMP-9 expression via p42/p44 MAPK, p38 MAPK, JNK, and nuclear factor-kappaB signaling pathways in human tracheal smooth muscle cells. J Cell Physiol. 2007; **211(3)**:759 – 70

Lin CW, Phillips SL, Brinckerhoff CE, Georgescu HI, Bandara G, Evans CH. Induction of collagenase mRNA in lapine articular chondrocytes by synovial factors and interleukin-1. Arch Biochem Biophys. 1988;**264(1)**:351 – 4.

Lindau T, Adlercreutz C, Aspenberg P. Cartilage injuries in distal radial fractures. Acta Orthop Scand. 2003; **74(3)**:327-31.

Lindblad S, Hedfors E. Arthroscopic and immunohistologic characterization of knee joint synovitis in osteoarthritis. Arthritis Rheum. 1987; **30(10)**:1081-8.

Lindblad S, Hedfors E. The synovial membrane of healthy individuals--immunohistochemical overlap with synovitis. Clin Exp Immunol. 1987; **69(1)**:41-7.

Lindsey ML. Novel strategies to delineate matrix metalloproteinase (MMP)-substrate relationships and identify targets to block MMP activity. Mini Rev Med Chem. 2006; **6(11)**:1243-8 *(Review)*.

Little CB, Flannery CR, Hughes CE, Mort JS, Roughley PJ, Dent C, Caterson B. Aggrecanase versus matrix metalloproteinases in the catabolism of the interglobular domain of aggrecan in vitro. Biochem J. 1999; **344 Pt 1**:61-8.

Little CB, Hughes CE, Curtis CL, Janusz MJ, Bohne R, Wang-Weigand S, Taiwo YO, Mitchell PG, Otterness IG, Flannery CR, Caterson B. Matrix metalloproteinases are involved in C-terminal and interglobular domain processing of cartilage aggrecan in late stage cartilage degradation. Matrix Biol. 2002; **21(3)**:271-88.

Lorenz H, Richter W. Osteoarthritis: cellular and molecular changes in degenerating cartilage. Prog Histochem Cytochem. 2006; **40(3)**:135-63 *(Review)*.

Lotz M, Moats T, Villiger PM. Leukemia inhibitory factor is expressed in cartilage and synovium and can contribute to the pathogenesis of arthritis. J Clin Invest. 1992; **90(3)**:888 – 96

Lozada CJ, Altman RD. Management of limb joint osteoarthritis: Osteoarthritis and related disorders. In *Rheumatology* (Ed Hochberg MC, Silman AJ, Smolen JS, Weinblatt ME, Weisman MH). pp 1853 – 1862.Elsevier 2003.

Lusky M, Christ M, Rittner K, Dieterle A, Dreyer D, Mourot B, Schultz H, Stoeckel F, Pavirani A, Mehtali M. In vitro and in vivo biology of recombinant adenovirus vectors with E1, E1/E2A, or E1/E4 deleted. J Virol. 1998; **72(3)**:2022-32.

Lust G, Pronsky W, Sherman DM. Biochemical and ultrastructural observations in normal and degenerative canine articular cartilage. Am J Vet Res. 1972; **33(12)**:2429 – 40

Ma Y, Thornton S, Duwel LE, Boivin GP, Giannini EH, Leiden JM, Bluestone JA, Hirsch R. Inhibition of collagen-induced arthritis in mice by viral IL-10 gene transfer. J Immunol. 1998; **161(3)**:1516-24.

Malemud CJ, Islam N, Haqqi TM. Pathophysiological mechanisms in osteoarthritis lead to novel therapeutic strategies. Cells Tissues Organs. 2003; **174(1-2)**:34-48 *(Review)*.

Malemud CJ. Cytokines as therapeutic targets for osteoarthritis. BioDrugs. 2004; **18(1)**:23-35 *(Review)*.

Mankin HJ, Lippiello L. Biochemical and metabolic abnormalities in articular cartilage from osteo-arthritic human hips. J Bone Joint Surg Am. 1970; **52(3)**:424-34.

Mankin HJ, JohnsonME, Lippiello L. Biochemical and metabolic abnormalities in articular cartilage from osteoarthritic human hips. III. Distribution and metabolism of amino sugar-containing macromolecules. J Bone Joint Surg Am. 1981; **63(1)**: 131 – 9

March CJ, Mosley B, Larsen A, Cerretti DP, Braedt G, Price V, Gillis S, Henney CS, Kronheim SR, Grabstein K, et al. Cloning, sequence and expression of two

distinct human interleukin-1 complementary DNAs. Nature. 1985; **315(6021)**:641-7.

Marles PJ, Hoyland JA, Parkinson R, Freemont AJ. Demonstration of variation in chondrocyte activity in different zones of articular cartilage: an assessment of the value of in-situ hybridization. Int J Exp Pathol. 1991; **72(2)**:171-82.

Marshall KW, Chan AD. Bilateral canine model of osteoarthritis. J Rheumatol. 1996; **23(2)**:344-50.

Martel-Pelletier J, Alaaeddine N, Pelletier JP. Cytokines and their role in the pathophysiology of osteoarthritis. Front Biosci. 1999; **4**:D694-703 *(Review)*.

Martel-Pelletier J, McCollum R, DiBattista J, Faure MP, Chin JA, Fournier S, Sarfati M, Pelletier JP. The interleukin-1 receptor in normal and osteoarthritic human articular chondrocytes. Identification as the type I receptor and analysis of binding kinetics and biologic function. Arthritis Rheum. 1992; **35(5)**:530-40.

Martel-Pelletier J, Mineau F, Jolicoeur FC, Cloutier JM, Pelletier JP. In vitro effects of diacerhein and rhein on interleukin 1 and tumor necrosis factor-alpha systems in human osteoarthritic synovium and chondrocytes. J Rheumatol. 1998; **25(4)**:753-62.

Martel-Pelletier J, Pelletier JP. New insights into the major pathophysiological processes responsible for the development of osteoarthritis. Semin Arthritis Rheum. 2005; **34(6 Suppl 2)**:6-8 *(Review)*.

Martel-Pelletier J, Welsch DJ, Pelletier JP. Metalloproteases and inhibitors in arthritic diseases. Best Pract Res Clin Rheumatol. 2001; **15(5)**:805-29 *(Review)*.

Martin G, Bogdanowicz P, Domagala F, Ficheux H, Pujol JP. Rhein inhibits interleukin-1 beta-induced activation of MEK/ERK pathway and DNA binding of NF-kappa B and AP-1 in chondrocytes cultured in hypoxia: a potential mechanism for its disease-modifying effect in osteoarthritis. Inflammation. 2003; **27(4)**:233-46.

Martin JA, Buckwalter JA. Aging, articular cartilage chondrocyte senescence and osteoarthritis. Biogerontology. 2002; **3(5)**:257-64 *(Review)*.

Martin JA, Buckwalter JA. The role of chondrocyte-matrix interactions in maintaining and repairing articular cartilage. Biorheology. 2000; **37(1-2)**:129-40.

Mason L, Moore RA, Derry S, Edwards JE, McQuay HJ. Systematic review of topical capsaicin for the treatment of chronic pain. BMJ. 2004; **328(7446)**:991 *(Review)*.

Mason RM, Chambers MG, Flannelly J, Gaffen JD, Dudhia J, Bayliss MT. The STR/ort mouse and its use as a model of osteoarthritis. Osteoarthritis Cartilage. 2001; **9(2)**:85-91 *(Review)*.

Masuhara K, Nakai T, Yamaguchi K, Yamasaki S, Sasaguri Y. Significant increases in serum and plasma concentrations of matrix metalloproteinases 3 and 9 in patients with rapidly destructive osteoarthritis of the hip. Arthritis Rheum. 2002; **46(10)**:2625-31.

May MJ, D'Acquisto F, Madge LA, Glockner J, Pober JS, Ghosh S. Selective inhibition of NF-kappaB activation by a peptide that blocks the interaction of NEMO with the IkappaB kinase complex. Science. 2000; **289(5484)**:1550-4.

Mazieres B, Garnero P, Gueguen A, Abbal M, Berdah L, Lequesne M, Nguyen M, Salles JP, Vignon E, Dougados M. Molecular markers of cartilage breakdown and synovitis at baseline as predictors of structural progression of hip osteoarthritis. The ECHODIAH Cohort. Ann Rheum Dis. 2006; **65(3)**:354-9.

McAlindon TE, Snow S, Cooper C, Dieppe PA. Radiographic patterns of osteoarthritis of the knee joint in the community: the importance of the patellofemoral joint. Ann Rheum Dis. 1992; **51(7)**: 844 -9.

McCawley LJ, Matrisian LM. Matrix metalloproteinases: they're not just for matrix anymore! Curr Opin Cell Biol. 2001;**13(5)**:534 -40.

McIntyre KW, Shuster DJ, Gillooly KM, Dambach DM, Pattoli MA, Lu P, Zhou XD, Qiu Y, Zusi FC, Burke JR. A highly selective inhibitor of I kappa B kinase, BMS-345541, blocks both joint inflammation and destruction in collagen-induced arthritis in mice. Arthritis Rheum. 2003; **48(9)**:2652-9.

Meachim G. Age changes in articular cartilage. 1969. Clin Orthop Relat Res. 2001; **(391 Suppl)**:S6-13.

Mendes AF, Caramona MM, de Carvalho AP, Lopes MC. Diacerhein and rhein prevent interleukin-1beta-induced nuclear factor-kappaB activation by inhibiting the degradation of inhibitor kappaB-alpha. Pharmacol Toxicol. 2002; **91(1)**:22-8.

Mendler M, Eich-Bender SG, Vaughan L, Winterhalter KH, Bruckner P. Cartilage contains mixed fibrils of collagen types II, IX, and XI. J Cell Biol. 1989; **108(1)**: 191-7

Mengshol JA, Mix KS, Brinckerhoff CE. Matrix metalloproteinases as therapeutic targets in arthritic diseases: bull's-eye or missing the mark? Arthritis Rheum. 2002; **46(1)**:13-20 *(Review)*.

Mengshol JA, Vincenti MP, Coon CI, Barchowsky A, Brinckerhoff CE. Interleukin-1 induction of collagenase-3 (matrix metalloproteinase 13) gene expression in chondrocytes requires p38, c-JUN N-terminal kinase and nuclear factor κB. Arthritis Rheum 2000;**43 (4)**:801 – 811

Mi Z, Ghivizzani SC, Lechman E, Glorioso JC, Evans CH, Robbins PD. Adverse effects of adenovirus-mediated gene transfer of human transforming growth factor beta 1 into rabbit knees. Arthritis Res Ther. 2003; **5(3)**:R132-9.

Middleton JF, Tyler JA. Upregulation of insulin-like growth factor I gene expression in the lesions of osteoarthritic human articular cartilage. Ann Rheum Dis. 1992; **51(4)**:440 -7

Milner JM, Cawston TE. Matrix metalloproteinase knockout studies and the potential use of matrix metalloproteinase inhibitors in the rheumatic diseases. Curr Drug Targets Inflamm Allergy. 2005; **4(3)**:363-75 *(Review)*.

Milner JM, Rowan AD, Cawston TE, Young DA. Metalloproteinase and inhibitor expression profiling of resorbing cartilage reveals pro-collagenase activation as a critical step for collagenolysis. Arthritis Res Ther. 2006; **8(5)**:R142.

Moldovan F, Pelletier JP, Hambor J, Cloutier JM, Martel-Pelletier J. Collagenase-3 (matrix metalloprotease 13) is preferentially localized in the deep layer of human arthritic cartilage in situ: in vitro mimicking effect by transforming growth factor beta. Arthritis Rheum. 1997; **40(9)**:1653-61.

Moldovan F, Pelletier JP, Mineau F, Dupuis M, Cloutier JM, Martel-Pelletier J. Modulation of collagenase 3 in human osteoarthritic cartilage by activation of extracellular transforming growth factor beta: role of furin convertase. Arthritis Rheum. 2000; **43(9)**:2100 – 9

Moore AR, Greenslade KJ, Alam CA, Willoughby DA. Effects of diacerhein on granuloma induced cartilage breakdown in the mouse. Osteoarthritis Cartilage. 1998; **6(1)**:19-23.

Moreland LW. Intra-articular hyaluronan (hyaluronic acid) and hylans for the treatment of osteoarthritis: mechanisms of action. Arthritis Res Ther. 2003; **5(2)**:54 -67

Morgelin M, Heinegard D, Engel J, Paulsson M. Electron microscopy of native cartilage oligomeric matrix protein purified from the Swarm rat chondrosarcoma reveals a five-armed structure. J Biol Chem. 1992; **267(9)**:6137-41.

Moseley TA, Haudenschild DR, Rose L, Reddi AH. Interleukin-17 family and IL-17 receptors. Cytokine Growth Factor Rev. 2003; **14(2)**:155-74 *(Review)*.

Moskowitz RW, Holderbraum D. Clinical and laboratory findings in osteoarthritis. In *Arthritis and Allied Conditions. A textbook of rheumatology*. (Ed Koopman WJ). pp 2216 – 2245. Lippincott Williams & Wilkins 2001.

Murphy G, Knauper V, Atkinson S, Butler G, English W, Hutton M, Stracke J, Clark I. Matrix metalloproteinases in arthritic disease. Arthritis Res. 2002; **4 Suppl 3**:S39-49 *(Review)*

Murrell GA, Jang D, Williams RJ. Nitric oxide activates metalloprotease enzymes in articular cartilage. Biochem Biophys Res Commun. 1995; **206(1)**:15 -21.

Myers SL, Brandt KD, Ehlich JW, Braunstein EM, Shelbourne KD, Heck DA, Kalasinski LA. Synovial inflammation in patients with early osteoarthritis of the knee. J Rheumatol. 1990; **17(12)**:1662 – 9.

Nagase H, Kashiwagi M. Aggrecanases and cartilage matrix degradation. Arthritis Res Ther. 2003; **5(2)**:94-103 *(Review)*.

Nagase H, Visse R, Murphy G. Structure and function of matrix metalloproteinases and TIMPs. Cardiovasc Res. 2006; **69(3)**:562-73 *(Review)*.

Nagase H, Woessner JF Jr. Matrix metalloproteinases. J Biol Chem. 1999; **274(31)**:21491-4 *(Review)*.

Naito K, Takahashi M, Kushida K, Suzuki M, Ohishi T, Miura M, Inoue T, Nagano A. Measurement of matrix metalloproteinases (MMPs) and tissue inhibitor of metalloproteinases-1 (TIMP-1) in patients with knee osteoarthritis: comparison with generalized osteoarthritis. Rheumatology (Oxford). 1999; **38(6)**:510-5.

Nakamura H, Yoshino S, Kato T, Tsuruha J, Nishioka K. T-cell mediated inflammatory pathway in osteoarthritis. Osteoarthritis Cartilage. 1999; **7(4)**:401-2.

Nakao T, Kim S, Ohta K, Kawano H, Hino M, Miura K, Tatsumi N, Iwao H. Role of mitogen-activated protein kinase family in serum-induced leukaemia inhibitory factor and interleukin-6 secretion by bone marrow stromal cells. Br J Pharmacol. 2002; **136(7)**:975-84.

Neidhart M, Muller-Ladner U, Frey W, Bosserhoff AK, Colombani PC, Frey-Rindova P, Hummel KM, Gay RE, Hauselmann H, Gay S. Increased serum levels of non-collagenous matrix proteins (cartilage oligomeric matrix protein and melanoma inhibitory activity) in marathon runners. Osteoarthritis Cartilage. 2000; **8(3)**:222-9.

Neitfeld JJ, Willbrink B, Helle M, van Roy JL, den Otter W, Swaak AJ, Huber-Bruning O. Interleukin-1-induced interleukin-6 is required for the inhibition of proteoglycan synthesis by interleukin-1 in human articular cartilage. Arthritis Rheum. 1990; **33(11)**:1695 - 701

Nguyen Q, Murphy G, Roughley PJ, Mort JS. Degradation of proteoglycan aggregate by a cartilage metalloproteinase. Evidence for the involvement of stromelysin in the generation of link protein heterogeneity in situ. Biochem J. 1989; **259(1)**:61-7.

Nishida M, Higuchi H, Kobayashi Y, Takagishi K. Histological and biochemical changes of experimental meniscus tear in the dog knee. J Orthop Sci. 2005; **10(4)**:406-13.

Nowell MA, Richards PJ, Horiuchi S, Yamamoto N, Rose-John S, Topley N, Williams AS, Jones SA. Soluble IL-6 receptor governs IL-6 activity in experimental arthritis: blockade of arthritis severity by soluble glycoprotein 130. J Immunol. 2003; **171(6)**:3202-9.

Nuijten MJ, Engelfriet P, Duijn K, Bruijn G, Wierz D, Koopmanschap M. A cost-cost study comparing etanercept with infliximab in rheumatoid arthritis. Pharmacoeconomics. 2001; **19(10)**:1051-64.

Oberholzer A, Oberholzer C, Moldawer LL. Cytokine signaling--regulation of the immune response in normal and critically ill states. Crit Care Med. 2000; **28(4 Suppl)**:N3-12 *(Review)*.

Obermaier B, Dauer M, Herten J, Schad K, Endres S, Eigler A. Development of a new protocol for 2-day generation of mature dendritic cells from human monocytes. Biol Proced Online. 2003; **5**:197-203.

Ockey DA, Dotson JL, Struble ME, Stults JT, Bourell JH, Clark KR, Gadek TR. Structure-activity relationships by mass spectrometry: identification of novel MMP-3 inhibitors. Bioorg Med Chem. 2004; **12(1)**:37-44.

Okada Y, Konomi H, Yada T, Kimata K, Nagase H. Degradation of type IX collagen by matrix metalloproteinase 3 (stromelysin) from human rheumatoid synovial cells. FEBS Lett. 1989; **244(2)**:473-6.

Ollivierre F, Gubler U, Towle CA, Laurencin C, Treadwell BV. Expression of IL-1 genes in human and bovine chondrocytes: a mechanism for autocrine control of cartilage matrix degradation. Biochem Biophys Res Commun. 1986; 141(3):904 – 11

O'Reilly S, Doherty M. Clinical features of osteoarthritis and standard approaches to the diagnosis. In *Osteoarthritis* (ed Brandt KD, Doherty M, Lohmander LS). pp. 197 – 217. Oxford University Press 2000.

Osten P, Grinevich V, Cetin A. Viral vectors: a wide range of choices and high levels of service. Handb Exp Pharmacol. 2007; **178**:177-202 *(Review)*.

Palayoor ST, Youmell MY, Calderwood SK, Coleman CN, Price BD. Constitutive activation of IkappaB kinase alpha and NF-kappaB in prostate cancer cells is inhibited by ibuprofen. Oncogene. 1999; **18(51)**:7389-94.

Pardo A, Selman M. MMP-1: the elder of the family. Int J Biochem Cell Biol. 2005; **37(2)**:283-8 *(Review)*.

Pasternack SG, Veis A, Breen M. Solvent-dependent changes in proteoglycan subunit conformation in aqueous guanidine hydrochloride solutions. J Biol Chem. 1974; **249(7)**:2206-11.

Pattoli MA, MacMaster JF, Gregor KR, Burke JR. Collagen and aggrecan degradation is blocked in interleukin-1-treated cartilage explants by an inhibitor of IkappaB kinase through suppression of metalloproteinase expression. J Pharmacol Exp Ther. 2005; **315(1)**:382-8.

Paulsson M, Morgelin M, Wiedemann H, Beardmore-Gray M, Dunham D, Hardingham T, Heinegard D, Timpl R, Engel J. Extended and globular protein domains in cartilage proteoglycans. Biochem J. 1987; **245(3)**:763-72.

Paulus HE, Whitehouse MW. Nonsteroid anti-inflammatory agents. Annu Rev Pharmacol. 1973; **13**:107-25 *(Review)*.

Pelletier JP, Boileau C, Boily M, Brunet J, Mineau F, Geng C, Reboul P, Laufer S, Lajeunesse D, Martel-Pelletier J. The protective effect of licofelone on experimental osteoarthritis is correlated with the downregulation of gene expression and protein synthesis of several major cartilage catabolic factors: MMP-13, cathepsin K and aggrecanases. Arthritis Res Ther. 2005; **7(5)**:R1091-102.

Pelletier JP, Boileau C, Brunet J, Boily M, Lajeunesse D, Reboul P, Laufer S, Martel-Pelletier J. The inhibition of subchondral bone resorption in the early phase of experimental dog osteoarthritis by licofelone is associated with a reduction in the synthesis of MMP-13 and cathepsin K. Bone. 2004; **34(3)**:527-38.

Pelletier JP, DiBattista JA, Roughley P, McCollum R, Martel-Pelletier J. Cytokines and inflammation in cartilage degradation. Rheum Dis Clin North Am. 1993; **19(3)**:545-68 *(Review)*.

Pelletier JP, Martel-Pelletier J, Abramson SB. Osteoarthritis, an inflammatory disease: potential implication for the selection of new therapeutic targets. Arthritis Rheum. 2001; **44(6)**:1237-47 *(Review)*.

Pelletier JP, Martel-Pelletier J, Raynauld JP. Most recent developments in strategies to reduce the progression of structural changes in osteoarthritis: today and tomorrow. Arthritis Res Ther. 2006; **8(2)**:206 *(Review)*.

Pelletier JP, Martel-Pelletier J. New trends in the treatment of osteoarthritis. Semin Arthritis Rheum. 2005; **34(6 Suppl 2)**:13-4 *(Review)*.

Pelletier JP, Martel-Pelletier J. Evidence for the involvement of interleukin 1 in human osteoarthritic cartilage degradation: protective effect of NSAID. J Rheumatol Suppl. 1989; **18**:19 – 27

Pelletier KP, Martel-Pelletier J, Howell DS. Etiopathogenesis of OA. In *Arthritis and Allied Conditions. A textbook of rheumatology.* (Ed Koopman WJ). pp 2195 – 2215. Lippincott Williams & Wilkins 2001.

Pelletier JP, McCollum R, Cloutier JM, Martel-Pelletier J. Synthesis of metalloproteases and interleukin 6 (IL-6) in human osteoarthritic synovial membrane is an IL-1 mediated process. J Rheumatol Suppl. 1995; **43**:109-14.

Petersson IF, Jacobsson LT. Osteoarthritis of the peripheral joints. Best Pract Res Clin Rheumatol. 2002; **16(5)**:741-60 *(Review).*

Pfander D, Rahmanzadeh R, Scheller EE. Presence and distribution of collagen II, collagen I, fibronectin, and tenascin in rabbit normal and osteoarthritic cartilage. J Rheumatol. 1999; **26(2)**:386-94.

Pham T, Le Henanff A, Ravaud P, Dieppe P, Paolozzi L, Dougados M. Evaluation of the symptomatic and structural efficacy of a new hyaluronic acid compound, NRD101, in comparison with diacerein and placebo in a 1 year randomised controlled study in symptomatic knee osteoarthritis. Ann Rheum Dis. 2004; **63(12)**:1611 -7.

Podolin PL, Callahan JF, Bolognese BJ, Li YH, Carlson K, Davis TG, Mellor GW, Evans C, Roshak AK. Attenuation of murine collagen-induced arthritis by a novel, potent, selective small molecule inhibitor of IkappaB Kinase 2, TPCA-1 (2-[(aminocarbonyl)amino]-5-(4-fluorophenyl)-3-thiophenecarboxamide), occurs via reduction of proinflammatory cytokines and antigen-induced T cell Proliferation. J Pharmacol Exp Ther. 2005; **312(1)**:373-81.

Poole AR, Kojima T, Yasuda T, Mwale F, Kobayashi M, Laverty S. Composition and structure of articular cartilage: a template for tissue repair. Clin Orthop Relat Res. 2001; **(391 Suppl)**:S26-33. *(Review).*

Poole AR, Pidoux I, Reiner A, Rosenberg L. An immunoelectron microscope study of the organization of proteoglycan monomer, link protein, and collagen in the matrix of articular cartilage. J Cell Biol. 1982; **93(3)**:921-37.

Poole AR. Complexity of proteoglycan organization in articular cartilage: recent observations. J Rheumatol Suppl. 1983; **11**:70-5.
Poole AR. Proteoglycans in health and disease: structures and functions. Biochem J. 1986; **236(1)**:1-14 *(Review).*

Poole CA, Matsuoka A, Schofield JR. Chondrons from articular cartilage. III. Roc Morphologic changes in the cellular microenvironment of chondrons isolated from osteoarthritic cartilage. Arthritis Rheum. 1991; **34(1)**:22-35.

Porter AG. Human tumour necrosis factors-alpha and -beta: differences in their structure, expression and biological properties. FEMS Microbiol Immunol. 1990; **2(4)**: 193 – 9

Porter S, Clark IM, Kevorkian L, Edwards DR. The ADAMTS metalloproteinases. Biochem J. 2005; **386(Pt 1)**:15-27 *(Review)*.

Priestle JP, Schar HP, Grutter MG. Crystallographic refinement of interleukin 1 beta at 2.0 A resolution. Proc Natl Acad Sci USA. 1989; **86(24)**:9667 – 71.

Pritzker KP. Animal models for osteoarthritis: processes, problems and prospects. Ann Rheum Dis. 1994; **53(6)**:406-20. *(Review)*.

Pynsent PB, Carter SR, Bulstrode CJ. The total cost of hip-joint replacement; a model for purchasers. J Public Health Med. 1996; **18(2)**:157-68.

Qi WN, Scully SP. Extracellular collagen regulates expression of transforming growth factor-beta1 gene. J Orthop Res. 2000; **18(6)**:928-32.

Quasnichka HL, Anderson-MacKenzie JM, Bailey AL. Subchondral bone and ligament changes precede cartilage degradation in guinea pig osteoarthritis. Biorheology. 2006; 43**(3 – 4)**:389 – 97.

Quinn M, Deering A, Stewart M, Cox D, Foley B, Fitzgerald D. Quantifying GPIIb/IIIa receptor binding using 2 monoclonal antibodies: discriminating abciximab and small molecular weight antagonists. Circulation. 1999; **99(17)**:2231-8.

Radin EL, Paul IL, Lowy LM. A comparison of the dynamic force transmitting properties of subchondral bone and articular cartilage. J Bone Joint Surg. 1970: **52(3)**: 444 – 56

Ralphs JR, Benjamin M. The joint capsule: structure, composition, ageing and disease. J Anat. 1994; **184 (Pt 3)**:503-9 *(Review)*.

Ratcliffe A, Tyler JA, Hardingham TE. Articular cartilage cultured with interleukin 1. Increased release of link protein, hyaluronate-binding region and other proteoglycan fragments. Biochem J. 1986; **238(2)**:571-80.

Raven PH, and Johnson GB, (1999). Biology 5th Edition. pp. 922. McGraw-Hill Companies Inc.

Regnier CH, Song HY, Gao X, Goeddel DV, Cao Z, Rothe M. Identification and characterization of an IkappaB kinase. Cell. 1997; **90(2)**:373-83.

Reig E. Tramadol in musculoskeletal pain--a survey. Clin Rheumatol. 2002; **21**:S9-11

Reuben PM, Cheung HS. Regulation of matrix metalloproteinase (MMP) gene expression by protein kinases. Front Biosci. 2006; **11**:1199-215 *(Review)*.

Revell PA, al-Saffar N, Fish S, Osei D. Extracellular matrix of the synovial intimal cell layer. Ann Rheum Dis. 1995; **54(5)**:404-7 *(Review)*.

Revell PA, Mayston V, Lalor P, Mapp P. The synovial membrane in osteoarthritis: a histological study including the characterisation of the cellular infiltrate present in inflammatory osteoarthritis using monoclonal antibodies. Ann Rheum Dis. 1988; **47(4)**:300-7.

Richards PJ, Williams AS, Goodfellow RM, Williams BD. Liposomal clodronate eliminates synovial macrophages, reduces inflammation and ameliorates joint destruction in antigen-induced arthritis. Rheumatology (Oxford). 1999; **38(9)**:818-25.

Riordan JR. Therapeutic strategies for treatment of CF based on knowledge of CFTR. Pediatr Pulmonol Suppl. 1999;**18**:83-7 *(Review)*.

Roman-Blas JA, Jimenez SA. NF-kappaB as a potential therapeutic target in osteoarthritis and rheumatoid arthritis. Osteoarthritis Cartilage. 2006; **14(9)**:839-48 *(Review)*.

Roos H, Adalberth T, Dahlberg L, Lohmander LS. Osteoarthritis of the knee after injury to the anterior cruciate ligament or meniscus: the influence of time and age. Osteoarthritis Cartilage. 1995; **3(4)**:261-7.

Rosenberg L. Chemical basis for the histological use of safranin O in the study of articular cartilage. J Bone Joint Surg Am. 1971; **53(1)**:69-82.

Rosenecker J, Huth S, Rudolph C. Gene therapy for cystic fibrosis lung disease: current status and future perspectives. Curr Opin Mol Ther. 2006; **8(5)**: 439-45 *(Review)*.

Roshak AK, Callahan JF, Blake SM. Small-molecule inhibitors of NF-kappaB for the treatment of inflammatory joint disease. Curr Opin Pharmacol. 2002; **2(3)**:316-21 *(Review)*.

Roughley PJ, White RJ, Poole AR. Identification of a hyaluronic acid-binding protein that interferes with the preparation of high-buoyant-density proteoglycan aggregates from adult human articular cartilage. Biochem J. 1985; **231(1)**:129-38.

Roughley PJ. Structural changes in the proteoglycans of human articular cartilage during aging. J Rheumatol. 1987; **14 Spec No**:14-5.

Roughley PJ, Lee ER. Cartilage proteoglycans: structure and potential functions. Microsc Res Tech. 1994; **28(5)**: 385 - 397

Rountree RB, Schoor M, Chen H, Marks ME, Harley V, Mishina Y, Kingsley DM. BMP receptor signaling is required for postnatal maintenance of articular cartilage. PLoS Biol. 2004; **2(11)**:e355.

Roy S. Ultrastructure of synovial membrane in osteo-arthritis. Ann Rheum Dis. 1967; **26(6)**:517-27.

Ruben SM, Klement JF, Coleman TA, Maher M, Chen CH, Rosen CA. I-Rel: a novel rel-related protein that inhibits NF-kappa B transcriptional activity. Genes Dev. 1992; **6(5)**:745-60.

Ryseck RP, Bull P, Takamiya M, Bours V, Siebenlist U, Dobrzanski P, Bravo R. RelB, a new Rel family transcription activator that can interact with p50-NF-kappa B. Mol Cell Biol. 1992; **12(2)**:674-84.

Sabatini M, Lesur C, Thomas M, Chomel A, Anract P, de Nanteuil G, Pastoureau P. Effect of inhibition of matrix metalloproteinases on cartilage loss in vitro and in a guinea pig model of osteoarthritis. Arthritis Rheum. 2005; **52(1)**:171-80.

Sadouk MB, Pelletier JP, Tardif G, Kiansa K, Cloutier JM, Martel-Pelletier J. Human synovial fibroblasts coexpress IL-1 receptor type I and type II mRNA. The increased level of the IL-1 receptor in osteoarthritic cells is related to an increased level of the type I receptor. Lab Invest. 1995; **73(3)**:347-55.

Sanchez-Serrano I. Success in translational research: lessons from the development of bortezomib. Nat Rev Drug Discov. 2006; **5(2)**:107-14.

Sandell LJ, Chansky H, Zamparo O, Hering TM. Molecular Biology of cartilage proteoglycans and link protein. In *Osteoarthritic Disorders* (ed Kuettner KE, Goldberg VM). pp 117 – 131. American Academy of Orthopaedic Surgeons 1995.

Sandy JD, Neame PJ, Boynton RE, Flannery CR. Catabolism of aggrecan in cartilage explants. Identification of a major cleavage site within the interglobular domain. J Biol Chem. 1991; **266(14)**:8683-5.

Santhanam U, Ghrayeb J, Sehgal PB, May LT. Post-translational modifications of human interleukin-6. Arch Biochem Biophys. 1989; **274(1)**:161-70.

Sasmono, T. R., and Hume, D.A., (2004). The biology of macrophages. In *The innate immune response to infection* (ed. Kaufmann, S., *et al.*) pp. 71 – 94.

Saxne T, Heinegard D. Cartilage oligomeric matrix protein: a novel marker of cartilage turnover detectable in synovial fluid and blood. Br J Rheumatol. 1992; **31(9)**:583-91. Erratum in: Br J Rheumatol 1993; **32(3)**:247.

Scharstuhl A, Vitters EL, van der Kraan PM, van den Berg WB. Reduction of osteophyte formation and synovial thickening by adenoviral overexpression of transforming growth factor beta/bone morphogenetic protein inhibitors during experimental osteoarthritis. Arthritis Rheum. 2003; **48(12)**:3442-51.

Schnell MA, Zhang Y, Tazelaar J, Gao GP, Yu QC, Qian R, Chen SJ, Varnavski AN, LeClair C, Raper SE, Wilson JM. Activation of innate immunity in nonhuman primates following intraportal administration of adenoviral vectors. Mol Ther. 2001; **3(5 Pt 1)**:708-22.

Schopf L, Savinainen A, Anderson K, Kujawa J, DuPont M, Silva M, Siebert E, Chandra S, Morgan J, Gangurde P, Wen D, Lane J, Xu Y, Hepperle M, Harriman G, Ocain T, Jaffee B. IKKbeta inhibition protects against bone and cartilage destruction in a rat model of rheumatoid arthritis. Arthritis Rheum. 2006; **54(10)**:3163-73.

Schouten JS, van den Ouweland FA, Valkenburg HA, Lamberts SW. Insulin-like growth factor-1: a prognostic factor of knee osteoarthritis. Br J Rheumatol. 1993; **32(4)**:274 -80

Schreiber J, Efron PA, Park JE, Moldawer LL, Barbul A. Adenoviral gene transfer of an NF-kappaB super-repressor increases collagen deposition in rodent cutaneous wound healing. Surgery. 2005; **138(5)**:940-6.

Schreiber S, Nikolaus S, Hampe J, Hamling J, Koop I, Groessner B, Lochs H, Raedler A. Tumour necrosis factor alpha and interleukin 1beta in relapse of Crohn's disease. Lancet. 1999; **353(9151)**:459 – 61.

Schwartz NB, Pirok EW 3rd, Mensch JR Jr, Domowicz MS. Domain organization, genomic structure, evolution, and regulation of expression of the aggrecan gene family. Prog Nucleic Acid Res Mol Biol. 1999; **62**:177-225 *(Review)*.

Scott DL. Etanercept in arthritis. Int J Clin Pract. 2005; **59(1)**:114-8 *(Review)*.

Sen R, Baltimore D. Multiple nuclear factors interact with the immunoglobulin enhancer sequences. Cell 1986; **46**:705-716.

Senftleben U, Cao Y, Xiao G, Greten FR, Krahn G, Bonizzi G, Chen Y, Hu Y, Fong A, Sun SC, Karin M. Activation by IKKalpha of a second, evolutionary conserved, NF-kappa B signaling pathway. Science. 2001; 293(5534):1495 – 9.

Shalom-Barak T, Quach J, Lotz M. Interleukin-17-induced gene expression in articular chondrocytes is associated with activation of mitogen-activated protein kinases and NF-kappaB. J Biol Chem. 1998; 273(42):27467 – 73

Sharif M, Kirwan JR, Elson CJ, Granell R, Clarke S. Suggestion of nonlinear or phasic progression of knee osteoarthritis based on measurements of serum cartilage oligomeric matrix protein levels over five years. Arthritis Rheum. 2004; **50(8)**:2479-88.

Sharma L, Lou C, Felson DT, Dunlop DD, Kirwan-Mellis G, Hayes KW, Weinrach D, Buchanan TS. Laxity in healthy and osteoarthritic knees. Arthritis Rheum. 1999; **42(5)**:861-70.

Shepard N, Mitchell N. Simultaneous localization of proteoglycan by light and electron microscopy using toluidine blue O. A study of epiphyseal cartilage. J Histochem Cytochem. 1976; **24(5)**:621-9.

Shingleton WD, Jones D, Xu X, Cawston TE, Rowan AD. Retinoic acid and oncostatin M combine to promote cartilage degradation via matrix metalloproteinase-13 expression in bovine but not human chondrocytes. Rheumatology (Oxford). 2006; **45(8)**:958-65.

Siebenlist U, Franzoso G, Brown K. Structure, regulation and function of NF-kappa B. Annu Rev Cell Biol. 1994; **10**:405-55 *(Review)*.

Silverstein E, Sokoloff L. Natural history of degenerative joint disease in small laboratory animals. 5. Osteoarthritis in Guinea Pigs. Arthritis Rheum. 1958; **1**: 82 – 6

Singer II, Scott S, Kawka DW, Bayne EK, Weidner JR, Williams HR, Mumford RA, Lark MW, McDonnell J, Christen AJ, Moore VL, Mudgett JS, Visco DM. Aggrecanase and metalloproteinase-specific aggrecan neo-epitopes are induced in the articular cartilage of mice with collagen II-induced arthritis. Osteoarthritis Cartilage. 1997; **5(6)**:407-18.

Skoumal M, Kolarz G, Klingler A. Serum levels of cartilage oligomeric matrix protein. A predicting factor and a valuable parameter for disease management in rheumatoid arthritis. Scand J Rheumatol. 2003; **32(3)**:156-61.

Slack HG. Some notes on the composition and metabolism of connective tissue. Am J Med. 1959; **26(1)**:113-24.

Slover J, Espehaug B, Havelin LI, Engesaeter LB, Furnes O, Tomek I, Tosteson A. Cost-effectiveness of unicompartmental and total knee arthroplasty in elderly low-demand patients. A Markov decision analysis. J Bone Joint Surg Am. 2006; **88(11)**:2348-55.

Smith GN Jr, Myers SL, Brandt KD, Mickler EA, Albrecht ME. Diacerhein treatment reduces the severity of osteoarthritis in the canine cruciate-deficiency model of osteoarthritis. Arthritis Rheum. 1999; **42(3)**:545-54.

Smith GN Jr. The role of collagenolytic matrix metalloproteinases in the loss of articular cartilage in osteoarthritis. Front Biosci. 2006; **11**:3081-95 *(Review)*.

Smith MD, Barg E, Weedon H, Papengelis V, Smeets T, Tak PP, Kraan M, Coleman M, Ahern MJ. Microarchitecture and protective mechanisms in synovial tissue from clinically and arthroscopically normal knee joints. Ann Rheum Dis. 2003; **62(4)**:303-7.

Smith MD, O'Donnell J, Highton J, Palmer DG, Rozenbilds M, Roberts-Thomson PJ. Immunohistochemical analysis of synovial membranes from inflammatory and non-inflammatory arthritides: scarcity of CD5 positive B cells and IL2 receptor bearing T cells. Pathology. 1992; **24(1)**:19-26.

Smith MD, Triantafillou S, Parker A, Youssef PP, Coleman M. Synovial membrane inflammation and cytokine production in patients with early osteoarthritis. J Rheumatol. 1997; **24(2)**:365-71.

Smith RL. Degradative enzymes in osteoarthritis. Front Biosci. 1999; **4**:D704-12 *(Review)*.

Spalding JR, Hay J. Cost effectiveness of tumour necrosis factor-alpha inhibitors as first-line agents in rheumatoid arthritis. Pharmacoeconomics. 2006; **24(12)**:1221-32.

Stabellini G, De Mattei M, Calastrini C, Gagliano N, Moscheni C, Pasello M, Pellati A, Bellucci C, Gioia M. Effects of interleukin-1beta on chondroblast viability and extracellular matrix changes in bovine articular cartilage explants. Biomed Pharmacother. 2003; **57(7)**:314-9.

Stancovski I, Baltimore D. NF-kappaB activation: the I kappaB kinase revealed? Cell. 1997; **91(3)**:299-302 *(Review)*.

Stanton H, Rogerson FM, East CJ, Golub SB, Lawlor KE, Meeker CT, Little CB, Last K, Farmer PJ, Campbell IK, Fourie AM, Fosang AJ. ADAMTS5 is the major aggrecanase in mouse cartilage in vivo and in vitro. Nature. 2005; **434(7033)**:648-52.

Steinmeyer J, Konttinen YT. Oral treatment options for degenerative joint disease--presence and future. Adv Drug Deliv Rev. 2006; **58(2)**:168-211 *(Review)*.

Sternlicht MD, Werb Z. How matrix metalloproteinases regulate cell behavior. Annu Rev Cell Dev Biol. 2001; **17**:463 - 516

Stockwell RA. The ultrastructure of cartilage canals and the surrounding cartilage in the sheep fetus. J Anat. 1971; **109(Pt 3)**:397-410.

Su S, Grover J, Roughley PJ, DiBattista JA, Martel-Pelletier J, Pelletier JP, Zafarullah M. Expression of the tissue inhibitor of metalloproteinases (TIMP) gene family in normal and osteoarthritic joints. Rheumatol Int. 1999; **18(5-6)**:183-91.

Szatmary Z. Tumor necrosis factor-alpha: molecular-biological aspects minireview. Neoplasma. 1999; **46(5)**:257-66 *(Review)*.

Szlosarek P, Charles KA, Balkwill FR. Tumour necrosis factor-alpha as a tumour promoter. Eur J Cancer. 2006; **42(6)**:745-50 *(Review)*.

Sztrolovics R, Alini M, Roughley PJ, Mort JS. Aggrecan degradation in human intervertebral disc and articular cartilage. Biochem J. 1997; **326 (Pt 1)**:235-41.

Sztrolovics R, Recklies AD, Roughley PJ, Mort JS. Hyaluronate degradation as an alternative mechanism for proteoglycan release from cartilage during interleukin-1beta-stimulated catabolism. Biochem J. 2002; **362(Pt 2)**:473-9.

Takagi N, Mihara M, Moriya Y, Nishimoto N, Yoshizaki K, Kishimoto T, Takeda Y, Ohsugi Y. Blockage of interleukin-6 receptor ameliorates joint disease in murine collagen-induced arthritis. 1998; **41(12)**:2117 – 21

Tamura T, Kosaka N, Ishiwa J, Sato T, Nagase H, Ito A. Rhein, an active metabolite of diacerein, down-regulates the production of pro-matrix metalloproteinases-1, -3, -9 and -13 and up-regulates the production of tissue inhibitor of metalloproteinase-1 in cultured rabbit articular chondrocytes. Osteoarthritis Cartilage. 2001; **9(3)**:257-63.

Taskiran D, Stefanovic-Racic M, Georgescu H, Evans C. Nitric oxide mediates suppression of cartilage proteoglycan synthesis by interleukin-1. Biochem Biophys Res Commun. 1994; **200(1)**:142 -8.

Tchetverikov I, Lohmander LS, Verzijl N, Huizinga TW, TeKoppele JM, Hanemaaijer R, DeGroot J. MMP protein and activity levels in synovial fluid from patients with joint injury, inflammatory arthritis, and osteoarthritis. Ann Rheum Dis. 2005; **64(5)**:694-8.

Thivierge M, Stankova J, Rola-Pleszczynski M. Toll-like receptor agonists differentially regulate cysteinyl-leukotriene receptor 1 expression and function in human dendritic cells. J Allergy Clin Immunol. 2006; **117(5)**:1155-62.

Thomas CE, Ehrhardt A, Kay MA. Progress and problems with the use of viral vectors for gene therapy. Nat Rev Genet. 2003; **4(5)**:346-58 *(Review)*.

Thonar EJ, Buckwalter JA, Kuettner KE. Maturation-related differences in the structure and composition of proteoglycans synthesized by chondrocytes from bovine articular cartilage. J Biol Chem. 1986; **261(5)**:2467-74.

Timmermans PB, Wong PC, Chiu AT, Herblin WF, Benfield P, Carini DJ, Lee RJ, Wexler RR, Saye JA, Smith RD. Angiotensin II receptors and angiotensin II receptor antagonists. Pharmacol Rev. 1993; **45(2)**:205-51 *(Review)*.

Toogood PL, Progress toward the development of agents to modulate the cell cycle. Curr Opin Chem Biol. 2002; **6(4)**:472 – 8.

Tortorella MD, Malfait AM, Deccico C, Arner E. The role of ADAM-TS4 (aggrecanase-1) and ADAM-TS5 (aggrecanase-2) in a model of cartilage degradation. Osteoarthritis Cartilage. 2001; **9(6)**:539-52. Erratum in: Osteoarthritis Cartilage 2002; **10(1)**:82.

Towheed TE, Maxwell L, Anastassiades TP, Shea B, Houpt J, Robinson V, Hochberg MC, Wells G. Glucosamine therapy for treating osteoarthritis. Cochrane Database Syst Rev. 2005; **(2)**:CD002946 *(Review)*.

Towheed TE, Maxwell L, Judd MG, Catton M, Hochberg MC, Wells G. Acetaminophen for osteoarthritis. Cochrane Database Syst Rev. 2006; **(1)**:CD004257 *(Review)*.

Trnavsky K, Fischer M, Vogtle-Junkert U, Schreyger F. Efficacy and safety of 5% ibuprofen cream treatment in knee osteoarthritis. Results of a randomized, double-blind, placebo-controlled study. J Rheumatol. 2004; **31(3)**:565 -72.

Tyler JA. Chondrocyte-mediated depletion of articular cartilage proteoglycans in vitro. Biochem J. 1985; **225(2)**:493-507.

Unemori EN, Bair MJ, Bauer EA, Amento EP. Stromelysin expression regulates collagenase activation in human fibroblasts. Dissociable control of two metalloproteinases by interferon-gamma. J Biol Chem. 1991; **266(34)**:23477-82.

van Beuningen HM, van der Kraan PM, Arntz OJ, van den Berg WB. Protection from interleukin 1 induced destruction of articular cartilage by transforming growth factor beta: studies in anatomically intact cartilage in vitro and in vivo. Ann Rheum Dis. 1993; **52(3)**:185-91.

van Damme J, Bunning RA, Conings R, Graham R, Russell G, Opdenakker G. Characterization of granulocyte chemotactic activity from human cytokine-stimulated chondrocytes as interleukin 8. Cytokine. 1990; **2(2)**:106 -11

van de Loo FA, Joosten LA, van Lent PL, Arntz OJ, van den Berg WB. Role of interleukin-1, tumor necrosis factor alpha, and interleukin-6 in cartilage proteoglycan metabolism and destruction. Effect of in situ blocking in murine antigen- and zymosan-induced arthritis. Arthritis Rheum. 1995; **38(2)**:164-72.

van den Berg WB, Joosten LA, Kollias G, van De Loo FA. Role of tumour necrosis factor alpha in experimental arthritis: separate activity of interleukin 1beta in chronicity and cartilage destruction. Ann Rheum Dis. 1999; **58 Suppl 1**:I40-8 *(Review)*.

van den Berg WB. Anti-cytokine therapy in chronic destructive arthritis. Arthritis Res. 2001; **3(1)**:18-26 *(Review)*.

van den Berg WB. Lessons from animal models of osteoarthritis. Curr Opin Rheumatol. 2001; **13(5)**:452-6 *(Review)*.

van den Berg WB. The role of cytokines and growth factors in cartilage destruction in osteoarthritis and rheumatoid arthritis. Z Rheumatol. 1999; **58(3)**:136-41 *(Review)*.

van den Berg WB, van der Kraan, van Beuningen et al. Synovial mediators of cartilage damage and repair in OA. In *Osteoarthritis* (ed Brandt KD, Doherty M, Lohmander LS). pp. 157 – 167. Oxford University Press 2000.

van der Kraan PM, Vitters EL, van Beuningen HM, van de Putte LB, van den Berg WB. Degenerative knee joint lesions in mice after a single intra-articular collagenase injection. A new model of osteoarthritis. J Exp Pathol (Oxford). 1990; **71(1)**:19-31.

van der Kraan PM, Vitters EL, van Beuningen HM, van den Berg WB. Proteoglycan synthesis and osteophyte formation in 'metabolically' and 'mechanically' induced murine degenerative joint disease: an in-vivo autoradiographic study. Int J Exp Pathol. 1992; **73(3)**:335-50.

van der Kraan PM, Vitters EL, van de Putte LB, van den Berg WB. Development of osteoarthritic lesions in mice by "metabolic" and "mechanical" alterations in the knee joints. Am J Pathol. 1989; **135(6)**:1001-14.

van Meurs J, van Lent P, Holthuysen A, Lambrou D, Bayne E, Singer I, van den Berg W. Active matrix metalloproteinases are present in cartilage during immune complex-mediated arthritis: a pivotal role for stromelysin-1 in cartilage destruction. J Immunol. 1999; **163(10)**:5633-9.

van Meurs J, van Lent P, Stoop R, Holthuysen A, Singer I, Bayne E, Mudgett J, Poole R, Billinghurst C, van der Kraan P, Buma P, van den Berg W. Cleavage of aggrecan at the Asn341-Phe342 site coincides with the initiation of collagen damage in murine antigen-induced arthritis: a pivotal role for stromelysin 1 in matrix metalloproteinase activity. Arthritis Rheum. 1999; **42(10)**:2074-84.

van Osch GJ, van den Berg WB, Hunziker EB, Hauselmann HJ. Differential effects of IGF-1 and TGF beta-2 on the assembly of proteoglycans in pericellular and territorial matrix by cultured bovine articular chondrocytes. Osteoarthritis Cartilage. 1998; **6(3)**:187-95.

van Osch GJ, van der Kraan PM, van Valburg AA, van den Berg WB. The relation between cartilage damage and osteophyte size in a murine model for osteoarthritis in the knee. Rheumatol Intl. 1996; **16(3)**:115 – 9

van Osch GJ, van der Kraan PM, van den Berg WB. Site-specific cartilage changes in murine degenerative knee joint disease induced by iodoacetate and collagenase. J Orthop Res. 1994; **12(2)**:168-75.

van Osch GJ, van der Veen SW, Buma P, Verwoerd-Verhoef HL. Effect of transforming growth factor-beta on proteoglycan synthesis by chondrocytes in relation to differentiation stage and the presence of pericellular matrix. Matrix Biol. 1998; **17(6)**:413-24.

Vanden Berghe W, Vermeulen L, De Wilde G, De Bosscher K, Boone E, Haegeman G. Signal transduction by tumor necrosis factor and gene regulation of the inflammatory cytokine interleukin-6. Biochem Pharmacol. 2000; **60(8)**:1185-95 *(Review)*.

Veje K, Hyllested-Winge JL, Ostergaard K. Topographic and zonal distribution of tenascin in human articular cartilage from femoral heads: normal versus mild and severe osteoarthritis. Osteoarthritis Cartilage. 2003; **11(3)**:217-27.

Vellet AD, Marks PH, Fowler PJ, Munro TG. Occult posttraumatic osteochondral lesions of the knee: prevalence, classification, and short-term sequelae evaluated with MR imaging. Radiology. 1991; **178(1)**: 271 - 6

Venn G, Nietfeld JJ, Duits AJ, Brennan FM, Arner E, Covington M, Billingham ME, Hardingham TE. Elevated synovial fluid levels of interleukin-6 and tumor necrosis factor associated with early experimental canine osteoarthritis. Arthritis Rheum. 1993; **36(6)**:819-26.

Vergunst CE, Tak PP. Chemokines: their role in rheumatoid arthritis. Curr Rheumatol Rep. 2005; **7(5)**:382-8 *(Review)*.

Vincenti MP, Brinckerhoff CE. Transcriptional regulation of collagenase (MMP-1, MMP-13) genes in arthritis: integration of complex signaling pathways for the recruitment of gene-specific transcription factors. Arthritis Res. 2002; **4(3)**:157-64 *(Review)*.

Visse R, Nagase H. Matrix metalloproteinases and tissue inhibitors of metalloproteinases: structure, function, and biochemistry. Circ Res. 2003; **92(8)**:827-39 *(Review)*.

von Porat A, Roos EM, Roos H. High prevalence of osteoarthritis 14 years after an anterior cruciate ligament tear in male soccer players: a study of radiographic and patient relevant outcomes. Ann Rheum Dis. 2004; **63(3)**:269-73.

Wagner JA, Gardner P. Toward cystic fibrosis gene therapy. Annu Rev Med. 1997;**48**:203-16 *(Review)*.

Wakamatsu K, Nanki T, Miyasaka N, Umezawa K, Kubota T. Effect of a small molecule inhibitor of nuclear factor-kappaB nuclear translocation in a murine model of arthritis and cultured human synovial cells. Arthritis Res Ther. 2005; **7(6)**:R1348-59.

Walton M. Degenerative joint disease in the mouse knee; histological observations. J Pathol. 1977; **123(2)**:109-22.

Walton M. Degenerative joint disease in the mouse knee; radiological and morphological observations. J Pathol. 1977; **123(2)**:97-107.

Wang J, Verdonk P, Elewaut D, Veys EM, Verbruggen G. Homeostasis of the extracellular matrix of normal and osteoarthritic human articular cartilage chondrocytes in vitro. Osteoarthritis Cartilage. 2003; **11(11)**:801-9.

Warren JS. Interleukins and tumor necrosis factor in inflammation. Crit Rev Clin Lab Sci. 1990; **28(1)**:37-59 *(Review)*.

Webb GR, Westacott CI, Elson CJ. Osteoarthritic synovial fluid and synovium supernatants up-regulate tumor necrosis factor receptors on human articular chondrocytes. Osteoarthritis Cartilage. 1998; **6(3)**:167-76.

Westacott CI, Atkins RM, Dieppe PA, Elson CJ. Tumor necrosis factor-alpha receptor expression on chondrocytes isolated from human articular cartilage. J Rheumatol. 1994; **21(9)**:1710 -5

Westacott CI, Sharif M. Cytokines in osteoarthritis: mediators or markers of joint destruction? Semin Arthritis Rheum. 1996; **25(4)**:254-72 *(Review)*.

Wieland HA, Michaelis M, Kirschbaum BJ, Rudolphi KA. Osteoarthritis - an untreatable disease? Nat Rev Drug Discov. 2005; **4(4)**:331-44 *(Review)*. Erratum in: Nat Rev Drug Discov. 2005; **4(7)**:543.

Wilczynska KM, Gopalan SM, Bugno M, Kasza A, Konik BS, Bryan L, Wright S, Griswold-Prenner I, Kordula T. A novel mechanism of tissue inhibitor of metalloproteinases-1 activation by interleukin-1 in primary human astrocytes. J Biol Chem. 2006; **281(46)**:34955-64.

Wilson CG, Palmer AW, Zuo F, Eugui E, Wilson S, Mackenzie R, Sandy JD, Levenston ME. Selective and non-selective metalloproteinase inhibitors reduce IL-1-induced cartilage degradation and loss of mechanical properties. Matrix Biol. 2006; *[Epub ahead of print]*.

Wilson W, van Burken C, van Donkelaar C, Buma P, van Rietbergen B, Huiskes R. Causes of mechanically induced collagen damage in articular cartilage. J Orthop Res. 2006; **24(2)**:220-8.

Wislowska M, Jablonska B. Serum cartilage oligomeric matrix protein (COMP) in rheumatoid arthritis and knee osteoarthritis. Clin Rheumatol. 2005; **24(3)**:278-84.

Wong PK, Campbell IK, Egan PJ, Ernst M, Wicks IP. The role of the interleukin-6 family of cytokines in inflammatory arthritis and bone turnover. Arthritis Rheum. 2003; **48(5)**:1177-89 *(Review)*.

Wrighton CJ, Hofer-Warbinek R, Moll T, Eytner R, Bach FH, de Martin R. Inhibition of endothelial cell activation by adenovirus-mediated expression of I kappa B alpha, an inhibitor of the transcription factor NF-kappa B. J Exp Med. 1996; **183(3)**:1013-22.

Wu JJ, Eyre DR. Structural analysis of cross-linking domains in cartilage type XI collagen. Insights on polymeric assembly. J Biol Chem. 1995; **270(32)**:18865-70.

Wu CY, Hseih HL, Jou MJ, Yang CM. Involvement of p42/p44 MAPK, p38 MAPK, JNK and nuclear factor-kappa B in interleukin-1beta-induced matrix metalloproteinase-9 expression in rat brain astrocytes. J Neurochem. 2004; **90(6)**:1477 – 88

Wysocki GP, Brinkhous KM. Scanning electron microscopy of synovial membranes. Arch Pathol. 1972; **93(2)**:172 – 7

Yamanishi Y, Boyle DL, Clark M, Maki RA, Tortorella MD, Arner EC, Firestein GS. Expression and regulation of aggrecanase in arthritis: the role of TGF-beta. J Immunol. 2002; **168(3)**:1405-12.

Yaron A, Gonen H, Alkalay I, Hatzubai A, Jung S, Beyth S, Mercurio F, Manning AM, Ciechanover A, Ben-Neriah Y. Inhibition of NF-kappa-B cellular function via specific targeting of the I-kappa-B-ubiquitin ligase. EMBO J. 1997; **16(21)**:6486-94.

Yasuda T. Cartilage destruction by matrix degradation products. Mod Rheumatol. 2006; **16(4)**:197-205 *(Review)*.

Yates LL, Gorecki DC. The nuclear factor-kappaB (NF-kappaB): from a versatile transcription factor to a ubiquitous therapeutic target. Acta Biochim Pol. 2006; **53(4)**:651 – 62.

Yin MJ, Yamamoto Y, Gaynor RB. The anti-inflammatory agents aspirin and salicylate inhibit the activity of I(kappa)B kinase-beta. Nature. 1998; **396(6706)**:77-80.

Yoshida Y, Katoh T, Tetskua T, Uno K, Matsui N, Okamoto T. Involvement of thioredoxin in rheumatoid arthritis: its costimulatory roles in the TNF-alpha-induced production of IL-6 and IL-8 from cultured synovial fibroblasts. J Immunol.1999;**163(1)**:351-8.

Yoshihara Y, Nakamura H, Obata K, Yamada H, Hayakawa T, Fujikawa K, Okada Y. Matrix metalloproteinases and tissue inhibitors of metalloproteinases in synovial fluids from patients with rheumatoid arthritis or osteoarthritis. Ann Rheum Dis. 2000; **59(6)**:455-61.

Youn I, Choi JB, Cao L, Setton LA, Guilak F. Zonal variations in the three-dimensional morphology of the chondron measured in situ using confocal microscopy. Osteoarthritis Cartilage. 2006; **14(9)**:889-97.

Young MF. Mouse models of osteoarthritis provide new research tools. Trends Pharmacol Sci. 2005; **26(7)**:333-5.

Yuan GH, Masuko-Hongo K, Sakata M, Tsuruha JI, Onuma H, Nakamura H, Aoki H, Kato T, Nishioka K. The role of C-C chemokines and their receptors in osteoarthritis. Arthritis Rheum. 2001;**44(5)**:1056 – 1070.

Zhang YP, Yao XX, Zhao X. Interleukin-1 beta up-regulates tissue inhibitor of matrix metalloproteinase-1 mRNA and phosphorylation of c-jun N-terminal kinase and p38 in hepatic stellate cells. World J Gastroenterol. 2006; **12(9)**:1392-6.

APPENDIX

Rheumatology 2007;46:752–758
Advance Access publication 11 January 2007

doi:10.1093/rheumatology/kel419

Interleukin-1β induced activation of nuclear factor-κb can be inhibited by novel pharmacological agents in osteoarthritis

S. N. Lauder, S. M. Carty, C. E. Carpenter, R. J. Hill[1], F. Talamas[1], J. Bondeson, P. Brennan[2] and A. S. Williams

Objectives. To investigate the importance of activation of the transcription factor, nuclear factor-κB (NF-κB) by interleukin-1β (IL-1β) and tumour necrosis factor-α (TNF-α) in the pathogenesis of osteoarthritis (OA) and assess its suitability as a target for therapy by determining its role in the induction of the cytokine IL-6 and the degenerative enzymes, matrix metalloproteinase (MMP)-1 and MMP-3 *in vitro*.

Methods. Three distinct cellular models, derived from primary OA tissue, were employed, namely, fibroblast-like synoviocytes (OA-SF); co-cultures containing phenotypic macrophage-like and fibroblast-like cells (OA-COCUL); and primary OA synovial tissue explants (OA-EXP). These were treated with specific inhibitors of IL-1β, TNF-α and NF-κB to assess their differential role in the production of pathologically relevant mediators, specifically IL-6, MMP-1, MMP-3 and the tissue inhibitor of metalloproteinases-1 (TIMP-1), which were quantified by enzyme-linked immunosorbent assay.

Results. Inhibition of NF-κB by a novel agent, RO100 at a dose of 0.1 μM, exerted significant ($P < 0.05$) repression of IL-6, MMP-1 and MMP-3 production in OA-SF. Notably, neither TIMP-1 production nor cell viability was significantly affected at the dose tested. These data were reproduced in OA-EXP, which might be considered as having greater physiological relevance. Interestingly, comparable efficacy was noted using IL-1β and TNF-α neutralizing antibodies in OA-COCUL.

Conclusions. We have demonstrated that a novel pharmacological inhibitor of NF-κB, RO100 inhibits pathological mediators of OA progression with equivalent efficacy as established IL-1β and TNF-α neutralizing strategies. Our findings highlight a potential for developing NF-κB targeted therapeutics for positively regulating disease activity and improving clinical outcome in OA.

Key words: Osteoarthritis, Therapeutics, Matrix Metalloproteinases, NF-κB, Cytokines.

As a debilitating, progressive disease affecting the joints, osteoarthritis (OA) is the most prevalent joint disorder globally. Now considered the eighth most frequent cause of disability [1], patients experience chronic pain and stiffness in the affected joint as a result of deterioration of the articular cartilage surface. Historically believed to be a consequence of 'wear and tear', OA was considered to involve non-inflammatory disease processes. A change in perception occurred as a result of a pioneering study in the 1970s that provided evidence that cohorts of OA patients experienced an acute inflammatory episode at disease onset [2]. The inflammation exhibited was not as severe as that seen in rheumatoid arthritis (RA) but sufficient to disprove the original belief that OA was simply an erosive process. Subsequent studies support this theory with OA now considered to be a complex multifactorial disease with sufferers classified as heterogeneous patient population, exhibiting varying degrees of inflammation, in some cases comparable with RA [3–6].

Whilst the aetiology of OA remains unclear, it appears that OA is initiated as a consequence of altered mechanical loading due to injury or excessive stress [7, 8]. In this context the chondrocytes become activated and increase levels of IL-1β and TNF-α [9] expression in the affected joint. The upregulation of IL-1β and TNF-α acts in both an autocrine and paracrine fashion [10] orchestrating in the formation of superficial fractures and fissures in the articular cartilage [11]. As the disease progresses, synovial hyperplasia and hypertrophy develop, and joint architecture becomes compromised.

The matrix metalloproteinase (MMP) family encompasses 23 enzymes that differentially mediate the degradation of each component of extracellular matrix. Key MMPs implicated in the pathogenesis of OA include the collagenases (MMP-1, -8 and -13), a gelatinase (MMP-9) and stromeolysin-1 (MMP-3) [12, 13]. Several studies suggest that MMP-13 is the critical MMP responsible for cartilage destruction [14, 15]. Levels of MMP-1 (a collagenase that is not as specific in its cleavage of collagen) expression is, however, 200-fold greater than MMP-13 in OA [11]. The stromeolysin MMP-3 has the ability to degrade many proteins including aggrecan, an early indicator of proteoglycan depletion in articular cartilage during the aetiopathogenesis of OA [16]. Perhaps of greater importance is the ability of MMP-3 to activate pro-MMP-1 and pro-MMP-9, which damage collagen fibrils and thereby disturb the highly organized structure of articular cartilage [17–19]. Apart from stimulating MMP production by the chondrocytes, both IL-1β and TNFα induce IL-6 release by the chondrocytes [20] and synovial cells [21]. IL-6 is reported to be instrumental in perpetuating synovial inflammation and intensifying cartilage depletion within the joint [22].

IL-1β and TNF-α primarily elicit their effects through inducing NF-κB activation [23]. This in turn results in the formation of the IκB kinase (IKK) complex, resulting in the phosphorylation and degradation of IκB-α. The loss of IκBα permits the translocation of NF-κB into the nucleus where it can turn on gene expression [24, 25], upregulating a plethora of cytokines and MMPs [23]. It has previously been shown that in cells derived from the osteoarthritic synovium that IL-6 production can be altered by targeting NF-κB [26]. The ERK, p38, MAPKs, AP-1 and NF-κB signalling cascades are all associated with MMP production [27–30]. It is hypothesized that inhibition of one or more of these signalling cascades may reveal a potential target for OA therapy and therefore warrant further investigation.

The aim of our present study was therefore to assess the potential of targeting NF-κB activation as a therapeutic strategy for OA. To achieve our objectives we used three distinct *in vitro*

Rheumatology Research Laboratory, Cardiff University, Heath Park, Cardiff, CF14 4XN, UK, [1]Roche, Palo Alto, CA 93404, USA and [2]Medical Biochemistry and Immunology, Henry Wellcome Building, Cardiff University, Heath Park, Cardiff CF14 4XN, UK.

Submitted 26 May 2006; accepted 9 November 2006.

Correspondence to: S. Lauder, Rheumatology Research Laboratory, Cardiff University, Heath Park, Cardiff CF14 4XN, UK. E-mail: LauderSN@cardiff.ac.uk

model systems, selected IL-6 as a relevant marker of synovial inflammation, MMP-1 and MMP-3 as relevant cartilage depleting enzymes and the endogenous regulator of MMP activity tissue inhibitor of metalloproteinases-1 (TIMP-1) as readouts that would provide a balanced perspective of efficacy.

Materials and methods

Experimental model systems

Three *in vitro* model systems derived from OA synovial samples namely, fibroblast-like synoviocytes (OA-SF), synovial co-cultures (OA-COCUL) and synovial tissue explants (OA-EXP) were utilized for this study. In all cases, synovium was obtained from consenting patients diagnosed with end-stage OA who were undergoing synovectomy at the time of joint replacement surgery. Ethical approval was obtained from Bro-Taf Health Authority (Cardiff, Wales, UK) prior to commencement of the study.

Fibroblast-like synoviocytes (OA-SF)

OA-SF were generated from synovium that had been cut into small fragments and digested with collagenase (1 mg/ml) and DNAse (2000 Kunitz units) for 2 h at 37°C with mechanical shaking. Following digestion the heterogeneous population of primary OA synovial cells, referred to as OA-COCUL, were distributed into T25 tissue culture flasks (Nunc, USA) and cultured overnight before the non-adherent cells were removed. Adherent cells were grown in DMEM F12 (supplemented with 2 mM L-glutamine, 10 units/ml penicillin–streptomycin, 1% insulin-transferring-slenium and 10% heat-inactivated fetal calf serum). At confluence, cells were passaged 1:2. By passage 3, the cells represented a homogeneous population of OA-SF. All experimental investigations conducted used OA-SF between passages 4 and 6.

OA synovial co-cultures (OA-COCUL)

Synovial digestion (described previously) generated OA-COCUL. OA-COCUL were dispensed into 12-well plates (Nunc) at 2×10^6 cells/well for experimental analysis.

OA synovial explants (OA-EXP)

OA-EXP were excised at random from synovial tissue, and their weight recorded prior to experimental investigation. OA-EXP were dispensed into 1.5 ml of DMEM F12 (supplemented as described previously) in 12-well plates and then allowed to equilibrate for 18 h. Supernatant samples taken at this time provided baseline measurements for each mediator prior to initiation of treatment protocols. The baseline value (100% mediator production) for each well was used as the reference point against which subsequent responses to individual treatment was compared. To accommodate the intra-variability present within each synovial sample, treatment conditions were conducted in triplicate or quadruplicate depending upon the size of the original synovial specimen and the mean calculated for each treatment strategy.

Electrophoretic mobility shift assay

OA-SF were dispensed at a concentration of 1×10^6 cells/well into 6-well plates. Cells were stimulated with IL-1β (20 ng/ml) for 30 min before terminating the stimulation using ice-cold PBS. Nuclear extracts were prepared as described previously [30]. Briefly, cells were detached using mechanical agitation, collected and centrifuged at 3000*g*. Cells were washed in buffer A (10 mM HEPES pH 7.9, 1.5 mM $MgCl_2$, 10 mM KCl) and centrifuged at 12 000*g*. OA-SF were treated with 400 μl of buffer A + 0.5 mM DTT, 0.5 mM PMSF, 5 μg/ml aprotinin, 5 μg/ml pepstatin, 30 μg/ml leupeptin, 0.125% IPEGAL (equivalent to the non-ionic surfactant Nonidet-P40) on ice for 5 min. OA-SF were centrifuged at 12 000*g* for 5 min and the resulting pellet treated with 100 μl of buffer C + 0.5 mM DTT, 0.5 mM PMSF, 5 μg/ml aprotinin, 5 μg/ml pepstatin, 30 μg/ml leupeptin and incubated at 4°C with mechanical shaking for 60 min. OA-SF were centrifuged at 13 000*g*, before the supernatant was collected and 100 μl of buffer D (8 mM HEPES pH 7.9, 0.5 mM DTT, 25 mM KCl, 0.1 mM EDTA, 8% glycerol) added. The protein content of each nuclear extract was established using a BCA protein assay kit (Pierce, USA). Four micrograms of protein was incubated with 10× Binding Buffer (40% Glycerol, 10 mM EDTA, 50 mM DTT, 100 mM Tris pH 7.5, 1 M NaCl, 1 mg/ml nuclease-free BSA), 2 μg of non-specific DNA competitor (polydIdC) and 1 μl of radiolabelled ^{32}P probe for NF-κB (5′-AGT TGA GGG GAC TTT CCC AGG C-3′, 3′-TCA ACT CCC CTG AAA GGG TCC G-5′) at room temperature for 30 min. For the cold competitor and non-self EMSA, 25-fold excess of unlabelled NF-κB oligo or 10-fold excess of AP-1 consensus oligo (5′-CGC TTG ATG ACT CAG CCG GAA-3′, 3′-GCG AAC TAC TGA GTC GGC CTT- 5′) or 10-fold excess of AP-1 mutant oligo (5′-CGC TTG ATG ACT TGG CCG GAA-3′3′-GCG AAC TAC TGA ACC GGC CTT-5′) was added to the samples and incubated on ice for 30 min prior to addition of radiolabelled probe. Protein–DNA complexes were resolved on a 4% polyacrylamide gel for 80 min and visualized by autoradiograph.

Cell viability

OA-SF were routinely examined under the microscope and at the conclusion of each experiment an Almar Blue Assay (Biosource International, USA) was performed to assess the viability of OA-SF according to manufacturer's guidelines.

Inhibition of the NF-κB signalling pathway

Two pharmacological inhibitors developed specifically to inhibit NF-κB signalling via IKK in OA, were employed in both the OA-SF and OA-EXP model systems. RO100 and RO919 were a kind gift of Roche Palo Alto, CA USA, and were administered at a known dose or dose range. The IKK inhibitors had been previously demonstrated to be effective in HUVECs. The enzyme IC50s for IKKB activity for both RO100 and RO919 are 2 nM. The IC50s of NF-κB activation were 100 nM and 30 nM, respectively for RO100 and RO919.

Anti-cytokine strategies

OA-COCUL were treated with etanercept, a soluble TNF-receptor Ig fusion protein (100 μg/ml), a depleting anti-IL-1β antibody (10 μg/ml), a combination of the two agents or left untreated for 48 h. OA-EXP were treated with the combination of etanercept and anti-IL-1β for 24 h (at the doses stated previously). At the conclusion of each investigation supernatants were harvested and cytokine and MMP levels measured by specific enzyme-linked immunosorbent assay (ELISA).

Enzyme-linked immunosorbent assay (ELISA)

Cytokines and MMP levels were quantified from the supernatants harvested from experimental OA-SF, OA-COCUL and OA-EXP. IL-1β, TNF-α, IL-6 and MMP-3 levels were measured using specific Biosource Europe ELISA kits (Human IL-1β Cytoset-CHC1214, Human TNF-α Cytoset-CHC1754, Human IL-6 Cytoset-CHC1264 & Human MMP-3 Cytoset-CHC1544) following the manufacturer's protocol supplied with each kit. TIMP-1 levels were quantified using an R&D Systems ELISA kit (Human TIMP-1 Duoset–DY970). The levels of MMP-1 were established using a matched antibody pair system. Briefly, 96-well ELISA plates (Nunc) were coated with 100 μl of monoclonal anti-human MMP-1 antibody (MAB901, R & D Systems) at 1 μg/ml diluted in

PBS overnight with mechanical shaking. Following incubation the antibody was discarded and plates were blocked for 1 h at room temperature with 300 μl of 1% BSA/PBS. Plates were washed four times in PBS with 0.05% Tween-20 (pH 7.2–7.4) added. 100 μl of diluted recombinant human MMP-1 (901-MP, R & D Systems) standards (3.125–200 ng/ml) were added in duplicate. 100 μl of each sample diluted in 1% BSA/PBS (1 : 2–1 : 100 depending on experimental investigation and *in vitro* model system) were added accordingly and incubated for 1.5 h at room temperature with mechanical shaking. After four washes 100 μl of biotinylated anti-human MMP-1 antibody (BAF901, R & D Systems) at 0.03 μg/ml diluted in 1% BSA/PBS was added and incubated for 1 h at room temperature with mechanical shaking. Following four washes, 100 μl of purified streptavidin–horseradish peroxidase conjugate (Biosource Europe) at 1 μg/ml was added and incubated for 30 min at room temperature with mechanical shaking. After four final washes, 100 μl of developing solution (containing 0.01% tetramethyl benzidine) was added and the colour was developed at room temperature. The reaction was terminated by the addition of 50 μl of 12.5% H_2SO_4. The optical density of the plates was measured at 450 nm (0.1 s) using a Wallac Victor 2 plate reader.

Statistical testing

All statistical differences determined in this study used the paired means Student's *t*-test. A two-tailed test was performed for Fig. 1 (A–D) and Fig. 2 (A and B), a one-tailed test was performed for Fig. 3 (A–H). $P \leq 0.05$ were considered significant, with values of ≤ 0.01 considered highly significant. The non-parametric Wilcoxon match pairs test was additionally performed for Fig. 4 (A–D).

Results

IKK inhibitors dysregulate IL-1β induced MMP-3 and TIMP-1 production in OA-SF

IKK inhibitors, RO100 and RO919 (1, 0.1, 0.03 μM), were employed to modulate IL-1β (20 ng/ml) induced NF-κB activation in OA-SF. EMSAs conducted on the nuclear extracts of treated OA-SF showed dose dependent inhibition of NF-κB activation (Fig. 1A). Densitometric analysis demonstrated a significant ($P \leq 0.05$) reduction in NF-κB nuclear signalling at the 1 μM dose (Fig. 1B). Binding specificity was confirmed by competition assays against unlabelled oligonucleotides of identical NF-κB sequence and using unrelated AP-1 consensus or mutant sequences.

When culture supernatants were analysed both MMP-3 and TIMP-1 production (mean ± S.E.M., ng/ml) increased significantly from 1 ± 0.9 and 265 ± 53.0 to 163 ± 63.9 and 399 ± 63.3, respectively in response to IL-1β stimulation (Fig. 1C and D). Both RO100 & RO919 elicited significant ($P \leq 0.05$) dose dependent reduction of IL-1β induced MMP-3 production, with maximum inhibition noted at the 1 μM dose for each agent (Fig. 1C and D). Interestingly, at doses below 1 μM, MMP-3 production was inhibited without affecting TIMP-1 significantly.

Amelioration of NF-κB activation inhibits IL-1β induced cytokine and MMP expression in OA-SF

Upon IL-1β activation, IL-6 production was significantly ($P \leq 0.05$) repressed by a 0.1 μM dose of RO100 or RO919 (Fig. 2A and B). Both RO100 and RO919 also inhibited MMP-3 production, but the effect was most pronounced upon MMP-1, with a highly significant ($P \leq 0.01$) 80% and 66% reduction with RO100 and RO919, respectively. Neither inhibitor elicited a notable effect upon TIMP-1 induction. These effects were not attributable to cell death, as cell viability was >95% at endpoint for each data point reported.

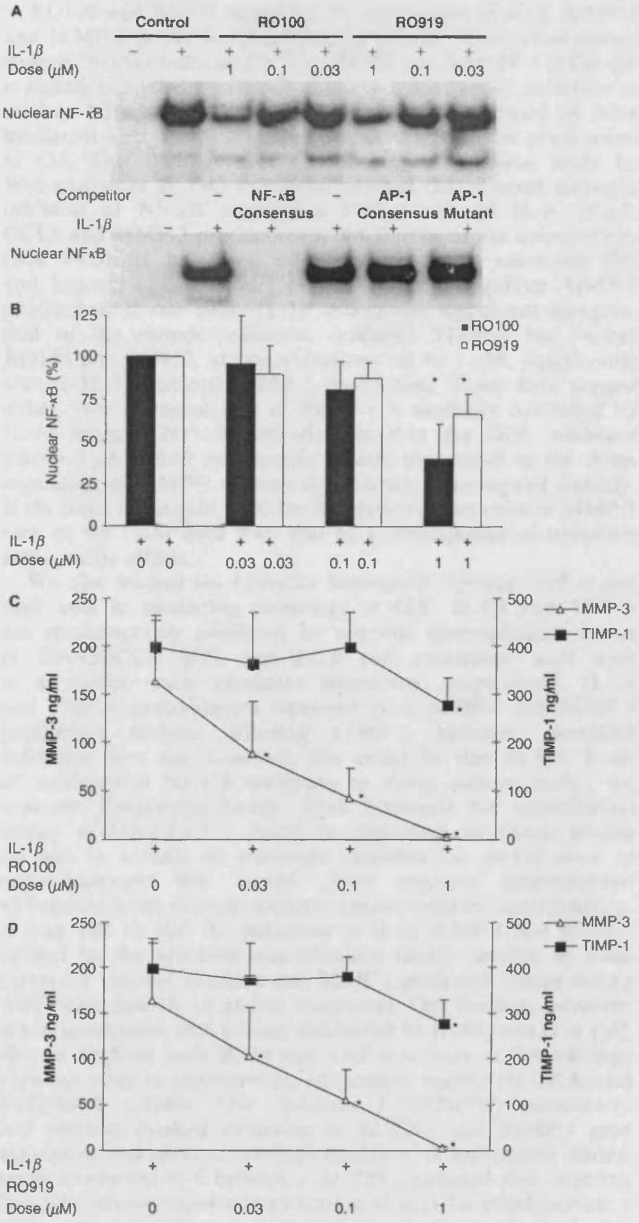

FIG. 1. The effect of RO100 and RO919 upon the IL-1β induced OA-SF model. Nuclear extracts were prepared from OA-SF treated with a dose range of RO100 and RO919 and subsequently stimulated with IL-1β (20 ng/ml). Extracts were analysed by EMSA (A), with 25-fold excess of self and 10-fold excess of non-self competitor added to determine specificity. Densitometric analysis (B) was conducted on EMSAs derived from four individual OA patients using NIH image software with results expressed as the mean ± S.E.M., percentage of nuclear NF-κB. MMP-3 and TIMP-1 levels were measured by ELISA from the supernatants of OA-SF treated with a dose range of RO100 and RO919 (C and D). Results are given as the mean ± S.E.M., ng/ml ($n = 5$). (*$P \leq 0.05$).

IL-1β and TNF-α regulate IL-6, MMP-1 and MMP-3 in OA-COCUL

IL-1β and TNF-α were neutralized in culture using a specific anti-IL-1β antibody (10 μg/ml) and etanercept (100 μg/ml). Anti-IL-1β and etanercept administered either solely or in combination resulted in marked reduction in NF-κB activation (Fig. 3A and B). Anti-IL-1β did not significantly affect TNF-α production whilst etanercept did not elicit a significant reduction in IL-1β levels (Fig. 3C and D). Combination

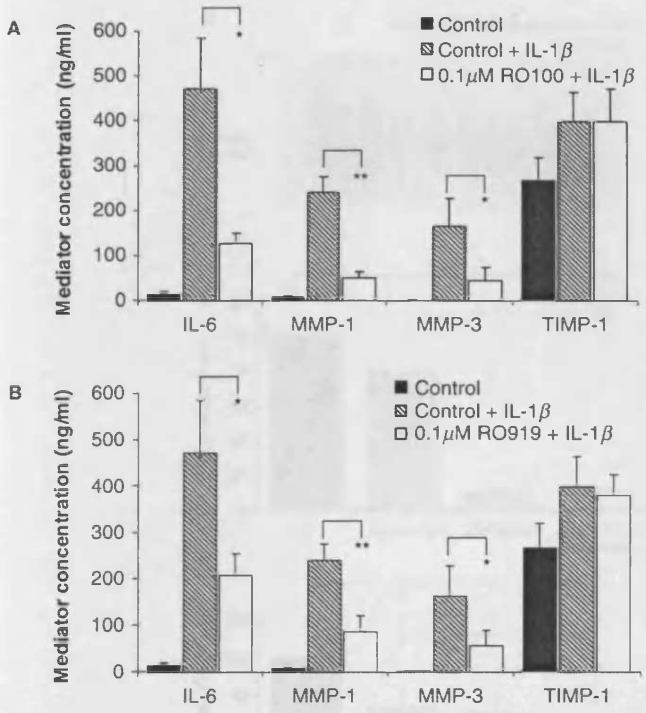

FIG. 2. Effect of NF-κB inhibition upon the pathogenic mediators produced by IL-1β stimulated OA-SF. OA-SF were treated with a 0.1 μM dose of RO100 and RO919 and subsequently stimulated with IL-1β (20 ng/ml). The levels of IL-6, MMP-1, MMP-3 and TIMP-1 were quantified by specific ELISA. Results are expressed as mean ± S.E.M., ng/ml ($n = 5$ individual patients) (A and B). ($^*P \leq 0.05$, $^{**}P \leq 0.01$).

therapy evoked a greater reduction in cytokine and MMP production, than either agent alone (Fig. 3E–H). These observations demonstrated that IL-6, MMP-1 and MMP-3 expression in OA-COCUL was dependent on both IL-1β and TNF-α expression.

Anti-IL-1β, etanercept and a novel NF-κB inhibitor reduce IL-6 and MMP-1 production in OA-EXP

Consistent with previous studies [31], histological analysis of OA-EXP revealed that the degree of inflammation and angiogenesis varied tremendously between OA patients (data not shown). OA-EXP treated with a combination of etanercept and anti-IL-1β or a 0.1 μM dose of RO100 elicited a significant ($P \leq 0.01$) reduction in IL-6 and MMP-1 production (Fig. 4A and C). However, neither MMP-3 nor TIMP-1 were significantly affected (Fig. 4B and D).

Discussion

Our studies demonstrated that IL-1β and TNF-α activation of the NF-κB signalling cascade regulate IL-6, MMP-1 and MMP-3 production in OA. We have clearly shown that the NF-κB signalling cascade can be targeted to achieve inhibition of a range of critical mediators implicated in the pathogenesis of OA, and is therefore of therapeutic interest.

Our data supports the current opinion that in OA, IL-1β and TNF-α drive disease progression by inducing MMPs (critical mediators of cartilage destruction) [32, 33] and IL-6, unique in eliciting a significant role both in synovial inflammation and cartilage destruction within the joint [21, 22]. The present study sought to investigate the role of the NF-κB signal transduction pathway in OA, specifically employing two novel inhibitors of IKK namely, RO100 and RO919.

RO100 and RO919 repressed the production of IL-6, MMP-1 and MMP-3 in the IL-1β stimulated OA-SF. Such observations suggest that the induction of IL-6, MMP-1 and MMP-3 in OA-SF is tightly regulated by NF-κB. Indeed, a diminutive reduction in nuclear NF-κB activation caused significant inhibition of these mediators that are so important in accelerating the progression of OA. Our findings are supported by a previous study by Wakamatsu *et al.* [34] who demonstrated that a small molecule inhibitor of NF-κB suppressed TNF-α induced IL-6, CCL2, CCL5 and MMP-3 production in RA fibroblast like synoviocytes (RA FLS). It has been established in both astrocytes [35] and hepatic stellate cells [36] that IL-1β upregulates TIMP-1 production. In our study IL-1β also caused significant upregulation of the chondroprotective mediator TIMP-1 but neither RO100 nor RO919, at concentrations up to 1 μM, significantly altered IL-1β induced TIMP-1 production. These data suggest either, that the regulation of TIMP-1 is modestly controlled by IL-1β induced NF-κB activation or that the IKK inhibitors (above 1 μM) elicit non-specific effects that result in the down regulation of TIMP-1 without significantly affecting cell viability. If the latter is the case, then the dramatic amelioration of MMP-3 seen at the 1 μM dose may also be a consequence of unknown non-specific effects.

We also studied the interplay between IL-1β and TNF-α and their role in mediating pathology in OA. IL-1β and TNF-α are spontaneously produced by synovial macrophages present in OA-COCUL [37], anti-IL-1β and etanercept were used to neutralize each cytokines bioactivity, respectively. IL-1β and TNF-α neutralization repressed IL-6, MMP-1 and MMP-3 production without affecting TIMP-1. However, complete inhibition was not achieved; this could be due to low levels of unidentified NF-κB activators in tissue culture media, for example, lipopolysaccharide. With hindsight the experimental design of OA-COCUL could be improved, in future studies we aim to include an overnight equilibration period prior to commencement that would allow accurate determination of baseline levels of each mediator before cytokine neutralization. It may well be that the reduction in IL-6, MMP-1 and MMP-3 elicited by the cytokine neutralization maybe masked to some extent by residual cytokine and MMP's generated before dosing with either anti-IL-1β and/or etanercept. Our findings, however, are in accordance with a study conducted by Kobayashi *et al.* [38], they neutralized both IL-1β and TNF-α activity in OA cartilage explants using recombinant IL-1β receptor agonist (IL-1RA) and PEGylated soluble TNF receptor I (sTNFRI) respectively and showed marked reduction in MMP-1 and MMP-3 gene expression and reduced cartilage depletion. A subsequent clinical study conducted by Chevalier *et al.* [39] concluded that targeting IL-1β by intraarticular administration of IL-1RA could provide a viable target for therapy in OA. Currently there are no studies published that have targeted TNF-α for treatment of OA, although, targeting TNF-α using etanercept or infliximab, for example, has revolutionized the management of RA [40, 41]. The results of our present study and those of others, detailed previously [38, 39], show that IL-1β and TNF-α act synergistically and that a treatment strategy that targets both cytokines may be more beneficial than targeting either cytokine alone in OA. In order to clarify the role of IL-1β and TNF-α in OA further studies are required.

We tested RO100 and RO919 in OA-COCUL but found that even at the lowest concentration (0.03 μM) both agents were extremely toxic. We attributed the high sensitivity of the cells to the aggressive collagenase and DNAse digestion required to prepare OA-COCUL. Consequently, a more robust *ex vivo* model was developed using OA synovial explants. Both RO100 and etanercept with anti-IL-1β reduced IL-6 and MMP-1 production without significantly affecting TIMP-1 or MMP-3. There may be many reasons for this, firstly, several signalling pathways induce MMP expression and it would appear

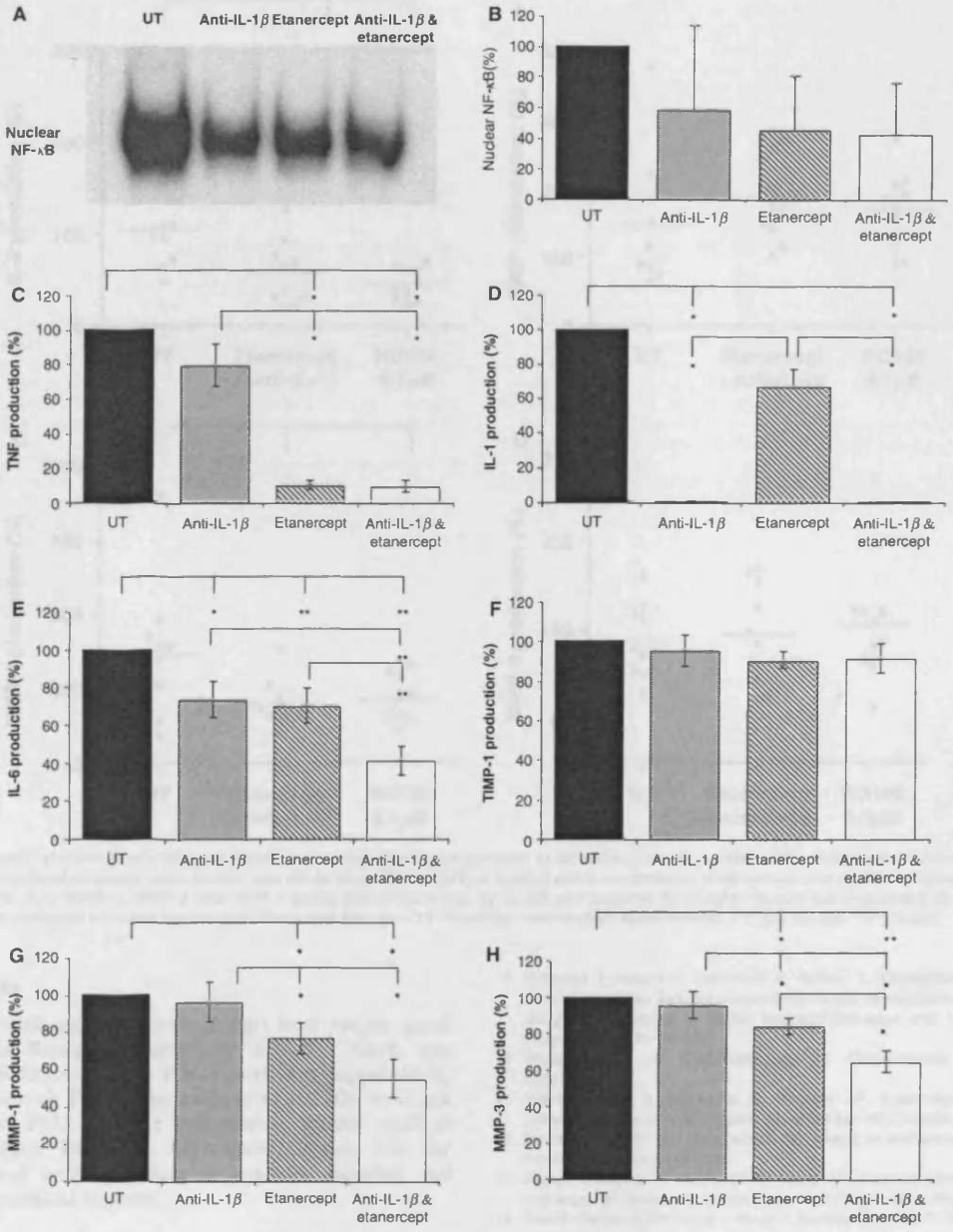

FIG. 3. Effect of anti-cytokine strategies employed in OA-COCUL. Nuclear extracts were prepared from OA-COCUL treated with either etanercept (10 μg/ml), anti-IL-1β antibody (100 μg/ml), the two agents in combination or left untreated (UT). The extracts were analysed by EMSA, note only the protein–DNA complexes are shown (A). Densitometric analysis was conducted on EMSAs using NIH image software, with the results given as the mean ± S.E.M. expressed as a percentage of nuclear NF-κB (B). TNF-α (C), IL-1β (D), IL-6 (E), TIMP-1 (F), MMP-1 (G) and MMP-3 (H) levels were quantified by specific ELISA. Data are expressed as mean ± S.E.M. as a percentage. ($n=9$ individual experiments). ($^*P \leq 0.05$ and $^{**}P \leq 0.01$).

that MMP-3 production is not primarily dependent upon NF-κB signalling in OA-EXP. Secondly, MMP-3 is most active in early OA affecting proteoglycan depletion in cartilage, OA-EXP were derived from end-stage patients where MMP-3 levels are comparatively low [14] thus IKK inhibitors could not affect further down-regulation of this enzyme.

To conclude, our study supports the view that an intrinsic network of cytokines and MMP's exist in OA and that the subsequent interactions between them is complex. We have demonstrated, using novel IKK inhibitors (RO100 and RO919) and anti-cytokine agents (etanercept and anti-IL-1β) the genuine potential of inhibiting pathogenic mediators by targeting the NF-κB pathway specifically. The observations have important implications with regard to developing new specific therapies for OA aimed at inhibiting cartilage depletion.

Rheumatology key messages

- NF-κB is an integral signalling pathway involved in the pathogenesis of OA.
- Novel pharmacological inhibitors of the NF-κB pathway elicit significant suppression of key pathological mediators associated with disease progression.
- Therapeutic targeting of the NF-κB pathway has the potential to modulate disease activity.

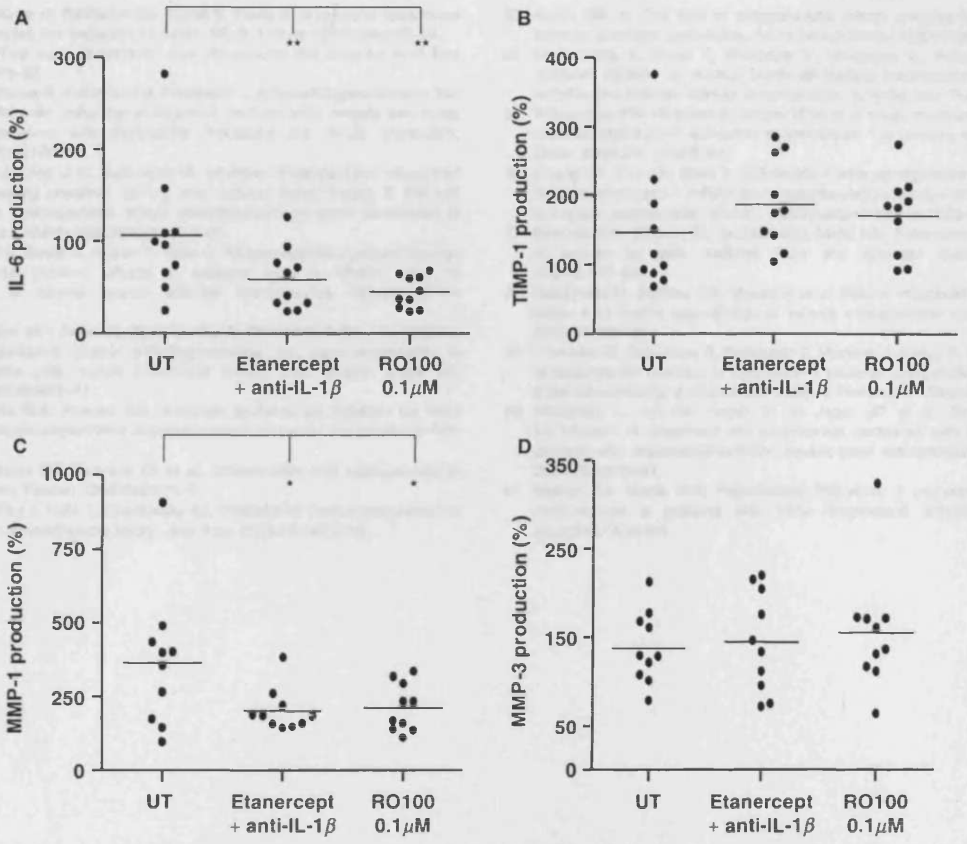

FIG. 4. OA-EXP represent a physiologically relevant model for studying disease progression *in vitro*. OA-EXP were prepared as described previously in the materials and methods. After an 18 h equilibration period each explant was either left untreated (UT) or treated with a combination of etanercept and anti-IL-1β (doses previously stated) or a 0.1 μM dose of RO100. IL-6, MMP-1, MMP-3 and TIMP-1 levels were established by ELISA and adjusted for weight. Results are expressed as a percentage, with the mean of each treatment condition indicated by the solid horizontal line. ($n = 10$ individual, independent experiments). ($^*P \leq 0.05$ and $^{**}P \leq 0.01$).

Acknowledgements

S.N.L. and J.B.'s work was supported in part by a project grant from the Arthritis Research Campaign. S.M.C.'s work was supported by the Wellcome Trust. P.B.'s work was supported by the Leukaemia Research Fund. The authors would like to thank Dr R. Goodfellow, PhD and the orthopaedic theatre staff at the Royal Glamorgan Hospitial, Llantrisant, Wales, UK for the ethical approval and collection of synovial samples and Mr N. Amos for technical support.

The authors have declared no conflicts of interest.

References

1 Birchfield PC. Osteoarthritis Overview. Geriatr Nurs 2001;22:124–31.
2 Ehrlich GE. Osteoarthritis beginning with inflammation. JAMA 1975;232:691–3.
3 Smith MD, Triantafillou S, Parker A, Youssef PP, Coleman S. Synovial membrane inflammation and cytokine production in patients with early osteoarthritis. J Rheum 1997;24:365–71.
4 Benito MJ, Veale DJ, Fitzgerald O, van den Berg WB, Breshinan B. Synovial tissue inflammation in early and late osteoarthritis. Ann Rheum Dis 2005;65:1263–7.
5 Loeuille D, Chary-Valckenaere I, Champigneulle J *et al.* Macroscopic and microscopic features of synovial membrane inflammation in the osteoarthritic knee. Arthritis Rheum 2005;52:3492–501.
6 Kristoffersen H, Torp-Pedersen S, Terslev L *et al.* Indications of inflammation visualized by unltrasound in osteoarthritis of the knee. Acta Radiolog 2006;47:281–6.
7 Huser CAM, Davies EM. Validation of an *in vitro* single-impact load model of the initiation of osteoarthritis-like changes in articular cartilage. J Orthopaed Res 2006;24:725–32.
8 Wilson W, van Burken C, van Donkelaar C, Buma P, van Rietbergen B, Huiskes R. Causes of mechanically induced collagen damage in articular cartilage. J Orthopaed Res 2006;24:220–8.
9 Fujisawa T, Hattori T, Takahashi K, Kuboki T, Yamashita A, Takigawa M. Cyclic mechanical stress induces extracellular matrix degradation in cultured chondrocytes via gene expression of matrix metalloproteinases and interleukin-1. J Biochem (Toyko) 1999;125:966–75.
10 Martel-Pelletier J. Pathophysiology of Osteoarthritis. Osteoarthr Cartilage 2004;12:S31–3.
11 Martel-Pelletier J, Alaaedine N, Pelletier JP. Cytokines and their role in the pathophysiology of osteoarthritis. Front Biosci 1999;4:d694–703.
12 Burrage PS, Mix KS, Brinckerhoff CE. Matrix metalloproteinases: role in arthritis. Front Biosci 2006;11:529–43.
13 Aigner T, Sachse A, Gebhard PM, Roach HI. Osteoarthritis: pathobiology – targets and ways for therapeutic intervention. Adv Drug Deliver Rev 2006;58:1–22.
14 Bau B, Gebhard PM, Haag J, Knorr T, Bartnik E, Aigner T. Relative messenger RNA expression profiling of collagenases and aggrecanases in human articular chondrocytes *in vivo* and *in vitro*. Arthritis Rheum 2002;46:2648–57.
15 Kevorkian L, Young DA, Darrah C *et al.* Expression profiling of metalloproteinases and their inhibitors in cartilage. Arthritis Rheum 2004;50:131–41.
16 Lin PM, Chen CTC, Torzilli PA. Increased stromeolysin-1 (MMP-3), proteoglycan degradation (3B3- and 7D4) and collagen damage in cyclically load-injured cartilage. Osteoarthr Cartilage 2004;12:485–96.
17 van Meurs J, van Lent P, Holthuysen A *et al.* Active matrix metalloproteinases are present in cartilage during immune complex-mediated arthritis: a pivotal role for stromeolysin-1 in cartilage destruction. J Immunol 1999;163:5633–9.
18 Unemori EN, Bair MJ, Bauer EA, Amento EP. Stromeolysin expression regulates collagenase activation in human fibroblasts. J Biol Chem 1991;266:23477–82.
19 Dreier R, Grassel S, Fuchs S, Schaumburger J, Bruckner P. Pro-MMP-9 is a specific macrophage product and is activated by osteoarthritic chondrocytes via MMP-3 or MT1-MMP/MMP-13 cascade. Exp Cell Res 2004;297:303–12.
20 Bender S, Haubeck HD, Van de Leur E *et al.* Interleukin-1β induces synthesis and secretion of interleukin-6 in human chondrocytes. FEBS 1990;263:321–4.
21 Pelletier JP, McCollum R, Coultier JM, Martel-Pelletier J. Synthesis of metalloproteases and interleukin-6 (IL-6) in human osteoarthritic synovial membrane is an IL-1 mediated process. J Rheumatol 1995;22:S110–4.
22 Flannery CR, Little CB, Hughes CE, Curtis CL, Caterson B, Jones SA. IL-6 and its soluble receptor augment aggrecanase-mediated proteoglycan catabolism in articular cartilage. Matrix Biol 2000;19:549–53.
23 Hayden MS, Ghosh S. Signaling to NFκB. Genes Dev 2004;18:2195–224.

24 DiDonato JA, Hayakawa M, Rothwarf DM, Zandi E, Karin M. A cytokine responsive IκB kinase that activates the transcription factor NFκB. Nature 1997;388:548–54.
25 Baldwin AS. The NFκB and IκB proteins: new discoveries and insights. Annl Rev Immunol 1996;14:649–81.
26 Amos N, Lauder S, Evans A, Feldmann M, Bondeson J. Adenoviral gene transfer into osteoarthritis synovial cells using the endogenous inhibitor IκBα reveals that most, but not all, inflammatory and destructive mediators are NFκB dependent. Rheumatology 2006;45:1201–9.
27 Liacini A, Sylvester J, Qing Li W, Zafarullah M. Inhibition of interleukin-1-stimulated MAP kinases, activating protein-1 (AP-1) and nuclear factor kappa B (NF-κB) transcription factors downregulates matrix metalloproteinase gene expression in articular chondrocytes. Matrix Biol 2002;21:251–62.
28 Fan Z, Yang H, Bau B, Soder S, Aigner T. Role of mitogen-activated protein kinases and NFκB on IL-1β induced effects of collagen type II, MMP-1 and 13 mRNA expression in normal human articular chondrocytes. Rheumatol Int 2006;26:900–03.
29 Mengshol JA, Vincenti MP, Coon CI, Barchowsky A, Brinckerhoff CE. Interleukin-1 induction of collagenase-3 (matrix metalloproteinase 13) gene expression in chondrocytes requires p38, c-JUN N-terminal kinase and nuclear factor κB. Arthritis Rheum 2000;43:801–11.
30 Dignam JD, Lebovitz RM, Roeder AG. Accurate transcription initiation by RNA polymerase II in a soluble extract from isolated mammalian nuclei. Nucleic Acids Res 1983;11:1475–89.
31 Haywood L, McWilliams DF, Pearson CI *et al.* Inflammation and angiogenesis in Osteoarthritis. Arthritis Rheum 2003;48:2173–7.
32 Kurz B, Lemke AK, Fay J, Pufe T, Grodzinsky AJ, Schunke M. Pathomechanisms of cartilage destruction by mechanical injury. Ann Anat 2005;187:473–85.
33 Smith GN Jr. The role of collagenolytic matrix metalloproteinases in the loss of articular cartilage destruction. Front Biosci 2006;11:3081–95.
34 Wakamatsu K, Nanki T, Miyasaka N, Umezawa K, Kubota T. Effect of a small molecule inhibitor of nuclear factor-κB nuclear translocation in a murine model of arthritis and cultured human synovial cells. Arthritis Res Ther 2005;7:R1348–59.
35 Wilczynska KM, Gopalan S, Bugno M *et al.* A novel mechanism of tissue inhibitor of metalloproteinases-1 activation by interleukin-1 in primary human astrocytes. J Biol Chem 2006;281:34955–64.
36 Zhang YP, Yao XX, Zhao X. Interleukin-1 beta up-regulates tissue inhibitor of matrix metalloproteinases-1 mRNA and phosphorylation of c-jun N-terminal kinase and p38 in hepatic stellate cells. World J Gastroenter 2006;12:1392–6.
37 Brennan FM, Chantry D, Jackson AM, Maini RN, Feldmann M. Cytokine production in culture by cells isolated from the synovial membrane. J Autoimmun 1989;2:177–86.
38 Kobayashi M, Squires GR, Mousa A *et al.* Role of interleukin-1 and tumour necrosis factor α in matrix degradation of human osteoarthritic cartilage. Arthritis Rheum 2005;52:128–35.
39 Chevalier X, Giraudeau B, Conrozier T, Marliere J, Kiefer P, Goupille P. Safety study of intraarticular injection of interleukin 1 receptor antagonist in patients with painful knee osteoarthritis: a multicenter study. J Rheumatol 2005;32:1317–23.
40 Klareskog L, van der Heijde D, de Jager JP *et al.* Therapeutic effect of the combination of etanercept and methtrexate compared with each treatment alone in patients with rheumatoid arthritis: double blind randomised controlled trial. Lancet 2004;363:675–81.
41 Bathon JM, Martin RW, Fleischmann RM *et al.* A comparison of etanercept and methotrexate in patients with early rheumatoid arthritis. New Engl J Med 2000;343:1586–93.